University of Nottingham

School of Medicine

Mental Health and Clinical Neuroscience

Neural Mechanisms of Treatment for Mental Disorders

Abdulrhman Mohammad M Shalabi

Thesis submitted for the degree of Doctor of Philosophy

December 2022

Acknowledgements

I must express my deepest gratitude towards the one who prepared, equipped, supported, and guided me until I wrote this thesis, and I pray that he will keep guiding me afterwards. He who enabled and commanded me to read, learn, apply, and deliver the knowledge. First and foremost, all thanks, gratitude, and praise to Allah.

Then, to the two who spent the time teaching me and directing my journey in the depths of the folded cortex. They marked the path towards the proper methods and approaches to tackle the scientific dilemma. Professor Peter Liddle and Dr Elizabeth Liddle, I cannot thank you enough but thank you.

Then to the reasons for my existence, those who seeded in me the passion for science and medicine. My mother, Dr Mona Banajah and my father, Dr Mohammad Shalabi, thank you for your generous love and patience. Thank you for your constant and endless support. Thank you for being there for me from the moment I was born.

To my smaller family, my beloved wife Alaa Jabalawi, and my sons Fares, Mohammad and Amir, thank you for supporting and joining me during the ups and downs of this journey.

Then to my colleagues in the IMH and the field. Thank you for your hard work exploring and discovering the hidden scientific gems using every possible way to achieve your goals.

Last but not least, to my sponsor who made this journey real, the University of Jeddah, Thank you.

Abstract

"Cognitive control" refers to the ability to regulate thoughts and actions in the service of goals or plans (Braver, 2012). Coordination between the central and peripheral autonomic nervous systems (ANS) maintains arousal and attention levels, which are essential for effective cognitive control. Diamond (2013) proposed a cognitive control model that builds on three core cognitive functions: cognitive flexibility, inhibitory control, and working memory. Abnormality in active inhibitory cognitive control is implicated in a broad range of psychiatric and personality disorders, including schizophrenia, attention deficit hyperactivity disorder (ADHD), impulsivity, and substance abuse, among many others. Transcranial direct current stimulation (tDCS) and cognitive training are two neuromodulation techniques which have the potential to modulate cortical functions to introduce long-lasting neuronal plasticity. The antisaccade task is a visual inhibitory control task frequently used to assess cognitive control. It requires the participant to suppress an automatic stimulus-driven saccadic eye movement and instead make a goal-driven saccade in the opposite direction.

In this thesis, by conducting two separate studies, we used the antisaccade task to examine the effect of tDCS and computerised cognitive training on inducing neuroplastic changes for the oculomotor control network (OCN). Chapter 1¢introduces relevant concepts to the subject of this thesis with a technical account of the methods used. The details of the **first study** are discussed in Chapter 2 - Chapter 4, where we used eye-tracking during antisaccade performance with the continuous assessment of cortical activity using Magnetoencephalography (MEG). Chapter 2 will discuss the short-term neuroplastic changes introduced by the tDCS on the functional connectivity within the resting state networks assessed using MEG. We found evidence of increased connectivity following the engagement in the antisaccade task for both active tDCS and sham conditions, but with different spatial patterns. Following tDCS delivered over the frontal cortex, there was increased connectivity with the frontal cortex. In contrast, in the sham condition there was increased connectivity with the posterior cortex. The effects of tDCS stimulation on

the ANS activity during the task performance were further assessed via pupillometry as a measure of Locus Coeruleus (LC) activity in Chapter 3. Our results showed that faster pupil dilation, reflecting increased arousal and sympathetic activity, was associated with faster saccade reaction times. In Chapter 4, we investigated the immediate effects of tDCS stimulation on the cerebral cortex during active cognitive inhibition followed by a correct saccadic response. The tDCS introduced neuromodulatory changes in the putative Alpha and low-Beta band during the anticipatory and post-stimulus periods, reflecting enhanced cortical engagement in a task-beneficial pattern.

Chapter 5 reports on **the second study** in which we used functional magnetic resonance imaging (fMRI) to evaluate the neuromodulatory effects of prolonged computerised cognitive training games (RECOGNeyes) on the resting state functional connectivity of the OCN and pupil dilation. Following gaze-control training, the connectivity within the left hemisphere was strengthened, while the intra-right hemisphere and the interhemispheric connectivity were diminished. Chapter 6 provides a summary of the findings and concluding remarks. Our result furthers our knowledge of the processes involved in the performance of the antisaccade task, the mechanisms of action and the neuroplastic effects of two neuromodulation techniques. However, the exact mechanisms underlying these methods' beneficial effects demand further exploration.

Statement of Contribution

I hereby confirm that the work presented in this thesis is original and my own, whereby the thoughts and ideas of others are appropriately acknowledged.

Both studies discussed in this thesis were team projects. The experimental designs and ethical approval were confirmed before I joined the project's team. The Chief investigator for the tDCS and inhibitory control study (the first study reported) was Professor Peter Liddle, and I was one of the key researchers. I contributed, with other team members, in all aspects of this study, from participant recruitment, data acquisition, and artefact rejection—a team member conducting the scoring and statistical analysis of the self-reported measure of impulsivity and schizotypy. The rest of the data pre-processing and analyses reported for this study in this thesis were conducted by me.

Dr Elizabeth Liddle was the Chief Investigator for the RECOGNeyes study (the second study reported). I contributed to some data acquisition and pre-processing and conducted all the pre-processing and analysis of the fMRI data reported in this thesis. The rest of the processes and analysis of this study, including participants recruitment, data collection and analysis of the MEG data, pupillometry, antisaccade task, and behavioural measures, were conducted by other team members.

Table of Contents

ABSTRACT **3**

TABLE OF CONTENTS **6**

TABLE OF FIGURES **10**

LIST OF TABLES **12**

LIST OF ABBREVIATIONS **13**

CHAPTER 1 INTRODUCTION **17**

1.1 NEUROPLASTICITY 17

1.2 NEUROPLASTICITY AND MENTAL HEALTH 18

1.3 NEUROMODULATION 19

1.4 MEASURING NEURAL ACTIVITY 22

1.4.1 Neural oscillations and magnetoencephalography 22

1.4.2 Functional magnetic resonance imaging and functional networks 24

1.5 COGNITIVE PROCESSING AND ATTENTION NETWORKS 28

1.5.1 Arousal and attentional networks 28

1.5.2 Cognitive Control 31

1.5.3 Cognitive Training and neurofeedback 32

1.6 THE ANTI-SACCADE TASK 34

1.7 OCULOMOTOR CONTROL NETWORK 36

1.8 THESIS SCOPE AND RATIONALE 39

CHAPTER 2 MEG RESTING-STATE NETWORKS AND NEUROMODULATION 40

2.1 INTRODUCTION 40

2.1.1 Magnetoencephalography 41

2.1.2 Alpha and Beta oscillations 44

2.1.3 Aims and questions 45

2.2 METHODS 46

2.2.1 Participants and recruitment 46

2.2.2 Study design 47

2.2.3 Imaging data acquisition 50

2.2.4 Analysis methods 51

2.2.5 Resting State Connectivity data analysis 52

2.3 RESULTS 55

2.3.1 Sample demographics *55*
2.3.2 Impulsivity, mood and schizotypy results *55*
2.3.3 MEG data quality *57*
2.3.4 Resting-state functional connectivity changes *59*
2.3.5 Regional centrality *65*
2.4 DISCUSSION 72

CHAPTER 3 PUPIL DILATATION, NEUROMODULATION, AND COGNITIVE CONTROL 75

3.1 INTRODUCTION 75
3.1.1 Aims and questions *76*
3.2 METHODS 77
3.2.1 Participants and study design *77*
3.2.2 The Anti-saccade task *77*
3.2.3 Pupillometry analysis and task performance *79*
3.3 RESULTS 83
3.3.1 Behavioural performance *83*
3.3.2 Pupillometry results *85*
3.4 DISCUSSION 90

CHAPTER 4 TDCS AND COGNITIVE CONTROL 92

4.1 INTRODUCTION 92
4.1.1 Communication Through Coherence *93*
4.1.2 Visual-spatial remapping *93*
4.1.3 Antisaccade and the OCN *94*
4.1.4 Aims and questions *96*
4.2 METHODS 97
4.2.1 Participants recruitment, study design, the antisaccade task, MEG pre-processing and co-registration *97*
4.3 RESULTS 102
4.3.1 Anticipatory period *102*
4.3.2 Anticipatory modulation in the Visual cortex *112*
4.3.3 Anticipatory period summary *113*
4.3.4 Post-stimulus period analysis *115*
4.4 DISCUSSION 127

CHAPTER 5 COGNITIVE TRAINING AND INHIBITORY CONTROL 132

5.1 INTRODUCTION 132
5.1.1 Specific learning difficulties *133*
5.1.2 Attention deficit hyperactivity disorder *134*

5.1.3 RECOGNeyes 135
5.1.4 Locus coeruleus 137
5.1.5 fMRI 138
5.1.6 Aims and questions 139
5.2 METHODS 140
5.2.1 Participants and recruitment 140
5.2.2 RECOGNeyes Gaze Training 141
5.2.3 The antisaccade task 144
5.2.4 ROI definition 144
5.2.5 MRI Data Acquisition 144
5.2.6 Image pre-processing 146
5.2.7 Denoising the functional data 148
5.2.8 Functional connectivity estimation 149
5.3 RESULTS 150
5.3.1 Participants and sample demographics 150
5.3.2 Training Exposure 151
5.3.3 Antisaccade performance 151
5.3.4 Pupil dilation changes 152
5.3.5 Data pre-processing quality 152
5.3.6 Resting-state functional connectivity patterns 157
5.3.7 RECOGNeyes training effects on the OCN 159
5.3.8 Locus coeruleus functional connectivity 160
5.4 DISCUSSION 162
CHAPTER 6 GENERAL DISCUSSION AND CONCLUDING REMARKS 164
6.1 RESTING-STATE CHANGES ASSOCIATED WITH TREATMENT CONDITIONS 164
6.2 ENGAGEMENT OF THE AUTONOMIC NERVOUS SYSTEM DURING THE ANTISACCADE TASK 166
6.3 EFFECTS OF TREATMENT CONDITIONS ON CEREBRAL ACTIVITY DURING THE ANTISACCADE TASK PERFORMANCE 167
6.3.1 Shared modulation between Treatment conditions 167
6.3.2 Effects of active tDCS 170
6.4 EFFECT OF GAZE CONTROL TRAINING ON RESTING STATE FUNCTIONAL CONNECTIVITY 171
6.5 LIMITATIONS 173
6.6 IMPACTS AND FUTURE DIRECTIONS 175
6.7 CONCLUSION 177
REFERENCES 178
APPENDICES 214

Appendix I: tDCS advertising flyer 214
Appendix II: E-mail to approach society and clubs 215
Appendix III: tDCS Participant information sheet 217
Appendix IV: tDCS Safety Questionnaire 223
Appendix V: Time-frequency spectrograms of the antisaccade task 224
Appendix VI: Profile of Mood status (POMS) questionnaire 230
Appendix VII Urgency premeditation, perseverance, sensation seeking and positive urgency (UPPS-P) scale 231
Appendix VIII Schizotypal personality questionnaire (SPQ) 234
Appendix IX: SPMIC MRI safety questionnaire 236
Appendix X: RECOGNeyes advertising flyer 237
Appendix XI: RECOGNeyes participant information sheet 238

Table of Figures

FIGURE 1.1 TRIPLE NETWORK MODEL OF PSYCHOPATHOLOGY 27

FIGURE 1.2 THE RELATIONSHIP BETWEEN TASK PERFORMANCE AND THE LC ACTIVITY 30

FIGURE 1.3 THE CORTICAL AND SUBCORTICAL REGIONS IMPLICATED IN THE PERFORMANCE OF THE ANTISACCADE TASK.. 38

FIGURE 2.1 THE FORWARD AND INVERSE PROBLEM INHERENT IN PROCESSING MEG SIGNAL 42

FIGURE 2.2 A PREPARED SUBJECT WITH FIDUCIAL COILS AND MR-COMPATIBLE TDCS ELECTRODES 49

FIGURE 2.3 THE ILLUSTRATED MEG RESTING-STATE ANALYSIS PIPELINE FROM ACQUISITION TO STATISTICAL ANALYSIS... 53

FIGURE 2.4 TRIALS AVAILABLE POST DATA FILTERING 59

FIGURE 2.5 THE FUNCTIONAL CONNECTIVITY MATRICES FOR THE SHAM CONDITION 61

FIGURE 2.6 THE FUNCTIONAL CONNECTIVITY MATRICES FOR THE ACTIVE TDCS CONDITION 62

FIGURE 2.7 THE CHANGE IN FUNCTIONAL CONNECTIVITY MATRICES FOR BOTH TREATMENT CONDITIONS 63

FIGURE 2.8 ALPHA BAND REGIONAL CENTRALITY, EFFECT OF TIME BY REGIONS BY HEMISPHERE INTERACTION 66

FIGURE 2.9 THE EFFECT OF REGIONS BY TREATMENT CONDITION INTERACTION IN ALPHA BAND CENTRALITY 67

FIGURE 2.10 BETA BAND REGIONAL CENTRALITY, EFFECT OF TIME BY REGIONS BY HEMISPHERE INTERACTION 68

FIGURE 2.11 THE ALPHA-BETA CROSS-FREQUENCY REGIONAL CENTRALITY 69

FIGURE 2.12 THE CHANGES IN THE ALPHA BAND CENTRALITY..... 70

FIGURE 2.13 THE CHANGES IN THE BETA BAND CENTRALITY..... 71

FIGURE 3.1 THE ANTISACCADE TASK TIMELINE 79

FIGURE 3.2 THE PUPILLOMETRY DATA ANALYSIS PIPELINE 80

FIGURE 3.3 FREQUENCY DISTRIBUTION OF THE SACCADIC RESPONSE REACTION TIMES 84

FIGURE 3.4 THE TIME COURSE OF PUPIL SIZE..... 85

FIGURE 3.5 THE PDR 86

FIGURE 3.6 THE ER-PDR..... 87

FIGURE 3.7 SPEARMAN'S CORRELATIONS (RT WITH THE ERPDR) 88

FIGURE 3.8 PEARSON CORRELATION (ANTISACCADE RT AND STIMULUS TO SACCADE ERPDR)..... 89

FIGURE 4.1 MEG DATA PROCESSING AND ANALYSIS PIPELINE..... 97

FIGURE 4.2 THE EFFECT OF TIME BY REGIONS INTERACTION IN THE ALPHA BAND 103

FIGURE 4.3 THE HEMISPHERE BY TRIAL TYPE INTERACTION IN THE DLPFC FOR ALPHA BAND..... 105

FIGURE 4.4 THE EFFECT OF HEMISPHERE BY TREATMENT CONDITIONS..... 106

FIGURE 4.5 THE ANTICIPATORY LOW-BETA BAND, EFFECT OF TIME BY REGIONS INTERACTION..... 107

FIGURE 4.6 ANTICIPATORY LOW-BETA BAND, EFFECT OF TIME BY TREATMENT CONDITIONS INTERACTION 109

FIGURE 4.7 HIGH-BETA BAND ANTICIPATORY, EFFECTS OF TIME BY REGION INTERACTION 110

FIGURE 4.8 THE TIME COURSE OF THE VISUAL CORTEX'S ALPHA, LOW-BETA, AND HIGH-BETA BANDS 112

FIGURE 4.9 THE POST-STIMULUS, EFFECT OF TIME BY STIMULUS LATERALITY INTERACTION..... 116

FIGURE 4.10 LEFT PEF ALPHA MODULATION, EFFECT OF TIME BY TRIAL TYPE BY STIMULUS LATERALITY..... 117

FIGURE 4.11 THE EFFECT OF TREATMENT CONDITION BY STIMULUS LATERALITY BY TRIAL TYPE ON ALPHA BAND..... 119

FIGURE 4.12 LOW-BETA BAND TRIAL TYPE MODULATION IN THE PEF DURING THE POST-STIMULUS PERIOD..... 121

FIGURE 4.13 THE FEF LOW-BETA BAND LATERALITY INDEX, EFFECT OF TREATMENT CONDITION BY TRIAL TYPE BY STIMULUS LATERALITY INTERACTION 123
FIGURE 4.14 THE LOW-BETA BAND LATERALITY INDEX'S TIME COURSE IN THE RIGHT HEMISPHERE, EFFECT OF TREATMENT CONDITION BY TRIAL TYPE BY STIMULUS LATERALITY INTERACTION 125
FIGURE 4.15 THE TIME COURSE OF HIGH-BETA BAND MODULATION IN THE HOMOTOPIC OCN REGIONS 126
FIGURE 5.1 RECOGNEYES TRAINING EQUIPMENT SETUP 142
FIGURE 5.2 SCREENSHOTS OF RECOGNEYES GAME 143
FIGURE 5.3 THE LC MAP AND THE TEN OCN REGIONS 145
FIGURE 5.4 THE FMRI RESTING-STATE ANALYSIS PIPELINE 147
FIGURE 5.5 QUALITY ASSESSMENT PARAMETERS OF THE ACQUIRED FMRI DATA 153
FIGURE 5.6 THE QUALITY OF THE SEGMENTATION AND CO-REGISTRATION PROCESS 155
FIGURE 5.7 THE EFFECTS OF PERFORMING THE DENOISING PROCESS 156
FIGURE 5.8 THE RESTING STATE FUNCTIONAL CONNECTIVITY BETWEEN THE OCN REGIONS AND THE LC 158
FIGURE 5.9 PEARSON CORRELATION BETWEEN THE ANTISACCADE PD RATE AND THE LC-V1 CONNECTIVITY 161

List of Tables

TABLE 1.1 THE THREE PRIMARY FUNCTIONAL RESTING STATE NETWORKS 27
TABLE 2.1 TDCS STUDY SAMPLE DEMOGRAPHIC 55
TABLE 2.2 THE PSYCHOMETRIC DESCRIPTIVE RESULTS FOR THE TDCS STUDY 56
TABLE 2.3 STATISTICAL RESULTS SUMMARY FOR TIME EFFECT ON POMS 57
TABLE 2.4 STATISTICS RESULTS SUMMARY FOR THE AVAILABLE TRIALS POST VISUAL INSPECTION OF THE MEG DATA. 58
TABLE 2.5 A LIST OF THE 78 AAL REGIONS USED IN THE ANALYSIS ARRANGED BY LOBE AND CORTICAL SURFACE 64
TABLE 3.1 REACTION TIME DESCRIPTIVE STATISTICS 84
TABLE 4.1 THE OCN REGIONS' COORDINATES IN MNI SPACE 99
TABLE 4.2 THE DESCRIPTION OF LATERALITY 101
TABLE 5.1 THE GAZE-CONTROL TASKS TARGETED IN EACH RECOGNEYES GAME 137
TABLE 5.2 RECOGNEYES SAMPLE DIAGNOSTIC INFORMATION 150
TABLE 5.3 RECOGNEYES TRAINING ALLOCATION AND TOTAL MINUTES TRAINED 151

List of Abbreviations

ACC	Anterior Cingulate Cortex
AdCS	Adjusted Change Score
ADHD	Attention Deficit Hyperactivity Disorder
AMPAR	α-Amino-3-Hydroxy-5-Methyl-4-Isoxazolepropionic Acid Receptor
ANS	Autonomic Nervous System
BEM	Boundary Element Method
BOLD	Blood Oxygenation Leve-Dependent
CEN	Central Executive Network
CiC	Confidence in Concept
CTC	Communication through Coherence
DA	Dopamine
dACC	Dorsal Anterior Cingulate Cortex
DAN	Dorsal Attention Network
Day1	First day session before engaging in the cognitive training
Day2	Second day session after the completion of the cognitive training
DBS	Deep Brain Stimulation
DLFC	Dorsolateral Frontal Cortex

DLPFC	Dorsolateral Prefrontal Cortex
DMN	Default Mode Network
dmPFC	Dorsomedial Prefrontal Cortex
ECT	Electroconvulsive Therapy
EEG	Electroencephalograph
er-PDR	Event Related Pupil Dilation Rate
ERSP	Event-Related Spectral Perturbation
ERSP	Event-Related Spectral Perturbation
FDR	False Discovery Rate
FEF	Frontal Eye Fields
FEM	Finite Element Method
FHMS	Faculty of Medicine and Health Sciences
fMRI	Functional Magnetic Resonance Imaging
FWHM	Full-Width Half Maximum
GABA	γ-Aminobutyric acid
HPI	Head Position Indicators
LC	Locus Coeruleus
LCMV	Linear-Constraint Minimum-Variance
LTD	Long-Term depression
LTP	Long-Term Potentiation
MDD	Major Depression Disorder

MEG	Magnetoencephalography
MNI	Montreal Neurological Institute
mPFC	Medial Prefrontal Cortex
MRC	Medical Research Council
MRI	Magnetic Resonance Imaging
NE	Norepinephrine
NMDAR	N-methyl-D-aspartate receptor
OCN	Oculomotor Control Network
PCC	Posterior Cingulate Cortex
PD	Pupil Dilation
PDR	Pupil Dilation Rate
PEF	Parietal Eye Fields
PFC	Prefrontal Cortex
POMS	Profile of Mood Status
PPC	Posterior Parietal Cortex
Rest1	Resting state before task/training completion
Rest2	Resting state after task/training completion
RS-fMRI	Resting-State Functional Magnetic Resonance Imaging
rTMS	Repetitive Transcranial Magnetic Stimulation
SC	Superior Colliculus
SDE	Saccade Directional Error

SMG	Supramarginal Gyrus
SPQ	Schizotypal Personality Questionnaire
SQUID	Superconducting Quantum Interference Device
SRT	Saccade Reaction Time
STG	Superior Temporal Gyrus
STS	Superior Temporal Sulcus
TBS	Theta Burst Stimulation
tDCS	Trans Cranial Direct Current Stimulation
TPM	Tissue Probability Maps
UPPS	Urgency, (lack of) Premeditation, (lack of) Perseverance, Sensation seeking
VAN	Ventral Attentional Network
VPFC	Ventral Prefrontal cortex

Chapter 1 Introduction

In this chapter, I will introduce principles of importance to the subject of this thesis. It will explore the concepts of neuroplasticity, neuromodulation methods, and the relevance of neuromodulation as a therapeutic tool. Then, I will review cognitive processing and control, introducing the antisaccade task and the oculomotor control network. Next, I'll describe the methods of measuring neural activity and networks.

1.1 Neuroplasticity

The nervous system has an innate ability to cope with the persisting internal and/or external stimuli by modulating its synaptic structure, connections and/or function (Mateos-Aparicio and Rodríguez-Moreno, 2019, Jackson et al., 2006). A healthy balance between the excitatory glutamatergic and the inhibitory GABAergic systems regulates this neurodevelopmental process (Sears and Hewett, 2021, Perica et al., 2022). These different neuroplastic modulations can either potentiate the synaptic efficacy of the circuit or depress it. The resulting modulatory effect could last for a short-term (milliseconds to several minutes) or a long-term (hours to days). Each modulation type is achieved via a different mechanism and serves a distinct physiological purpose (for review, see (Zucker and Regehr, 2002, Malenka and Bear, 2004, Citri and Malenka, 2008)).

Despite various forms of neuroplasticity, most converge to alter calcium membrane permeability and concentrations at the presynaptic, synaptic, or postsynaptic level (Chindemi et al., 2022, Lisman, 1989). The arrival of action potential to the presynaptic membrane opens the voltage-gated channels of calcium that permit the influx of calcium ions. The presynaptic increase in calcium concentration facilitates neurotransmitters' vesicle release into the synaptic cleft. The modulation of presynaptic calcium ions concentrations is circuit dependent and is correlated with the level of synaptic enhancement or depression in the short-term forms of the neuroplasticity (Zucker and Regehr, 2002).

Conversely, long-term neuroplasticity is under the glutamatergic system regulation via the postsynaptic voltage-dependent N-methyl-D-aspartate receptor

(NMDAR) calcium influx (Gasiorowska et al., 2021). The activation of the NMDAR requires prior postsynaptic depolarisation by the activated AMPAR (α-amino-3-hydroxy-5-methyl-4-isoxazole propionic acid receptor) (Citri and Malenka, 2008). This neuroplasticity form has gained more interest in the research field than any other form of plasticity. It has been associated with hippocampus memory consolidation and Hebbian learning theory. Hebbian learning theory proposes that long-term potentiation (LTP) or depression (LTD) is enhanced by a correlated activation between the presynaptic and postsynaptic neurons (Lynch, 2004, Munakata and Pfaffly, 2004).

1.2 Neuroplasticity and mental health

Neuroplastic processes are maintained by a continuous interaction between epigenetic (nature) and activity-dependant (nurture) factors to produce more efficient functional networks by strengthening or eliminating synapses (Friston, 1998, Clayton et al., 2020, Markham and Greenough, 2004). Epigenetic factors regulate the activation and inhibition of inherited genes responsible for the neurogenesis, synaptogenesis and pruning processes from conception through adulthood. On the other hand, activity-dependent neuroplasticity results from either spontaneous intrinsic activity in a neural network or elicited by an experience with the surrounding environment (experience-driven) (Markham and Greenough, 2004).

Abnormalities in the neuroplastic processes could develop into several mental disorders. For example, Feinberg (1982) proposed that an abnormality in the synaptic pruning process, which leads to partial dysconnectivity (Friston, 1998, Friston et al., 2016), is an underlying cause of the symptoms of schizophrenia. The theory received support from several lines of evidence, including; A) post-mortem synaptic density analysis showing a decreased synaptic density in the temporal and frontal lobes (Garey et al., 1998, Berdenis van Berlekom et al., 2020), B) reduced cortical grey matter volume and gyrification index in the temporal, frontal regions (Rapoport et al., 1999, Rosa et al., 2021), C) reduced synaptic protein (synaptophysin) in the hippocampus and frontal regions (Osimo et al., 2019) (for a detailed review see (McGlashan and Hoffman, 2000, Howes et al., 2023)).

These structural abnormalities are reflected in measures of functional connectivity. Li et al. (2019) conducted a meta-analysis comparing the resting state functional connectivity of 2,567 healthy control and 2,588 schizophrenia patients using an independent component analysis. The authors concluded that schizophrenia patients exhibited diffuse hypoconnectivity in several key cortical hubs, including temporal and frontal regions (Li et al., 2019). Moreover, the observable functional connectivity changes in the DMN are highly correlated with symptom severity (as measured by the positive and negative syndrome scale (PANSS)) (Tang et al., 2013), which could be used as a treatment response predictor (Mehta et al., 2021).

Although the samples examined in the work of this thesis are not clinical samples, it aims to examine the underpinning mechanisms of neuroplastic changes associated with neuromodulation techniques that could be used as treatment options for mental disorders.

1.3 Neuromodulation

Neuromodulation is becoming an essential tool to appreciate the complexity underpinning mental processes, to restore an impaired neuronal function as a prosthetic device, and to provide a possible alternative treatment strategy for psychiatric illnesses (Lewis et al., 2016, Luan et al., 2014). Neuromodulators are innovative techniques that grant scientists in-vivo interaction with the human brain. It introduces a reversible modulation to the brain's structure and function. The term neuromodulation encompasses a wide range of interventional methods. Thus, it is suitable for this thesis to consider the use (continuous or intermittent) of a controllable clinical intervention (non-invasive, invasive, or pharmacological), which produces functional changes in a neuronal network (central or peripheral) as a tool of neuromodulation (Sakas et al., 2007, DeFelipe and Fariñas, 1992, Holsheimer, 2003, Nadim and Bucher, 2014, Horn and Fox, 2020). The neuromodulation source can be either intrinsic or extrinsic relative to the neural circuit's level (Katz and Frost, 1996, Salvador et al., 2021, Nadim and Bucher, 2014). Extrinsic neuromodulators are further classified based on the approach used to; a) chemical, b) acoustic, c) electric, d) magnetic, e) thermal, or f) optogenetic neuromodulators (for a comprehensive

review, see (Luan et al., 2014)). Neuromodulators can potentially introduce long-term changes to the structure and function of the involved cortical regions (Jackson et al., 2006), which, with proper use, would produce beneficial outcomes for mental health and interested parties of the general population.

Among the approved neuromodulation techniques for the treatment of mental disorders is deep brain stimulation (DBS). DBS is an invasive neuromodulation method which requires the implantation of stimulation electrodes into predefined target cortical regions. Then implanted electrodes are connected to an external pulse generation device responsible for delivering the stimulation program. It is a current treatment option for patients suffering from movement disorders (Schwalb and Hamani, 2008, Udupa and Chen, 2015), major depression (Puigdemont et al., 2015), and epilepsy (Li and Cook, 2018). However, there is a significant increase in suicidal rates associated with the use of DBS and the risks associated with the surgical electrode implantation procedure, including infections, electrodes misplacement, lead fractures and skin erosion (Appleby et al., 2007, Hamani and Lozano, 2006).

Recently, electroconvulsive therapy (ECT) was reclassified from a high-risk to a moderate-risk treatment device in cases of treatment-resistant depression by the Food and Drug Administration (2018). ECT is a non-invasive neuromodulation method with proven efficacy in treating mood disorders (Lisanby, 2007) and schizophrenia (Tharyan and Adams, 2005). The main factors limiting the use of ECT are the moderate risk associated with ECT, the required clinical settings, the stigma associated with ECT, and the limited knowledge of the ECT mechanisms of action (Espinoza and Kellner, 2022).

Repetitive transcranial magnetic stimulation (rTMS) is a non-invasive brain stimulation tool that induces an electrical current in the brain tissue by applying a focal repetitive magnetic (Gaynes et al., 2014). This induced neuronal depolarisation depends on different parameters of the applied rTMS, which results in an LTD or LTP (Rossi et al., 2009, Rossi et al., 2021). In 2007, The Food and Drug Administration approved the application of rTMS over the left dorsolateral prefrontal cortex (DLPFC) as a treatment regime for Major Depression Disorder (MDD) and treatment-resistant

MDD (Lan et al., 2016, Gaynes et al., 2014). Furthermore, using rTMS effectively induces structural cortical change by increasing the grey matter volume of the right angular gyrus, left anterior cingulate cortex, left superior temporal gyrus and left insula (Lan et al., 2016). Theta burst stimulation (TBS) is a modality of rTMS that entails three high-frequency (50 Hz) bursts of pulses repeated in the range of theta oscillation (5 Hz) (Ni et al., 2017). TBS has the advantage of achieving the desired outcome (LTP or LTD) in a shorter time window and with better accuracy depending on the parameter used (intermitted or continuous) (Chung et al., 2015). However, the use of TMS requires advanced training, specialised clinical equipment and brain imaging for precise stimulation.

Transcranial direct current stimulation (tDCS) is a non-invasive brain stimulation tool which utilises a weak direct current ranging from 1 – 2 mA applied via scalp electrodes. The applied current modulates cortical excitability in a polarity-dependent manner. Anodal stimulation increases cortical excitability, and cathodal stimulation hyperpolarises it (Stagg et al., 2009). The cortical oscillations exhibit different modulation patterns for the applied current (Antal et al., 2004). A gathering of evidence implies the effectiveness of tDCS in modulating the resting state functional connectivity (Sehm et al., 2012, Keeser et al., 2011).

Notturno et al. (2014) compared the effect of three separate anodal tDCS stimulation sessions to cathodal stimulation and sham condition over the primary motor area. They measured changes in event-related spectral perturbation (ERSP) to a finger-tapping task before and after the tDCS session. Their anodal stimulation increased the low Alpha and Beta bands event-related desynchronisation compared to the sham and cathodal tDCS. Moreover, Stagg et al. (2011) examined the effect of timing tDCS before or during the task on motor learning between anodal, cathodal and sham conditions. Their results showed a significant modulatory effect of anodal tDCS during sequence motor tasks on shortening the time required to learn the task compared to cathodal stimulation and sham condition. There was no effect of tDCS before task performance on their behavioural results, which indicates that tDCS modulates the active cortical components during the stimulation. These modulatory effects are mediated via the NMDAR LTP and LTD effects (Nitsche et al., 2003,

Liebetanz et al., 2002) and result in the modulation of GABA (γ-Aminobutyric acid) and Glutamate neurotransmitters (Stagg et al., 2009). The produced modulation has a prolonged aftereffect lasting for a few days and, in some cases, weeks after tDCS has ceased, indicating a strengthening of synaptic transmission (for detailed review (Stagg and Nitsche, 2011)). However, solid conclusions regarding tDCS efficacy and mechanism of action cannot be drawn from the available literature.

1.4 Measuring neural activity

There are several methods to measure neural activity. These techniques could be invasive implantation of microelectrodes or patch-clamping neurons providing high-temporal and spatial resolution of neuronal activity with the cost of direct neuronal and cortical damage (Bjornsson et al., 2006, Biran et al., 2005). On the other hand, non-invasive techniques do not cause tissue damage and could provide either high-temporal or spatial resolution at the expense of the other. In the following sections, we will discuss two non-invasive methods used in this thesis to measure neural activity.

1.4.1 Neural oscillations and magnetoencephalography

The electrical neural activity in the brain produces measurable scalp oscillations. The measured electrical signal is produced by the potential electrical change of the extracellular environment associated with the synchronous activity of hundreds of neurons arranged in a perpendicular array to the cortical surface, primarily in cortical layers V and III. Although the cortical pyramidal cells are believed to be the primary source of the measured signals, their activity is highly modulated by a different subcortical structure, such as the thalamus (Jackson and Bolger, 2014, Portillo-Lara et al., 2021, Hallez et al., 2007, Buzsáki et al., 2012). These oscillations are categorised into five frequency bands: Delta (1-4), Theta (4-8), Alpha (8-13), Beta (14 - 30 Hz), and Gamma (> 30 Hz) (Cole and Voytek, 2017, Marzbani et al., 2016), which are measured using electroencephalography (EEG) or Magnetoencephalography (MEG). Modern EEG systems employ an array of

electrodes placed over the scalp to record the fluctuating voltage differences between the volume conducted electrical fields at predefined scalp positions.

Rather than measuring the scalp's electrical potential changes, D.S. Cohen (1968) successfully measured the subtle magnetic fields surrounding human subjects' heads using a magnetoencephalography (MEG) system with a single superconducting quantum interference device (SQUID). With further developments, modern MEG systems are now equipped with over 250 SQUIDs submerged in cooling liquid helium measuring the subtle magnetic field changes surrounding the scalp. The MEG employs the electromagnetic principles explained by Maxwell's equation and Ampère's law, which states that changes in electrical current generate a circulating magnetic field. The induced magnetic fields cross the meninges, skull, and scalp layers unaltered. This feature gives MEG the advantage of high spatial resolution down to the millimetre scale of the neuronal activity (for details, see section 4.1) (Troebinger et al., 2014) (for review, see (Proudfoot et al., 2014, Schwartz et al., 2010, Hämäläinen et al., 1993, Gross, 2019)).

Functional network findings from the BOLD fMRI signal have recently been translated to EEG/MEG analysis (Brookes et al., 2011b, De Pasquale et al., 2010). The resting state connectivity patterns observed using BOLD are best represented by correlation patterns in the Beta band (Brookes et al., 2011a, De Pasquale et al., 2012). This transition of functional connectivity analysis to MEG is associated with a substantial increase in the possible extractable information. MEG data has greater temporal resolution allowing the evaluation of instantaneous connectivity changes within the network compared to the fMRI. Moreover, neuronal oscillations grant a more comprehensive range of analyses as the measured neurophysiological signal encompasses five primary frequency bands. Each frequency independently relates to certain physiological functions and has multiple distinct parameters (e.g. amplitude, phase, amplitude envelopes) (Başar, 2013).

The Delta band reflects motivational system involvement (limbic regions) and deep sleep status. Theta band prevails in emotion regulation and memory processing (Knyazev, 2007). The increase in the Alpha band amplitude is associated with

suppressing the visual attention (Foxe et al., 1998) and active inhibition of the visuospatial distractors (Kelly et al., 2006). It disengages task-irrelevant cortical regions (Jensen and Mazaheri, 2010).

On the other hand, Beta band activity in the somatosensory area is related to the active control and delaying of the movement initiation (Khanna and Carmena, 2017). It shows decreased amplitude in conditions with active motor movements and increased power when movement inhibition or postural maintenance is required (Chakarov et al., 2009). Moreover, the Beta band demonstrates increased activity in conditions associated with the top-down attentional processing (Kamiński et al., 2012, Saleh et al., 2010) (for review of Beta band functional roles, see (Engel and Fries, 2010)). A communication through coherence (CTC) theory proposes that the Alpha and Beta bands mediate the active top-down influence of distant cortical communication, which activates remote local cortical circuits (Fries, 2015).

1.4.2 Functional magnetic resonance imaging and functional networks

Ogawa et al. (1990) were the first to describe Blood Oxygenation Level-Dependent (BOLD) MRI changes related to blood flow in the brain. These changes in the BOLD signal represent the regional cortical processing capacity (Logothetis et al., 2001). As the regional neural activity increases, so does its oxygen and glucose consumption, which causes an increase in blood flow to the active neural regions. This increased blood flow and associated deoxyhemoglobin rise are measured using the BOLD signals in fMRI within a 2 seconds time window of the actual neural activity (Kim et al., 1997) (for an extensive review, see (Heeger and Ress, 2002, Logothetis, 2008, Amaro and Barker, 2006)).

The growing evidence using the fMRI as a measure of neuronal function suggested the presence of BOLD activation patterns involving several brain regions during cognitive task performance or resting state with many mental disorders. This evidence indicates the existence of different functional correlation patterns that reflect functional cortical connectivity. Functional connectivity is evaluated using a statistical correlation between the neurophysiological time courses of a particular

event. These functional correlations either reflect the sequential temporal influence of one cortical region activity on another (effective connectivity) or represent the presence of temporal coactivation patterns between distinct regions regardless of evidence of influence (functional connectivity) (Friston, 1994)

Biswal et al. (1995) first reported resting-state functional connectivity. They reported a resting state's time-course correlation for the measured BOLD signal in the sensorimotor cortex in the left and right hemispheres. The replication of this finding increased the confidence in the used fMRI functional connectivity analysis methods (Cordes et al., 2000, Xiong et al., 1999). It led to the demonstration that resting-state functional connectivity can be observed within networks engaged in cognitive processes including the visual, language (Cordes et al., 2000), auditory (Hampson et al., 2002), and attention (Fox et al., 2005) processing.

Based on a comparison of brain activity patterns in the resting state with that during various tasks, Raichle et al. (2001) proposed the presence of an organised, baseline default mode of brain function that is suspended during specific goal-directed behaviours. The brain regions involved in a proposed pattern of resting state activity included midline frontal and parietal regions and bilateral angular gyrus. Subsequently, Greicius et al. (2003) used fMRI to demonstrate functional connectivity between these brain regions in the resting state. They proposed the existence of a default mode network (DMN) active prominently during rest locked to the posterior cingulate cortex (PCC), which was a consistent pattern confirmed across other samples (Damoiseaux et al., 2006, De Luca et al., 2006).

Fox et al. (2005) described a second network with inversed correlation to the DMN. It exhibited resting-state functional activity between regions engaged during attention-demanding tasks, including the intraparietal sulcus, frontal eye field (FEF), dorsal lateral prefrontal cortex (DLPFC), ventral prefrontal cortex and insula. For this reason, they called it the task-positive network. Their DMN network was reported to involve the medial prefrontal, lateral parietal and posterior cingulate cortex, consistent with the defined DMN by Raichle et al. (2001).

These findings were extended further by Seeley et al. (2007). They reported a significant correlation between anxiety and functional connectivity in a salience network of reward, emotion and conflict processing centres. The primary cortical regions implicated were the frontal insula and anterior cingulate cortex. Both regions have extensive connectivity to the limbic lobe and other subcortical structures. Moreover, their report on the executive control system (central executive network (CEN) / task-positive) was consistent with Fox et al. (2005) task-positive network, including the frontoparietal regions, DLPFC, ventrolateral PFC, intraparietal sulcus and superior parietal lobules. Seeley et al. (2007) reported an inverse correlation between the functional connectivity in the executive control network and task processing time. Interestingly, there was no association overlap between anxiety level and executive control network or between task performance and salience network connectivity, which confirms the functional dissociation between these networks. This evidence and others (Menon, 2011, Hamilton et al., 2013, Hampson et al., 2006) suggest that typical human attention, emotion, cognitive and executive functions are modulated by the interaction of three major networks out of 17 detectable functional networks using fMRI (Yeo et al., 2011). These three networks are the DMN, CEN and the salience network.

The DMN is the prevailing network at rest and is related to the self-appraisal processes (Raichle et al., 2001, Raichle, 2015). Abnormal DMN connectivity is documented in mental disorders with increased internal mentation processes, such as major depressive disorder (MDD), Autism, and schizophrenia (Brakowski et al., 2017, Sheline et al., 2009, Nixon et al., 2014). The CEN is the active network during active cognitive processing and goal-directed behaviour (Menon, 2011). Abnormal CEN connectivity was reported in autism during resting state and in psychosis during active task performance (Sarpal et al., 2022). The salience network activity grants the active switching between the network, which depends on the interoceptive integration of memories and goals with the external environment conditions. Disturbances in the salience network have been associated with anxiety, addiction, and schizophrenia (Sridharan et al., 2008, Seeley et al., 2007, Kühn et al., 2012).

Table 1.1 The three primary functional resting state networks, their abnormalities, and primary cortical nodes. mPFC: medial prefrontal cortex, PCC: posterior cingulate cortex, dACC: dorsal anterior cingulate cortex, DLPFC: dorsolateral prefrontal cortex, dmPFC: dorsomedial prefrontal cortex, FEF: frontal eye fields, PPC: posterior parietal cortex.

	Default Mode Network	**Salience Network**	**Central Executive Network**
Function	Self-referential processing. Mind wandering. Emotion regulation	-Processing of salient stimuli. -Switching active network according to functional demand	Implicated in cognitive functioning and including attention and working memory.
Abnormality	MDD, Autism, schizophrenia	Addiction, anxiety, schizophrenia	Psychosis, autism
Cortical Regions	- mPFC - PCC - Precuneus - Lateral parietal cortex	- dACC - Insula - Temporal pole	- DLPFC - dmPFC - FEF - PPC - Paracingulate

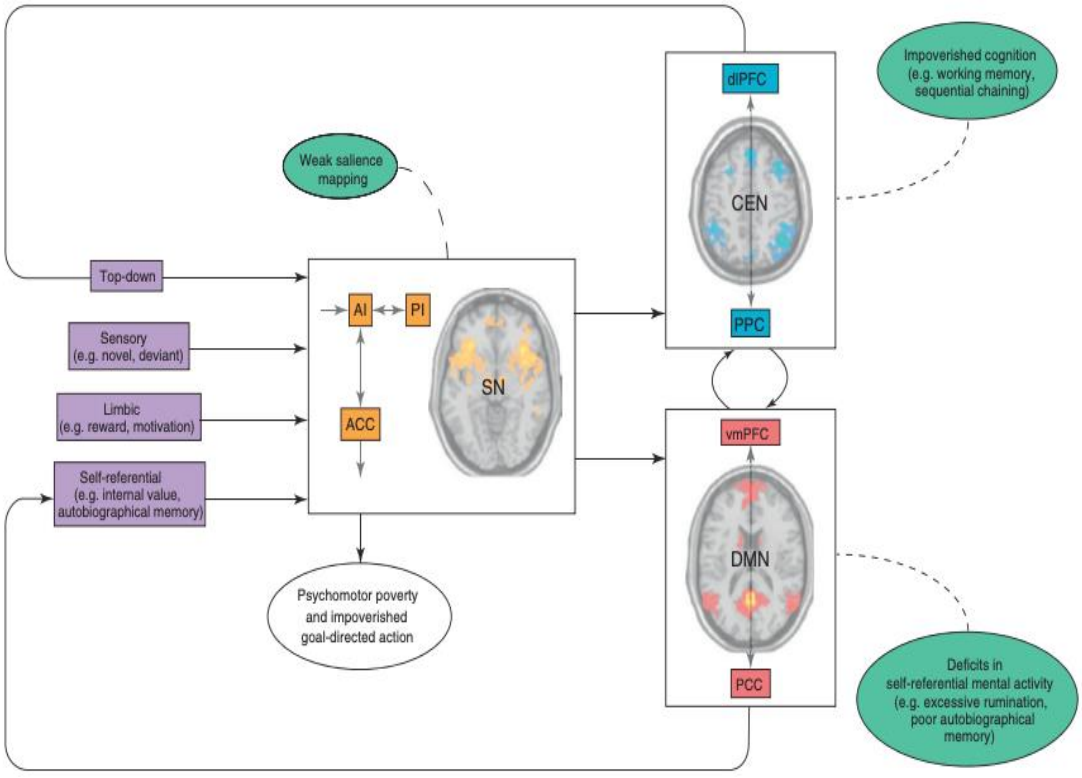

Figure 1.1 Triple network model of psychopathology. The three major resting state networks and the resulting psychopathological symptoms relating to abnormal connectivity. AI: anterior insula, PI posterior insula, ACC: anterior cingulate cortex, PCC: posterior cingulate cortex, vmPFC: ventromedial prefrontal cortex, dlPFC: dorsolateral prefrontal cortex, PPC: posterior parietal cortex. Reprinted from (Menon, 2011) with permission from Elsevier.

1.5 Cognitive processing and attention networks

Cognitive processing is the ability to perceive, process, store information, and execute behaviour (Eysenck and Keane, 2020). These mental processes are categorised into two main categories: bottom-up (lower-order) and top-down processes (higher-order). The bottom-up processes refer to the reflexive behaviours elicited by perceived sensory input that engages the attentional system. A noticeable change in the environment first orients the attention system towards its sensory modality, which increases the alertness state to identify a stimulus (target) allowing faster execution of a reflexive response to that stimulus (Posner, 1980, Petersen and Posner, 2012). Each of the orienting, alerting and target detection processes activates a subset network of cortical regions that are part of the more extensive functional attentional network using different neurotransmitters (Posner and Rothbart, 2007). The top-down processes reflect the active-willed controlled execution of behaviour to achieve pre-planned goals, which is referred to by many as the cognitive control (Miller and Wallis, 2009). The next two sections will introduce the attentional networks and the cognitive control process.

1.5.1 Arousal and attentional networks

The orientation process begins with an initial phase of a covert attention orientation towards the modality and the location of a salient environmental stimulus, which is followed by an overt orientation of attention. Both processes activate distinct cortical regions using the neurotransmitter acetylcholine (Posner and Rothbart, 2007) and exhibit a specific increase in the Gamma and Beta band post-spatial cue presentation (Fan et al., 2007). The covert orientation attention process creates a spatial map to detect relevant stimuli without executing physical movements (Corbetta and Shulman, 2002). It is believed to take place in the frontal and parietal eye fields (FEF and PEF, respectively) (Fan et al., 2005), which jointly form the dorsal attentional network (DAN) (Corbetta and Shulman, 2002). Overt orientation (or reorientation) is a goal-dependent motor movement to bring the stimuli into the focus of the attention (Rizzolatti et al., 1987). It is associated with activity in the temporoparietal junction, supramarginal gyrus, superior temporal

gyrus, superior temporal sulcus, anterior cingulate cortex, and the ventral and medial frontal cortices. These cortical regions jointly form the ventral attentional network (VAN) (Petersen and Posner, 2012, Fan et al., 2005, Corbetta et al., 2008).

Posner and Petersen (1990) described alerting as "the ability to prepare and sustain alertness to process high-priority signals", referring to a preparatory process that follows orienting attention towards sensory input of interest and precedes target detection and response execution. The alerting network uses norepinephrine to connect between its brain regions that include the locus coeruleus (LC), right frontal and parietal cortices (Posner and Rothbart, 2007). Its activation is associated with decreased Theta, Alpha and Beta bands power 200-450 post-cue presentation (Fan et al., 2007). Norepinephrine (NE) evokes specific excitation or inhibition states in the target region via the activation of physiologically and histologically different adrenergic neuroreceptors (for detailed review, see (Berridge, 2008, Berridge and Waterhouse, 2003)). The sole source of noradrenergic in the cerebral cortex is the LC, which has extensive projections to cortical and sub-cortical regions to regulate arousal levels.

Furthermore, the alertness state decreases response time by increasing sensitivity to detectable targets, but with the cost of an increased error rate (Posner and Petersen, 1990). According to Yerkes-Dodson law, an optimum level of arousal is required to achieve peak performance in a relationship illustrated by an inverted U-curve (Figure 1.2) (Yerkes and Dodson, 1908). A similar relationship is observable between the LC-NE activity and cognitive task performance (Aston-Jones and Cohen, 2005, Howells et al., 2012, Aston-Jones et al., 1999). Low arousal causes drowsiness, inattention, and sleepiness, and increased arousal is associated with high distractibility, anxiety and acute stress (Berridge, 2008, Sara and Bouret, 2012). This indicates that arousal levels induced by LC modulate the alerting network activity to effectively deploy attentional resources (Petersen and Posner, 2012, Aston-Jones et al., 1999), which we aim to consider in this thesis.

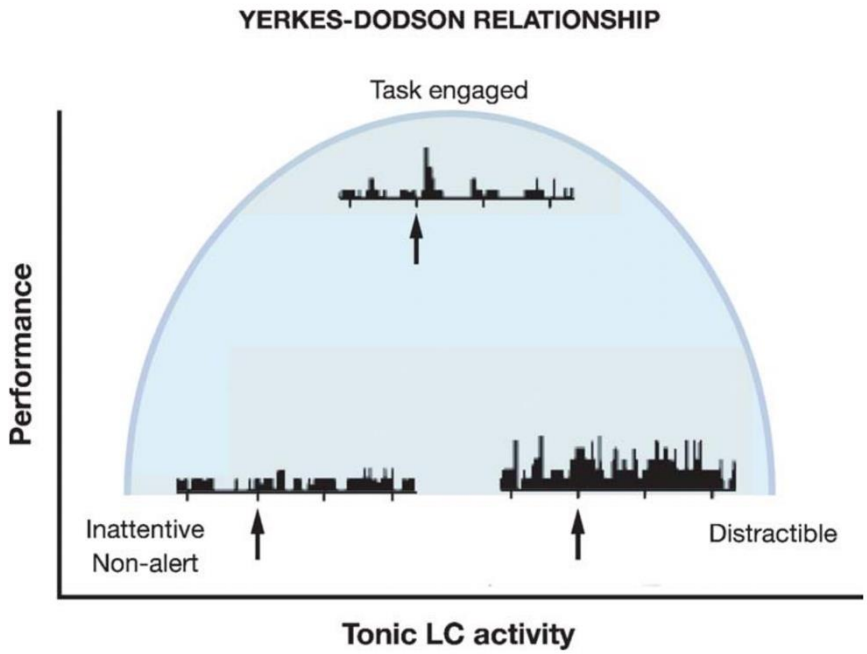

Figure 1.2 The relationship between task performance and the LC activity depicts the inverted U-shape Yerkes-Dodson description of the relationship between arousal and performance. Task performance is minimized at low and high arousal levels (low tonic activity). An optimum level of arousal is required for the initiation of phasic activity essential for the best performance on a task. The arrow indicate imperative stimulus presentation. Reprinted from (Aston-Jones and Cohen, 2005) with permission conveyed through Copyright Clearance Center, Inc.

The adaptive gain theory postulates that the LC has two modes of activity in response to sensory stimuli: tonic and phasic (Aston-Jones and Cohen, 2005). The tonic mode is the baseline activity that promotes environment exploration and the search for salient stimuli and represents baseline arousal levels. An optimum level of tonic mode is a prerequisite for effective transition and activation of the phasic mode (Howells et al., 2012). The phasic mode represents bursts of LC activity promoting the exploitation of a salient stimulus by a behavioural response. Activation of the phasic mode precedes the behavioural response by about 230 ms and adjusts the responsivity (gain) of the task-relevant region (Aston-Jones and Cohen, 2005).

The LC activity is directly regulated by an excitatory and inhibitory control of the prefrontal cortex (PFC) (Sara and Herve-Minvielle, 1995, Jodoj et al., 1998). The anterior cingulate cortex and the orbitofrontal cortices are implicated in this regulation process (Chandler et al., 2014). This top-down frontal control of the LC activity ensures the optimum utilisation of task-relevant regions based on the balanced decision between the reward and cost (Aston-Jones and Cohen, 2005). This

cognitive control role is consistent with the functional role of the executive attention network described by Petersen and Posner (2012). The executive attention network activates the anterior cingulate, ventrolateral/dorsolateral prefrontal cortex, and basal ganglia using dopamine as a neurotransmitter (Posner and Rothbart, 2007, Petersen and Posner, 2012). This network monitors performance and controls switching between tasks (rule selection) (Petersen and Posner, 2012) and its activity is associated with changes in the Alpha, Beta and Gamma bands (Fan et al., 2007).

1.5.2 Cognitive Control

The scientific community has yet to reach a consensus on the explicit definition of executive functions, which are often referred to as cognitive functions, and cognitive control. However, most of the research in the field converges towards a general understanding that executive functions are mental processes which aim to 1) direct behaviour, 2) regulate and monitor tasks, and 3) are applicable to the behavioural, socioemotional and cognitive domains (Baggetta and Alexander, 2016, Miyake and Friedman, 2012). Diamond (2013) has postulated a relatively concise theory that builds executive functioning on three major cognitive processes: 1) inhibitory control, 2) working memory, and 3) cognitive flexibility.

Inhibitory cognitive control is the higher-order executive amendment of lower-order reflexive or unplanned impulsive behaviour (Aron, 2007). It enables us to focus our attention selectively to choose and plan actions wisely (Diamond, 2013). Inhibitory control deficit leads to impulsivity, a core feature of multiple mental disorders (see section 2.1). To decide on an appropriate response, one must hold (for a short term) and manipulate thoughts (goals and plans), which is the definition of working memory, the second core executive function according to Diamond (2013). The third core executive function is cognitive flexibility, which describes the ability to switch between tasks, change perspective (spatially or interpersonally) or adjust planes and priorities (Diamond, 2013). Growing evidence implicates the PFC in all three core cognitive control functions. It is essential for the inhibitory control (Miller and Cohen, 2001, Hwang et al., 2010), working memory (Eldreth et al., 2006) and cognitive flexibility (Rushworth et al., 2002, Sarafyazd and Jazayeri, 2019)

1.5.3 Cognitive Training and neurofeedback

Cognitive training and neurofeedback are non-pharmacological modalities for treating ADHD with uncertain effectiveness in improving core symptoms (Caye et al., 2019, Abikoff, 1991, Arns et al., 2014). However, the evidence supporting its effectiveness in improving specific cognitive processes (Wiest et al., 2022) and modulating cortical activity is growing (de Oliveira Rosa et al., 2020, Van Doren et al., 2019), which calls for further exploration and refinement (Kirk et al., 2016, Kirk et al., 2015).

Cognitive training is a behavioural intervention of repeated exposure to a specific cognitive task (or tasks) intending to produce a task gain transfer to other cognitive abilities. The most targeted cognitive processes include attention, multitasking, working and episodic memory (for a detailed review, see (von Bastian et al., 2022)). Cognitive training is associated with changing the synaptic density (McNab et al., 2009), increasing the structural (Takeuchi et al., 2010) and functional connectivity (Geraldo et al., 2022, Lampit et al., 2015, van Balkom et al., 2020) in the targeted networks. As cognitive training is associated with neuroplastic changes, it is reasonable to consider it a non-invasive form of neuromodulation technique.

Recent systematic reviews of the cognitive training efficacy illustrate a small to moderate effect in improving targeted cognitive abilities in people with dementia (Bahar-Fuchs et al., 2019, Hill et al., 2016), Parkinson's disease (Leung et al., 2015), in adolescents and children with ADHD (Veloso et al., 2020, Cortese et al., 2015) and autism spectrum disorder (Pasqualotto et al., 2021). However, this evidence must be considered with caution as the reviews' authors converged to highlight several limitations in the included studies. These limitations include A) increased risk of bias due to lack of blinding, B) small sample size, C) heterogeneity of cognitive training paradigms and reported outcome measures, D) limited follow-up evaluation and E) limited transfer to general cognitive ability.

Neurofeedback is a technique that trains participants to control their brain neural dynamics. It employs a brain-computer interface that measures the trainees' neural activity and presents performance feedback to them regarding their neural

dynamics regulation (Lubianiker et al., 2022). Several training sessions are required to observe a beneficial effect, each of which lasts between 15-50 minutes depending on the case and the targeted effects (Marzbani et al., 2016). There are three commonly used measures for neurofeedback paradigms and investigated in depth, which are A) Theta to Beta ratio, B) slow cortical potential, C) sensorimotor rhythms (for detailed reviews see (Arns et al., 2014, Enriquez-Geppert et al., 2019, Marzbani et al., 2016, Sitaram et al., 2017).

In a recent systematic review of neurofeedback randomised controlled trials, Moreno-García et al. (2022) found a long-term reduction in the symptoms of ADHD associated with neurofeedback treatment in "over half" of the included 67 trials. Arns et al. (2020) evaluated the evidence of neurofeedback effectiveness and efficacy in ADHD. They concluded that neurofeedback is an "efficacious and specific" treatment option for ADHD with a medium-large effect size lasting 6-12 months. However, this conclusion was based on evaluating two "recent" meta-analyses of randomised control studies, and the other identified studies. Their reported selection methods emphasised that the review should have been published in the preceding two years from their search date. The first included meta-analysis found a medium to a large effect size of neurofeedback on improving ADHD symptoms on a 6-12 months follow-up (Van Doren et al., 2019). Despite being out of their suggested search date range, the second review and meta-analysis did not find a significant effect of neurofeedback on ameliorating ADHD symptoms (in the short-term) when evaluated by a "probably blinded" assessor (Cortese et al., 2016). Furthermore, two more recent meta-analyses found that neurofeedback did not show beneficial effects in ADHD on executive functions (Louthrenoo et al., 2021) or reported symptoms (Rahmani et al., 2022). These discrepancies behind neurofeedback effectiveness demand larger randomised control studies and further research to investigate it.

Combined cognitive and neurofeedback training is a novel technique with promising potential. Hosseini et al. (2016) compared the executive function changes associated with working memory training in active and sham neurofeedback conditions (ten healthy participants in each arm). They found a significant performance improvement in the active neurofeedback group compared to the sham

condition in working memory and task switching. Moreover, they found a decreased right middle and inferior frontal regions activity in the active treatment relative to the sham condition, which was correlated with post-training working memory accuracy (Hosseini et al., 2016). Furthermore, in a quasi-experimental study, Rezaei Sharif et al. (2022) compared the effect of working memory training in neurofeedback, cognitive training, combined training and control groups in a hundred children with SpLD. Their results showed a significantly superior improvement in the combined treatments group compared to other groups and a significantly enhanced working memory performance in the cognitive training group relative to the neurofeedback one. The combined approach significantly reduced ADHD symptoms, as reported by most likely blinded assessors (Johnstone et al., 2017). In the later chapters of this thesis, we will assess the neuromodulation changes associated with a similar approach, which combines cognitive training with visual feedback.

1.6 The anti-saccade task

The antisaccade task is one method of investigating inhibitory cognitive control. Hallett (1978) introduced the antisaccade task while examining the motives and mechanisms of saccadic eye movements by separating the goal of the saccade from the location of presented stimuli. This disengagement examines the participants' top-down cognitive control abilities of a) inhibiting the physiological reflex from foveating towards the stimulus and b) initiating a saccadic eye movement in the opposite direction, which employs several cognitive processes, including working memory, executive function, and attention control (Munoz and Everling, 2004, Coe and Munoz, 2017). The task typically begins with a fixation point in the centre of a display (fixation point). Then, a peripheral stimulus is presented. The participants must foveate towards it for prosaccade trials. In antisaccade trials, they must refrain from looking towards the stimulus and gaze in the opposite direction. The trial is counted as a directional error if the participants fail to suppress the automatic reflex and perform a saccade towards the stimulus.

There are two main performance metrics extracted from the antisaccade task; a) the percentage of saccade directional errors (SDE) trials to correct saccadic response trials provides a measure of performance effectiveness. b) The latency between stimulus presentation and motor saccade performance (i.e. saccade reaction time (SRT)) is a measure of the processing efficiency (Eysenck et al., 2007). Klein and Foerster (2001) illustrated that prefrontal cortex maturation with age significantly improves the performance metrics of the antisaccade task in healthy subjects. Furthermore, this development of cognitive control is positively correlated with the PFC functional and effective connectivity to cortical and subcortical regions involved in the oculomotor control (Hwang et al., 2010). Whilst healthy individuals exhibit around 20% of antisaccade trials as SDE, several studies have reported that a significantly more directional error and longer RT are associated with different neurological and psychiatric disorders (Hutton and Ettinger, 2006, Schaeffer et al., 2013, Evdokimidis et al., 2002, Ainsworth and Garner, 2013).

Several task paradigms enhance the examination of specific aspects of reflexive or top-down behaviour. For example, the peripheral stimulus presentation could overlap with the fixation point presentation or follows its disappearance by a 150-200 ms temporal gap, which shortens the SRT by 20–30 ms. The prosaccade trials typically exhibit an SRT within 200-250 ms of stimulus presentation. The antisaccade trials show a 100-150 ms longer SRT than the prosaccade trials. This latency reflects the cognitive control process and the executive functioning required for the antisaccade performance (Ptak and Müri, 2013, Ramat et al., 2006, Saslow, 1967, Basanovic et al., 2022).

However, there are earlier saccadic responses reported for both trial types around 100 ms (Paré and Munoz, 1996, Fischer and Weber, 1993). These saccadic responses are regarded as express saccades. It is hypothesised to represent an optomotor reflex that does not involve the higher cortical regions of the visual attention system (Fischer and Weber, 1993).

1.7 Oculomotor Control Network

Several cortical and subcortical regions are involved in controlling saccadic eye movements. These regions are either involved in the sensory processing of the visual signal or the motor planning and execution of the saccadic eye movement. The main regions implicated in this system are the primary visual cortex (V1), the thalamus, the lateral geniculate nucleus, the superior colliculus (SC), the frontal and parietal eye fields (FEF and PEF, respectively), the anterior cingulate cortex (ACC), the insular cortex and the DLPFC (Pierrot-Deseilligny et al., 1991a, Pierrot-Deseilligny et al., 1991b, Munoz and Everling, 2004). The cortical and subcortical regions implicated in the OCN and the performance of the antisaccade task are illustrated in Figure 1.3. The cortical OCN regions investigated in this thesis are illustrated in Figure 5.3.

The flow of the visual signal begins from the retina. Then it travels via the retino-geniculo-cortical pathway to the visual cortex or the SC via the retinotectal pathway (Munoz and Everling, 2004). The visual cortex sends afferent neurons to the PEF. The PEF is involved in the spatial coding of salient stimuli and directly connects to the frontal lobe regions (DLPFC, supplementary eye field and FEF) and the superior colliculus (SC). When the PEF or its connection with the SC is damaged, all contralateral saccades become inaccurate with a decrease in gain (the amplitude of saccade ratio to target eccentricity). However, when subjects with damaged PEF-SC connection are informed of the stimulus location and the expected saccade direction, they regain their performance metrics. This evidence indicates that PEF sends spatial information towards the frontal lobes for further processing rather than to the SC directly (Gaymard et al., 1998). The SRT for bilateral saccade directions in memory-guided saccades was significantly affected in patients with a right PEF lesion. However, in left PEF, only ipsilateral saccade exhibited prolonged SRT (Pierrot-Deseilligny et al., 1991a). Bidirectional SDE was higher in patients with right PEF but not left PEF damage. This gathering evidence suggests the dominant role of the right PEF in the bottom-up processing of prosaccades and the visual-spatial remapping (Pisella et al., 2011). The visual-spatial remapping is a process that predicts the changes in the visual field depending on a planned saccadic movement and warrants further discussion detailed in section 4.1.2 (Wurtz, 2008).

The FEF region is close to the precentral and the superior frontal sulcal junction. Intracranial stimulation of the FEF elicits a saccadic eye movement (Grosbras et al., 2005, Lobel et al., 2001). It is involved in planning and executing internally generated saccadic eye movements, which are not triggered by external stimuli (Pierrot-Deseilligny et al., 1991a). The PEF and the DLPFC send direct projects towards the FEF, which acts as a coordination and execution centre. It receives the spatial information from the PEF and the execution commands from the DLPFC and projects these signals to the SC for the execution of saccade (Munoz and Everling, 2004, Gaymard et al., 1999, Rivaud et al., 1994). A human lesion study demonstrated the implication of the left FEF in a) guiding contralateral saccade based on the retinotopic coordinates. b) disengaging the eye from central fixation during task performance, and c) predicting saccadic response (Rivaud et al., 1994). Moreover, another lesion study confirmed the crucial role of the FEF in performing memory-guided saccades and suggests that reflexive saccadic responses do not involve FEF recruitment (Gaymard et al., 1999).

The dorsolateral prefrontal cortex (DLPFC) receives direct input from several sensory and motor regions (Miller and Cohen, 2001, Haber et al., 2022). It is implicated in cognitive inhibitory control (Hwang et al., 2010, Walker et al., 1998), role-selection (Jensen and Bonnefond, 2013) and task preparation (MacDonald et al., 2000). Patients with left DLPFC damage exhibit higher rates of SDE in both directions. In contrast, right-sided DLPFC injury led to higher SDE only for the contralateral saccades. Damage to either DLFC (dorsolateral frontal cortex) increased the SRT for both directions (Pierrot-Deseilligny et al., 1991a). Another human lesion study from three patients with DLPFC lesions reported a significant bilateral increase in SDE in the antisaccade task, variable amplitude errors in memory-guided saccade, and a decrease in performance on a predictive saccade task. Their conclusion suggests that the DLPFC is involved in reflexive saccade inhibition and short-term spatial memory (Pierrot-Deseilligny et al., 2003). These findings implicate the crucial role of the DLPFC, with left hemisphere dominance, in a) inhibitory cognitive control and b) planning the direction and execution of the saccade in response to external stimuli.

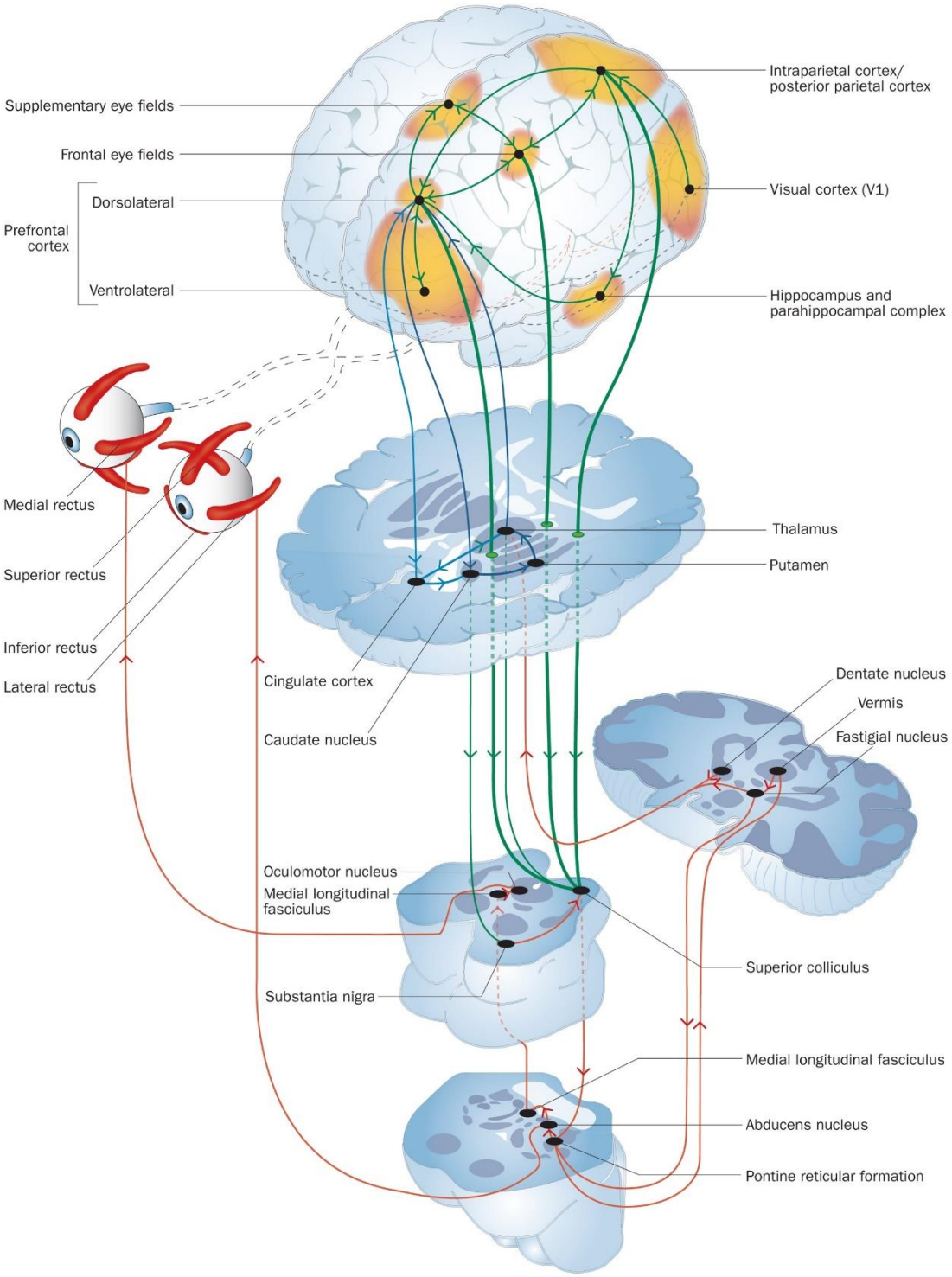

Figure 1.3 The cortical and subcortical regions implicated in the performance of the antisaccade task. The green lines are connection between the cortical OCN regions. The red lines represent connection to the brainstem oculomotor control regions. The dark blue line indicate loops of working memory. The light blue line reflects connections of executive cognitive functioning. The visual input signals flow from the retina to the occipital primary visual regions, which sends it to the PEF for spatial mapping. The PEF sends efferent to the PFC and the FEF for executive planning. The SC receives spatial input from the PEF and executive input from the PFC and FEF guiding the saccadic response. The frontal regions communicate with the caudate nucleus in the basal ganglia that sends inhibitory projection to the SC inhibiting saccadic movements (Munoz and Everling, 2004). The illustration is reprinted from (Fielding et al., 2015) and Reproduced with permission from Springer Nature.

1.8 Thesis scope and rationale

The work in this thesis investigates the effect of brain stimulation on the function of the oculomotor control network. We employed two methods of brain stimulation: computer-based cognitive training and non-invasive transcranial direct current stimulation (tDCS). We aim to examine the following hypotheses:

- A single session of tDCS delivered during the antisaccade task performance will lead to plastic changes in the resting-state network connectivity, assessed using MEG. The changes in resting state connectivity relate to the modulation patterns of brain activity observed during the antisaccade task (Chapter 2).
- Engagement in the antisaccade task during both active tDCS and sham tDCS will be associated with the engagement of the autonomic nervous system reflected in pupil dilation (Chapter 3).
- Concurrent tDCS with the antisaccade task will modulate the OCN neural activity during task performance, providing a more precise timing of activity (Chapter 4).
- Computer-based cognitive training will be associated with changes in resting state connectivity, assessed using fMRI, before and after two weeks of training. The change in connectivity correlates with the amount of training performed (Chapter 5).
- Changes in arousal, assessed by the rate of pupil dilation during the preparation of responses in the antisaccade task, correlate with the functional connectivity between the locus coeruleus and nodes of the oculomotor control network (Chapter 5).

Chapter 2 MEG resting-state networks and neuromodulation

In this chapter, we will examine the effect of tDCS delivered during the performance of the antisaccade task on resting state functional connectivity to test the hypothesis that a single session of tDCS will produce plastic changes in connectivity that persist at least for a short period after cessation of treatment. Considering the potential therapeutic value of tDCS for impulse control disorders, we recruited individuals identified on the basis of activities that tend to involve impulsive behaviour.

2.1 Introduction

A recent meta-analysis explored the potential of transcranial Direct Current Stimulation (tDCS) as a treatment for disorders of impulsivity (Teti Mayer et al., 2020). The analysis was conducted on randomised control studies examining the effect of tDCS application in an adult population (either healthy or diagnosed with a mental disorder) on impulsivity-related tasks. Over 80% of the 92 included studies in the analysis demonstrated an improvement in the examined impulsivity facet in the active tDCS group. However, the heterogeneity of tDCS parameters and the cognitive tasks hinder the formulation of a solid conclusion and demand further research to explore the different stimulation protocols to use tDCS as a therapeutic tool.

The use of tDCS during an active sequence-learning task was associated with learning speed depending on the stimulation polarity. Anodal stimulation led to faster learning, and cathodal stimulation was associated with slower learning (Stagg et al., 2011). The effect of anodal tDCS in the facilitation of learning was reported for the motor skills (Reis et al., 2009) and working memory (Pupíková et al., 2021, Zaehle et al., 2011), among many other cognitive functions (for review, see (Coffman et al., 2014, Kuo and Nitsche, 2012)). Furthermore, the tDCS has the potential to modulate cortical excitability in different frequency oscillations and alter intrinsic functional connectivity (FC), including default mode network (DMN) and central executive network (CEN) (Nitsche et al., 2008, Filmer et al., 2014, Sehm et al., 2012, Notturno et al., 2014, Keeser et al., 2011, Zaehle et al., 2011). It has been proposed to act on

the prolonged strengthening of synaptic transmission, which produces an aftereffect lasting beyond the cessation of tDCS (for detailed review (Stagg and Nitsche, 2011, Reis et al., 2009).

Impulsivity is an essential feature of multiple psychiatric and personality disorders (e.g. substance abuse, gambling, binge eating, antisocial personality, ADHD, and conduct disorder), which has been associated with harmful consequences for individuals and others (e.g., self-harm, violence). (Hollander and Rosen, 2000, Moeller et al., 2001). It describes a failure of inhibitory control processes, resulting in unplanned actions with little consideration of the consequences. Impulsivity has two fundamental categories. The first is rapid response impulsivity, characterised by an inability to resist initiating pre-potent action or stop an ongoing one. The second category is delayed-reward impulsivity, where a large, delayed reward is rejected in favour of an immediately smaller one (Bari and Robbins, 2013, Swann et al., 2002).

2.1.1 Magnetoencephalography

As we aim to evaluate the subtle short-term effects of tDCS application during cognitive task performance. Thus, it is most suitable to use MEG to capture the minute neurophysiological activity changes, as discussed in section 1.4.1. However, although MEG provides an instantaneous measure of cortical activity and inter-regional brain interactions with high spatial resolution, accurate cortical source localisation presents major challenges. There are challenges in estimating expected signals at the sensors distributed over the scalp from a hypothetical distribution of sources (the forward problem) and in the estimation of sources within the brain that might account for the pattern of signals observed in the scalp sensors (the inverse problem) (Baillet et al., 2001). The forward problem deals with modelling the EEG/MEG signal from the neuronal source to its measurement at the sensor level. The solution for the forward problem involves employing; a) a source model for the electrical current generated in the synchronising pyramidal cells. This model could be either a current dipole or multipole. b) A head model that encompasses the source model to resemble human heads' inhomogeneous shape and conductivity. Currently, used head models range from simple spherical head models (single or multiple shells)

to more complex models such as the boundary element method (BEM) and finite element method (FEM), among many others. The BEM and the FEM model employ three distinct boundaries extracted from structural MRI or CT images. These boundaries delineate the scalp, inner and outer skull boundaries, which are then used to calculate the measured signals at the sensor level (for a review, see (Hallez et al., 2007, Hämäläinen et al., 1993, Baillet et al., 2001)).

In contrast, the inverse problem identifies the signal's source from an indefinite number of possible solutions, which can be limited using certain constraining assumptions. The least-squares source estimation assumes a priori-fixed number of sources within the brain. It minimises the least squared error between the computed forward model and the recorded data from these sources. Another approach to solving the inverse problem is beamforming, which is not limited by a prior assumed number of sources.

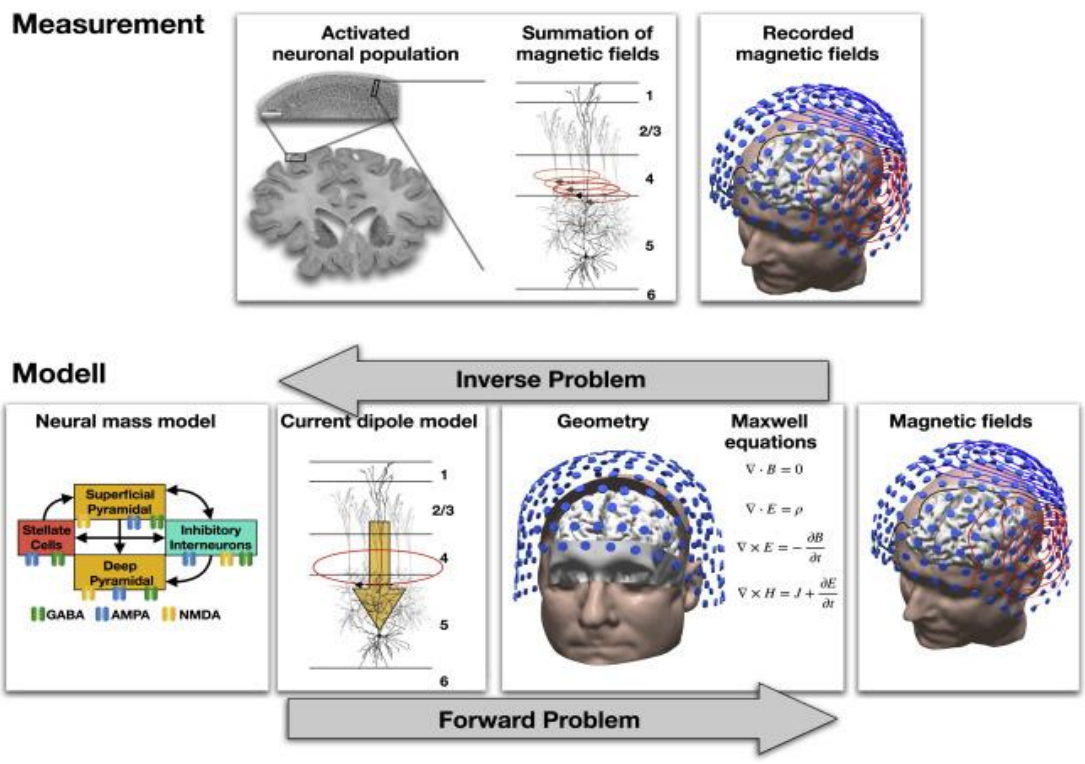

Figure 2.1 The forward and inverse problem inherent in processing MEG signal. The forward problem is involved in creating a plausible model for measured magnetic signals at the sensors level, which requires definition of head shape (or geometry) and position in the scanner. The inverse problem is concerned with finding the source and orientation of the measured signal. This figure is reprinted from (Gross, 2019) with permission from Elsevier to illustrate the mentioned concepts. It embraces the neural mass forward-model (David and Friston, 2003) that is different from the ones we used in the analysis and described in the method sections.

Beamforming describes a process of spatial data filtering developed for use in radars, which utilises a sensor array to strengthen a signal of interest originating from a specific location and attenuating signals from other regions (Veen and Buckley, 1988). The beamformer weighs the contribution of each sensor's signal differently before summing the overall array's output for each voxel in the brain. The given weights act as adjustable signal apertures, which compute the electrical signal at each grid node (voxel, dipole) location that encompasses the brain (or the cortical surface) at specific time points. The weights are sensitive estimates based on the electromagnetic data covariance and provide high spatial resolution for incoherent and weakly coherent sources (Barnes and Hillebrand, 2003). Linear-constraint minimum-variance (LCMV) beamforming is one of the widely used computational methods to influence the beamformer's response to detecting signals coming from a specific direction with a predefined temporal frequency. LCMV is most useful when only the direction of an incoming signal is known (Huang et al., 2004, Van Veen et al., 1997).

The richness of MEG data provides an abundance of extractable functional parameters that provide a plethora of potential physiological markers. There are several methods to measure functional connectivity in MEG/EEG data, which include and not limited to amplitude envelope correlation (AEC), spectral coherence, and phase estimation. Colclough et al. (2016) examined twelve connectivity metrics to conclude that AEC is the most consistent approach for analysing resting-state functional connectivity.

The estimated sources' time course for a spatial location is highly contaminated by the field spread or the linear spatial leakage for the adjacent regions (Schoffelen and Gross, 2009). This leakage results from the methods used for solving the forward and inverse problems. This spatial leakage between the distinct neighbouring regions introduces an artificial functional correlation. However, the spatial leakage is an instantaneous artefact with a zero-time lag between the different sources. Thus, zero-lag temporal correction provides a possible solution for the field spread (Colclough et al., 2015).

2.1.2 Alpha and Beta oscillations

Converging evidence suggests that alpha oscillations play a role in suppressing contextual inappropriate brain activity by inhibiting the flow of information to task-irrelevant regions in a process currently known as gating by inhibition or cortical idling (Jensen and Mazaheri, 2010, Haegens et al., 2011, Palva and Palva, 2007). Furthermore, converging EEG evidence from visuospatial studies demonstrated increased Alpha band power in the parietal and occipital regions contralateral to the unattended hemifield relative to the attended one (Worden et al., 2000, Sauseng et al., 2005). This lateralisation of Alpha power was correlated with successfully inhibiting the visual attention (Händel et al., 2011) and is diminished in children and adults with ADHD (Vollebregt et al., 2016, Guo et al., 2019, Deiber et al., 2020), which suggests a deficit in Alpha modulation mechanism in ADHD patients (Lenartowicz et al., 2018). Moreover, a TMS stimulation in the alpha band range of the parietal and occipital regions impaired visual perception of the presented stimuli (Romei et al., 2010). This indicates an increase in alpha band oscillation is to be expected in cortical regions not directly engaged in task performance at hand and act as a mechanism to ignore certain stimuli or modality (Foxe and Snyder, 2011).

On the other hand, beta band oscillation is proposed to have a central role in the long-range top-down recruitment (activation) of distant cortical regions (Fries, 2015, Spitzer and Haegens, 2017, Sherman et al., 2016), the maintenance of the cognitive and motor state at rest (Engel and Fries, 2010, Barone and Rossiter, 2021). Hwang et al. (2014) suggested that top-down inhibitory control is mediated via cross-frequency connectivity between Alpha and Beta bands; whereby frontal Beta band activity precedes Alpha band surge of activity in the effector cortical regions. Hence, we aim to examine the functional connectivity in the Alpha, Beta and cross-frequency Alpha-Beta connectivity.

The functional networks (for details, see sections 1.4.2 and 1.5) exhibit distinct neuroplastic changes in relation to cognitive task performance. Using fMRI Wang et al. (2012) demonstrated an increase in the DMN functional connectivity with the frontal and temporal regions and a decreased connectivity to the occipital lobe

during task performance compared to the pre-task resting state. Moreover, they reported a decreased connectivity DMN to the middle temporal pole and the superior orbitofrontal regions. The observed neuroplastic modulation in the resting state networks seems to reflect the effect of task engagement as semantic-matching task (Wang et al., 2012) exhibit different neuroplastic changes from a memory encoding task (Tambini et al., 2010) or a visual shape-discrimination task (Lewis et al., 2009).

2.1.3 Aims and questions

We aim to compare the effect of tDCS as an external non-invasive neuromodulation technique to the Sham condition on modulating the impact of the inhibitory control task on the resting-state functional connectivity for the Alpha, Beta band and cross-frequency connectivity.

We predict that the functional connectivity measured by the AEC in the post-task resting state will show a different modulation pattern in the tDCS condition from the sham group. These modulation patterns will reflect the short-term plastic changes associated with the asymmetric tDCS over the right frontal regions during the performance of an antisaccade task. We expect this modulation to be more in the Alpha band due to its inhibitory role in the antisaccade task.

As discussed in section 1.7, diverse brain regions are engaged in the control of saccades (see Figure 1.3). Therefore, we will examine functional connectivity between all pairs of regions within 78 brain regions spanning the cerebral cortex. To quantify the change in connectivity from before to after the treatment, we will compute the change in the degree centrality of each of the 78 brain regions, where we defined centrality as the mean functional connectivity between a brain region of interest and all other brain regions.

In this chapter, we seek to answer the following questions:

- Does active tDCS alter participants' self-reported POMS?
- Does the performance of the antisaccade task modulate the resting state functional connectivity reflecting the inhibitory control mechanisms?
- Does the active asymmetric tDCS modulate the changes produced by the antisaccade task in the resting state functional connectivity?

2.2 Methods

The data collected in this study is part of the tDCS and Inhibitory Control study, funded by the Medical Research Council (MRC) as a Confidence in Concept (CiC) grant via the University of Nottingham. The study was ethically approved by the Faculty of Medicine and Health Sciences (FHMS) Research Ethics Committee, University of Nottingham, before the commencement.

2.2.1 Participants and recruitment

As the aim of the study is to examine rapid response impulsivity, we recruited participants for the study by advertising online in the University of Nottingham societies and sports clubs associated with a high degree of risk and thrill-seeking behaviour (e.g., mountain climbing, wrestling, and mixed martial arts)(Self et al., 2006). We contacted the societies and clubs via their web pages and Facebook groups. In addition, we distributed study posters at the Jubilee and Park University of Nottingham campuses.

We aimed to recruit 60 healthy volunteers from the student and staff population of the University of Nottingham. Interested volunteers were provided (emailed) with an information package, including the required study details. G*Power3 software by Faul et al. (2007) was used to estimate sample size based on an independent sample t-test to detect medium size effect (n=60, 30 in each group, the effect size of d = 0.65, 80% power, & alpha error probability $\alpha = 0.05$, one-tailed testing). Volunteers who showed interest in participating were phone interviewed initially to confirm their eligibility and ability to participate in the study.

We used the following inclusion and exclusion criteria to limit the number of confounding variables in our results:

- *Inclusion criteria*

  Participants were included if they were:

- Aged 18-40.
- Able to give consent.
- Capable of identifying medium-sized shapes and colours (a few centimetres in size), which are displayed 80 centimetres away without the need to wear correction glasses (participants were asked to wear contact lenses on the day of scans if needed).

- *Exclusion criteria*

  Participants were excluded if they had:

- A medical history of epilepsy or neurological disorder.
- A history of significant head injury.
- A diagnosis of a major mental disorder or currently receiving psychotropic medication.
- Reported current substance misuse
- Failed to pass MRI safety questionnaire.
- Participated in other studies in the last three months.

2.2.2 Study design

This study was a single-blind, randomised control study. Participants had to visit the Sir Peter Mansfield Imaging centre for about four hours. On arrival, a team member provided a detailed information package about the study and explained the study procedure and protocol. Then, participants had to complete a tDCS and MRI safety questionnaires. Once eligibility was confirmed, participants provided their written consent and were randomised and matched by age and gender to either active tDCS or sham group using a computer randomisation code.

Pre-scan questionnaires and training

Post-randomization, subjects were asked to complete a computer-based self-report measure. These included measures of schizotypy personality questionnaire (SPQ (Raine and Benishay, 1995)), impulsivity (UPPS-P (Lynam et al., 2006)) and the profile of mood states (POMS (McNair et al., 1992)). Participants only completed the POMS questionnaire a second time after completing the study scans. Following the questionnaires, the subjects received a brief anti-saccade task training. The task was displayed on a laptop screen, and a keyboard was used to input the participants' responses rather than eye movements. The training continued until the participant could score six correct saccades and nine correct anti-saccades trials.

MEG scan preparation

The participants were then prepared for the tDCS/MEG session. They were provided disposable scrubs and were asked to remove any jewellery, metals, or make-up. Three electromagnetic head position indicators (HPI) were attached to the subject's nasion, right and left preauricular points as fiducial markers. These coils were marked on a 3D head surface model and used throughout the tDCS/MEG session to continuously evaluate head movement and position relative to the MEG sensors. The 3D head model was created using a 3D digitiser (Polhemus Inc.), and to ensure the best coordinate measurements, we asked the participant to wear an EEG cap to trace and digitise the head surface. We extended the digitisation process to include the forehead, eyebrows, and nose to enhance the anatomical co-registration process with the structural MRI.

tDCS preparation and setup

We applied the 10-20 electrode positioning system to define the location of F4 (right frontal electrode 4) and Fp1 (left prefrontal) electrodes. We prepared two MRI-compatible rubber electrodes using Ten20 conductive paste (by WEAVER and company) and placed the anode at F4 and the cathode on the position of the Fp1 electrode. We employed a neuroConn DC stimulator device (Rogue Resolutions Ltd.) to deliver 1.25 mA stimulation ramping up/down for 10 seconds. For the active tDCS group, the stimulation persisted for the whole duration of the anti-saccade task, 1200

seconds. The sham group received 10 seconds of ramping up, 15 seconds of 1.25 mA stimulation and 10 seconds of ramping down.

The participant preparation method was the result of experimenting with several combinations of skin preparation, electrode types, and electro-conducting options. The following choices produced our best results: A) using cotton pads soaked with Micellar cleansing solution to scrub the skin at the electrode placement sites to cleanse remaining make-up, dirt, or excessive sebum, providing good cleansing with minimal to no skin irritation compared to other methods. B) We used 5*5 cm MRI rubber electrodes as they are reusable, provide excellent conductivity and are MRI-compatible. C) Preparing the electrodes with a thick layer of a conductive paste (≈ 2-3mm thickness), which permeated hair layers to reach the participant's scalp. The conductive paste preparation solved two issues; first, increasing the electrode stability throughout the session, even on scalps with thick hair without adding straps or caps, and it granted optimum current delivery by decreasing the impedance level.

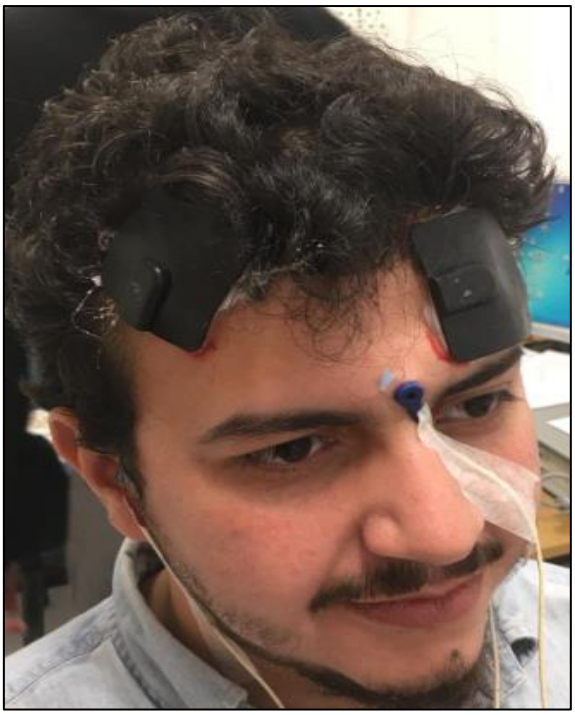

Figure 2.2 A prepared subject with fiducial coils and MR-compatible tDCS electrodes. The three fiducial coils are continuously energized during the MEG data acquisition to monitor head position relative to MEG sensors. The tDCS anode electrode is placed on the F4 and the cathode is placed at the Fp1 electrode position using the 10/20 electrode positioning system.

2.2.3 Imaging data acquisition

MEG data

MEG data were collected using 275 CTF Omega MEG system (Canadian Thin Films, MISL, Coquitlam, BC, Canada) in a three-layer magnetically shielded room. We used a sampling rate of 600 Hz and applied a 150 Hz anti-aliasing filter. The prepared participant sat in an upright MEG seat, electromechanically adjusted to accommodate the participant's head inside the MEG helmet. To optimise sensor-source distance and reduce the signal-to-noise ratio, the participants reported that once they felt the MEG helmet touching the top of their heads. Then to provide comfort, centralise, and increase head stability, researchers supported the participant's head inside the helmet using sponge pads where needed. Once the participant was comfortable, team members connected the HPI and tDCS cables and tested and explained communication methods to the participants. Then, we positioned the eye-tracker and the projection display and calibrated the eye-tracker. The team monitored the participants' video, and a two-way intercom was used for audio communication.

We divided the MEG scan into three separate sessions. Eight minutes session of resting-state, followed by active/sham tDCS stimulation concurrent with participant's performance of the antisaccade task for 20 minutes, and finally another eight minutes session of resting-state. During the MEG sessions, the participants were instructed to stay as still as possible. For resting state sessions, participants were asked to fix their vision at a displayed red cross.

MRI data

We used Philips Achieva (TX)-DS MR system (Philips Medical Systems, Best, The Netherlands) to acquire structural T1 weighted MRI images for each subject. We used MPRAGE sequence protocol (3000ms short interval, TR/TE/FA=2.2 ms/ 4.5 ms/ 8°, FOV= 256 x 256 mm, 1mm slice thickness, SENSE factor=1). All MRI scans were done after the MEG sessions to prevent possible magnetisation effects on the MEG data quality.

2.2.4 Analysis methods

2.2.4.1 MEG data pre-processing

We segmented and filtered datasets using customised algorithms encoded in Unix, Bash, and MATLAB scripts. Third-order synthetic gradiometers were employed during MEG data acquisition to filter neural magnetic activity from other magnetic fields in the scanner environment. The resting-state datasets were segmented into 245 epochs (2 seconds/epoch). Antisaccade/tDCS datasets were segmented into saccade and anti-saccade trials (3 seconds/trial) using the recorded trial event markers within each dataset. We removed data segments demonstrating more than a 5 mm deviation from the dataset's mean head motion.

We used DataEditor software (VSM, MedTech Systems Inc., Coquitlam, BC, Canada. Release 5.2.1-Linux-20060623) to inspect and filter the datasets. We applied a bandpass filter (high-pass filter =1 Hz, low-pass filter=150 Hz) to filter the data from extremely low/high-frequency signals. Then, trained team members visually inspected the datasets to remove data segments, which contained visible artefacts such as blinks, muscle contractions, squid resets or other features that did not resemble typical MEG data signals.

2.2.4.2 MRI/MEG co-registration

The 3D digital head model created using the Polhemus 3D digitiser (described in section 2.2.3) was aligned with the high-resolution T1-weighted MRI image to enable accurate anatomical location of the sources of the MEG signal.

The series of DICOM files, containing one slice of MRI data per file, was restructured to produce a single 3D volume (256x256x256 mm) using MRI Viewer software (VSM MedTech systems Inc., Coquitlam, BC, Canada. Release: 5.2.1-Linux-20060809). The neck and oral cavity were excised from the MRI image, while the head shape and facial details from the tip of the nose upwards were retained to produce a head-shape model. Using customised MATLAB software, this MRI head shape model was co-registered with the Polhemus 3D head model. The accuracy of co-registration

was confirmed by visual inspection of the imported locations of the three head position indicators on the MRI image.

2.2.5 Resting State Connectivity data analysis

The analysis process used is illustrated in Figure 2.3 and detailed as follows.

A multi-layer network approach described by Brookes et al. (2016) was applied to assess functional connectivity within alpha and beta frequency bands and between bands connectivity. Given the limited MEG spatial resolution, we excluded the subcortical regions and only used the 78 parcellated cortical regions from the automated anatomical labelling atlas (AAL) (Tzourio-Mazoyer et al., 2002) (Table 2.5). A 4 mm regular voxel grid covering each region was used to derive the centre of mass measure for the parcellated region. A band-pass filter (1-150 Hz) was used. Then, an LCMV scalar beamformer spatial filter (Robinson, 1999) was used to compute the estimated electrophysiological time course activity for each voxel in a time window spanning the whole resting-state session to minimise the error of the covariance matrix (Brookes et al., 2008). The forward model was based on a multiple local sphere head model (Huang et al., 1999) and a dipole approximation (Sarvas, 1987). Tikhonov method was used for regularisation with regularisation parameter = 5% of the maximum eigenvalue of the unregularised covariance matrix.

We used a symmetric multivariate leakage correction (Colclough et al., 2015), which utilises the zero-time lag correlation exhibited by signal leakage from separate regions' beamformer projected time courses (Brookes et al., 2012, Hipp et al., 2012). Linear regression was used to eliminate these zero-time lag linear correlations before estimating the connectivity.

For each cortical AAL region, the time course of the MEG signal across each resting state was derived by computing a weighted average of the time course in each voxel in the defined region, weighted according to the inverse distance of the voxel from the region's centroid. Band-pass filtering was applied to extract signal time course in two frequency bands, alpha (8 Hz – 13 Hz) and beta (13 Hz – 30 Hz), using a finite impulse response filter with a least-squares linear-phase design.

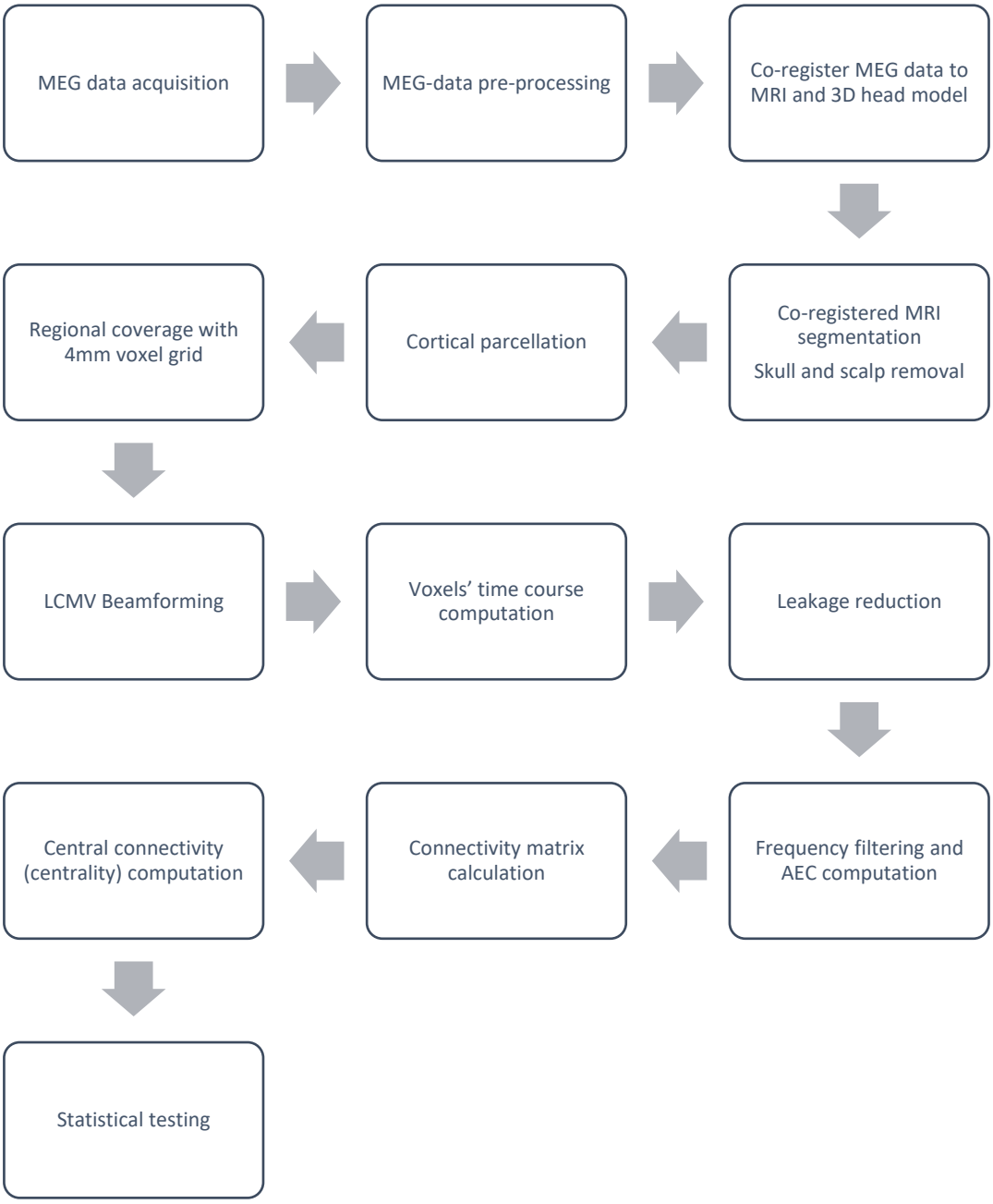

Figure 2.3 The illustrated MEG resting-state analysis pipeline from acquisition to statistical analysis.

After leakage correction, we computed Hilbert amplitude envelopes for the orthogonalised seed and test region's time course using the absolute value of the Hilbert transformation analytical signal for the predefined 2-second epochs. We then computed the amplitude envelope correlations (AEC) using the Pearson correlation coefficient between the amplitude envelopes of the seed and test regions within each time epoch. We applied this process for each frequency band and cross-frequency connectivity within each resting state. Each resting state functional connectivity was then derived from the mean correlation coefficients across subjects for each

condition. This process produced six functional connectivity adjacency matrices per Treatment condition, three matrices for each resting state representing Alpha, Beta, and cross-frequency (Alpha to Beta). The adjacency matrices exhibit a diagonal symmetry, whereby the correlation between seed and test regions is identical for inversed relationships (source regions becoming test regions). Then to contrast the change in functional connectivity for the post-task resting state from the pre-task, we subtracted the pre-task from the post-task resting states' correlation coefficients. The illustrated matrices (Figure 2.5, Figure 2.6 and Figure 2.7) represent the 78 by 234 (78 regions x 3 frequency bands) connectivity matrix. It is arranged from left to right to represent Alpha, Beta, and Alpha-to-Beta connectivity. The cortical regions are arranged according to Table 2.5 from top to bottom and from left to right (repeated for each frequency), and due to limited space not all are labelled.

Then, we computed the average degree centrality for each region (node) by computing the mean correlation coefficient for each region per resting state. It estimates the node strength and connectivity to the rest of the cortical regions (Zuo et al., 2012, Wang et al., 2010), demonstrating task-specific changes relative to the resting state (Buckner et al., 2009). This measure was computed for each region by averaging the Fisher Z-transformation of the 77 pairwise AECs between that region and the other 77 regions for each rest period. A Four-way mixed design ANOVA was employed to compare the variation of centrality across time and brain region in the two treatment conditions. Centrality was the dependent variable. Time (two-level: before and after tDCS/task performance) and AAL region (78-level) were the within-subject factors, and treatment condition (2 levels, active tDCS and sham) was the between-subject factor. Separate ANOVAs were performed for each frequency band and the cross-frequencies centrality.

2.3 Results

2.3.1 Sample demographics

A total of 43 healthy subjects (22 males, 21 females) were initially recruited and randomised before the withdrawal of one female participant who could not complete the MEG scanning session. This sums to 42 participants included in the study who completed the required tasks and scanning sessions. There were no significant differences between the active tDCS group and the sham group on age or gender. The demographic details are summarised in Table 2.1.

Table 2.1 tDCS study sample demographic

	Overall (*n*=42)	**tDCS (*n*=21)**	**Sham (*n*=21)**	***p***
Age	21 (3.45)	21.33 (4.08)	20.67 (3.65)	0.874
Gender	22 M, 20 F	11 M, 10 F	11 M, 10 F	1

2.3.2 Impulsivity, mood and schizotypy results

The self-reported measures of impulsivity (UPPS-P), schizotypal personality questionnaire (SPQ) and mood (POMS) were examined using independent samples t-test for between Treatment conditions group differences. There were no significant differences between the Treatment groups on any of the examined measures or subscales (Table 2.2). However, the descriptive results of the self-reported measure indicate that sensation-seeking behaviour is elevated in our sample.

The POMS was the only measure acquired before and after the completion of the data acquisition. We examined the effect of study performance on the POMS subscale for each treatment condition. For each POMS subscale, we conducted a mixed-design ANOVA with treatment condition as the between-subjects factor and the time (two-level; before and after the study) as the within-subject factor. The results are summarised in Table 2.3.

There was no significant effect of the Treatment condition on any subscales. However, across the sample, there was a significant change in esteem, vigour, fatigue, tension, and depression after the completion of the study relative to before the commencement (Table 2.3). To examine these changes, we conducted a paired sample t-test on the whole sample for each subscale. Across the sample, there was a significant increase in fatigue and a significant decrease in esteem, vigour, tension, and depression (Table 2.3).

*Table 2.2 The psychometric descriptive results for the tDCS study. The p-value indicates the significance level on the independent samples t-test for the difference between treatment groups. * a constant of 100 was added to each subject's TMD result to eliminate negative results. Greater scores on the UPPS and the SPQ are indicative of a greater tendency for impulsivity or the presence of personal schizotypy traits*

	Overall Mean (SD)	**tDCS Mean (SD)**	**Sham Mean (SD)**	***p***
Impulsivity (UPPS-P)				
Negative urgency	26.12 (6.79)	26.19 (6.87)	26.05 (6.87)	.947
Sensation seeking	35.55 (8.96)	33.48 (9.45)	37.62 (8.15)	.136
Lack of perseverance	20.36 (5.54)	19.95 (5.25)	20.76 (5.92)	.642
Lack of premeditation	21.76 (5.61)	22.62 (5.55)	20.9 (5.67)	.328
Positive urgency	25.4 (8.15)	26.52 (8.82)	24.29 (7.46)	.380
Profile of mood states (POMS)				
Total mood disturbance (TMD) T1*	95.71 (11.71)	96.62 (12.88)	94.81 (10.66)	.623
Total mood disturbance (TMD) T2*	96.98(12.58)	99 (13.86)	94.95 (11.12)	.303
Schizotypal Personality Questionnaire (SPQ)				
Ideas of reference	24.29 (7.58)	24.24 (7.6)	24.33 (7.75)	.968
Excessive social anxiety	15.98 (8.32)	17.62 (8.46)	14.33 (8.04)	.204
Odd beliefs and magical thinking	24.38 (3.91)	23.29 (4.72)	25.48 (2.54)	.069
Unusual perceptual experiences	27.02 (5.25)	27.05 (5.56)	27 (5.05)	.977
Odd eccentric	16.62 (7.62)	17.9 (8.54)	15.33 (6.51)	.279
No close friends	25.05 (6.15)	25.86 (5.71)	24.24 (6.59)	.400
Odd speech	19.31 (8.18)	21.48 (8.52)	17.14 (7.39)	.086
Constricted affect	20.81 (6.93)	21.81 (6.94)	19.81 (6.94)	.356
Suspiciousness	21.62 (6.58)	20.62 (7.14)	22.62 (5.96)	.331

Table 2.3 Statistical results summary for time effect on POMS for the mixed-design ANOVA (between groups difference) and the paired-sample t-tests (whole sample, two-sided p-value) for each POMS subscale. The negative mean value indicates a decrease in the subscales' mean score.

POMS	*Time*		*Paired t-test*		
Subscale	*F*(1, 40)	*p*	*M*	*t(41)*	*p*
Esteem	11.746	.001	-1.071	3.464	.001
Vigour	8.423	.006	-1.381	-2.902	.006
Fatigue	8.572	.006	1.595	2.914	.006
Confusion	.013	.908	-0.048	.117	.907
Tension	12.381	.001	-1.762	-3.561	.001
Anger	.442	.51	-0.143	-.666	.509
Depression	4.882	.033	-0.833	-2.224	.032

2.3.3 MEG data quality

The application of tDCS is a possible source of noise and artefact generation in the MEG system (Marshall et al., 2016). These artefacts might be during the delivery of tDCS or affect the MEG sensors' sensitivity. Hence, we compared the number of available trials after head motion correction and the visual inspection for artefacts in both treatment conditions for the different scanning sessions.

Resting-state data quality

Across all subjects, the total number of trials excluded due to head motion correction (HMC) in the first resting state was 0.38% of the collected data (39 epochs, 22 Sham and 17 tDCS). Then visual inspection for artefacts excluded 8.9% of the head motion corrected data (902 epochs, 568 Sham, 373 tDCS). In the second resting state, 2.5% of collected data was excluded in head motion corrections (252 epochs, 18 Sham, 234 tDCS), and further 900 epochs (454 Sham, 698 tDCS) were excluded due to visually inspected artefacts. After the cleaning process completion, 9349 epochs (90.86%) of the first resting state and 9138 epochs (88.8%) of the second resting state were available for analysis (Figure 2.4). Despite the higher number of excluded trials in the active tDCS condition in the second resting state due to visual artefacts (M= 211.76, SD = 30.08) compared to the Sham condition (*M* = 233.38, *SD* = 16.03), there was no significant effect of visually excluded trials, $t(30.55) = -1.57$, $p = .128$.

Task data

We excluded three subjects from the tDCS group during task MEG data filtering. Two subjects had less than 50% trials available for analysis after correction for head motion. The third subject had excessive head motion and multiple artefacts on visual inspection, which led to the exclusion of more than 50% of their task data after visual inspection. These exclusions caused a significant between-groups effect ($F(1,37)=4.36$, $p = 0.044$), which was corrected by excluding three matchings (for age and gender) subjects from the sham group ($F(1,34)=3.4$, $p = 0.74$).

To examine the effect of tDCS on MEG data, we conducted independent samples t-test comparing the numbers of available trials (epochs) remaining after head movement correction and visual artefact inspection before, during and after the task between the two groups. The tDCS group demonstrated significantly lower average trials per subject compared to sham in antisaccade trials (M= -7.33, t(34)=-2.73, p = 0.01), and between trials rest (M=-18.2, t(34)=-3.51, p = 0.001). There was no significant difference between treatment groups in prosaccade trials or resting state periods (Table 2.4, Figure 2.4).

Table 2.4 Statistics results summary for the between groups mean difference of the available trials post visual inspection of the MEG data.

	t	df	p	Mean Difference
Antisaccade trials	-2.734	34	0.01	-7.333 (2.683)
Prosaccade trials	-1.57	34	0.126	-4.111 (2.618)
Trials rest	-3.514	34	0.001	-18.222 (5.185)
Resting-state 1	1.563	34	0.127	9.278 (5.937)
Resting-state 2	-1.641	23.636	0.114	-12.222 (7.447)

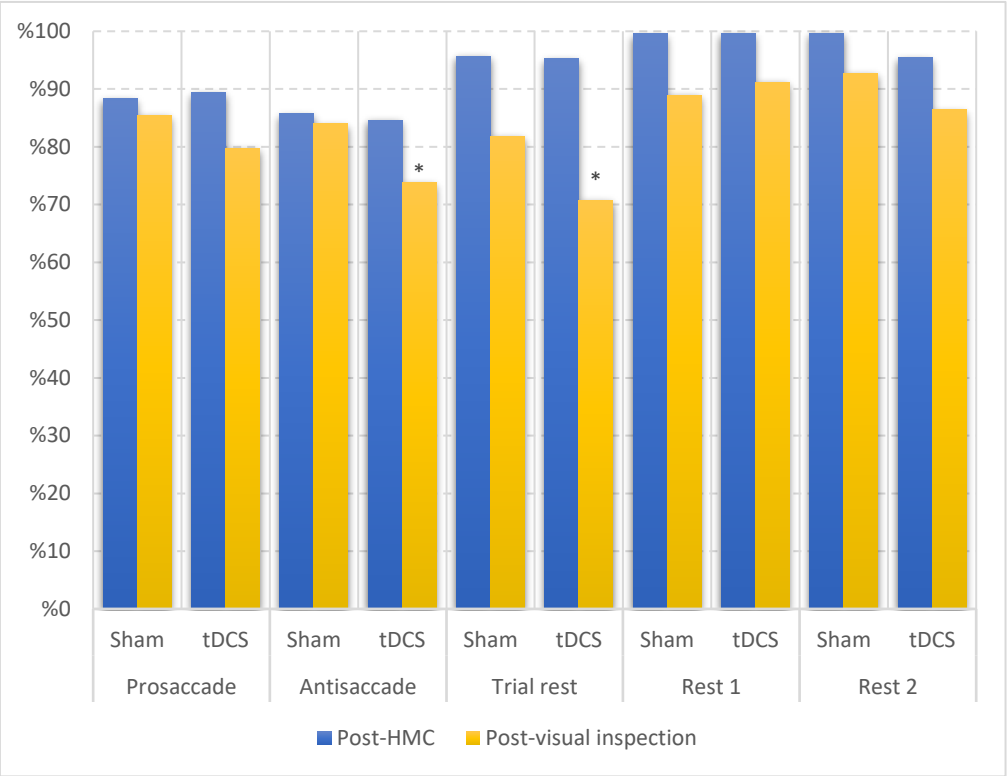

Figure 2.4 Trials available post data filtering of head motion correction (HMC), and visual inspection for visible artefacts (% of tatal number of trials). The asterisk (*) represents a significant between group difference (p <.05).

2.3.4 Resting-state functional connectivity changes

Our method of computing the functional connectivity captures the average connectivity fluctuation of the active functional networks during the resting state condition. Participants were asked to fixate their vision on a fixation cross displayed on the screen during the resting state. The average connectivity fluctuations for Rest1 and Rest2 are illustrated in, Figure 2.5 for the Sham condition and Figure 2.6 for the active tDCS condition.

Overall, both Treatment conditions showed a more robust Alpha band connectivity within both resting states than the Beta band and the cross-frequency connectivity. The averaged functional connectivity in Rest1 was prominent in the medial frontal (supplementary motor area (SMA), paracentral lobule), lateral parietal (superior parietal gyrus), medial parietal (angular gyrus and precuneus), lateral occipital (superior, middle, inferior occipital gyri), medial occipital (Calcarine fissure,

cuneus), and cingulate regions of the limbic lobe (median and posterior cingulate). The temporal lobe had less connectivity fluctuation than other cortical regions during Rest1 for both conditions. Both conditions in Rest2 exhibited an increase in functional connectivity of the lateral parietal (superior and inferior parietal gyri), lateral occipital, lateral temporal, median and posterior cingulate regions. The tDCS group showed more connectivity in frontal regions relative to the sham group.

Subtracting the functional connectivity in Rest1 from Rest2 (Rest3) contrasted the task performance effect on modulating the resting state network connectivity in both Treatment conditions (Figure 2.7). The change in resting state connectivity illustrated an interestingly divergent effect of Treatment conditions. In Rest3, the Sham condition functional connectivity increase in the parietal regions to the occipital, limbic and temporal regions, predominantly in the right hemisphere. In contrast, the active tDCS condition illustrated a dominance of the left hemisphere and increased functional connectivity between the frontal, temporal, limbic and parietal regions. This finding supports our prediction of different ¢connectivity modulation patterns per Treatment condition.

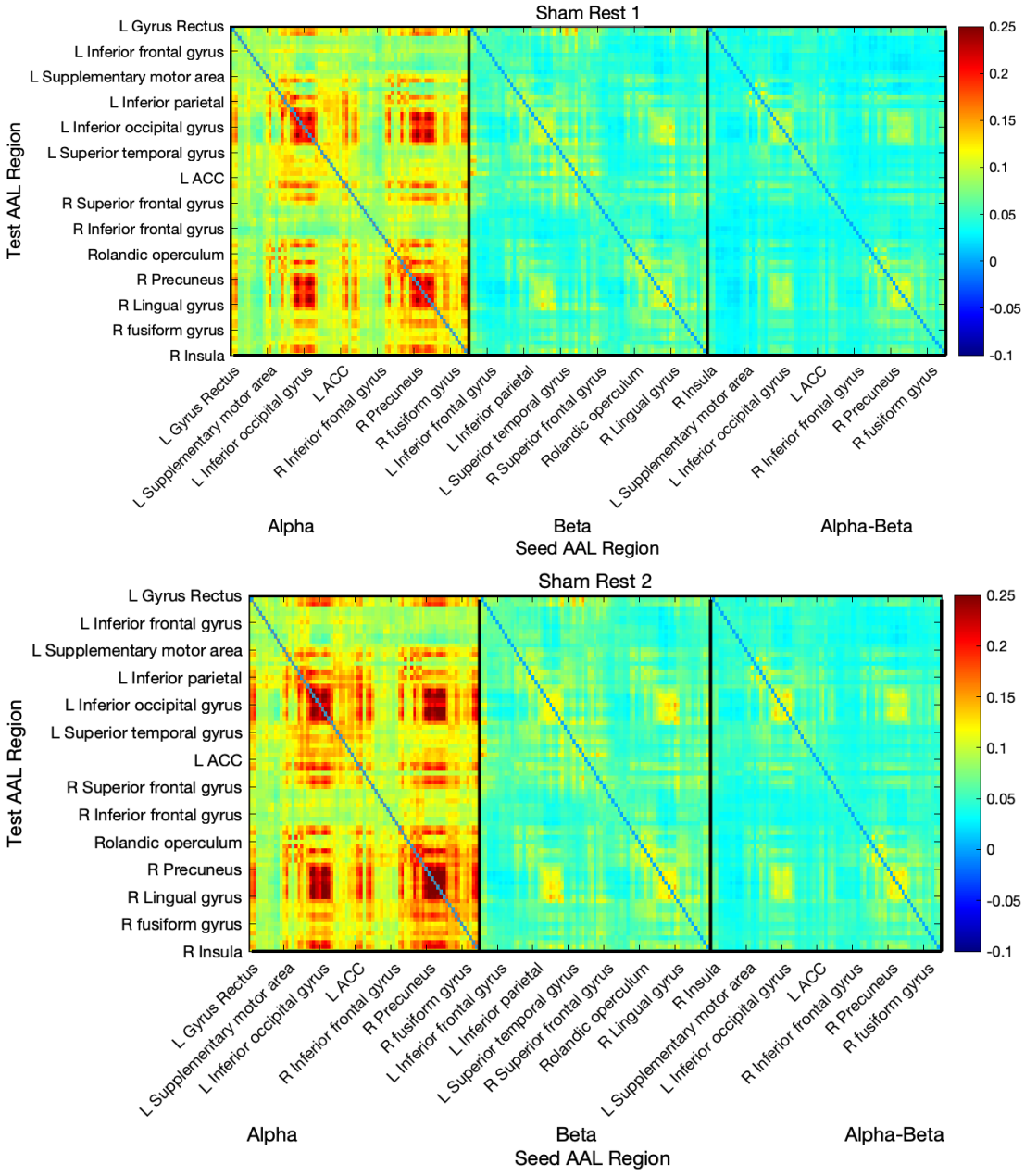

Figure 2.5 The functional connectivity matrices for the sham condition illustrating in A) pre-task resting state (Rest 1) and in B) post-task resting state (Rest 2). In both resting state there was greater connectivity in the occipital regions reflecting the active engagement of the visual network. In addition, there was increased functional connectivity in the orbital and medial frontal, superior parietal, angular, precuneus, lateral occipital, median and posterior cingulate regions. In Rest 2 compared to Rest 1 there was increase connectivity in the temporal and occipital functional connectivity. The adjacency matrices are arranged from left to right to represent Alpha, Beta, and Alpha-to-Beta connectivity between the 78 cortical regions (arranged according to Table 2.5 from top to bottom and from left to right). Due to limited space, not all regions are labelled.

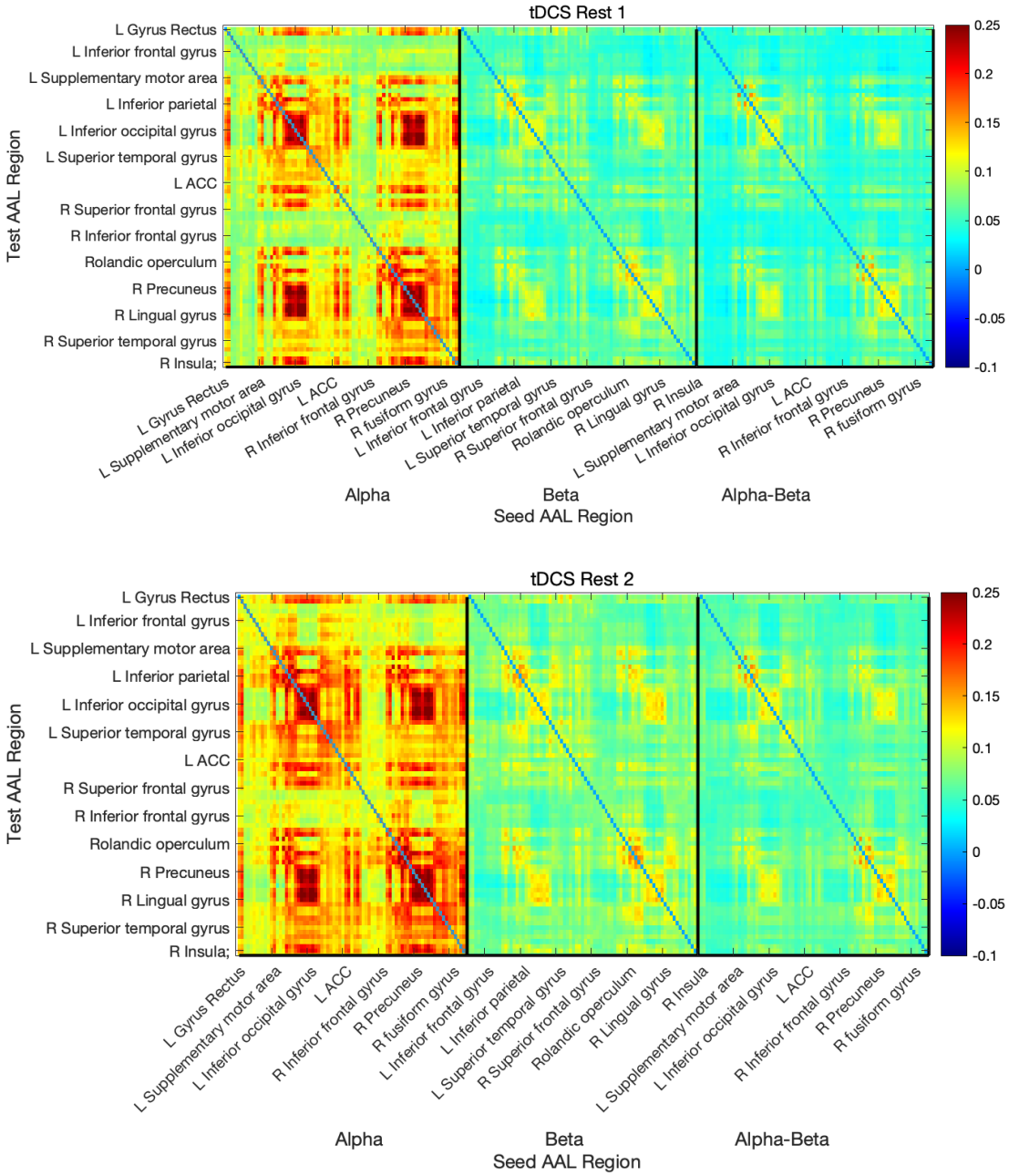

Figure 2.6 The functional connectivity matrices for the active tDCS condition illustrating in A) pre-task resting state (Rest 1) and in B) post-task resting state (Rest 2). In both resting state there was greater connectivity in the occipital regions reflecting the active engagement of the visual network. In addition, there was increased functional connectivity in the orbital and medial frontal, superior parietal, angular, precuneus, lateral occipital, median and posterior cingulate regions. In Rest 2 compared to Rest 1 there was increase connectivity in the frontal and parietal regions' functional connectivity. The adjacency matrices are arranged from left to right to represent Alpha, Beta, and Alpha-to-Beta connectivity between the 78 cortical regions (arranged according to Table 2.5 from top to bottom and from left to right). Due to limited space, not all regions are labelled.

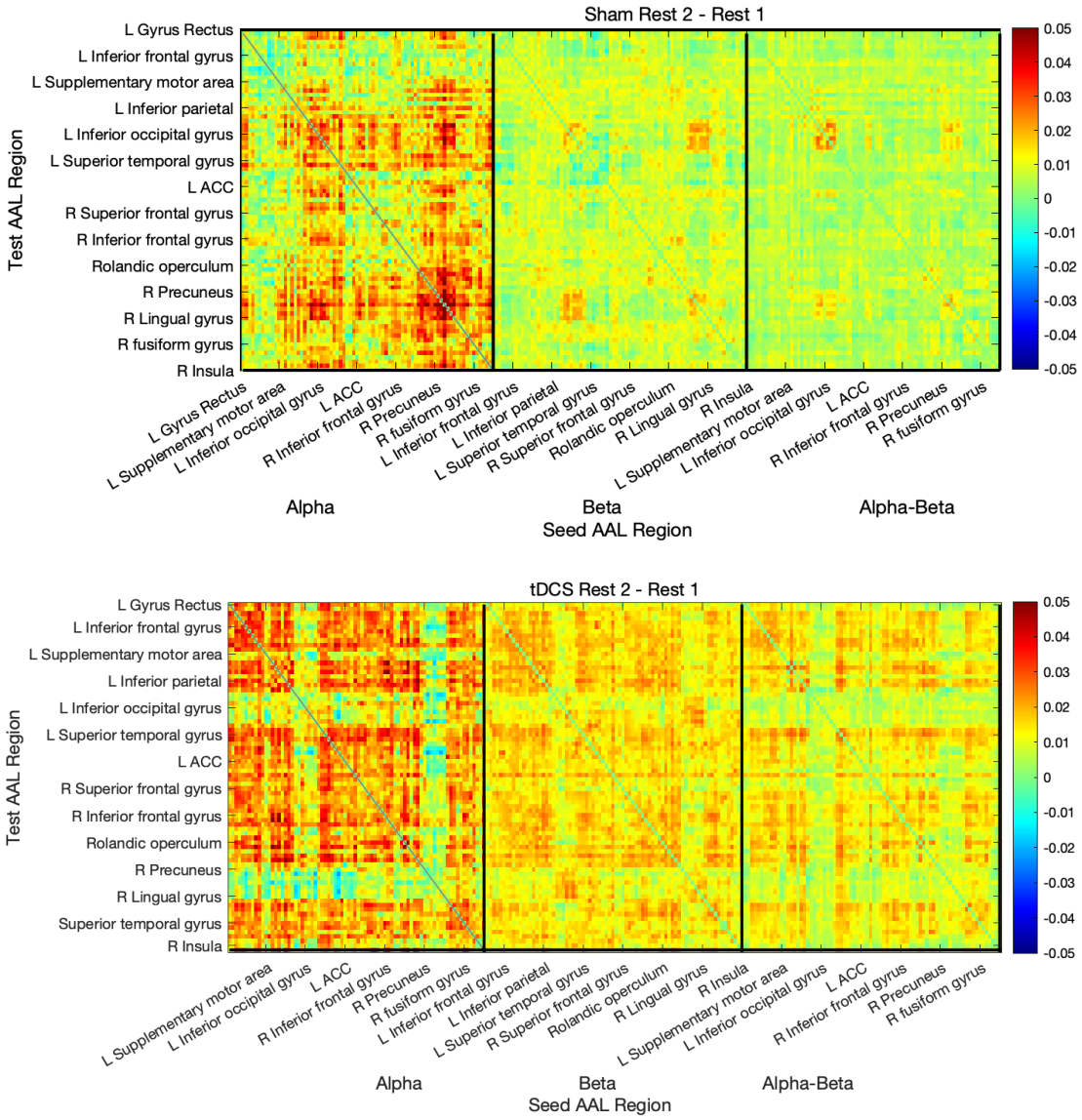

Figure 2.7 The change in functional connectivity matrices for both Treatment conditions illustrate a contrasting difference between Treatment conditions. While the sham condition exhibited an increased change of connectivity in the occipital regions bilaterally, the active tDCS condition illustrated an increased change of connectivity in between frontal, temporal and parietal region. The adjacency matrices are arranged from left to right to represent Alpha, Beta, and Alpha-to-Beta connectivity between the 78 cortical regions (arranged according to Table 2.5 from top to bottom and from left to right). Due to limited space, not all regions are labelled.

Table 2.5 A list of the 78 AAL regions used in the analysis arranged by lobe and cortical surface. The numbering indicates their arrangement in the adjacency matrix.

Lobe	Surface	Region	Left	Right
Frontal lobe	**Orbital**	Gyrus rectus	1	40
		Olfactory cortex	2	41
		Superior frontal gyrus, orbital part	3	42
		Superior frontal gyrus, medial orbital	4	43
		Middle frontal gyrus, orbital part	5	44
		Inferior frontal gyrus, orbital part	6	45
	Lateral	Superior frontal gyrus, dorsolateral	7	46
		Middle frontal gyrus	8	47
		Inferior frontal gyrus, opercular part	9	48
		Inferior frontal gyrus, triangular part	10	49
	Medial	Superior frontal gyrus, medial part	11	50
		Supplementary motor area	12	51
		Paracentral lobule	13	52
	Central	Precentral gyrus	14	53
		Rolandic operculum	15	54
		Postcentral gyrus	16	55
Parietal lobe	**Lateral**	Superior parietal gyrus	17	56
		Inferior parietal	18	57
		Supramarginal gyrus	19	58
		Angular gyrus	20	59
	Medial	Precuneus	21	60
Occipital lobe	**Lateral**	Superior occipital gyrus	22	61
		Middle occipital gyrus	23	62
		Inferior occipital gyrus	24	63
	Medial and inferior	Calcarine fissure and surrounding cortex	25	64
		Cuneus	26	65
		Lingual gyrus	27	66
		Fusiform gyrus	28	67
		Heschl gyrus	29	68
Temporal lobe	**Lateral**	Superior temporal gyrus	30	69
		Middle temporal gyrus	31	70
		Inferior temporal gyrus	32	71
Limbic lobe	**Temporal pole**	Superior temporal gyrus	33	72
		Middle temporal gyrus	34	73
	Parahippocampal	Parahippocampal gyrus	35	74
	Cingulate	Anterior cingulate and paracingulate gyri	36	75
		Median cingulate and paracingulate gyri	37	76
		Posterior cingulate gyrus	38	77
Insula			39	78

2.3.5 Regional centrality

2.3.5.1 Alpha band centrality

To compare the resting-state centrality in Rest1 and Rest2 for each frequency band and the cross-frequency connectivity. We used the computed centrality measure as the dependent factor to conduct a four-way mixed design ANOVA with Treatment condition as the between-subjects factors and three within-subjects factors; Hemisphere (two-level; left, right), Regions(39-level; 39 AAL regions) and Time (two-level; Rest1, Rest2).

Resting-state centrality demonstrated a significant main effect of Time, $F(1,40)= 62.928$, $p <.001$, in the Alpha band. However, there was a significant effect of Time by Hemisphere interaction, $F(1,40)= 10.337$, $p = .003$, Time by Regions interaction, $F(4.4, 174.8) = 20.213$, $p < .001$, and Time by Regions by Hemisphere interaction, $F (11.1, 445.6) =3.272$, $p < .001$ (Figure 2.8). These findings indicate that the pre-task resting-state Alpha-band centrality was significantly modulated after engaging in the antisaccade task. This modulation was different for different AAL regions bilaterally and in each hemisphere.

We then investigated the effect of the antisaccade task performance on the resting-state regional centrality for each Treatment condition independently. To achieve this, we examined the change in Rest2 by subtracting the Rest1 centrality measure. This contrast removes the shared baseline centrality and enhances the modulation effect of the engagement in the task.

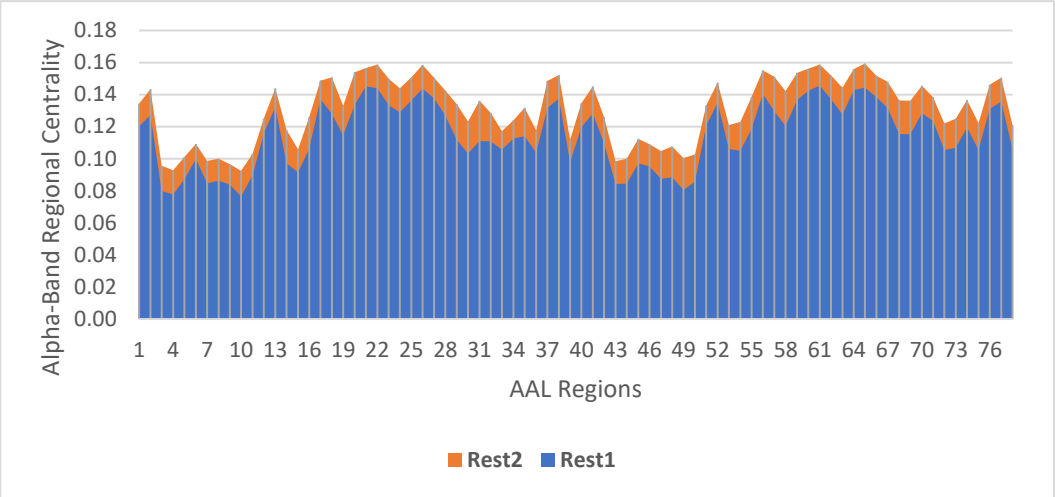

Figure 2.8 Alpha band regional centrality illustrates the significant effect of Time by Regions by Hemisphere interaction (p <.001). The centrality in Rest2 for all AAL regions has increased significantly from Rest1 averaged across conditions. The 78 AAL regions are arranged from the left hemisphere to the right (as labelled in Table 2.5).

Effects of Treatment Condition

The change of Alpha centrality exhibited a significant effect of Regions by Treatment Conditions, F (6.1, 244.4) = 3.461, p = .003. While the Sham condition illustrated increased Alpha centrality in the occipital regions, the active tDCS condition exhibited increased centrality in the frontal, temporal, parietal and limbic lobe regions (Figure 2.9 and Figure 2.12). The active tDCS condition had more pronounced modulation relative to the Sham condition in all cortical regions except for the bilateral supplementary motor area, supramarginal gyrus, angular gyrus, praecuneus, lateral and medial occipital regions and the right median cingulate and posterior cingulate regions. This regional distribution exhibiting greater centrality for the Sham condition embraces the visual cortex and the posterior DMN regions (including the angular gyrus and precuneus). This finding indicates that, in accordance with our prediction, the active tDCS condition exhibited an increase in the CEN and the salience network compared to the sham condition.

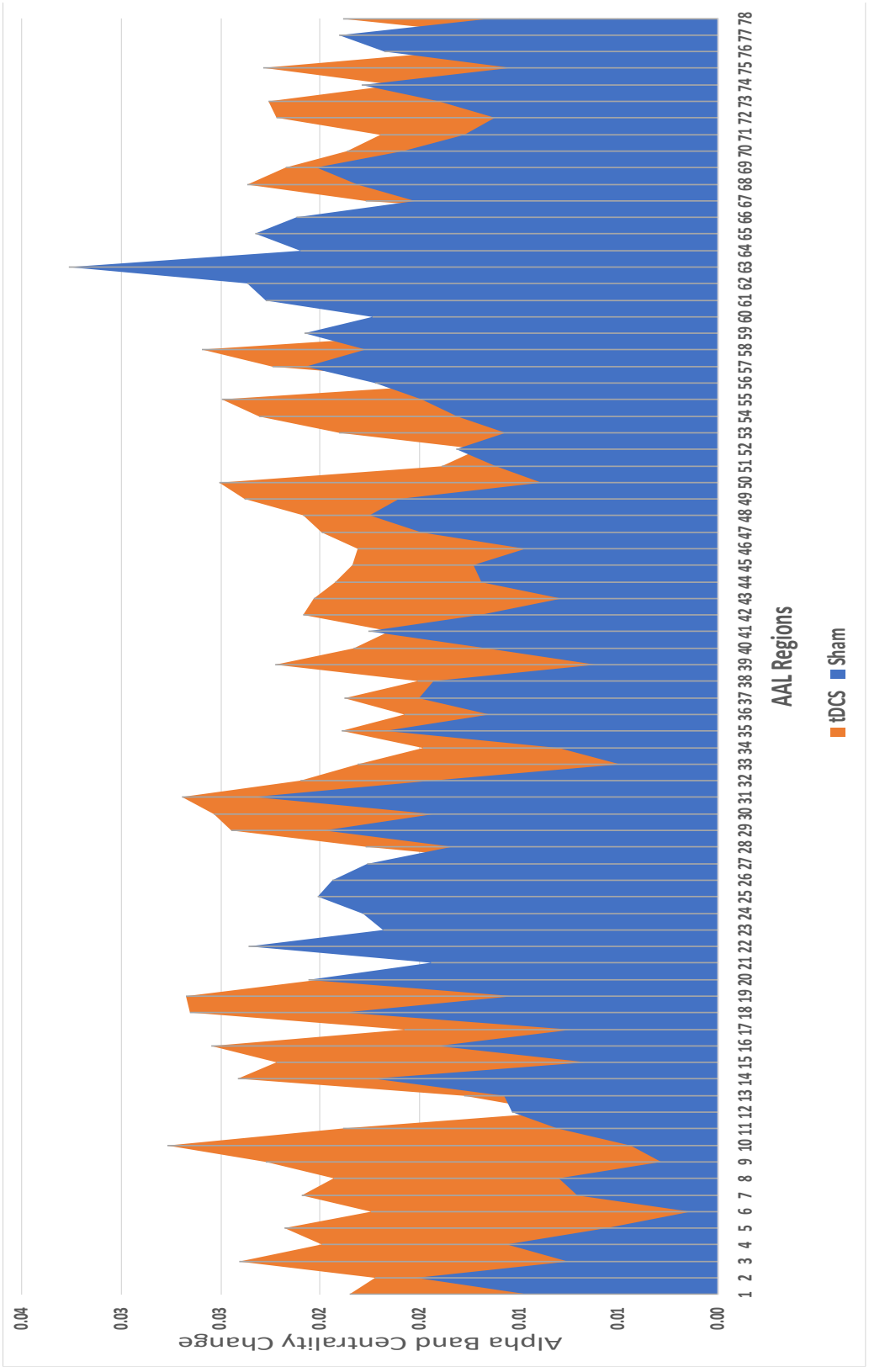

Figure 2.9 The modulatory effect of Regions by Treatment condition interaction for modulating the change in Alpha band centrality. While the Sham condition illustrate increased centrality (averaged across Hemispheres) in the occipital and inferior parietal regions, the active tDCS condition exhibited increased centrality in the frontal, temporal, superior parietal and limbic lobe regions for the active tDCS condition. The 78 AAL regions are arranged from the left hemisphere to the right (as labelled in Table 2.5).

2.3.5.2 Beta band centrality

The Beta band resting-state centrality demonstrated a significant main effect of Time, $F(1,40)= 160.506$, $p < .001$. However, there was a significant effect of Time by Hemisphere interaction, $F(1,40)= 4.666$, $p = .037$, Time by Regions interaction, $F(4.1, 163.5) = 18.333$, $p < .001$, and Time by Regions by Hemisphere interaction, $F(12.1, 482.68) = 1.921$, p .03 (Figure 2.10). This finding indicates that the Beta band centrality during the resting states changed significantly after engaging in the antisaccade task. This change was different for different regions in each hemisphere.

Despite the illustrated differences in Figure 2.13, the change in the Beta band centrality did not show any significant main effect or interactions involving the treatment condition.

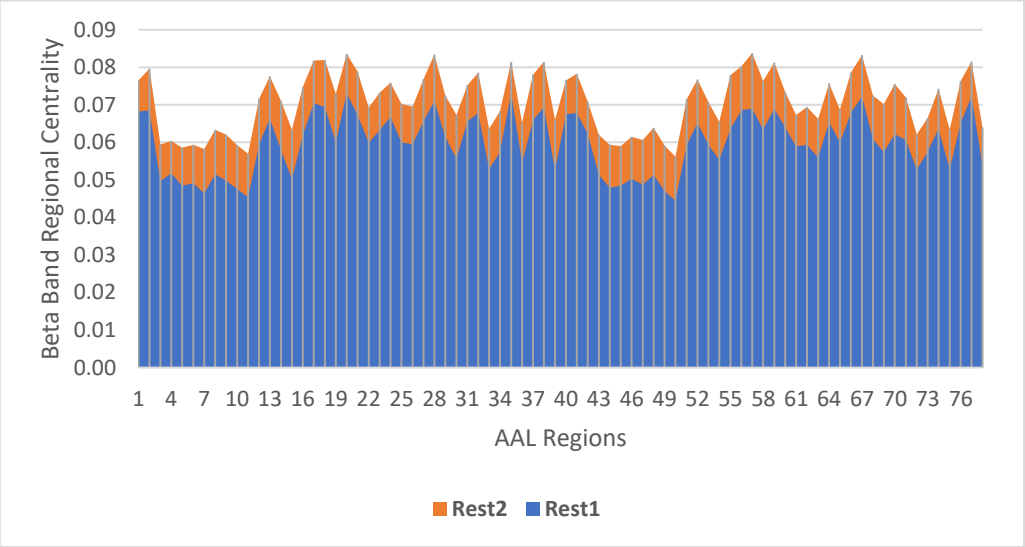

Figure 2.10 Beta band regional centrality illustrate the effect of Time by Regions by Hemisphere interaction (p <.05). The centrality in Rest2 for all AAL regions has increased significantly from Rest1 averaged across conditions. The 78 AAL regions are arranged from the left hemisphere to the right (as labelled in Table 2.5).

2.3.5.3 Alpha-Beta cross-frequency centrality

The Alph-Beta cross-frequency resting-state centrality demonstrated a significant main effect of Time, $F(1,40)= 7.057$, $p = .011$, Time by Regions interaction, $F(4.1, 284) = 17.498$, $p < .001$, and Time by Regions by Hemisphere interaction, $F(12.1, 527) = 4.628$, $p < .001$ (Figure 2.10). These findings indicate that the Alpha-Beta cross-frequency regional centrality during the resting states changed significantly after engaging in the antisaccade task. This change was different for different regions in each hemisphere. In Rest2, there was a decreased connectivity in the left rectus gyrus, paracentral lobule, superior parietal gyrus, the right middle and inferior temporal, and bilateral olfactory, posterior and median cingulate cortices.

The Alpha-Beta cross-frequency did not exhibit any significant effect or interactions in the change of centrality investigation for the effect of the Treatment condition.

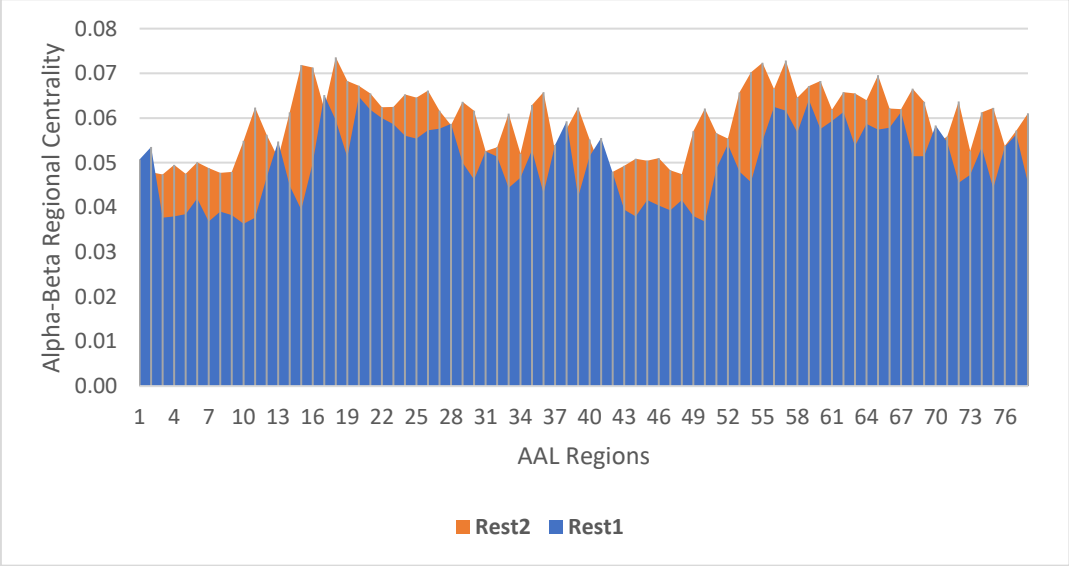

Figure 2.11 The Alpha-Beta cross-frequency regional centrality illustrating the effect of Time by Hemisphere by Regions interaction, which show overall increased centrality in Rest2 relative to Rest1. The 78 AAL regions are arranged from the left hemisphere to the right (as labelled in Table 2.5).

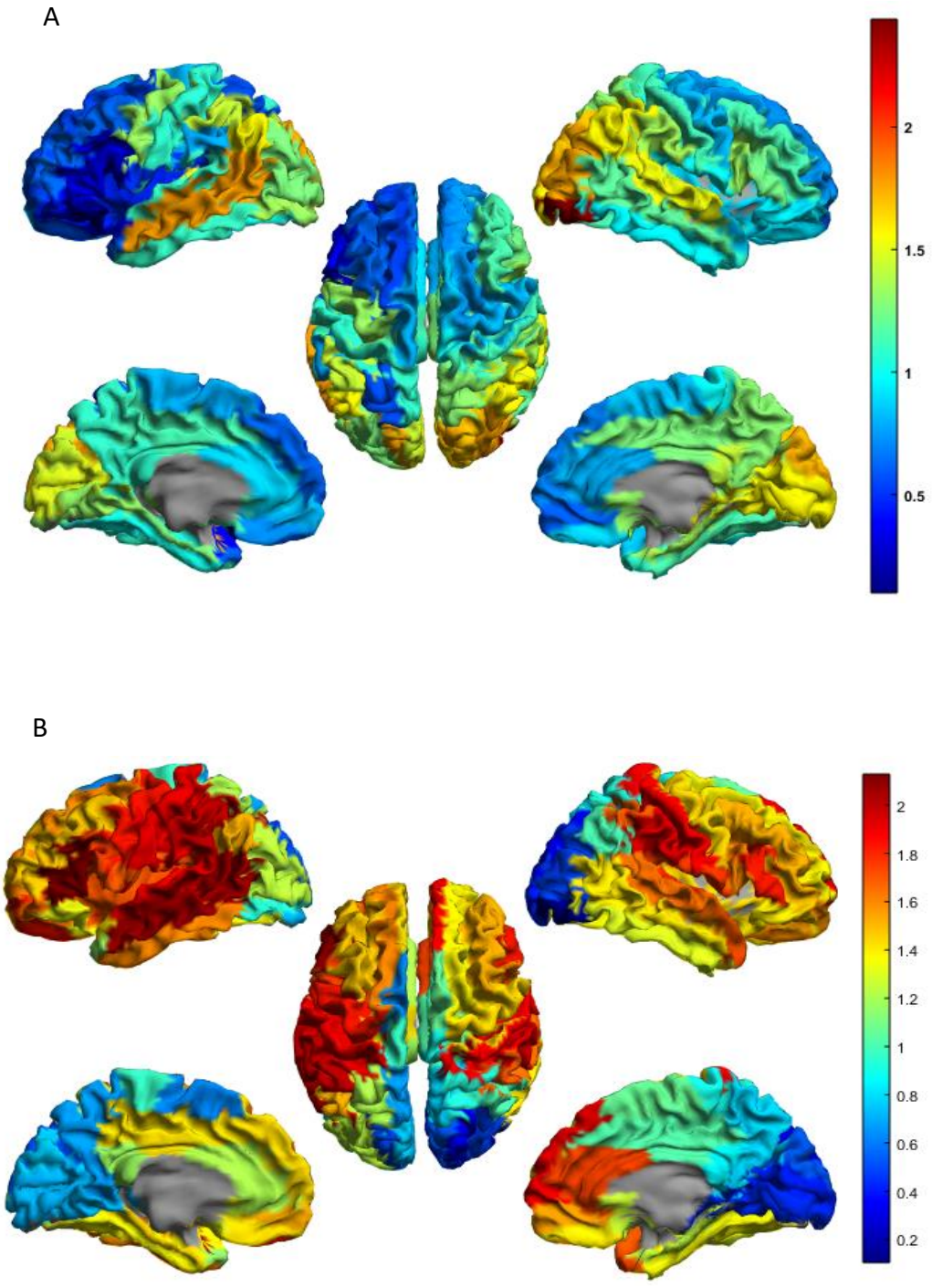

Figure 2.12 The changes in the Alpha band centrality for A) the Sham condition illustrated an increase in the occipital and posterior parietotemporal regions centrality. A regional distribution that involves the visual and posterior DMN regions. B) The active tDCS condition illustrated a prominent increase of centrality in the frontal, parietal, temporal and anterior cingulate regions than the occipital ones with left hemisphere tendency. This regional distribution encombasses regions of the CEN and salience network involved in the top-down control of behaviour.

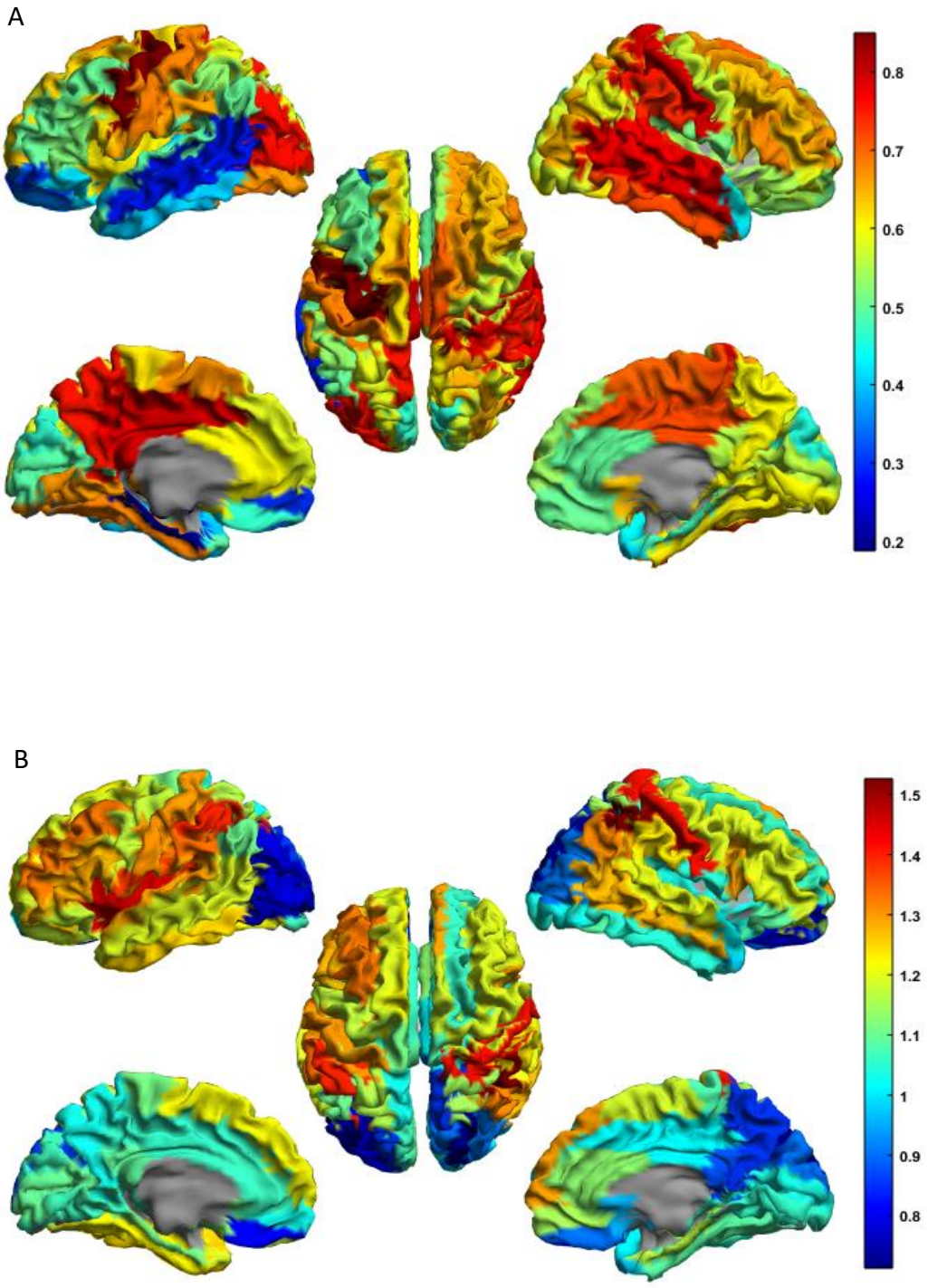

Figure 2.13 The changes in the Beta band centrality for A) the Sham condition illustrated a prevailing right hemisphere increased centrality in the temporal, Parietal and occipitial and left central regions. B) The active tDCS condition illustrated greater centrality overall compared to the Sham condition with left hemisphere dominance in the frontotemporal regions. The tDCS condition exhibited less centrality in the occipital regions relative to the other AAL regions.

Note the color scale differences for both conditions.

2.4 Discussion

- Does active tDCS alter participants' behavioural measures?

The baseline behavioural assessment of our sample indicated an elevated level of sensation-seeking behaviour, reflected in the UPPS-P scores. However, there were no differences between the two groups of treatment conditions in any of the psychometric self-reported measures. Regardless of the treatment condition, participation in the study increased fatigue levels. It decreased the tension, depression, esteem, and vigour levels across the whole sample, which might reflect the exhaustion resulting from the prolonged study duration and the postural steadiness required from the participants in the MEG scanner and the relief by completing the study.

Does the antisaccade task modulate the resting state functional connectivity?

Our results illustrated increased functional connectivity for Rest2 relative to Rest1 across the sample. The increased connectivity was spread across the cortex for the Alpha, Beta, and cross-frequency connectivity. This increase in connectivity was prominent in the lateral parietal (superior and inferior parietal gyri), lateral occipital, lateral temporal, median and posterior cingulate regions for both treatment conditions (Figure 2.5, Figure 2.6). This regional distribution is implicated in the visuospatial system (Beckmann et al., 2005) and the DMN (Greicius et al., 2003). The resting state condition in our study design involved active oculomotor engagement by fixating the vision on a displayed target. This visual fixation could explain the engagement of the visuospatial system and the DMN.

However, Subtracting the baseline (Rest1) from post-task functional connectivity removes the effect introduced by this visual processing. It provides a contrast to the effect of the antisaccade task performance (with the possible placebo effect) on the resting state functional networks. The application of this contrast (in the Sham condition) showed an increase in the parietal region's connectivity to the occipital, temporal and limbic regions, which was prominent in the right hemisphere (Figure 2.7). The right hemisphere is implicated in the posterior attentional network

that regulates the baseline attentional intensity (Sturm and Willmes, 2001, Petersen and Posner, 2012). Moreover, it is crucial for visual remapping (Pisella et al., 2011).

In summary, the performance of the antisaccade task in the sham condition modulated the resting state functional network by increasing the functional connectivity of the occipital and parietal cortices. This modulation indicates a strengthening of the bottom-up cognitive processing of orientation (alerting) within the posterior attention network (or VAN).

Does active tDCS modulate the antisaccade task performance effect on the resting state functional connectivity?

In the contrasted Rest3, the active tDCS condition increased connectivity of the frontal regions to the parietal, limbic and temporal regions but not the occipital ones. This change in connectivity was greater in the left hemisphere. The resulting modulation effect is a distinctly contrasted connectivity pattern for the active tDCS relative to the Sham condition (Figure 2.7). The left hemisphere is implicated in the alerting phase of attention that requires fast decision-making and response initiation. This role is evident in patients with left hemisphere lesions, showing slower reaction times and greater error rates (Sturm and Willmes, 2001). As part of the DAN, the frontal and anterior cingulate regions have a critical role in the regulation of NE release from the LC and in performing top-down control over the VAN (Petersen and Posner, 2012). Our finding suggests that active tDCS condition increased the functional connectivity of these pivotal regions of cognitive and attention control. Furthermore, the degree centrality changes supported this finding with a significant effect of the treatment condition on modulating the Alpha band nodal centrality Figure 2.9.

In summary, while the Sham condition exhibited greater connectivity within the occipital regions, the active tDCS condition showed increased centrality in the frontal cortical regions. The modulation of performing the antisaccade task in the Sham condition illustrates an increase in regions responsible for bottom-up cognitive processing. The active tDCS modulated this effect augmenting the top-down control of the visual inhibitory control system. These findings imply the neuromodulatory effect of combined inhibitory cognitive task performance with active tDCS and task performance with sham stimulation on inducing short-term neuroplastic effects in the cortical networks involved.

Chapter 3 Pupil dilatation, neuromodulation, and cognitive control

In the previous chapters, we introduced the antisaccade task and the modulatory effects of active tDCS. Then, we examined their modulatory effects on the resting-state networks following the performance of the antisaccade task with and without the active tDCS in a sample with impulsivity traits. In this chapter, we will focus on examining the effect of arousal changes during the performance of the antisaccade task on altering the pupil dilation (PD) response. We will examine the effects of Treatment conditions on this modulation.

3.1 Introduction

Pupillometry is the measurement of pupil size changes across time. It was established by Hess and Polt (1960), who reported gender differences in PD associated with the presentation of interesting visual stimuli (for a detailed review, see (Laeng et al., 2012)). Pupil size is under the direct control of the autonomic nervous system (ANS). Miosis is the pupil constriction reflex. It is a pupil response to increased luminance or focused near vision. It is mediated via acetylcholine, the primary parasympathetic neurotransmitter.

In contrast, pupil dilatation (mydriasis) is the pupil response to far vision and dimmed luminance in the environment. It is mediated via norepinephrine (NE), the primary sympathetic neurotransmitter. An increase in NE levels results from increased arousal levels or stress (Bouffard, 2019, Mathôt, 2018). The increase in NE is associated with pupil dilation (Gabay et al., 2011). The PD functional connection with the ANS makes PD a reasonably sensitive measure of the sympathetic activity in the LC despite the yet-to-be-known structural connectivity (Gilzenrat et al., 2010, Joshi et al., 2016).

The adaptive gain theory incorporates this relationship to detangle the interactions between the LC-NE activity, task performance optimisation and arousal (for LC-NE and attention details, see section 1.4) (Aston-Jones and Cohen, 2005). The

converging evidence reports high sensitivity for PD to reflect arousal levels associated with cognitive effort (Koelewijn et al., 2015), high-value memory encoding (Ariel and Castel, 2014, Kang et al., 2014), and emotional arousal (Bradley et al., 2008).

Geva et al. (2013) used the attention network task to examine PD changes associated with alertness, orientation, and executive attention to a visual stimulus (Petersen and Posner, 2012, Fan et al., 2002). In accordance with the adaptive gain theory, Geva et al. (2013) reported a dual-mode PD response in each of the cued-trial conditions they examined. The first is an alerting PD response with a peak dilation of around 360 ms post-cue presentation that was not recorded in non-cue trials. This response represents task engagement and recruitment of ANS resources for covert attention. The different task conditions did not modulate the alerting response. The second reported PD response had a more significant peak than the alerting response and was closely related to the response with around 600 ms post-cue presentation latency. It would have been more informative if they had reported a response-locked analysis to confirm this result.

3.1.1 Aims and questions

We seek to examine the arousal changes related to the performance of the antisaccade task as measured by the PD. Based on the findings of Waitt (2022) and Geva et al. (2013), we predict dual mode peaks of PD. The first peak will follow the cue presentation, and the second response will be more prominent in magnitude and precedes the response. We predict pronounced PD changes for antisaccade trials reflecting increased cognitive effort than prosaccade trials.

We aim to examine whether the active tDCS had a modulatory effect on the arousal as measured by the PD changes during the performance of antisaccade. We seek to answer the following questions.

- Are there differences between the antisaccade and prosaccade trials in measures of PD?
- Do the treatment conditions modulate the measures of PD differently for either trial type?

- Is there a difference between target and cue-induced PD changes?
- Is there a correlation between the induced PD measures and task performance?

3.2 Methods

The analyses reported in this chapter were conducted on the sample reported in the previous chapter.

3.2.1 Participants and study design

The participant recruitment process is detailed in section 2.2.1. The study design is described in section 2.2.2.

3.2.2 The Anti-saccade task

Using EyeLink® Experiment Builder (SR Research Ltd.), the research team designed the antisaccade task. The task included 12 blocks of pro-saccade and 12 blocks of antisaccade trials with 15 seconds of rest between blocks. An antisaccade block followed each pro-saccade one. The blocks included six trials; three trials of left targets were randomly presented with three right ones. The task was back-projected on a paper screen placed 1 m away from the upright setting participant's face.

Each trial begins by presenting a colour-coded fixation cross indicating the trial type (pink for antisaccade and blue for pro-saccade trials). The antisaccade task timeline is illustrated in Figure 3.1. After 300ms elapsed, two empty rectangular boxes appear on display for 800ms, representing a cue to prepare the participant for the upcoming target. The target is presented by a solid red rectangle filling one of the two boxes at 1100ms from the start of the trial. The saccadic response was expected from the participants within 500ms of the target presentation.

Participants were instructed to move their eyes only towards (in pro-saccade trials) or away from (in antisaccade trials) a presented stimulus in the subject's peripheral visual field to achieve a score. EyeLink® 1000 plus eye-tracker (SR Research Ltd., Canada) continuously recorded saccadic eye movements and changes

in pupil dilation during the task. The eye-tracker was calibrated for each participant before the task commencement and between blocks.

The following feedback messages were presented 200-700ms after each saccade; a) 'Early response' message if subjects attempted a saccade before the target presentation. b) Incorrect response will display a cantered '-1' feedback message and fill the box where the participant is looking to yellow. c) In case of correct response is recorded, the box to which the participant is looking will change colour to green, and a '+1' message indicates the achieved score. d) 'Slow response' if the participant performed saccade within the 501-990ms time-window post-target presentation. When the subject made no saccadic response or the attempt was >1000ms post-stimulus presentation, the feedback message 'No response' was presented.

The back projection and the continuous presentation of the fixation cross help maintain the luminance level throughout the trials and minimise the associated pupil light reflex with luminance changes. However, presenting the imperative stimulus and the feedback messages would introduce minimal luminance changes. The saccadic response is known to produce an artefactual reduction in pupil size in a stationary pupillometer device (Hayes and Petrov, 2016). This confound reduction is called pupil foreshortening error. It is due to the elliptical appearance of the moving pupil in the recording camera. We controlled for the effect of pupil foreshortening error by using around a one-meter distance between the eye-tracker and the subject and by limiting our pupillometry analysis to the period preceding saccade onset. The last step helps control for the effect of feedback message luminance changes but not for the effect of imperative stimulus presentation.

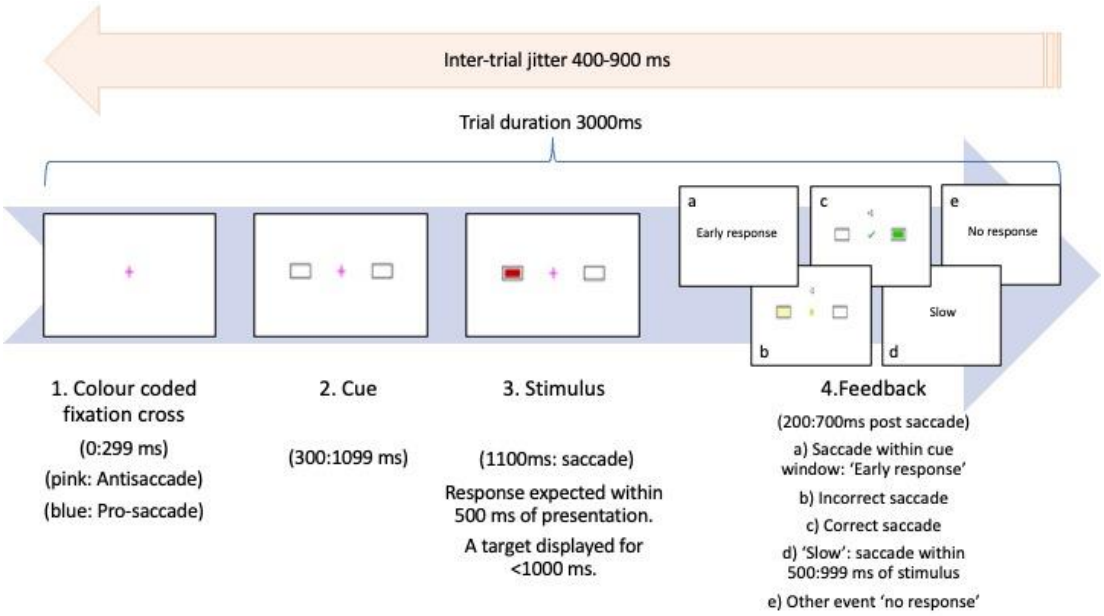

Figure 3.1 The antisaccade task timeline. The task begins by presenting a colour coded fixation cross for 300 ms. Two rectangular boxed are presented on both horizontal sides of the fixation cross for 800 ms representing the task's cue. The imperative stimulus is presented 1100 ms from trials' start and displayed up to a saccadic response is recorded. One of five feedback message is presented depending on the recorded saccadic response.

3.2.3 Pupillometry analysis and task performance

The EyeLink ® 1000 was used to capture the instantaneous PD changes (1000 Hz). The EyeLink software recorded several parameters required for the pupillometry data analysis. These parameters included a continuous measure of pupil size, a detailed trial time course with marked events (trial start, cue, stimulus, response, and trial end), and event specifications (stimulus presentation side, trial types, response type, and feedback message presented). However, pupillometry data is vulnerable to blink and movement artefacts which cause a gap in the PD time course.

We used a customised MATLAB code based on the data cleaning and analysis methods described by Waitt (2022) to pre-process our data. The pre-processing steps included correct response trial extraction, exclusion of trials with express saccades and then data filtering and interpolation for missing segments, as illustrated in Figure 3.2. We choose a time window of interest spanning over the first 1600 ms of the trial's timeline to include a baseline, anticipatory and response periods while excluding feedback-related changes in PD (see antisaccade task timeline Figure 3.1).

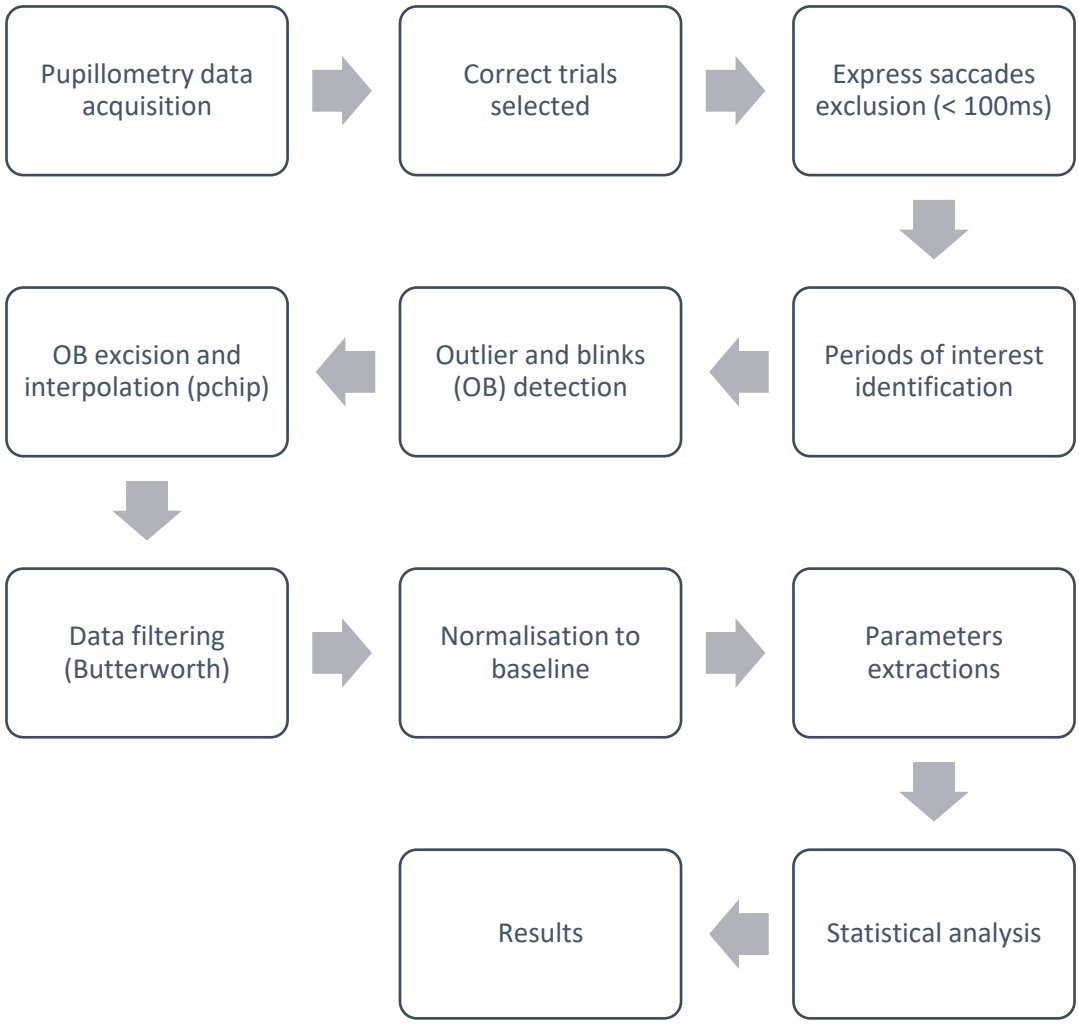

Figure 3.2 The illustrated pupillometry data analysis pipeline

We identified outliers and blinks as data points that lie off the third standard deviation of each trial's mean on a trial-by-trial basis. Moreover, data were evaluated for outliers every 4 ms, defined as data points exceeding a 15-unit deviation from the trials' mean PD. Waitt (2022) used a Piecewise Cubic Hermite Interpolating Polynomial (Pchip) to interpolate the missing data segment due to blink and other artefacts, which provides a smoother and more accurate reconstruction of the missed data (Dan et al., 2020). However, the number of samples interpolated was based on a study that used a similar device and sampling rate (Miles et al., 2017), which used linear interpolation (66 ms before and 132 ms after the blink) parameters justified by their previous work using a different eye-tracking device with a significantly lower sampling rate of 60 Hz (Siegle et al., 2008). We modified the number of interpolated samples to 33 ms before and 66 ms after the blinks and

outlier segments to preserve most of the actual data. Trials were excluded from the analysis if they had more than 30% missing data.

After interpolating missing data, a fourth-order low-pass Butterworth filter with a 4 Hz cut-off frequency was used to remove high-frequency noise and preserve the temporal resolution of the data attained to event markers. Then, we normalised the pupil dilation data using 100 ms from the pre-cue period as a baseline (25-125 ms relative to trial start).

The analyses covered the period from cue presentation up to 500 ms post imperative stimulus presentation, totaling 1400 ms (800 ms cue to target and 500 ms post-stimulus). This period included the saccadic response and up to 100 ms post-saccade. The time course was divided into thirteen-time bins; each bin contained the median pupil size, to control for outliers, in a period of 100 ms (averaged across subjects). This means the first bin includes the median pupil size from cue presentation up to 100 ms afterwards, and the second time bin includes pupil sizes from 100-200 etc. This measure provides insight into the pupil dynamic throughout the trial's time course, which is considered as a proxy measure for the tonic LC-NE activity (Aston-Jones and Cohen, 2005)

The change in pupil size was computed by subtracting the PD at each time point from its counterpart in the previous bin on a trial-by-trial basis to represent the PD changes for this time window. We used the PD changes to represent the rapid changes in arousal and in the LC-NE activity reflecting its phasic mode.

$$PD_{rate} = PD_X - PD_Z$$

PD_X represents the pupil size sample at time X, and Z= time X - 100ms, thus PD_Z = pupil size at time Z = PD_{X-100}

We defined three periods of interest, an anticipatory period (cue to stimulus presentation), post-stimulus (stimulus + 100 ms) and stimulus to saccadic response (stimulus to response). The rate of PD change (event-related PDR) was computed by subtracting the PD at event1 from the PD at event2 divided by the duration from event1 to event2 on a trial-by-trial basis. This method provides a more accurate comparison measure as PD rate per ms per period rather than computing the difference between two singular events.

$$event - related\ PDR\ = \frac{PD_{event2} - PD_{event1}}{event2_{time} - event1_{time}}$$

The rate of PD for each of the three events was correlated with the reaction time (RT), using Spearman's rank correlation on a trial-by-trial basis to investigate the relationship between the RT and PDR in each period. Then we sought to compare the trial-by-trial correlation's sensitivity to a more common and abstract measure of the median PD rate for each defined period separately for each trial type per subject and examined its correlation with the RT.

3.3 Results

3.3.1 Behavioural performance

We excluded one active tDCS subject from all eye-tracking analyses due to a technical error preventing pupillometry data acquisition. The total of subjects included in the behavioural performance and pupillometry analysis was 41 subjects (21 Sham condition, 20 active tDCS).

As expected, the results illustrated a longer RT for antisaccade trials averaged across the sample and in each treatment condition relative to prosaccade trials. Moreover, the Active tDCS exhibited a shorter RT for both trial types than the Sham condition. The descriptive statistical results are summarised in Table 3.1 and illustrated in Figure 3.3.

To examine the effect of trial types and treatment conditions on the RT, we used the median RT as the dependent variable to conduct a two-level mixed-design ANOVA with Treatment conditions (two-level; Sham, Active tDCS) as the between-subjects factor and Trial type (two-level; prosaccade, antisaccade) as the within-subjects factor. The results showed a significant main effect of Trial types, $F(1,39) = 29.807$, $p < .001$, whereby antisaccade trials exhibited greater RT than prosaccade. In line with previous reports of greater RT for antisaccade trials (Waitt, 2022, Wang et al., 2015), indicative of cognitive processing.

However, there was no significant main effect of the Treatment condition, $F(1, 39) = 1366.821$, $p = .342$, or effect of Trial types by Treatment condition interaction, $F(1, 39) = 140.662$, $p = .586$. These findings indicate that the subtle changes in the median RT between Treatment conditions (illustrated in Figure 3.3) need enhancement to reaching a significant level.

Table 3.1 Reaction time descriptive statisticsfor both trial types in each treatment condition and in the average across groups.

Trial Type	Group	N	Mean	Std. Deviation	Min	Max
Prosaccade	Sham	21	245.548	36.1133	172	304
	tDCS	20	240	24.0739	180.5	284
	Total	41	242.841	30.5819	172	304
Antisaccade	Sham	21	274.238	31.3311	236	337
	tDCS	20	263.45	31.7713	190	333
	Total	41	268.976	31.6243	190	337

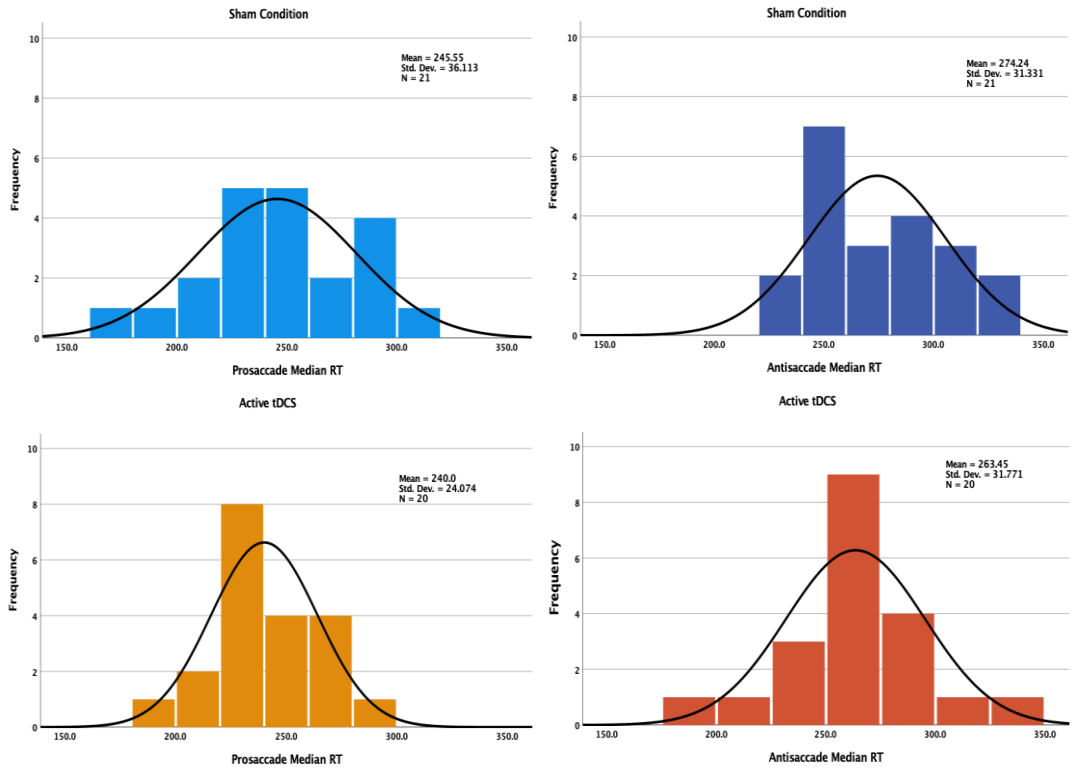

Figure 3.3 Frequency distribution of the saccadic response reaction times for Sham condition (top row), active tDCS condition (bottom row), prosaccades (left column), and antisaccade (right column). The normal distribution curve are plotted to ease the interpretation of the plots, whereby increased curve's height reflects increase central tendency and leftward shift indicate faster reaction times.

3.3.2 Pupillometry results

Pupil size

We aimed to examine the PD differences between Trial types for both treatment conditions during the cue to 500 ms post-stimulus period. To prevent spurious effects due to outliers, we used the median PD values as the dependent measure to conduct a three-way mixed-design ANOVA with the Treatment condition as the between-subjects factor and two within-subjects factors defined as Time bins (13-level: 13-time bins of 100 ms increments), and Trial Type (two-level; prosaccade, antisaccade).

There was a significant main effect of Time, $F(1.2, 49.6) = 100.587$, $p < .001$. However, there was a significant interaction effect between Time and Trial types, $F(2.7, 108.5) = 18.45$, $p = < .001$. These results imply differences between the PD time course of each Trial type. The prosaccade trials illustrated a greater pupil size than antisaccade trials up to 100 ms before the imperative stimulus presentation. In contrast, in the antisaccade trials, there was a larger pupil size from stimulus presentation time up to 500 ms post-stimulus (Figure 3.4).

The treatment conditions did not exhibit significant modulatory effects on the time course of pupil size.

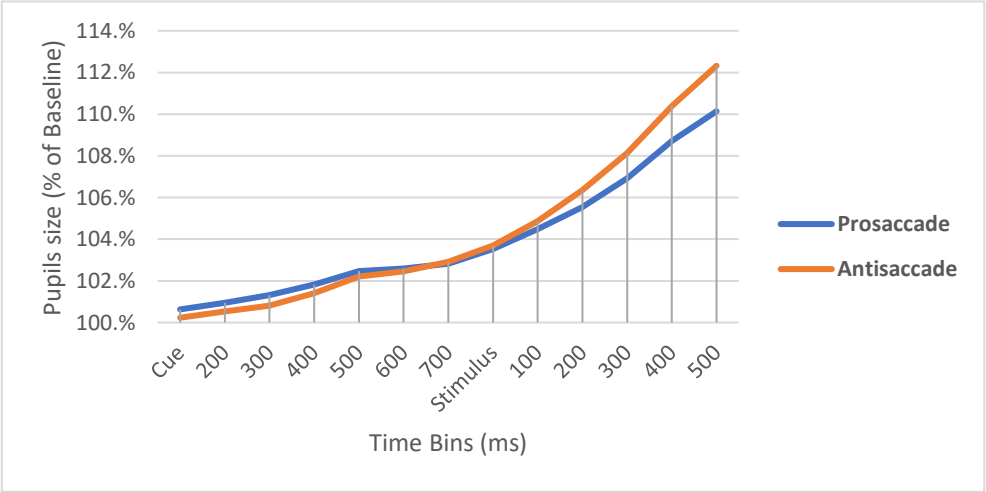

Figure 3.4 The time course of pupil size for each Trial type averaged across treatment conditions. The prosaccade trials exhibited greater PD up to 100ms pre-stimulus, when the antisaccade begins to illustrate a larger increase in PD. NOTE: we binned the median pupil size into 100 ms bins. Thus, each time point in this graph represents the median binned pupil size.

Pupil dilatation rate

We then examined if the increase in PD across trial time courses results from a different PD rate (PDR) between the time bins for each trial type, reflecting the phasic LC activity. We used the PDR as a dependent measure to conduct a three-way mixed-design ANOVA, the Treatment condition was the between-subjects factor, and two within-subjects factors were the Time intervals (12-level: 12 bins of the binned difference between pupil size at each two consecutive 100 ms time bins), and Trial Type (two-level; prosaccade, antisaccade).

There was a significant main effect of PDR, $F(3.7, 143.7)= 48.532$, $p < .001$, and a significant main effect of Trial types, $F(1, 39) = 39.011$, $p = < .001$. However, PDR was significantly affected by Trial type interaction, $F(5.5, 213.1) = 10.134$, $p = < .001$. The prosaccade trials exhibited greater PDR changes within the first 300 ms post-cue. In contrast, the antisaccade trials illustrated prominent PDR from 400 ms post-cue to 500 ms post-stimulus Figure 3.5.

The treatment conditions did not exhibit significant modulatory effects on the PDR during the examined periods (cue to 500 ms post-saccade).

Figure 3.5 The PDR for prosaccade and antisaccade trials, where antisaccade trials exhibited greater PDR from 400 ms post-cue up to 500 ms post-stimulus presentation. The post-cue increase in PDR represents the tonic attention changes. The post-stimulus increase reflects the phasic LC mode

Event-related PDR

The PDR illustrated in Figure 3.5 shows a bimodal change in PDR. The first mode is in the cue to stimulus period, and the second is from stimulus presentation up to 500 ms post-stimulus. We aimed to examine the effects of cue and stimulus presentation on eliciting this bimodal PDR. We used the median er-PDR (see section 3.2.3 for more details) for the cue to stimulus and for the stimulus to saccade computed on a trial-by-trial basis as a dependent variable to conduct a three-way mixed-design ANOVA with Treatment conditions as the between-subjects factor and defined within-subjects factor as; the time interval (two-level: cue-stimulus, stimulus-saccade) and Trial types (two-levels; prosaccade, antisaccade).

There was a significant main effect of Trial types, $F(1, 39) = 46.777$, $p < .001$, and a significant main effect of Time interval on er-PDR, $F(1, 39) = 141.146$, $p < .001$. However, there was a significant effect of Trial types by Time interval interaction, $F(1, 39) = 46.039$, $p < .001$, whereby the stimulus-saccade erPDR was significantly greater than the cue-stimulus erPDR. Furthermore, the antisaccade trials had greater erPDR in both events compared to the prosaccade trials. In accord with the accumulating evidence (Waitt, 2022, Wang et al., 2015). This finding indicates cues and imperative stimuli elicit different PD responses, which are effort-dependent, whereas antisaccade trials are associated with greater PDR.

There was no significant main effect or interaction of Treatment condition on modulation of the er-PDR.

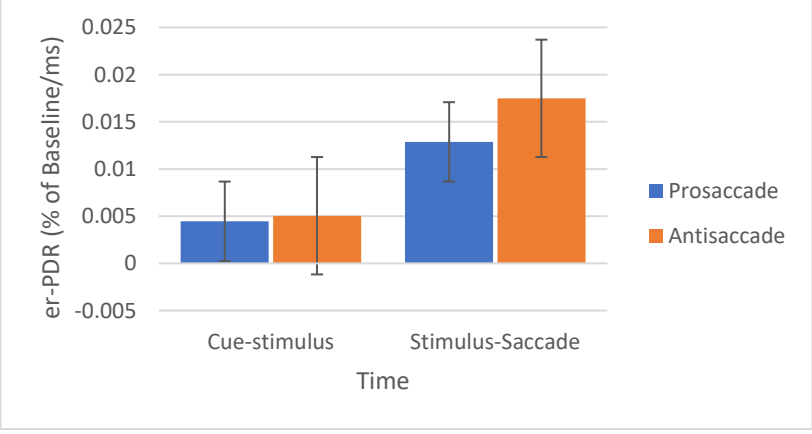

Figure 3.6 The illustrated significant different er-PDR during the cue-stimulus and stimulus-saccade periods for both trial types. The stimulus presentation elicited greater erPDR than cue presentation. The change of PDR was prominent for antisaccade trials in the post stimulus period. The error bars represent the standard error.

PD-RT correlations

We aimed to examine the relationship between RT and PDR for both Trial types and whether the Treatment conditions modulate this relationship. We used the z-transformed Spearman's correlation coefficient between the PDR and RT, computed on a trial-by-trial basis (see section 3.2.3 for more details), as a dependent variable to conduct a three-way mixed-design ANOVA with the Treatment condition as the between-subjects factor. The periods of interest (two-level; cue-stimulus, stimulus presentation to 500 ms post-stimulus) and Trial types (two-level; prosaccade, antisaccade) were the within-subjects factors.

As the dependent factor in this analysis is the mean PDR-RT correlation coefficients of all the trial types, the intercept of between-subjects effects indicates whether the averaged correlation across other factors differs from zero. In this case, the averaged correlation across trial types, periods of interest and treatment conditions differed significantly from zero, $F(1, 39) = 59.363$, $p < .001$. Moreover, there was a significant main effect for Periods of interest, $F(1, 39) = 27.41$, $p < .001$, which illustrated significantly more negative correlations (averaged across trial types) in the stimulus to saccade period than the cue to stimulus period (Figure 3.7).

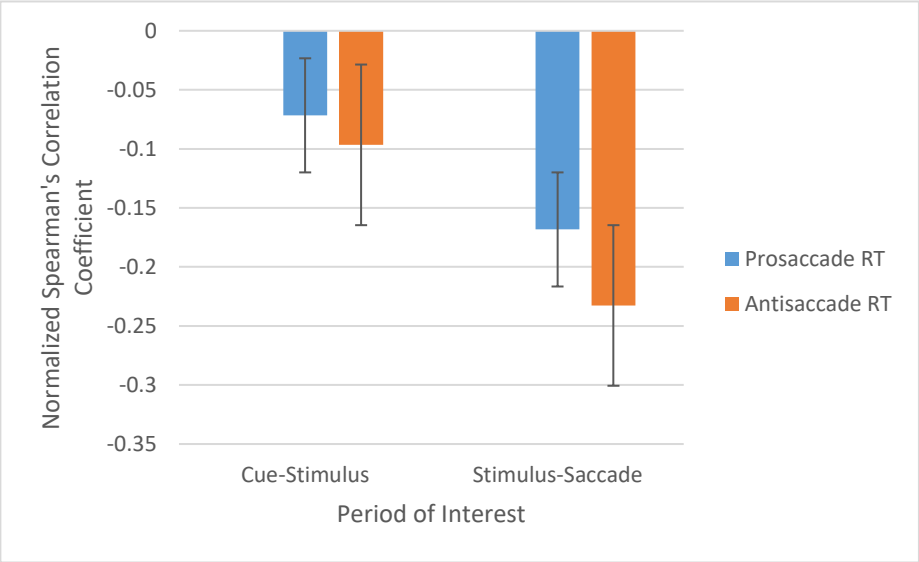

Figure 3.7 The normalised Spearman's correlations (on trial-by-trial basis) for the median RT of each trial types with the erPDR at each time period of interest. The correlations exhibited a negative direction indicating faster RT correlated with greater PDR on trial-by-trial basis.

Moreover, we used the Pearson correlation test to examine the correlation across subjects between each Trial type median RT (estimated across trials within each subject) and the erPDR of the Periods of interest (cue to stimulus and stimulus to saccade). Only the antisaccade RT exhibited a significant negative correlation with the stimulus to saccade PDR, $t(41) = -.425$, $p = .006$ (Figure 3.8). These results imply that on a trial-by-trial basis, the correlation between the RT and PDR is more sensitive than the correlation between averaged median RT and erPDR.

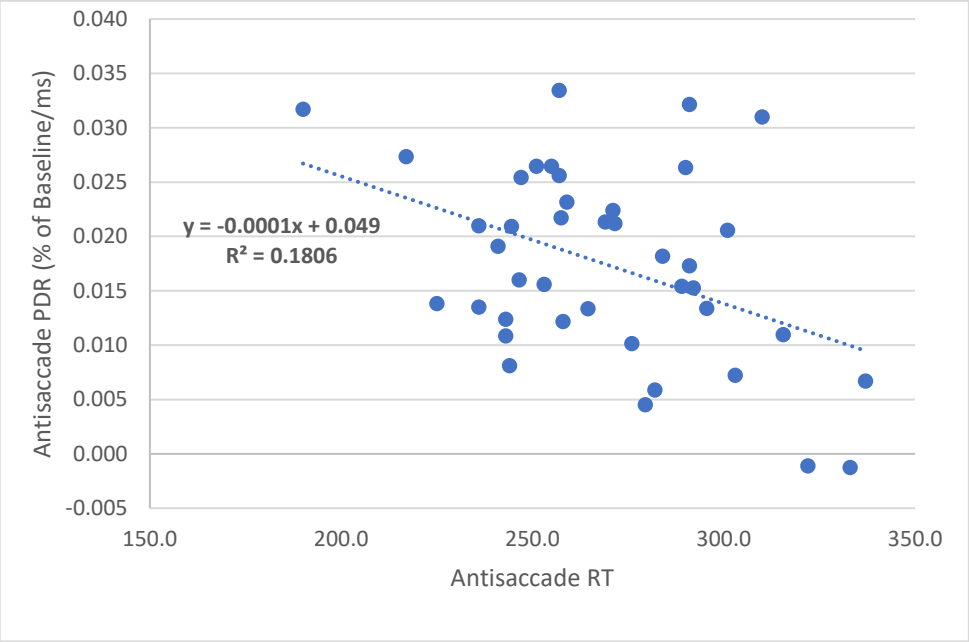

Figure 3.8 The significant Pearson correlation between the antisaccade RT and stimulus to saccade erPDR, whereby greater PDR is correlated with faster RT.

3.4 Discussion

- Does the average PD exhibit differences between antisaccade and prosaccade trials during the anticipatory period?

In accordance with the adaptive gain theory (Aston-Jones and Cohen, 2005), there was an increase in the tonic phase of the PD during the first 400 ms of the alerting phase of the antisaccade task anticipatory period, which indicates increased active engagement and covert attention shift towards task type. However, the theory predicted that greater tonic mode activation (baseline activity) negatively affects task performance, resulting in more false alarms. Instead, an optimum baseline activity level is required to allow for phasic mode initiation and the correct behavioural performance (Aston-Jones and Cohen, 2005, Howells et al., 2012). Our results showed 300 ms of decelerated PD after the initial alerting phase and before the imperative stimulus presentation. This deceleration could reflect an optimisation period of activity essential for making the correct response (Howells et al., 2012).

Our results illustrated differences between the antisaccade and prosaccade for the PD time course and the PD rate. While the prosaccade trials exhibited greater PD during the anticipatory period up to 100ms pre-stimulus presentation, the antisaccade exhibited greater PD during the post-imperative stimulus presentation than the prosaccade. On the other hand, the PD rate for both trial types were comparable during the first 300ms post-cue presentation. The antisaccade trials demonstrated greater rate of PD increase than prosaccades. In accordance with the association between arousal, cognitive effort levels and PD (Wang et al., 2015, Sara and Bouret, 2012, Gabay et al., 2011, Gilzenrat et al., 2010), this finding reflects the greater LC-NE activity associated with the antisaccade task.

- Is there a difference between target and cue-induced phasic PD changes?

According to the adaptive gain theory, the phasic LC activity is behaviour specific and only precedes the response by 230 ms (in monkeys) (Aston-Jones and Cohen, 2005, Aston-Jones et al., 1994). A significantly greater PDR was elicited during the period between imperative stimulus presentation and the saccade, which was

greater for the antisaccade than the prosaccade trials. Our findings support the role of phasic PD associated with increased cognitive effort and attentional allocation.

- Do the treatment conditions modulate the measures of PD differently for either trial type?

Our tDCS stimulation parameters did not elicit a modulatory effect on the PD or the PDR during the performance of the antisaccade task. This finding could be related to the low stimulation amplitude or the tDCS need for multiple dosing to illustrate behavioural effects (detailed in section 4.4). Due to the time constraints of the PhD, one of our limitations is that we did not examine the learning effect by examining the PD or the RT in early trials and comparing it to the late ones (Geva et al., 2013).

- Is there a correlation between the induced phasic PD measures and task performance?

In accordance with previous findings (Waitt, 2022, Wang et al., 2015), our results illustrated a significantly negative correlation between reaction times and PDR. We found that using trial-by-trial correlation produced more robust results between reaction time and the PDR during the cue-stimulus and stimulus-saccadic response period for both trial types. Our findings support that faster reaction times correlate with greater pupil size within the examined periods. However, when examining the correlations using the median PDR (averaged across subjects) for each period with the reaction times, only the stimulus to saccadic response PDR was negatively correlated with the reaction time in the antisaccade trials.

In this chapter, we investigated the modulatory effect of active tDCS on the LC-NE using PD as a measure of ANS activity. In the next chapter, we will examine the modulatory effect of the active tDCS during the performance of the antisaccade task on the ERSP within the OCN.

Chapter 4 tDCS and cognitive control

In the previous two chapters, we examined the effects associated with the performance of the antisaccade task on resting-state functional connectivity and the modulatory effect of active tDCS on this resting-state connectivity. We then investigated changes in the behavioural performance and the ANS neural correlates during the antisaccade task performance as indexed by the PD.

In this chapter, we resume our investigations of the modulatory effects of the active tDCS, as a possible neuromodulatory therapeutic tool, in a sample with an elevated impulsive trait. We aim to examine the modulatory effects of active tDCS on the event-related spectral perturbation within the OCN during the performance of the antisaccade task.

4.1 Introduction

The brain electrophysiological activity during cognitive or sensorimotor tasks could be analysed in several methods (for detailed reviews, see (Makeig et al., 2004, Roach and Mathalon, 2008, Huster and Raud, 2018)). Event-related potential (ERP) describes the averaged electrical potential (voltage) changes over several trials (or epochs) that have been time-locked to a specific trial's event, a specific response for example or an imperative stimulus. However, the measured ERP at any time point is formed in essence by complex dynamics of several frequencies that could be further explored using spectral decomposition to perform time-frequency analyses. An event-related spectral perturbation (ERSP) is a result of the ERP spectral decomposition, which details the event-induced amplitude changes in the frequency spectrum with time (Makeig, 1993). While an increase in oscillatory amplitude is referred to as event-related synchronisation, a decrease in amplitude is known as even-related desynchronisation reflecting synchronous changes in the neuronal activity (Pfurtscheller, 1992)

4.1.1 Communication Through Coherence

The communication through coherence (CTC) theory (Fries, 2015) postulates that postsynaptic gamma oscillatory activity creates a 3 ms phase-selective window of high and low synaptic input sensitivity to the incoming presynaptic signals. This temporal window grants matching input signals greater effective connectivity with the postsynaptic neuron. This gamma-band coherence provides cross-frequency bands interregional connectivity with precise, effective, and selective communication. Furthermore, it proposes a modulation of synaptic gain (i.e. postsynaptic sensitivity to presynaptic stimuli) by a top-down regulation of the rhythmic Gamma band synchronisation amplitude and frequency.

The CTC postulate that Alpha and Beta bands are the main mediators of top-down control. The PFC Alpha mediate the increase of local, regional Alpha synchronisation at the targeted regions. This regional Alpha activity represents an available mode that permits regional engagement on demand. In contrast, the Beta band act as a target circuit activator and elicits, via deep cortical feedback, an increase in gamma synchronisation in the superficial cortical layers of the targeted regions. Hence, an increase in the Beta band synchronisation indicates regional engagement and an increase in the Alpha band implies regional deactivation and disengagement.

4.1.2 Visual-spatial remapping

To scan the surrounding environment, we continuously move our eyes, heads, and bodies. These movements and scanning process provides an unremitting visual input to the visual cortex. However, we have a stable spatial perception of the surrounding environment that facilitate the identification of objects coordinates in real-world dimensions despite our movement. This perceived visual stability is theorised to result from the remapping process of the cortical retinotopic representation of the visual field (Bays and Husain, 2007, Mathôt and Theeuwes, 2011).

The remapping process accounts for the intended saccadic eye movement by generating a predicted representation of the visual input after the execution of the planned saccade. Creating this prediction requires a notion of the movement direction (corollary discharge) and a visual signal to interpolate the new retinotopic representation (for review, see (Wurtz, 2008, Bays and Husain, 2007, Mathôt and Theeuwes, 2011, Cavanagh et al., 2010, Sommer and Wurtz, 2008). Rolfs et al. (2011) reported that an attentional shift towards the preplanned saccade endpoint is associated with the efficiency of the retinotopic remapping process and precedes the execution of the saccade.

4.1.3 Antisaccade and the OCN

The antisaccade task is an oculomotor inhibitory control task, which activates the oculomotor control network (OCN) (see section 1.5.3 for more details about the antisaccade task). It requires participants to inhibit a prepotent prosaccade response towards a novel stimulus presented in the peripheral visual field and initiate a motor response in a different direction (Hallett, 1978). After stimulus presentation, successful performance in antisaccade trials involves a vector inversion process (vector remapping), which shifts participants' attention from the stimulus presentation hemifield towards the saccade endpoint direction.

Accumulating evidence points towards the PEF and the FEF as the cortical regions implicated in the predictive remapping process (Duhamel et al., 1992, Umeno and Goldberg, 1997, Sommer and Wurtz, 2006, Rolfs et al., 2011) and in vector inversion remapping process (Moon et al., 2007, Munoz and Everling, 2004, Medendorp et al., 2005, Belyusar et al., 2013). Both regions exhibit greater physiological activity for the contralateral presented stimuli than ipsilateral ones (Sereno et al., 2001, Everling and Munoz, 2000, Medendorp et al., 2005, Everling et al., 1998). This indicates that vector inversion involves a shift in the neurophysiological activities related to contralateral stimuli remapped to the cortical regions contralateral to the saccadic endpoint.

The neural activity in the FEF is associated with motor planning (preparation) and executive processing (for more details about the OCN, see section 1.7). At the same time, the PEF is mainly involved in the visuospatial processing (Connolly et al., 2002, Schall, 2004, Medendorp et al., 2005). The dorsolateral prefrontal cortex (DLPFC) is among the essential cortical regions in the antisaccade and other tasks of the response inhibition (Bari and Robbins, 2013, Munoz and Everling, 2004). The DLPFC activity involves multiple executive functions and is a central hub in the cognitive control processing (Miller and Cohen, 2001).

Hwang et al. (2014) proposed a top-down inhibitory control mechanism whereby an increase in the right DLPFC Beta-band (18-38Hz) activity during the anticipatory period precedes an increase in Alpha-band (6-14Hz) activity in the FEF by about 80ms. Compared to the prosaccade, antisaccade trials exhibited a significantly stronger Alpha-band increase in the FEF, which indicates increased functional inhibition. This observed increase in the preparatory Alpha band diminishes 204-24ms before the saccadic response suggesting a decrease in the functional inhibition. The authors proposed that PFC Beta activity is a signalling mechanism to increase Alpha band activity in a targeted system or network, which leads to a functional inhibition (Hwang et al., 2014). This functional role of the Alpha band is supported by the CTC (Fries, 2015) and the gating by inhibition theories (Jensen and Mazaheri, 2010).

4.1.4 Aims and questions

This study was designed to further our knowledge of the pathophysiological mechanisms of rapid response impulsivity and to examine whether anodal tDCS will improve the involved top-down inhibitory control processes. We aim to examine the modulatory effects of the active tDCS condition compared to sham stimulation on the OCN using MEG during active engagement in an inhibitory control task.

Given the proposed roles of the Alpha and Beta band in the CTC, gating by inhibition, and neurodynamics of inhibitory control. We predict an increase in Alpha and Beta late in the anticipatory period for the frontal OCN regions more than in occipital regions, especially for the FEF, reflecting the inhibition of premature responses. We expect the active tDCS condition to modulate the time course of the OCN regions to enhance the performance on the task more than the sham condition. Furthermore, given the asymmetry in the tDCS delivery, we expect Treatment conditions to manifest different hemispheric modulation.

My research questions for this chapter:

- Do Alpha and Beta rise more in the frontal OCN compared to occipital ones during the anticipatory period?
- Are there preparatory regional differences between antisaccade and prosaccade?
- What is the ERSP-associated vector inversion (saccade remapping)? Are the FEF and PEF involved in the process?
- What are the modulatory effects of the active tDCS compared to the Sham condition?

4.2 Methods

4.2.1 Participants recruitment, study design, the antisaccade task, MEG pre-processing and co-registration

The participant recruitment process is detailed in section 2.2.1. The study design is described in section 2.2.2. Methods of data acquisition are described in 2.2.3. The details of the antisaccade task paradigm used and the timeline of the task events are described in 3.2.2. Eye-tracking and pupillometry methods are detailed in section 3.2.3.

The preprocessing and co-registration steps are illustrated in Figure 4.1 and detailed in sections 2.2.4.1 and 2.2.4.2, respectively.

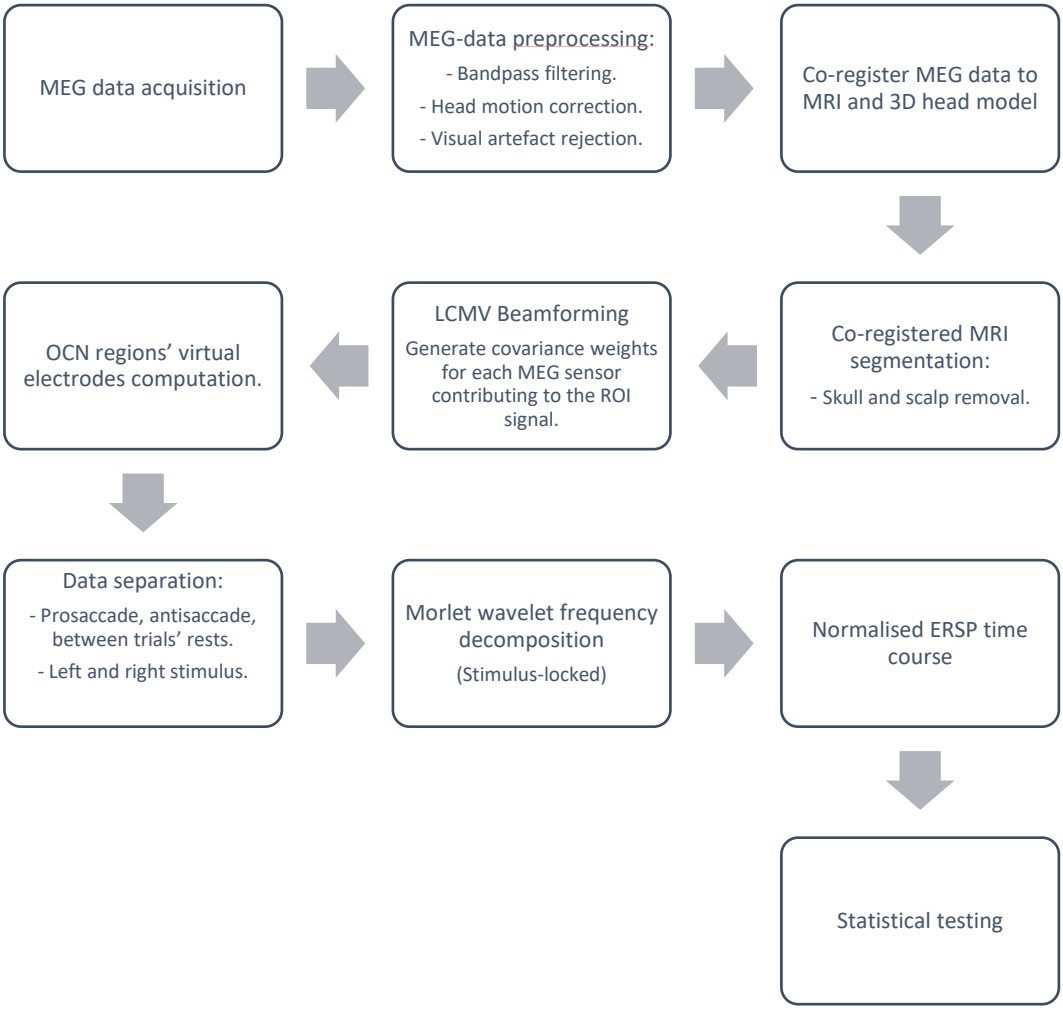

Figure 4.1 MEG data processing and analysis pipeline. Illustrated process of MEG data pre-processing and analysis steps applied for the data collected during the antisaccade task session.

We aimed to examine and compare the modulatory effects related to the inhibitory control process in the antisaccade task in both Treatment conditions for the Alpha and Beta bands. To achieve this, we computed a normalised time course of the event-related spectral perturbation (ERSP) for the Alpha and Beta bands. We used the rest between trial blocks as a baseline for the normalisation process. We used stimulus-locked analysis for the anticipatory period and the post-stimulus period.

4.2.1.1 Antisaccade task MEG data analysis

We prepared the MEG data during the tDCS/antisaccade for statistical analysis using customised scripts in MATLAB. These scripts incorporated functions from the FieldTrip toolbox (Oostenveld et al., 2011). For source localisation, we used a modified version of the pipeline developed by O'Neill et al. (2017). The co-registered subjects' MRIs were segmented to the scalp, skull, and brain, then prepared by removing the scalp and preserving brain volume.

We used IBM SPSS Statistics (IBM Corp. Released 2020. IBM SPSS Statistics for Windows, Version 27.0. Armonk, NY: IBM Corp) to perform our statistical analysis.

We used LCMV beamforming to estimate the signal at nine nodes of the oculomotor control network (OCN) (refer to section 2.1 for details about beamforming and section 1.7 for more details regarding the OCN). These coordinates were defined using an extensive literature search by Waitt (2022) (Table 4.1). This network is involved in the top-down regulation of eye movements. It is composed of the primary visual cortex (V1), parietal eye field (PEF), anterior insula (AntIns), frontal eye fields (FEF) and the dorsolateral prefrontal cortex (DLPFC). The cortical region V1 receives visual inputs from the retina and then projects them to the parietal and frontal regions. The DLPFC is an executive control centre responsible for inhibiting reflexive prosaccade and planning to execute an antisaccade is believed to take place. While the PEF processes visuospatial information as to where to look, the FEF coordinates the visuomotor aspect of the saccadic movement (how to move). The anterior insula regulates multiple functions, including attention, working memory, and salience processing.

Table 4.1 The OCN regions' coordinates in MNI space

ROI	x	y	z
R DLPFC	40.5	38.5	25
L DLPFC	-39.5	37.5	26.5
R FEF	31.15	-5.5	50.45
L FEF	-31	-4.7	50.5
R AntIns	40.5	12	0
L AntIns	-36	9	4
R PEF	25.5	-63	57.5
L PEF	-26	-61	55
V1	-0.82	-79.25	5.93

A standard Montreal Neurological Institute (MNI) space with a 4 mm grid resolution was used as a template to define the 9 ROIs of the OCN. We used these coordinates to find the nearest voxels in the MNI template and then warped the MNI-ROI template into each subject's prepared brain volume. We used LCMV adaptive beamformer (Robinson, 1999, Van Veen et al., 1997) for source localisation in a time window spanning the entire task session duration and a 1-150Hz frequency window (Brookes et al., 2008). To compute the forward fields, we employed a single-shell dipole approximation method (Nolte, 2003). Then, to optimise the signal-to-noise ratio (SNR), dipole orientation was modelled by concatenating the x, y, and z axes to a single electrode orientation using a non-linear search for the optimal SNR (Sekihara et al., 2004).

We used the Tikhonov regularisation method set to condition the regularised covariance matrix to a number of 100 (lambda= 0.01 of the eigenvalue's range of the covariance matrix). The covariance matrix regularisation generates spatial blurring, which promotes a more stable signal from the source space. The resulting signal from each voxel is a weighted average of its signal and contributions from the surrounding voxels. We performed the regularisation process to ascertain the inclusion of the most relevant data to the ROI activity from the adjacent voxels. The process produced an $m_R \times n_S$ matrix (where R is the number of ROIs, and S is the number of sensors), which contains the contribution signal weights for every MEG sensor to each ROI throughout the task session duration.

A virtual electrode (VE) time series for each ROI by multiplying the computed weights matrix by the time series (TS) signal from each sensor (S) for each trial type (TT) separately (rest/antisaccade/saccade). This produced nine-time courses (one for each ROI) for each trial type.

$$VE_{ROI} = W_{(ROI,S)} * TS_{(S,TT)}$$

We used the rest periods between trials' blocks as a baseline to normalise the antisaccade task modulation effect for Alpha (8-13Hz), low-Beta (13-20Hz) and high-Beta (20-30Hz). For the anticipatory period, the Morlet wavelet time-frequency transformation method (Tallon-Baudry et al., 1997) was employed using five Morlet cycles in three standard deviations Gaussian tapered time window centred at each 100 ms in the time of interest (TOI) window to examine the time-frequency power spectrum changes related to the antisaccade task main events. The wavelet transformation was computed in two-hertz increments for each frequency band.

Then, the frequency band modulation was computed by subtracting the averaged frequency band's amplitude between trials' rest periods from its counterpart signal in each trial type's signal. Then we divided the result by the average rest period frequency band's power spectrum.

$$modulated\ avg.pow\ trial_{type} = \frac{\text{avg. pow trial}_{\text{type}} - \text{ avg. pow trial}_{rest}}{\text{avg. pow trial}_{rest}}$$

Then for each frequency band, we averaged the power spectrum across the encompassing frequencies. This process produced $m_{ROI} * n_{time}$ matrix, where m is the number of ROIs and n is the averaged power spectrum at the prespecified ten 100 ms TOI windows for each period per trial type for the anticipatory period.

For the post-stimulus period, we increased the temporal resolution to 20 ms to examine the subtle time changes related to stimulus presentation and saccade response. Trials were divided into anticipatory (preparatory) and response periods. The anticipatory period was analysed using stimulus-locked analysis. The time of interest (TOI) for the anticipatory period begins at cue presentation and ends 100 ms post-stimulus presentation (-800 to 100 ms relative to the stimulus). We included the

first 500 ms post-stimulus presentation in the analysis. Only correct trials were used in the analysis, conditioned to have a response within 500 ms from stimulus presentation.

To examine the effect of the laterality, we categorised prosaccade and antisaccade trials into ipsilateral and contralateral trials. Trials laterality describes the stimulus presentation hemifield relative to the OCN ROIs hemisphere Table 4.2.

Table 4.2 The description of laterality in the anticipatory and post-stimulus periods (relative to stimulus presentation hemifield).

Stimulus presentation hemifield	**Region's hemisphere**	**Stimulus laterality**	
		Prosaccade	**Antisaccade**
Right	**Right**	Ipsilateral	Ipsilateral
Right	**Left**	Contralateral	Contralateral
Left	**Right**	Contralateral	Contralateral
Left	**Left**	Ipsilateral	Ipsilateral

Several methods were described to examine the effect of stimulus laterality on the attentional shift (Moon et al., 2007, Mazzetti et al., 2019, Belyusar et al., 2013, Sauseng et al., 2005). However, some of the described methods were computationally demanding or challenging to understand either contrasting the attention hemifield and neglecting the hemisphere or the other way around. We used a method similar to the one used by Sauseng et al. (2005) to compute a simple laterality index that accounts for both the hemisphere and hemifield at the same time for the same event. The laterality index was computed by subtracting the ipsilateral from the contralateral trial's time course, which contrasts the effect of the contralateral stimulus as positive values and the ipsilateral stimulus as negative values.

$$Laterality\ Index_x = Contralateral_x - Ipsilateral_x$$

4.3 Results

4.3.1 Anticipatory period

Given the described role of Alpha and Beta bands, we predict that Alpha and Beta will increase late in the anticipatory period for the frontal OCN regions more than in occipital regions, especially for the FEF, reflecting the inhibition of premature responses. Moreover, we expect Trial types to exhibit different Alpha and Beta bands modulation reflecting the inhibition of reflexive prosaccades.

We expect the active treatment condition to modulate the time course of the OCN regions to reach peak amplitude at a faster rate than the sham condition. Furthermore, given the asymmetry in the tDCS delivery, we expect Treatment conditions to manifest different hemispheric modulation.

4.3.1.1 Alpha band Modulation

To examine the Alpha band modulation, we used the change in Alpha band ERSP during the anticipatory period relative to the baseline (the rest between trial blocks) as our dependent measure to conduct the multivariate analyses reported in this section. We first conducted a five-way mixed-design **exploratory** ANOVA with Treatment conditions (two levels: tDCS or sham) as a between-subjects factor and four within-subjects factors defined as; Time course (17 levels: 17 50-ms time bins), Trial Type (two levels: prosaccade and antisaccade), Hemisphere (two levels: right or left), and OCN Regions (four levels DLPFC, FEF, anterior insula, and the PEF).

There was a significant main effect of Time, F (3.4, 116.4) = 4.09, p = .006, and a significant main effect of Regions, F(2.151, 73.128) = 5.194, p = .007. However, there was a significant effect of Time by Region interaction, F(6.1,208.5) = 8.715, p < .001. This finding indicates that the time course of the Alpha band during the anticipatory period exhibited significant differences between OCN Regions (illustrated in Figure 4.2). However, it does not indicate which regions exhibit significant anticipatory temporal changes.

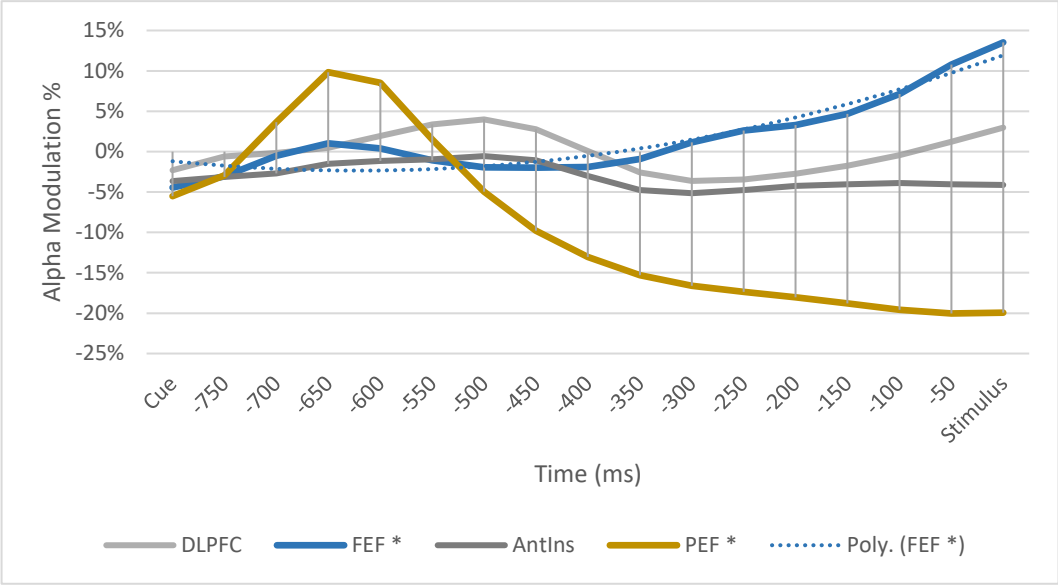

Figure 4.2 Illustrates the significant effect of Time by Regions interaction in the Alpha band. The time course of the FEF exhibited an increase in Alpha synchronisation 400 ms pre-stimulus up to the stimulus presentation time. The time course of the PEF demonstrated an initial synchronisation peak at 150-200 ms post-cue presentation, followed by a progressive decrease in Alpha synchrony until the stimulus presentation time. The asterisks (*) represent a significant main effect of Time (p <.05).

To find which regions exhibited significant Alpha band anticipatory changes with time. We conducted a **second** mixed-design ANOVA for each Region separately with Treatment conditions (two levels: tDCS or sham) as a between-subjects factor and three within-subjects factors defined as; Time (17 levels: 17 50-ms time bins), Trial Type (two levels: prosaccade and antisaccade), Hemisphere (two levels: right or left).

The changes in Alpha time course were significant for the FEF, $F(2.3, 78.8) = 3.636$, $p = .025$, and for the PEF, $F(3.4, 116) = 10.12$, $p < .001$. The FEF exhibited a significant quadratic polynomial contrast, $F(1, 34) = 6.581$, $p = .015$, which illustrated a peak in Alpha synchronisation at 150 ms post-cue followed by an increasing progressive synchronisation from 400 ms post-cue up to stimulus presentation (Figure 4.2). The PEF time course exhibited a peak Alpha band synchronisation within the 150-200 ms post-cue presentation, followed by progressive desynchronisation down to stimulus presentation (Figure 4.2). The main effect of time did not reach a significant level in the DLPFC, $F(3.5, 119.5) = 1.038$, $p = .385$, or in the anterior insula, $F(6.3, 214.6) = 1.448$, $p = .195$ (Figure 4.2). These results indicate that the significant differences in the Time by Regions interaction of the primary ANOVA represent the

different Alpha band time courses in the FEF and the PEF during the anticipatory period. In accord with the prediction that Alpha would increase late in the anticipatory period for the frontal OCN regions more than in occipital regions, reflecting the inhibition of premature responses.

The exploratory ANOVA revealed an expected significant modulatory effect of Trial type by Hemisphere by Regions interaction, $F(2.6, 86.6)$, $p = .004$. We examined this interaction in the second ANOVA. Only the DLPFC exhibited a significant effect for the Hemisphere by Trial type interaction, $F(1,34) = 8.633$, $p = 0.006$. This finding indicates different DLPFC hemispheric engagements based on the Trial type modulation of the Alpha band (illustrated in Figure 4.3). To find which DLPFC is move involved for each trial type, we conducted a mixed design ANOVA for each trial type independently, with treatment conditions as between the subjects' factor and two within-subjects factors (2 hemispheres x 17 time-bins).

There was a trend-level effect of Hemisphere differences (averaged across time) for the prosaccade trials, $F(1, 34) = 3.966$, $p = .055$, with greater Alpha synchronisation in the left hemisphere. There was no significant effect of Hemispheric differences for the antisaccade trials, $F(1, 34) = .891$, $p = .352$. These results imply that each DLPFC exhibited significantly different Alpha band modulation for each Trial type. The left DLPFC exhibited a pronounced Alpha band desynchronisation for antisaccade trials throughout the anticipatory period. The right DLPFC illustrated pronounced desynchronisation at 300 ms before the imperative stimulus presentation. These results suggest the engagement of the left DLPFC in preparation for antisaccade trials and the right DLPFC for prosaccade trials.

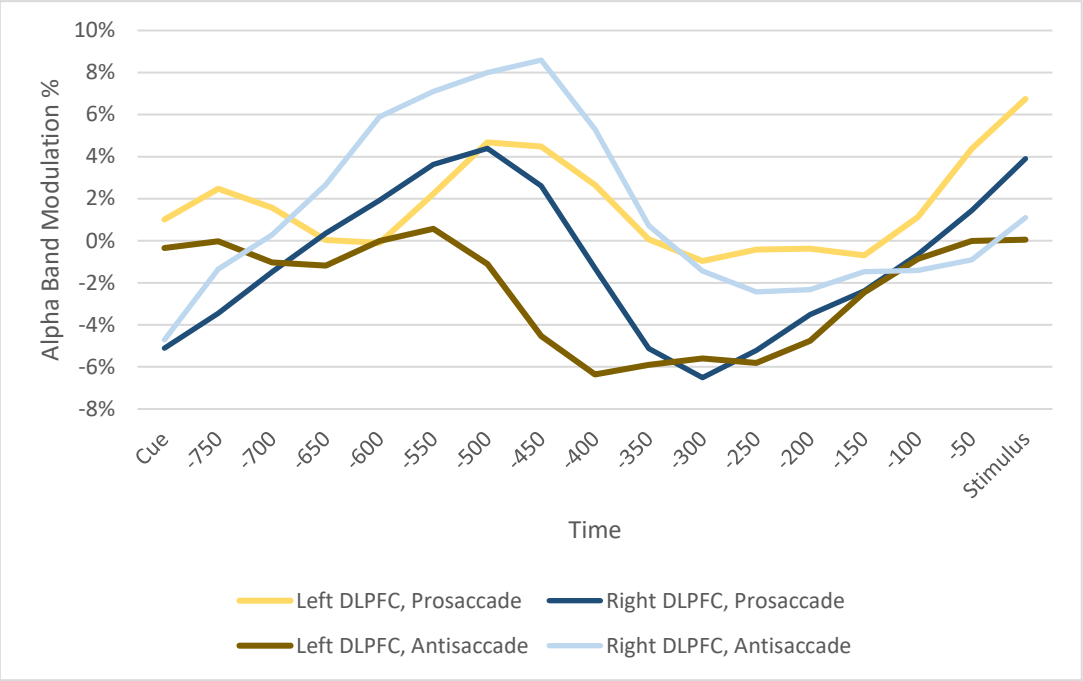

Figure 4.3 Illustrates the significant effect of The Hemisphere by Trial type interaction in the DLPFC for Alpha band modulation (p = .006). The Alpha band illustrated, on average across time and condition, a desynchronisation in the left DLPFC for antisaccade trials and the right DLPFC illustrated a synchronisation for antisaccade trials. The prosaccade exhibited Alpha synchronisation in the left DLPFC and desynchronisation in the right DLPFC.

Effects of treatment conditions

There was a significant effect for the Hemisphere by Treatment conditions interaction, $F(1, 34) = 8.172$, $p = .007$, which indicate a significant difference between treatment condition in the Alpha band averaged across each hemisphere. We further investigated this interaction by exploring the effect of treatment condition modulation on each Hemisphere separately. We conducted a four-way mixed ANOVA with three defined within-subjects factors; Trial Types (two-level; prosaccade, antisaccade), Regions (four-level; DLPFC, FEF, AntIns, PEF), Time (17-level; 17 50-ms time-bins), with the Treatment conditions being between the subject's factors.

There were no significant differences between treatment conditions in the left hemisphere, $F(1, 34) = 0.403$, $p = .53$. However, the right hemisphere illustrated a significant between-subjects effect of treatment condition, $F(1, 34) = 6.019$, $p = .019$, whereby the Sham condition exhibited Alpha band synchronisation. In contrast, the tDCS condition illustrated a desynchronisation of Alpha.

We then examined if the effect of each Treatment condition on the right Hemisphere significantly differed from its baseline by examining the intercept of a three-way repeated measure ANOVA with three within-subjects factors Trial Types (two-level; prosaccade, antisaccade), Regions (four-level; DLPFC, FEF, AntIns, PEF) Time (17-level; 17 50-ms time-bins) conducted for each Treatment group independently. The average change in the right hemisphere's Alpha band across all factors did not differ from the baseline (between trials' rests) in the sham condition, $F(1, 17) = 0.492$, $p = .0493$. However, the tDCS condition exhibited a significant difference from baseline, $F(1, 17) = 12.773$, $p = .002$ (Figure 4.4). This finding indicates the significant modulatory effect of tDCS on the preparatory Alpha band increased the right hemisphere desynchronisation during the anticipatory period relative to the between trial's rests. Furthermore, it supports our prediction that asymmetric active tDCS induces different hemispheric modulations prominent in the stimulated hemisphere.

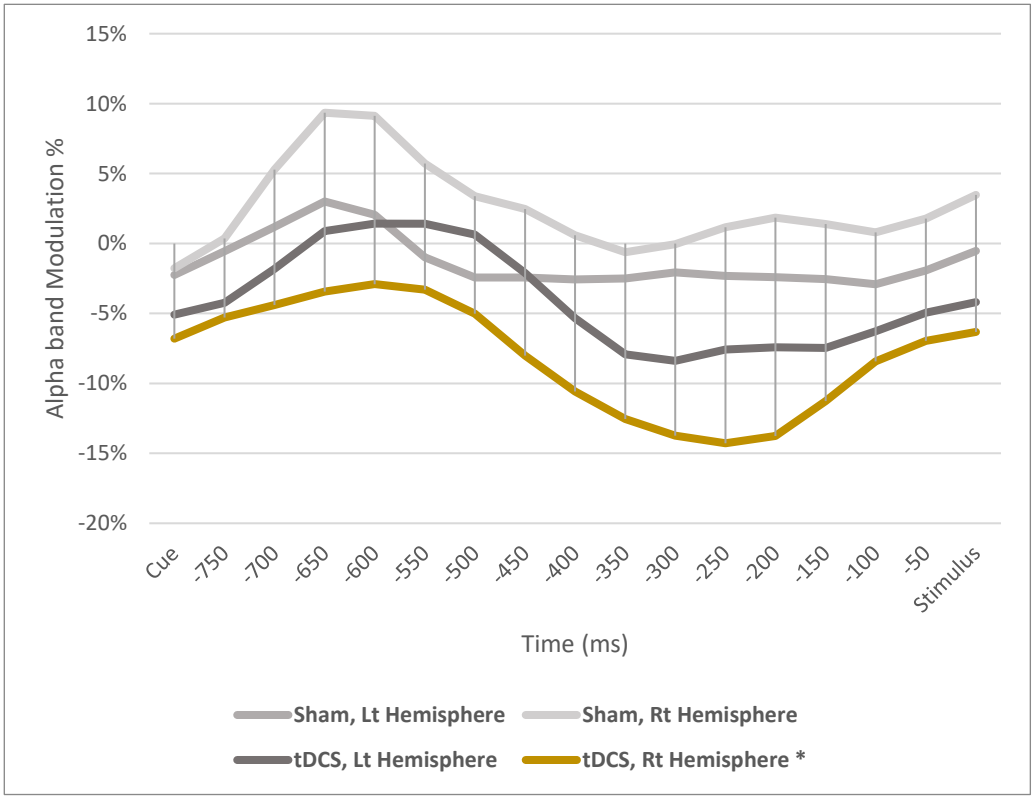

Figure 4.4 The effect of Hemisphere by Treatment conditions on the average change in Alpha band, across other factors, during the anticipatory period relative to the between trials' rests. The tDCS group illustrates more Alpha desynchronization in the right hemisphere, where the sham group exhibited a synchronization tendency. The asterisk (*) represent a significant deviation from the baseline (p = 0.002) on the averaged modulation in the right hemisphere of the active tDCS condition.

4.3.1.2 Low-Beta band Modulation

We used the change in low-Beta band modulation during the anticipatory period relative to the between trials' rests as the dependent variable to conduct the multivariate analyses reported in this section. We first performed an exploratory five-way mixed-design ANOVA with treatment conditions between the subject's factors and four within-subjects factors; Trial Types (two-level: antisaccade; prosaccade), Hemispheres (two-levels: right; left), Regions (four-level: DLPFC; FEF; AntIns; PEF), and Time (17-levels: 17 50ms time-bins).

There were a significant Beta-band changes with Time, $F(6.1, 206.7) = 4.349$, $p < .001$. and a significant different low-Beta band modulation between Regions, $F(2.2, 78) = 29.207$, $p < 0.001$. However, there was a significant effect of the Regions by Time interaction, $F(13.3, 450.6) = 3.681$, $p < .001$ (illustrated in Figure 4.5). To examine the Time by Regions interaction, we conducted a four-way mixed ANOVA in each Region, with Treatment conditions as the between-subjects factors and three within-subjects factors. These factors were: Time (17 levels: 17 50-ms time-bins), Hemisphere (two-levels: right; left), and Trial Type (two-levels: prosaccade; antisaccade).

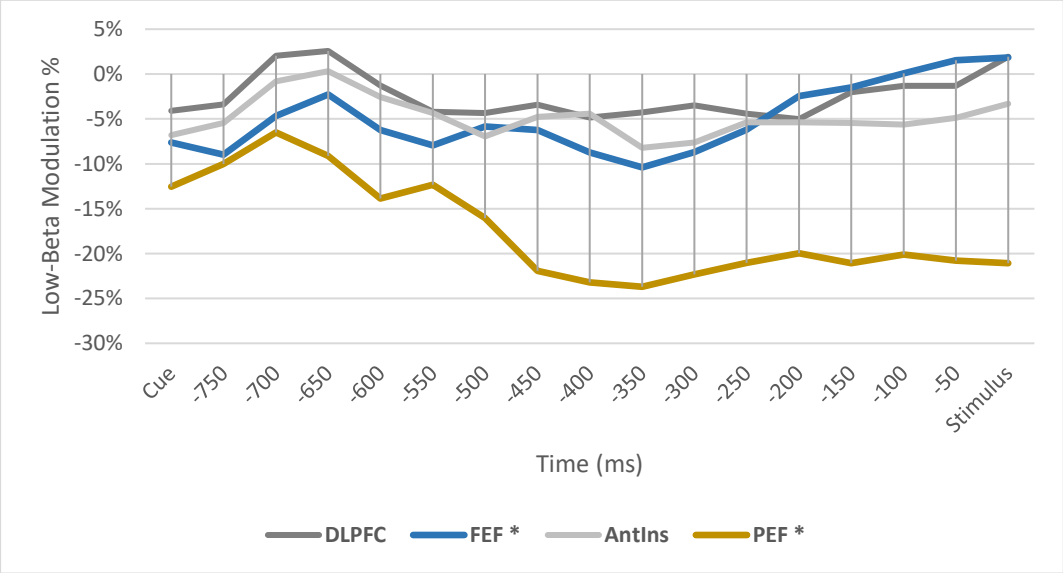

Figure 4.5 The anticipatory Low-Beta band modulation relative to the between trials' rests illustrates the significant effect of Time by Regions interaction. The frontal regions exhibit less low-Beta desynchrony than the PEF. The FEF exhibited a progressive increase in low-Beta synchronization 350 ms prestimulus up to stimulus presentation while the PEF maintained low-Beta desynchronization. The astrisks (*) represents a significant main effect of Time ($p < 0.001$) in the independent Region examination.

The changes in the low-Beta band time course, relative to the baseline, were significant for the PEF, $F(1, 34) = 8.549$, $p = < .001$, and for the FEF, $F(6.3, 215) = 3.769$, $p = .001$, which are illustrated in Figure 4.5. The PEF low-Beta band time course exhibited a desynchronisation trend overall with two peaks of decrease in desynchrony at 100 ms and 250 ms post-cue presentation followed by progressive desynchronisation to stimulus presentation. On the other hand, the FEF illustrated a low-Beta band time course with less desynchronisation than PEF and two peaks of decreased desynchrony following the ones in the PEF by 50 ms. Then the FEF time course exhibited a significant increase in synchronisation up to the stimulus presentation time. This finding suggests the active involvement of the FEF in suppressing the saccadic movement, consistent with the proposed role of the Beta band in the somatomotor area for maintaining position or inhibiting motor movement (Engel and Fries, 2010).

Effects of Treatment conditions

In the exploratory ANOVA, Treatment conditions exhibited significant differences in modulating the preparatory low-Beta band time course (effect of Time by Treatment conditions interaction), $F(6.1, 206.7) = 2.669$, $p = .016$. To investigate this interaction, we conducted a repeated measure ANOVA using four within-subjects factors; Trial Types (two-level: antisaccade; prosaccade), Hemispheres (two-levels: right; left), Regions (four-level: DLPFC; FEF; AntIns; PEF), and Time (17-levels: 17 50ms time-bins) for each Treatment condition indecently.

While the Sham condition illustrated non-significant changes in low-Beta band time course, $F(3.2, 54.2) = 1.374$, $p = .260$, the tDCS condition exhibited a significant main effect of Time, $F(3.1, 52) = 3.593$, $p = .019$, supported by a significant cubic polynomial contrast, $F(1, 34) = 14.641$, $p = .001$. Both Treatment conditions shared a similar low-Beta synchronisation pattern during the orientation phase; then, the active tDCS condition exhibited more low-Beta band desynchronisation up to the stimulus presentation. This finding indicates that active tDCS modulated the low-Beta band time course by provoking a more precise synchronisation timing with decreased desynchrony during the alertness phase to recruit essential cortical regions for the

task. There was an initial desynchronisation increase followed by a progressive gain of synchronisation during the anticipatory period (Figure 4.6).

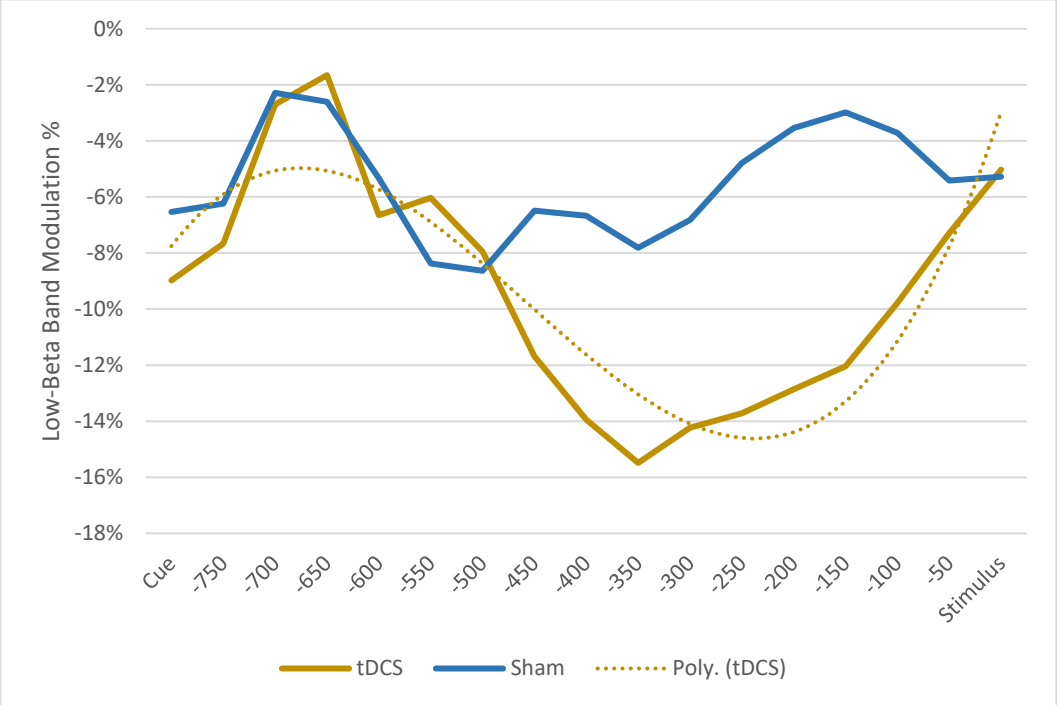

Figure 4.6 The change in anticipatory low-Beta band relative to the between trials' rests, illustrates the significant effect of Time by Treatment conditions interaction. Both treatment conditions share similar change in low-Beta synchrony for the first 300 ms post-cue presentation then diverge. The tDCS exhibit more desynchronization than the sham group. The tDCS condition time course exhibited a significant cubic polynomial contrast. The asterisk (*) represent a significant main effect of Time (p = 0.019) in the active tDCS condition.

4.3.1.3 High-Beta band Modulation

To examine the change in the high-Beta band during the anticipatory period relative to the between trials' rests, we used the change in high-Beta band modulation relative to the baseline (the rest between trials) as the dependent variable to conduct the analyses reported in this section. We first conducted a five-way mixed ANOVA with treatment conditions between the subject's factors and four within-subjects factors; Trial Types (two-level: antisaccade; prosaccade), Hemispheres (two-levels: right; left), Regions (four-level: DLPFC; FEF; AntIns; PEF), and Time (17-levels: 17 50ms time-bins).

There was a significant main effect of time, $F(6.2, 211.1) = 3.812$, $p = .001$,and main effect of Region, $F(2.8, 77.4)$, $p < .001$. However, there was a significant effect of Time by Regions interaction, $F(14.1, 477.9) = 2.891$, $p < .001$, which indicates that high-Beta modulation time course differed in each OCN Region. The Time by Region interaction is plotted in Figure 4.7.

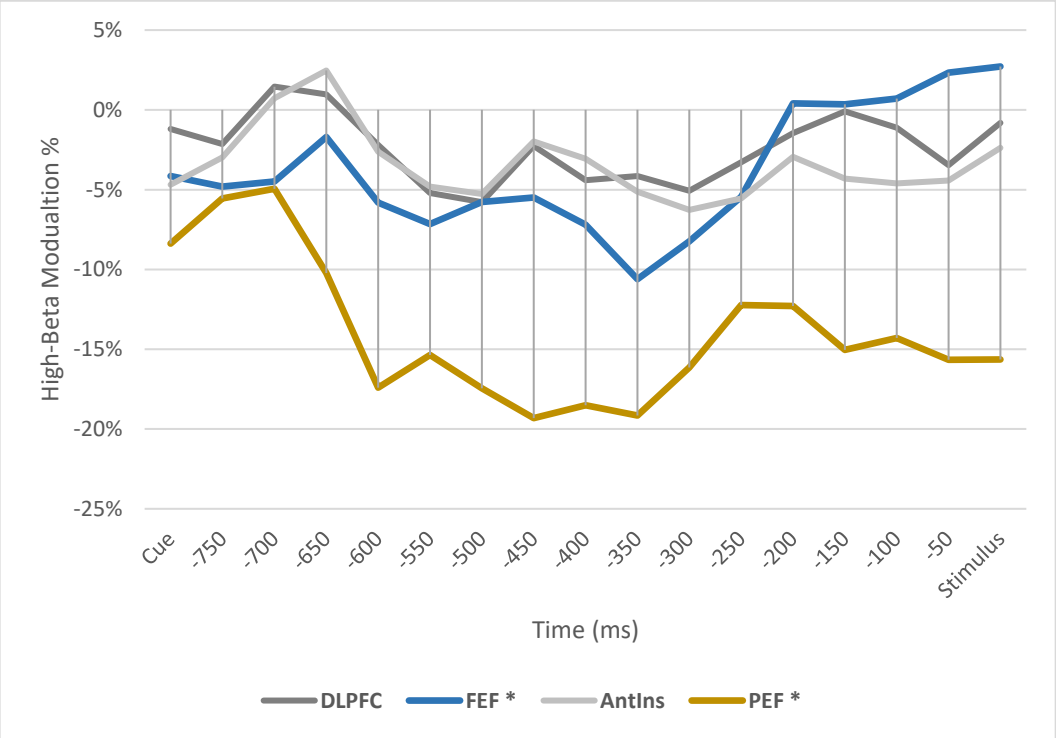

Figure 4.7 High-Beta band anticipatory illustrates modulation effects of Time by Region interaction. The FEF time course exhibited an increase in synchronisation at 150 and 350 ms post-cue presentation, followed by progressive synchronisation up to stimulus presentation. The time course of the PEF exhibited an increase in synchronisation at 100 ms and 550 ms post-cue presentation and maintained a desynchronisation trend overall. The asterisk (*) represents a significant main effect of Time in the independent Region examination (p <0.001).

We conducted four-way mixed ANOVA on each Region separately to investigate the Time by Regions interaction. The between-subjects factor was Treatment condition (two-levels: Active tDCS; Sham), and three within-subjects factors were defined as Hemisphere (two-level: left; right); Trial Type (two-level: antisaccade, prosaccade); Time (17-level: 17 50ms time-bins).

There was a significant main effect of Time for the PEF, $F(5.1, 173.1) = 6.01$, $p = < .001$, and for the FEF, $F(8.2, 278.1) = 4.275$, $p < .001$. The time course of the PEF illustrated two main peaks; the first was at 50-100 ms post-cue and a second peak at 550-600 ms post-cue presentation with high desynchronisation overall. The FEF, on the other hand, illustrated two synchronisation peaks at 150 ms and 350 ms post-cue presentation followed by progressive synchronisation gain up to stimulus presentation. This finding indicates that the difference in the PEF and the FEF high-Beta band time courses produced a significant Time by Regions interaction effect in the primary ANOVA.

There was no significant effect or interactions involving the Treatment condition in the high-Beta band.

4.3.2 Anticipatory modulation in the Visual cortex

We used the ERSP changes in the visual cortex during the anticipatory period (relative to the rests between trials) for each frequency band separately as a dependent variable to conduct three separate mixed-design ANOVAs with Treatment condition (two levels: tDCS or sham) as a between-subjects factor and two within-subjects factors defined as; Time course (17 levels: 17 50-ms time bins), and Trial Type (two levels: prosaccade and antisaccade).

There was a significant main effect of Time in the visual cortex for the Alpha-band, $F(3.2, 108) = 6.91$, $p < .001$, the low-Beta band, $F(5.7, 192.2) = 6.385$, $p < .001$, and in the high-Beta band, $F(7.7, 261.7) = 4.368$, $p < .001$, which are illustrated in Figure 4.8. The time course of the Alpha band in the visual cortex exhibited an initial decrease in desynchronisation during the first half of the anticipatory period peaking at 200 ms post-cue presentation, followed by a progressive increase in desynchronisation down to the stimulus presentation time. During the first half of the anticipatory period, the high and low Beta bands exhibited a dual peak of decreased in desynchrony at 100 and 250 ms post-cue presentation, followed by an increase in desynchronisation down to 400 ms post-cue. From 400 ms onward, the low-Beta illustrated a sustained level of desynchrony, while the high-beta exhibited a decreased desynchronisation.

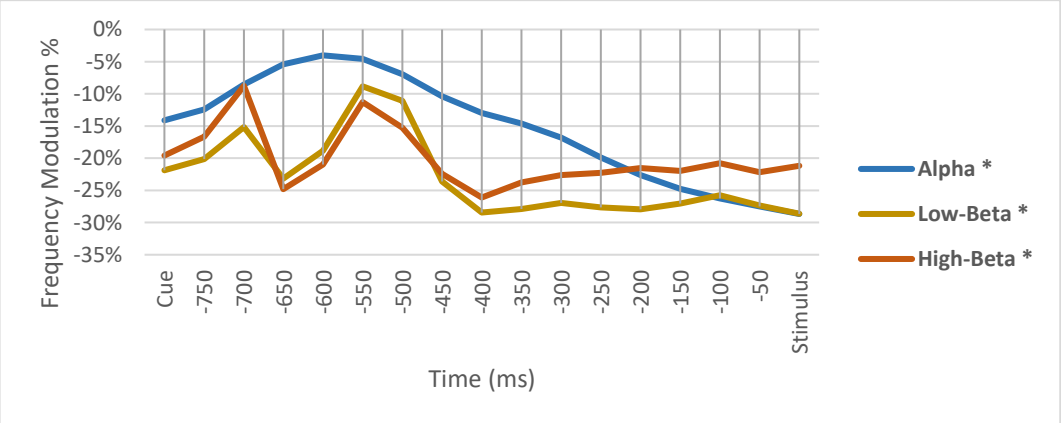

Figure 4.8 The illustrated time course of the visual cortex's Alpha, low-Beta, and high-Beta bands modulation during the anticipatory period relative to the between trials' rests. The Alpha band exhibited an initial decrease in desynchronisation followed by increasing progressive desynchronisation. The low- and high-Beta bands illustrated dual peaks in synchronisation at 100 and 250 ms post-cue presentation, followed by sustained desynchronisation levels in the low-Beta and decreased desynchronisation levels in the high-Beta band. The asterisk (*) represents a significant main effect of Time in independently examined frequency bands (p<0.001).

4.3.3 Anticipatory period summary

There were significant modulatory changes with Time in the examined Alpha and Beta bands for the FEF and the PEF time courses. In accord with the predicted increase in the FEF Alpha and Beta band in anticipation of the stimulus, the FEF sustained a stable synchronisation level in the first half of the anticipatory period and exhibited a progressive increase in synchronisation during the second half of the examined Alpha (Figure 4.2), low-Beta (Figure 4.5), and high-Beta bands (Figure 4.7).

The PEF illustrated an initial increase in synchronisation followed by progressive desynchronisation in the first half of the anticipatory period in the examined frequency bands. During the second half of the anticipatory period, the PEF exhibited progressive desynchronisation in the Alpha band (Figure 4.2), maintained desynchrony in the low Beta (Figure 4.5), and decreased desynchronisation in the high-Beta band (Figure 4.7).

There were significant trial-type modulated hemispheric differences in the DLPFC for the Alpha band (Figure 4.3). The prosaccade trials exhibited Alpha desynchronisation in the right DLPFC and synchronisation in the left DLPFC. In contrast, the antisaccade illustrated an Alpha band synchronisation in the right and desynchronisation in the left DLPFC.

The visual cortex exhibited a significant modulation time course in the frequency bands examined (Figure 4.8). The Alpha-band illustrated an initial synchronisation increase followed by progressive desynchronisation. Low- and High-Beta bands exhibited dual peaks in the first half of the anticipatory period. The low-Beta band maintained a high level of desynchrony during the second half of the anticipatory period, while the high-Beta showed a desynchronisation decrease. Considering the anticipated role of the Beta band in suppressing task-irrelevant brain activity, the sustained desynchronization of the putative Beta bands in the final 400 ms of the anticipatory period is consistent with the suppression of distracting brain activity in the preparatory period.

Effects of Treatment conditions

In the tDCS condition, there was a significant Alpha-band desynchronisation in the right hemisphere, which resulted in a significantly different interaction of Hemispheres by Treatment condition.

The tDCS low-Beta band time course differed significantly from the Sham condition's time course averaged across all other factors. Both Treatment conditions shared a similar synchronisation time course in the first half of the anticipatory period. The tDCS exhibited greater desynchronisation than the Sham condition up to stimulus presentation (Figure 4.6). This observation suggests that active tDCS enhances the effect of low beta oscillations in suppressing irrelevant brain activity immediately preceding the expected stimulus.

4.3.4 Post-stimulus period analysis

Based on the described gathering evidence, we predict that contralateral presented stimuli will elicit a greater ERSP modulation for the FEF and the PEF. Furthermore, the antisaccade task requires a shift of attention (vector inversion). We expect a modulation of the Alpha and Beta bands' time course of signal for antisaccade trials for the FEF and the PEF contralateral to stimulus reflecting this process.

4.3.4.1 Alpha band modulation

To investigate the stimulus-induced Alpha band modulation, we used the stimulus-locked changes in the Alpha band during the post-stimulus period relative to the baseline (the rest between trial blocks) as our dependent measure to conduct the multivariate analyses reported in this section.

We conducted an exploratory ANOVA to examine the ERSP changes in the OCN regions during the post-stimulus presentation period. We employed a six-way mixed-design ANOVA with Treatment condition (two levels: tDCS or sham) as a between-subjects factor and four within-subjects factors defined as; Time (twenty-six levels: twenty-six 20-ms time bins), Trial Type (two levels: prosaccade and antisaccade), Hemisphere (two levels: right or left), Stimulus Laterality (two levels: ipsilateral, contralateral stimulus relative to the Regions' hemisphere), and OCN Regions (four levels DLPFC, FEF, anterior insula, and the PEF).

There was a significant main effect of Time, $F(2.6, 87.4) = 15.203$, $p < .001$. However, there was a significant effect of the Time by Stimulus Laterality interaction, $F(2.5, 85.377) = 3.635$, $p = .022$. The contralateral presented stimulus exhibited earlier and greater Alpha band desynchronisation from stimulus presentation up to 320 ms post-stimulus. This finding indicates, per our prediction and findings of Medendorp et al. (2005), Händel et al. (2011), that contralateral presented stimuli were associated with greater Alpha synchronisation during the first 300 ms post-stimulus presentation compared to ipsilateral stimuli (Figure 4.9).

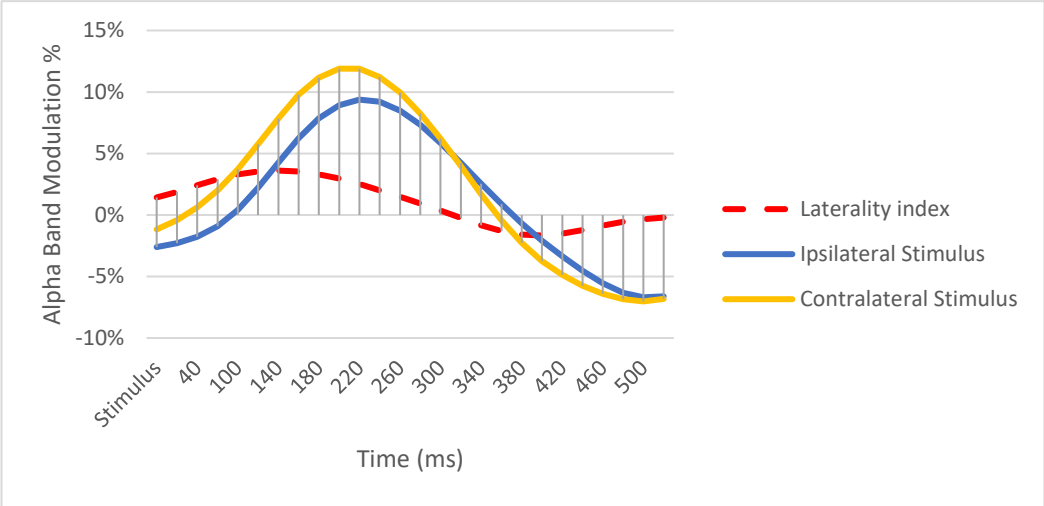

Figure 4.9 The post-stimulus modulatory effect of Time by Stimulus Laterality interaction relative to the baseline (between trials' rests) for the Alpha band averaged across all other factors. The ipsilateral stimulus exhibited less Alpha-band synchronisation in the initial 300 ms post-stimulus, and greater synchrony in the remaining post-stimulus period than the contralateral stimuli. The Laterality index illustrate the stimulus Laterality difference (contralateral-ipsilateral).

Furthermore, there was a significant effect of Stimulus Laterality by Trial Type by Regions by Hemisphere interaction, $F(2.6, 87.6) = 5.598$, $p = .002$, which implies Regional Hemispheric lateralisation differences of Alpha-band modulation for trial types and stimulus laterality. We further explored the effects of this interaction in each Region independently. We used five-way mixed ANOVA with three within-subjects factors; Time (twenty-six levels: twenty-six 20-ms time bins), Trial Type (two levels: prosaccade and antisaccade), Hemisphere (two levels: right or left), and Stimulus Laterality (two levels: ipsilateral, contralateral stimulus relative to the Regions' hemisphere), with Treatment Conditions as between-subjects factors.

Only the PEF exhibited significant modulatory differences of the Stimulus Laterality by Trial Type by Hemisphere, $F(1,34) = 8.431$, $p = .006$. We then asked which hemisphere is more sensitive to the modulatory effects of this interaction. We independently examined the effect of Stimulus Laterality by Trial type interaction in each hemisphere. The effect of Stimulus Laterality by Trial Type interaction was significant in the left PEF, $F(1, 34) = 14.229$, $p = .001$, but not in the right PEF, $F(1, 34) = 0.047$, $p = .830$. This finding implicates the left PEF in the vector inversion process involved in the antisaccade task.

To interpret the PEF engagement and response to each task category, we further investigated the modulatory effect of each Stimulus Laterality for each Trial Type in the left Hemisphere. All task categories had modulated the Alpha band significantly relative to the baseline. Interestingly the illustrated time course of these modulations showed greater Alpha desynchronisation for contralateral prosaccades compared to ipsilateral prosaccade. For the antisaccade trials, the contralateral stimulus was associated with initial greater Alpha desynchronisation that shifted towards less desynchronisation, relative to ipsilateral stimulus, at 150 ms post-stimulus presentation (Figure 4.10). These results suggest that the left PEF exhibit more task engagement for contralateral stimulus. In case the task was antisaccade, the left PEF illustrate an engagement shift towards the ipsilateral presented stimulus at around 150 ms post-stimulus presentation. These results support, partially (Moon et al., 2007)

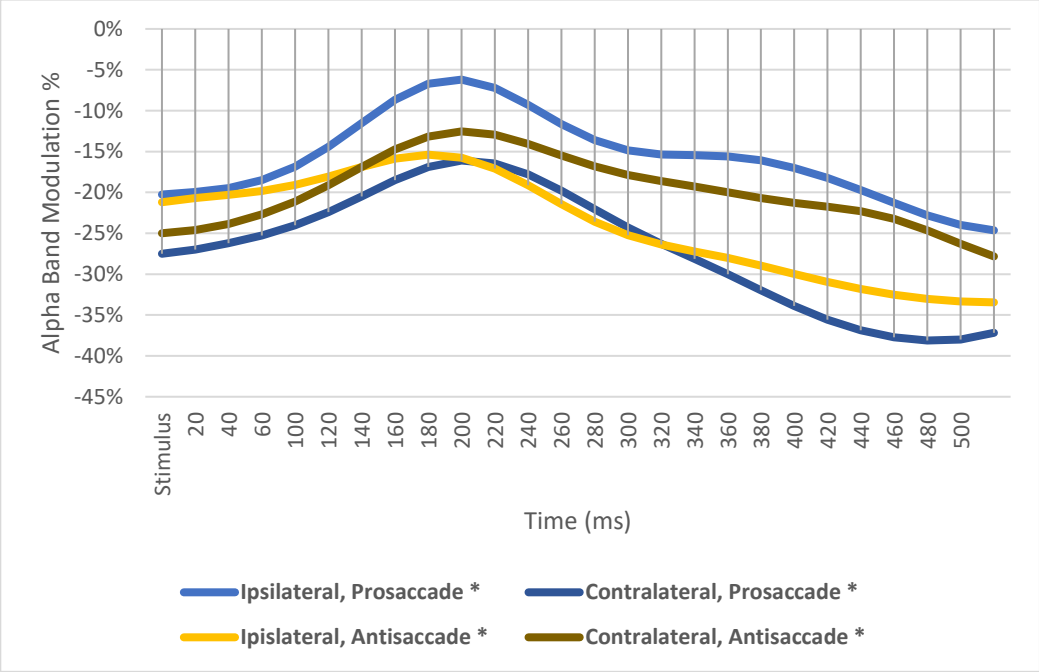

Figure 4.10 Left PEF Alpha modulation effect of Time by Trial type by Stimulus laterality illustrating greater Alpha desynchronisation in prosaccade trials for contralateral stimulus compared to ipsilateral prosaccade. Contralateral stimulus in antisaccade trials modulation exhibited a relative decrease in desynchronisation cross-over the increasing desynchronisation of ipsilateral stimulus. Asterisks (*) indicate averaged modulation (across time) significantly differ from the baseline (p <. 05).

Effects of Treatment condition

The exploratory ANOVA demonstrated a significant effect of the stimulus Laterality by Trial type by Treatment condition interaction, $F(1,34) = 5.831$, $p = .021$. However, there was a significant effect of the Treatment conditions by Hemispheres by Trial Type by Stimulus Laterality, $F(1, 34) = 11.315$, $p = .002$. This result implies that the modulatory effect of Treatment conditions on the Alpha-band was significantly different between task categories for each Hemisphere. We investigated which Hemisphere exhibited this significant effect by conducting a five-way mixed ANOVA with treatment condition as the between-subjects factor and four within-subjects factors: Laterality, Trial Type, Regions, and Time on Hemisphere independently.

The left Hemisphere did not show a significant effect of Treatment condition by Trial Type by Laterality interaction, $F(1,34) = 2.323$, $p = 0.137$. However, the right hemisphere exhibited a significant effect for this interaction, $F(1,34) = 18.375$, $p < 0.001$. This finding implies that Treatment conditions exhibited significant modulatory differences within the right hemisphere's Alpha-band activity between task categories. We investigated which Trial type was significantly modulated by the effect of the Treatment condition. We examined each Trial type independently in the right hemisphere by conducting a mixed-design ANOVA with the Treatment condition as the between-subjects factor and three within-subjects factors defined as Stimulus laterality, Regions, and Time.

The prosaccade trials did not show an effect of Treatment condition by Laterality interaction, $F(1, 34) = 11.172$, $p = .002$. On the other hand, the antisaccade trials had a significant Treatment condition by Laterality interaction, $F(1, 34) = 11.172$, $p = .002$, for which we examined the between-subject Treatment effect of ipsilateral and contralateral antisaccade trials independently.

The Ipsilateral antisaccade exhibited a non-significant between-subjects effect, $F(1, 34) = 0.271$, $p = .606$. The between-subjects effect of the Treatment condition was significant for contralateral presented stimuli for antisaccade trials in the right hemisphere, $F(1, 34) = 7.812$, $p = .008$. We then examined this effect in each Treatment condition independently using two-way repeated measures ANOVA with

Time and Regions as the within-subjects factors. In the active tDCS condition, the intercept of contralateral antisaccade did not differ significantly from the baseline, $F(1, 17) = 1.077$, $p = .314$. However, in the Sham condition, the modulatory effect of contralateral antisaccade exhibited a significant synchronisation relative to the baseline, $F=(1, 17) = 6.898$, $p = .018$.

These results indicate two points: first, in antisaccade trials, a contralateral presented stimulus is associated with greater Alpha synchronisation in the right hemisphere for the sham condition. Second, the active tDCS condition modulates the right hemisphere's Alpha band and nullifies this significant effect.

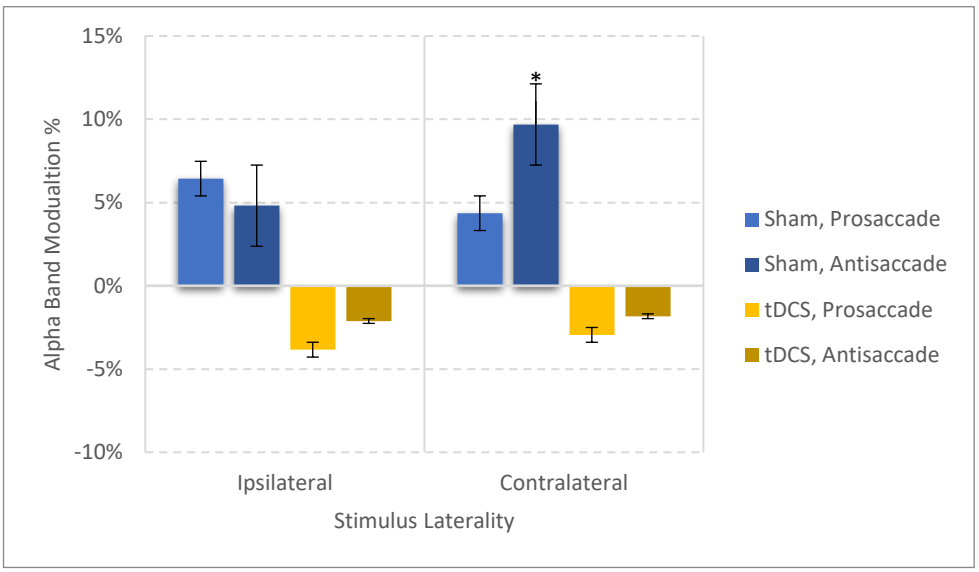

Figure 4.11 The modulatory effects of Treatment condition by Stimulus laterality by Trial type on Alpha band modulation in the right Hemisphere for all task categories in both treatment conditions. The contralateral antisaccade trials exhibited a significant synchronisation relative to the baseline (marked by the asterisk (*) $p < .05$). The active tDCS condition did not exhibit a significant effect.

4.3.4.2 Low-Bata Band modulation

We used the stimulus-locked changes in the low-Beta band during the post-stimulus period relative to the baseline (the rest between trial blocks) as the dependent variable to conduct the multivariate analyses reported in this section.

We conducted an exploratory ANOVA to examine the low-Beta band modulation in the OCN regions during the post-stimulus presentation period. We employed a six-way mixed-design ANOVA with Treatment condition (two levels: tDCS or sham) as a between-subjects factor and four within-subjects factors defined as; Time (twenty-six levels: twenty-six 20-ms time bins), Trial Type (two levels: prosaccade and antisaccade), Hemisphere (two levels: right or left), Stimulus Laterality (two levels: ipsilateral, contralateral stimulus relative to the Regions' hemisphere), and OCN Regions (four levels DLPFC, FEF, anterior insula, and the PEF).

There was a significant effect of low-Beta band modulation difference between Regions, $F(1.9, 65.7) = 25.525$, $p < .001$. However, there was a significant effect of Regions by Trial Type interactions, $F(2.3, 78.7) = 4.837$, *p = .007, which we investigated in each region independently using* five-way mixed ANOVA with treatment conditions as the between-subjects factor and four within-subjects factors: Hemisphere, Laterality, Trial Type, and Time.

The effect of the Trial Types was significant only in the PEF, $F(1, 34) = 24.418$, $p < .001$, whereby prosaccade trials, on average, exhibited less low-Beta desynchronisation with a noticeable decrease 200-300 ms post-stimulus relative to antisaccade trials. Considering the PEF's proposed role in spatial localisation, the Beta band in long-distance, regional activation and the timing of the prosaccade desynchronisation decrease, this finding could indicate a saccade direction initiation. However, further investigations are required to interpret this finding.

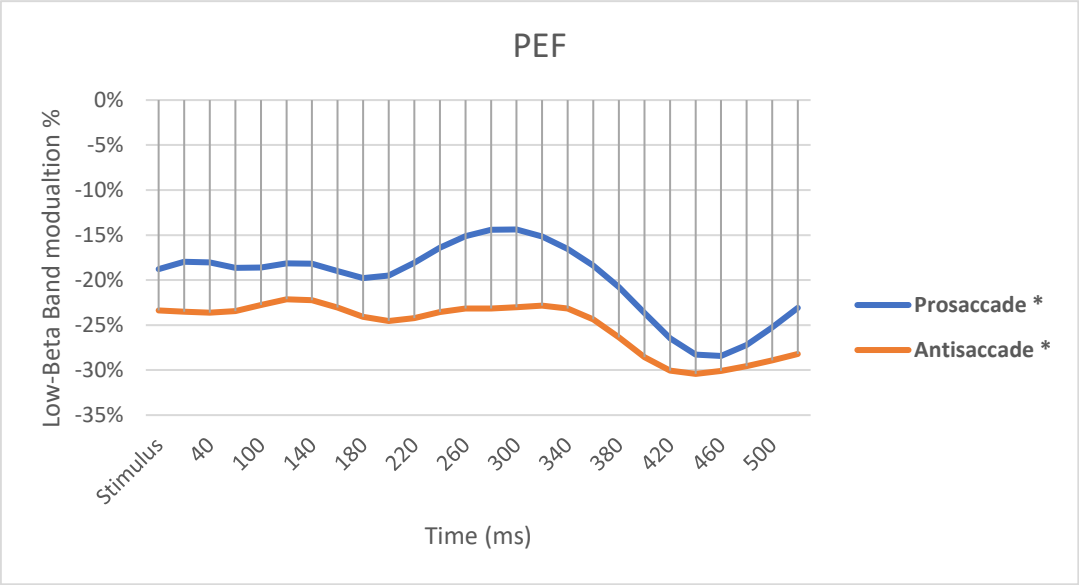

Figure 4.12 Low-Beta band Trial type modulation in the PEF exhibited a more significant desynchronisation for antisaccade than prosaccade trials during the post-stimulus period. The prosaccade trials illustrated a decrease in desynchronisation begins around 220 ms that could indicate a saccade direction signaling mechanism. Asterisks (*) indicate significant level of (p <.001)

Effects of Treatment conditions

In the exploratory ANOVA, there was a significant effect of the Treatment conditions by Regions by Trial Type interaction, *F(2.3, 78.7) = 3.477, p* = .03. However, There was a significant effect of the Treatment conditions by Regions by Trial Type by Stimulus Laterality interaction, *F*(2.2, 75.3) = 3.415*, p* = .034, which we explored in each Region independently, using a five-way mixed ANOVA with treatment condition as the between-subjects factor and four within-subjects factors: Hemisphere, Laterality, Trial Type, and Time.

The modulatory effect of the Treatment condition by Trial Type by Stimulus laterality interaction was only significant for the FEF, *F*(1, 34) = 6.003, *p* = .02. We then examined the effect of Treatment condition by Stimulus Laterality in each Trial Type independently. We used a four-way mixed ANOVA with the Treatment condition as the between-subjects factor and three within-subjects factors: Hemisphere, Laterality, Trial Type, and Time.

The effect of Treatment condition by Stimulus Laterality was significant for prosaccade trials, F(1, 34) = 9.475, *p* = .004, but not for antisaccade Trials, *F*(1, 34) = 0.634, *p* = .431. Then, we sought to examine which Treatment condition exhibited

greater differences for prosaccade stimulus laterality. We employed a three-way ANOVA with three within-subjects factors (2 x Hemisphere, 2 x Laterality and 26 x Time bins) to examine the differences between stimulus laterality for the prosaccade trials in each Treatment condition independently.

The Sham condition exhibited a significant difference for stimulus Laterality in the FEF, $\underline{F}(1, 17) = 7.428$, $p = .014$. However, the active tDCS condition did not show a significant difference for stimulus Laterality in prosaccade trials, $F(1, 17) = 3.012$, $p = .101$. We examined the intercept of two-way repeated measures ANOVA for each stimulus laterality independently in the Sham condition, using two within-subjects factors (Hemisphere and Time). Neither the ipsilateral, $F(1, 17) = 0.683$, $p = .42$, nor the contralateral stimulus exhibited a significant difference from the baseline, $F(1, 17) = 0.005$, $p = .945$. These results indicate that FEF low-Beta band modulation for ipsilateral stimulus differs significantly from the contralateral stimulus in the Sham condition. The active tDCS condition modulated the low-Beta band and decreased this difference to non-significant (Figure 4.13).

For illustration purposes, we plotted the stimulus laterality index for Trial Types by Treatment conditions (Figure 4.13), which illustrates that contralateral presented stimulus for prosaccade trials exhibited greater desynchronisation than ipsilateral stimulus during the post-stimulus period in the Sham condition. The antisaccade demonstrated a greater synchronisation for contralateral stimuli than ipsilateral ones. In contrast, in both trial types, the active tDCS demonstrated a similar pattern of initially greater low-Beta synchronisation for contralateral presented stimulus. Then the ipsilateral stimulus exhibited greater synchronisation at 200 ms and 260 ms post-stimulus presentation for antisaccade and prosaccade trials, respectively.

Collectively, these results imply a) active tDCS condition had a significant impact on changing the stimulus Laterality's low-Beta band modulation for prosaccade trials, in low-Beta band modulation for FEF. B) The FEF exhibits a stable low-Beta band activity for antisaccade trials that was not significantly modulated by

the active tDCS, but was reshaped into, what seems to be, a more precise timing of activity.

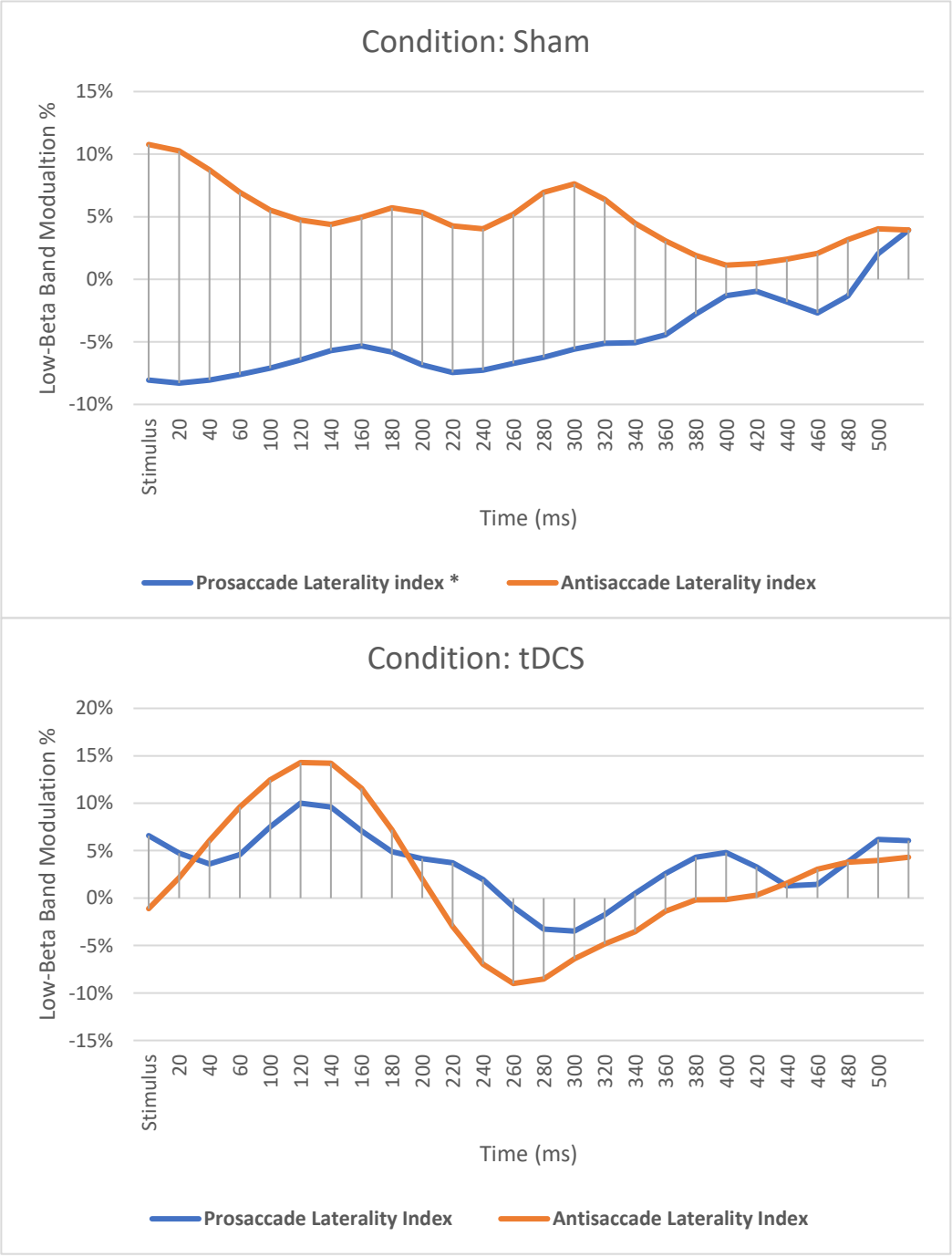

Figure 4.13 The FEF Low-Beta band Laterality index illustrates the effect of Treatment condition by Trial Type by Stimulus Laterality interaction. Positive laterality index reflects greater synchrony for contralateral trials and negative value implies more synchrony for ipsilateral stimulus. While prosaccade contralateral stimulus exhibit significantly less low-Beta synchronisation than ipsilateral stimulus, the opposite is true for the antisaccade stimulus (more synchronisation for contralateral than ipsilateral stimulus). This relationship between stimulus laterality and Trial types is distorted in the active tDCS condition. Asterisk (*) indicate significant difference between stimulus laterality in prosaccade trials (p <.05).

Furthermore, there was a significant effect of the Treatment conditions by Hemisphere by Trial Type by Stimulus Laterality interaction, $F(1, 34) = 8.392$, $p = .007$, on modulating the post-stimulus low-Beta band. We investigated this effect in each Hemisphere separately by conducting a five-way mixed ANOVA with treatment condition as the between-subjects factor and four within-subjects factors: Laterality, Trial Type, Regions, and Time. While the left Hemisphere did not show a significant effect of Treatment condition by Trial Type by Laterality interaction, the right hemisphere exhibited a significant effect, $F(1, 34) = 6.948$, $p = .013$. Then we examined the effect of Treatment condition by Laterality for each Trial Type independently within the right hemisphere. The Treatment condition by Laterality interaction exhibited a significant effect for prosaccade trials, $F(1, 34) = 5.186$, $p = .029$, but not for antisaccade trials, $F(1, 34) = 1.535$, $p = .224$.

We then examined the right Hemisphere Prosaccade stimulus Laterality effect in each Treatment condition independently by using repeated measures ANOVA with three within-subjects factors: laterality, Regions, and Time. The Laterality effect was significant for the Sham condition, $F(1, 17) = 9.726$, $p = .006$, and not significant for the active tDCS condition, $F(1, 17) = 0.015$, $p = .904$. Examining the intercept of ipsilateral and contralateral prosaccades independently in the right hemisphere for the Sham condition revealed a significant difference from the baseline for contralateral prosaccade, $F(1, 17) = 5.379$, $p = .033$, and a non-significant difference for ipsilateral trials, $F(1, 17) = 0.531$, $p = .476$. These results indicate that the active tDCS modulated the right hemisphere's low-Beta band during its active engagement in the prosaccade trials (Figure 4.14).

Figure 4.14 The low-Beta band Laterality index's time course in the right hemisphere illustrate the significant effect of Treatment condition by Trial Type by Stimulus Laterality interaction. The prosaccade index show more initial desynchronisation for contralateral trials followed by a shift in low-Beta synchrony at 160 ms later. This effect is smeared off in the active tDCS condition. The asterisk (*) represent the significant effect of Stimulus laterality for prosaccade trials ($p < .05$).

4.3.4.3 High-Beta band modulations

The dependent variable used to conduct the multivariate analyses reported in this section was the stimulus-locked changes in the low-Beta band during the post-stimulus period relative to the baseline (the rest between trial blocks). There was a significant main effect of Time, $F(4, 135.1) = 2.578$, $p = .041$. *However,* there was a significant effect of Time by Regions interaction, $F(9.8, 331.6)$, $p = .005$, illustrated in (Figure 4.15). To interpret this interaction, we conducted five-way mixed ANOVA with the Treatment condition as the between-subjects factor and four within-subject factors: Hemispheres (two-levels: left, right), Stimulus laterality (two-level: ipsilateral, Contralateral), and Trial Type (two-level: Prosaccade, antisaccade) in each Region separately.

The main effect of Time was significant in the DLPFC, $F(5.8, 196.2) = 3.057$, $p = .008$, in the FEF, $F(3.5, 119.4) = 2.588$, $p = .047$, and in the PEF, $F(4.2, 143.8) = 3.603$, $p = .007$. The time course of the FEF exhibited an initial high-Beta synchronisation for 160 ms post-stimulus, followed by desynchronisation. Given the role of the Beta-band in the somatosensory regions and the long-distance CTC theory, this shift in the FEF and PEF high-Beta synchrony could reflect the active regional communication and the transition from sustaining fixation and initiating active saccade.

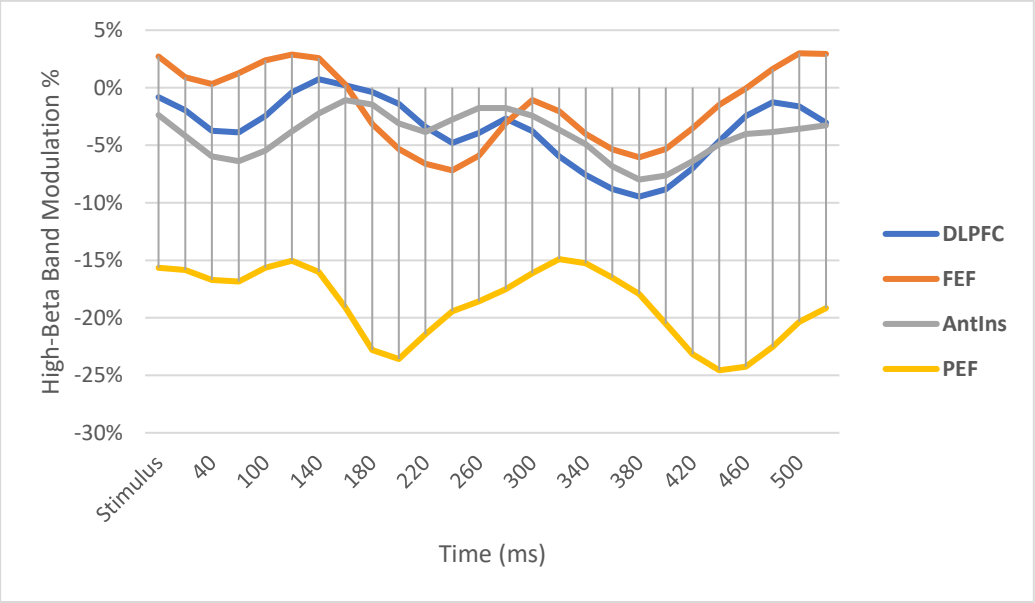

Figure 4.15 The time course of high-Beta band modulation in the homotopic OCN regions. The time by Region interaction was significant for the DLPFC, FEF, and PEF.

Effect of Treatment Condition

There was no significant effect or interaction of the Treatment condition in the high-Beta band.

4.4 Discussion

Do Alpha and Beta rise more in the frontal OCN than occipital ones during the anticipatory period?

Our results illustrated an increase in the FEF Alpha, low-Beta and high-Beta bands synchronisation during the second half of the anticipatory period up to stimulus presentation. The FEF is one of the higher-order regions implicated in voluntary saccade initiation. The CTC (Fries, 2015), among other gathering evidence (Hwang et al., 2014, Buschman and Miller, 2007), proposed a different functional role for the Alpha and Beta bands. Alpha is proposed to produce local-regional inhibition and as the prefrontal cortex (PFC) active inhibition signal for the disengagement (Fries, 2015, Jensen and Mazaheri, 2010, Hwang et al., 2014). On the other hand, the Beta band is implicated in the PFC long-distance communication and proposed to activate regions involved in task performance as an activation signal for regions involved in the task (Fries, 2015, Hwang et al., 2014).

Furthermore, the increase of the Beta band in the somatomotor regions is associated with active postural maintenance (isometric contraction) and preparation for movement (Khanna and Carmena, 2017). Considering these functional roles of Alpha, Beta and the FEF, our finding of increased Alpha and Beta during the second half of the preparatory period suggests that the increased Alpha disengages the premature saccade initiation process. At the same time, the increase in low- and high-Beta bands suggests an increased active suppression of saccades by maintaining ocular fixation on the alerting cue (resembling isometric contraction in the somatomotor region) in preparation for the imperative stimulus presentation. This finding is further supported by the progressive desynchronisation of the high-Beta band during the post-stimulus period, reaching maximum desynchronisation around 250 ms post imperative stimulus presentation. Interestingly, the average median

reaction time for both trial types is around 255 ms. These findings further support the role of the FEF Beta band in eliciting voluntary saccades.

Moreover, we found a persistent Alpha band desynchronisation during the second half of the preparatory period for the PEF. This desynchronisation indicates the active engagement of the PEF in preparation for spatial localisation of the imperative stimulus. Romei et al. (2010) used TMS at Alpha band frequency to stimulate the PEF before presenting visual stimuli. This stimulation impaired target detection in the contralateral visual field. Our results support this role of PEF sensitivity for stimulus lateralisation, as we found that only the PEF post-stimulus Alpha band was associated with stimulus presentation and laterality, showing initial higher sensitivity for contralateral presented stimuli (Figure 4.10) (Moon et al., 2007). The PEF hemifield sensitivity is further implicated in the vector inversion process of the antisaccade trials. The initial engagement of the PEF contralateral to the presented stimulus is reversed around 150 ms after the stimulus presentation towards a greater engagement for the ipsilateral PEF. This finding is supported by a gathering neuroimaging evidence suggesting the PEF pivotal role in the vector remapping process (Belyusar et al., 2013, Moon et al., 2007, Medendorp et al., 2005, Sereno et al., 2001, Corbetta et al., 2000)

- Are there preparatory regional differences between antisaccade and prosaccade?

Moreover, our results illustrated significant hemispheric differences in the DLPFC for trial types (Figure 4.3). In the prosaccade trials, the Alpha band exhibited a desynchronisation in the right DLPFC and synchronisation in the left DLPFC. For antisaccade, there was an Alpha synchronisation in the right and desynchronisation in the left DLPFC. Considering a) the proposed role of the DLPFC in cognitive control (Miller and Cohen, 2001, Buschman and Miller, 2007, Jensen and Bonnefond, 2013). b) The different hemispheric roles in the orientation of attention (Buschman and Miller, 2007, Posner and Petersen, 1990). c) The role of Alpha and Beta bands within the prefrontal cortex (Jensen and Bonnefond, 2013, Hwang et al., 2010) and in the CTC (Fries, 2015). This finding supports the engagement of the right DLPFC for prosaccade trials. The antisaccade trials exhibited a disengagement of the right DLPFC

and increased recruitment of the left DLPFC in preparation for fast decision taking during the phasic response period. However, we could not find a trial-type specific increase in the DLPFC for either of the putative Beta-bands as reported by Hwang et al. (2014). This discrepancy might be caused by the differences in the defined Beta-band oscillation range where we used 13-20Hz and 20-30Hz for low- and high-Beta-bands respectively, and they used a wider range for their analysis of Beta-band (18-38Hz). Moreover, we used an antisaccade task with an 800ms anticipatory period in contrast to their 1500ms preparatory period, which could obscure the increase in the right DLPFC they described to appear around 922ms post task-cue presentation.

What are the modulatory effects of active tDCS compared to sham stimulation?

Max et al. (2021) examined the effect of tDCS (1 mA and 2 mA) combined with a food-modified antisaccade task in a sample of people with binge eating disorder. They found decreased antisaccade reaction times in the group allocated to 2 mA and an increased RT in the 1 mA group. They reported a decrease in the binge eating episodes in the 2 mA group and no change in the other groups. Our finding illustrates enhanced reaction times for the active tDCS condition on both trial types compared to the sham condition (Table 3.1), which did not reach a significant level. This finding indicates an ameliorated effect of the 1.25 mA stimulation we used and implies a possible more significant effect with stimulation parameters modification or increasing number of tDCS sessions.

In line with our prediction, the asymmetric application of tDCS has modulated the right OCN regions' Alpha band activity during the anticipatory and response periods of the antisaccade task. The tDCS significantly decreased the right hemisphere Alpha band synchronisation during the anticipatory period (Figure 4.4). Moreover, it caused significant right hemisphere Alpha band suppression post-stimulus presentation in antisaccade trials compared to the sham condition (Figure 4.11). These findings could reflect the effect of asymmetric modulation of anodal tDCS over the right hemisphere. Alternatively, considering A) the right hemisphere's pivotal role in the DAN and in the preservation of tonic attention fundamental for the

bottom-up cognitive processing and B) the Alpha band functional inhibition effect (Petersen and Posner, 2012, Foxe and Snyder, 2011), these findings suggest a constructive impact of active tDCS in augmenting the functional recruitment of the right hemisphere responsible for the bottom-up cognitive processing and executing reflexive saccades.

Furthermore, active tDCS modulated the low-Beta band during the preparatory period across the putative OCN regions and during the post-stimulus period for the FEF and the right hemisphere. Active tDCS increased low-Beta band desynchronisation for the preparatory but not during the alerting phase of the anticipatory period across OCN regions and trial types (Figure 4.6). This finding implies that active tDCS decreased OCN engagement overall during the preparatory period to allow for more efficient antisaccade task-relative regions to be recruited, given the role of the Beta band in active long-distance top-down recruitment for regions essential for task performance (Fries, 2015). During the post-stimulus period, the active tDCS increased the FEF low-Beta band synchronisation post-stimulus for contralateral presented stimuli in prosaccade trials (Figure 4.13). Considering A) the implicated role of the FEF in initiating voluntary contralateral saccades (Bruce et al., 1985, Everling and Munoz, 2000, Gaymard et al., 1999), B) the greater neurophysiological response for contralateral stimuli in regions involved in the bottom-up processing (Sereno et al., 2001, Hsu et al., 2021), and C) the top-down cognitive control of Beta-band (Fries, 2015, Hwang et al., 2014), this finding suggests that active tDCS increases contralateral FEF engagement in response to the imperative stimulus presentation, which could produce with repeated exposure or better stimulation parameters in beneficial behavioural results. In addition, the active tDCS increased the low-Beta band synchronisation in the right hemisphere for contralateral presented stimuli in prosaccade trials. This finding suggests that active tDCS enhance the reflexive response associated with the right hemisphere roles in the bottom-up processing for prosaccade trials (Petersen and Posner, 2012). tDCS also decreased right hemisphere engagement (Beta-band synchronisation) for antisaccade trials, which demand a top-down cognitive control (Petersen and Posner, 2012).

In summary, our results support the functional inhibitory role of the Alpha band and the top-down control of Beta, which strengthen the executive control effect of FEF and the spatial localization of the PEF in the putative OCN. This finding confirms our prediction of increased Alpha and Beta band in frontal than occipital regions. Moreover, our results illustrated the involvement of the PEF in the vector remapping process of the antisaccade task. In addition, we found evidence of implicate the DLPFC in the decision-making process involved in the antisaccade task. We demonstrated the effects of active tDCS on constructive modulation for the Alpha and Beta bands of the OCN during the antisaccade task. The produced neuromodulations had a non-significant positive impact on the behavioural performance of the task.

This concludes our investigations on the neuromodulatory effect of active tDCS delivered during the performance of the antisaccade task. In the next chapter, we will discuss the neuromodulatory effect of cognitive training on resting state functional connectivity changes as measured by fMRI.

Chapter 5 Cognitive training and inhibitory control

5.1 Introduction

In the previous chapters, we examined the neuromodulatory effects of an external neuromodulator on altering the brain functions assessed using MEG and pupillometry. We investigated the short-term neuroplastic effect of the antisaccade task alone and concurrent with active tDCS on modulating cortical functional connectivity. Then, we examined the neural correlates of arousal, and ANS activation during the antisaccade task performance, for both Treatment conditions, assessed using measures of PD. Next, we investigated the ERSP during the performance of the antisaccade task. In this chapter, we aim to investigate the effect of two weeks of inhibitory cognitive control of oculomotor training (RECOGNeyes) as a neuromodulator on OCN functional connectivity assessed using fMRI.

The RECOGNeyes study was a confidence-in-concept study. It was designed to test the confidence in computerised gaze-control cognitive training as a possible therapeutic neuromodulation tool in young adults with a specific learning difficulty (SpLD) and/or ADHD (Collins, 2016, Waitt, 2022). In addition, it aims to delineate the neural and behavioural changes associated with RECOGNeyes Training. Before the commencement, the study received ethical approval from the Research Ethics Committee at the Faculty of Medicine and Health Sciences, the University of Nottingham. The University of Nottingham funded this study via a Confidence in Concept (CiC) grant from the Medical Research Council (MRC), part of the UK Research and Innovation.

The data analysed in this chapter is part of more extensive data collected and partially analysed elsewhere (Waitt, 2022). The scope of this chapter is to investigate the resting state functional connectivity (RSFC) changes in the OCN and the LC before and after randomly assigned participants to different training sessions of RECOGNeyes as inhibitory cognitive control training, assessed using resting state fMRI (RS-fMRI). We also investigated correlations between the amount of time spent training on RECOGNeyes, the antisaccade performance, and the resting state functional connectivity changes in the OCN.

5.1.1 Specific learning difficulties

There are normal variations between individuals' cognitive abilities. These variation causes an inclination towards certain learning styles and does not affect the overall academic performance of the individual. The presence of specific deficits in academic performance (1.5 – 2 standard deviations below the expected population average) with the perseverance of the general intellectual ability (as measured by the intelligence quotient IQ) is what defines specific learning difficulties (SpLD) (Hall, 2008, American Psychiatric, 2013). SpLD is a unique entity of learning difficulty and should be distinguished from general learning disabilities that is associated with a lower-than-average IQ (Hall, 2008). Individuals with SpLD show lower social skills and attention levels (Parhiala et al., 2015). They have a higher rate of having comorbid different SpLD, mood disorder (depression and anxiety) or behavioural disorder (conduct or attention deficit hyperactivity disorder) (Margari et al., 2013, Moll et al., 2020, Moll et al., 2014). SpLD could be either an isolated arithmetic (dyscalculia), reading (dyslexia), spelling (dysgraphia), motor coordination (dyspraxia), non-verbal learning difficulties or a combination of more than one type (Snowling, 2005, Hall, 2008, Moll et al., 2020).

Of the different SpLD categories, dyslexia is the most investigated and researched. The underpinning pathophysiological mechanism for SpLD needs to be better understood. A combination of genetic and environmental factors interaction is proposed to result in cognitive processing deficits in the dyslexia (Frith, 1999, Pennington and Olson, 2005, Pennington, 2006). The observed cognitive deficit implicates several visual and auditory processes that include working memory and attention (Ramus et al., 2003, Démonet et al., 2004, Alloway, 2009, Parhiala et al., 2015). The overlapping cognitive deficits between ADHD and SpLD suggest a shared pathological mechanism (Pennington, 2006, Moll et al., 2020). Growing neuroimaging evidence points towards a reduced left hemisphere connectivity prominent in the left parietal, occipital and temporal regions in patients with dyslexia relative to the controls (Démonet et al., 2004, Norton et al., 2015, Boets et al., 2013).

5.1.2 Attention deficit hyperactivity disorder

Over 63 million individuals worldwide suffer from attention deficit hyperactivity disorder (ADHD) (Polanczyk et al., 2015). On average, 5% of children are at risk of developing ADHD (Sayal et al., 2018). Furthermore, they have a 65% chance of persisting symptoms in their adulthood (Luo et al., 2019). Patients with ADHD have cognitive impairments (inattention and impulsivity), hindering their academic and social performance compared to their healthy peers (Kofler et al., 2018, Loyer Carbonneau et al., 2021). This developmental delay leads to comorbidity with anxiety, depression, and conduct disorder (Jensen et al., 2001, McGough et al., 2005). A heterogeneous combination of genetic and environmental risk factors is believed to be the precursor for the development of ADHD (Thapar et al., 2013).

Most theories seek to explain the neurobiological pathology underlying the symptoms of ADHD converge to an imbalance of the autonomic nervous system (ANS) neurotransmitters: dopamine (DA) and norepinephrine (NE) (Ziegler et al., 2016, Mehta et al., 2019). This imbalance induces abnormal brain structural development and atypical functional connectivity patterns (Vaidya, 2012, Qiu et al., 2011, Bouziane et al., 2018, Wang et al., 2021). The NE/DA imbalance in ADHD affects the normal regulation processes of the ANS with a tendency to decrease the arousal level (hypo-arousal) (Bellato et al., 2020).

The current pharmacological treatment strategies depend mainly on psychostimulants as first line of pharmacological treatment (amphetamines and methylphenidate), which require multiple daily doses for maximum efficacy (Wigal et al., 1999, Gau et al., 2008). The high frequency of doses affects patients' compliance and adherence to the prescription and, in turn, modifies its therapeutic effect (Paes et al., 1997, Gau et al., 2008). Not to mention the adverse effect of adhering to these psychostimulants could vary between emotional disturbances (anxiety, sadness), behavioural changes (insomnia, anorexia), neurological symptoms (tics and headaches), liver failure and sudden death (Wigal et al., 1999). Although the efficacy of psychostimulants in alleviating the symptoms of ADHD in the short term is evident (70-88% response rate), its efficacy diminishes with time. It requires continuous dose

adjustment to sustain the therapeutic effect (Group, 2004, Caye et al., 2019). However, combining pharmacological treatment with nonpharmacological behavioural therapy has a synergetic beneficial effect at lower medication doses (Group, 2004), elucidating the underrated effect of non-pharmacological treatment options.

5.1.3 RECOGNeyes

Engaging in play is imperative for the healthy progression of cognitive capacities, especially in the formative years of childhood (Piaget, 2013, Ahmad et al., 2016). Scientists have been studying the various aspects of play for centuries since ancient Greece, providing ample research materials (D'Angour, 2013). A major interesting facet of play is that it promotes learning and helps skills consolidation and mastery through repeated practice and skill testing in spontaneous, enjoyable, imaginary, unconstrained, self-absorbing situations (Wilkinson, 2016, Prensky, 2001).

On the other hand, games are considered a subcategory or a structured form of play with rules, goals, and objectives (Prensky, 2001, Deterding et al., 2011, Wilkinson, 2016). With the fast-paced advancement of technology, games have undergone a significant transformation from conventional card and board-based games to more sophisticated digital and video games (Prensky, 2001). The serious games genre Implements learning theories in its design to augment the planned outcome impact, which has shown fruitful applications in military, academic and mental health sectors (Prensky, 2001, Wu et al., 2012, Wilkinson, 2016, Fleming et al., 2017, Gentry et al., 2019). For example, serious games improve executive and global cognitive functions in older adults with cognitive impairment (Abd-alrazaq et al., 2022b, Abd-alrazaq et al., 2022a) and children and adolescents with autism spectrum disorder (Pasqualotto et al., 2021). Moreover, a recent meta-analysis showed that game-based therapeutic interventions are effective in reducing symptoms of ADHD as reported by parents and teachers (Oh et al., 2023). However, the neurophysiological mechanisms contributing to this cognitive improvement remain unclear.

RECOGNeye (remediating control of gaze: neuro-education for your eye) is a computer-based gaze-control training game designed to train attention in people with ADHD (Collins, 2016). The game builds on the suggestions of Buschkuehl and Jaeggi (2010) to maximise the beneficial effects of training and improving task transfer; the game should be A) adaptive and challenging within each trainee's performance capacity and B) complex enough to engage several cognitive processes (Collins, 2016). The game design employs adaptive performance-tracking algorithms that are based on the cognitive load theory (Paas and Van Merriënboer, 1994), which accounts for the mental effort imposed by environmental distractors (noise) and task complexity to optimise the difficulty levels and keeps it within the zone of proximal development where the trainee's skills could improve with guidance and supervision (McLeod, 2019, Vygotsky and Cole, 1978).

Furthermore, the game intrinsically integrates its goal of enhancing oculomotor cognitive control by using an eye-tracking device as a novel control method that demonstrated superior cognitive control training results relative to the traditional use of a mouse or a keyboard in a randomised control trial (García-Baos et al., 2019, Habgood and Ainsworth, 2011). The RECOGNeyes game encompasses six tasks in a fantasy theme, detailed in Table 5.1 (Figure 5.1), to encompass the different aspects of inhibitory cognitive control of the oculomotor system in several environmental interfaces to engage the trainees' attention. It provides immediate performance feedback through gained points (scores) to motivate and engage trainees (a demonstration video of the RECOGNeyes game is available at https://www.youtube.com/watch?v=HRjK8iJbkao).

Table 5.1 The gaze-control tasks targeted in each RECOGNeyes game

Task Name	Description
1. The sorcerer's stare	Is a **fixation control task**, the participant must focus on the central point while ignoring distractors in the peripheral visual field.
2. Inverse incantation	An **antisaccade task**. The participant should avoid looking towards the initiated fire in one of the Opticke and look in the opposite direction.
3. Arcane Abandon	A **go/no go task**, where the participants need to look quickly towards presented ice crystals and fixate their vision at the central point if a fire ring is presented.
4. Clockwork charm	In **a timing saccade task**, an ice crystal slowly forms in one of the Opticke lenses. The participant must time their saccade when it is fully formed.
5. Delayed divination	Two ice crystals are presented sequentially in a visually **guided delayed saccade task**. The participant must look at the first crystal only after the second one is presented. Otherwise, fire will attack the ice sprite if the saccade is performed before the second crystal presentation, or the crystals will break if looked at the second one.
6. Rune of reversal	In a **covert attention task**, a fire shield surrounds the Opticke and an ice crystal circles around it in a specific direction. Once the circling direction is reversed, the fire shield disappears, and the participant must make a saccade towards the ice crystal to save the ice sprite.

5.1.4 Locus coeruleus

Locus coeruleus (LC) is the primary source of NE in the brain. It is located on the floor of the fourth ventricle and has an elongated pyramidal shape (Keren et al., 2009). The LC is implicated in several functional roles, including attention recruitment, stress modulation, behavioural arousal, cognitive performance

regulation and emotional memory (Benarroch, 2018, Aston-Jones et al., 1999, Usher et al., 1999). Its pivotal role in attention, and arousal, among other functions, is detailed in sections 1.5 and 3.1. More importantly, it is involved in regulating pupil diameter changes via its tonic and phasic activity, whereby phasic PD is associated with better task performance (Joshi et al., 2016, Blaser et al., 2014). In addition to the decreased arousal in patients with ADHD, they share a decreased attention level with SpLD. Both cognitive deficits are modulated by the activity of the noradrenergic system, which is evident in the use of psychostimulants as one of the primary treatment options for ADHD. This makes the LC activity, and its neural correlates a possible biomarker for these disorders.

Moreover, neuromelanin is a dark-coloured substrate in the catecholaminergic (DA/NE) metabolism pathway (Wakamatsu et al., 2015). It has a high binding capacity and affinity to metal ions, including iron, which gives it paramagnetic (ferrous-like) properties in MRI scans (Enochs et al., 1997, Zucca et al., 2017, Sasaki et al., 2006). Keren et al. (2009) exploited the presence of neuromelanin pigment in the LC to produce a probabilistic map of the LC location in the Montreal Neurological Institute (MNI) standard coordinate space using a 3-Tesla MRI scanner. Then, they correlated the resulting LC map with the LC cells' density as reported from post-mortem studies (Keren et al., 2009). However, localising small-sized regions such as the LC is rather difficult in neuroimaging. This difficulty is related to the individual natural variability of the location and size of the regions and the limited spatial resolution of 3 Tesla relative to the 7 Tesla MRI scanners (Isaacs et al., 2020). In addition, the physiological cardiac and respiratory motion artefacts inherent to the MRI further impede the localisation process (Zaitsev et al., 2015). The combined effect of these factors increases the noise-to-signal ratio and decreases the extracted data validity from such small regions of interest.

5.1.5 fMRI

The measured fMRI BOLD signals are vulnerable to several artefacts related to physiological or scanner-related factors (Bianciardi et al., 2009). The physiological artefact generated by respiratory and cardiac cycles accounts for the increased

correlation of perivascular regions and “partially” of the grey matter, which introduces a non-neural correlation in the functional connectivity (Birn et al., 2008, Shmueli et al., 2007). Moreover, the subject’s head movement inside the scanner substantially impacts all functional connectivity measures. It should be considered and accounted for before examining the fMRI functional connectivity (Van Dijk et al., 2012, Satterthwaite et al., 2012).

Zarahn et al. (1997) introduced the term global signal, which describes all brain voxels' average time course fluctuations. The global signal is predominant in the low-frequency range (<0.05 Hz), which includes the shared artefactual noise from different sources (Macey et al., 2004, Zarahn et al., 1997). It does not represent a neurophysiological process and introduces a temporal autocorrelation in the BOLD signal. Accounting for the global signal as a covariate in a GLM normalises the data distribution and reduces the variance of false-positive rates, enhancing the functional connectivity measures (Fox et al., 2009).

5.1.6 Aims and questions

We aim to investigate the effect of intensive training using a computer-based cognitive training game (RECOGNeyes) designed to improve cognitive control over gaze direction on the oculomotor control network’s (OCN) functional connectivity.

In addition, we aim to investigate the relationship between the antisaccade performance, pupil dilation rate (as a measure of phasic LC function) and the functional connectivity between the locus coleus and the OCN. In this chapter, we seek to answer the following questions

- Does RECOGNeyes training alter the functional connectivity within the OCN?
- What are the functional connectivity changes related to RECOGNeyes training?
- Can we detect LC- cortical functional connectivity?
- Is there a relationship between the pupil dilation changes in the antisaccade task and LC connectivity to the OCN?

5.2 Methods

5.2.1 Participants and recruitment

We aimed to include adults seeking help with learning difficulties or clinically diagnosed with a specific learning difficulty (SpLD) or ADHD. Two advertisement methods were used for recruitment purposes; posters were displayed around the University of Nottingham campuses and through the Academic Support Services (ASS) mailing lists.

Participants were included in the study if they met the following criteria:

1. Age within 18-30 years.
2. No MR safety exclusions
3. Able to consent to the study.
4. Reported diagnosis of ADHD or SpLD (i.e. dyspraxia, dysgraphia, dyscalculia or dyslexia).
5. Normal or corrected to normal vision enables them to see medium-sized words/shapes at about 60 centimetres.
6. Willing and able to train 20-30 minutes per session for up to four weekly sessions in two weeks.
7. Not concurrently involved in other studies. A minimum of 3 months since the last participation in any previous study to reduce the risk of other interventions affecting the outcomes.

We approached participants by distributing posters and leaflets in the University of Nottingham Park campus (Academic Support, Student's Services Centre, Portland Building, University Park) and surrounding areas. Moreover, we sent emails to the registered emails with the Academic Support Unit.

A detailed explanation of the trial was provided to the candidates, and if they expressed further interest, they were phone interviewed to confirm their eligibility to participate in the study. After eligibility confirmation, participants gave their consent to participate before participating in the study. An inconvenience allowance of £60 was provided to the participants upon completion of the study, as approved by the Ethics committee.

Randomisation

We randomised participants' allocation using enclosed envelopes to take two, three or four training sessions. Participants were instructed that each training session lasts 20 - 30 min for either 2, 3 or 4 training sessions per week for two weeks. The randomisation was stratified by age and gender on a rolling basis as volunteers were recruited. The investigators were blind to the training instruction provided in the sealed envelopes until the data was processed.

5.2.2 RECOGNeyes Gaze Training

Participants were introduced to the RECOGNeyes gaze-control training game. After demonstrating the setup procedures and configuration (Figure 5.1), a laptop (Lenovo ThinkPad L560) and a portable eye-tracker (Tobii 4C) were provided to the participants to train at home. The provided laptop created a record of each participant's training compliance and progress. The participant plays with an ice sorcerer character, who guides the ice sprites away from the fire into a safe magical ice vertex formed by the correct saccadic responses or the inhibition of these responses (Figure 5.2). Upon the completion of a task, a feedback message reflecting the participant’s performance is displayed using three stars for each accuracy level (no stars for performance below 60%, 60-70% accuracy = single bronze star, two silver stars for 70-79% accuracy and three golden stars for accuracy above 80%) (Figure 5.2). The six different tasks are described in Table 5.1.

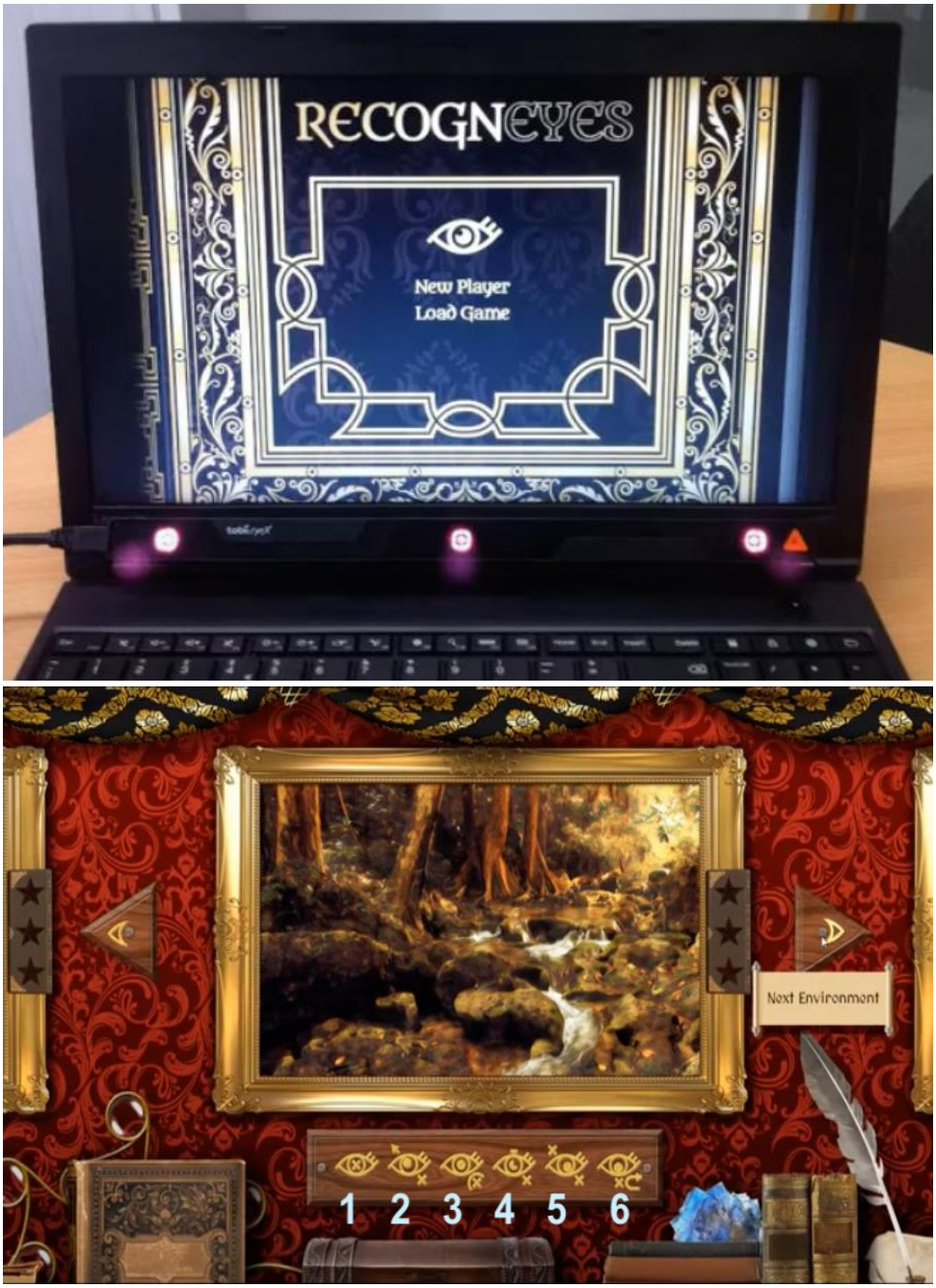

Figure 5.1 Illustrates in the top image, the RECOGNeyes training equipment's' setup and the eye tracker position at the bottom of the laptop's screen. The bottom image is a screenshot of the game display illustrating one of the available environments and the numbers reflects different available tasks, 1. The Sorcerer's stare, 2. Inverse carnation, 3. Arcane abandon, 4. Clockwork charm, 5. Delayed divination, 6. Rune of reversal.

Figure 5.2 The top image is a screenshot of the inverse incantation game. The nine lenses represent the Opticks in the middle of the screen, where the participant is asked to focus at the centre of the screen (number 1) and then look in the opposite direction marked by brackets (rectangle) to the circle on fire (star). The ice sprite (circled) follows the participant's eye movements. The bottom image is a screenshot of the feedback message after completing the task reflecting the participant's performance.

5.2.3 The antisaccade task

The antisaccade task used in this study and the tDCS and active inhibitory control study has the same task design. The task design is detailed in section 3.2.2.

5.2.4 ROI definition

For examining the LC, we used a version with two standard deviations LC probability map defined by Keren et al. (2009) to increase the probability of capturing BOLD signals related to the LC activity (Figure 5.3). For the OCN, we used ten OCN MNI space coordinates defined by Waitt (2022) based on the comparative finding from animal and human studies (Table 4.1,Figure 5.3).

5.2.5 MRI Data Acquisition

The participants underwent two scanning sessions using a 3.0T Philips Achieva (TX)-DS Scanner at Sir Peter Mansfield Imaging Centre. The first baseline session (Day1) was acquired after the participants performed 20 minutes of concurrent MEG/antisaccade task and before demonstrating RECOGNeyes training. The second session was after the two weeks of training were completed (Day2) and after 20 minutes of concurrent MEG/antisaccade task was done on the same day. Each MRI session included a structural MRI and a resting-state functional MRI (RS-fMRI).

A high-resolution anatomical MRI was acquired using a T1-weighted 3D MPRAGE sequence (TR/TE/FA= 4.5 ms/2.2 ms/ 8^{o}, FOV= 256 x 256, 1 mm slice thickness). A short interval of 3000 ms and a SENS factor 1 for image registration.

The RS-fMRI data were acquired using a 32-channel head coil with SENSE factor 1 in the anterior-posterior direction, blood oxygenation level-dependent (BOLD) sensitive, T2*- weighted, echo planar images (TR/TE/FA= 2000 ms/35 ms/85^{o}, FOV=240 x 240 mm, voxel size= 3 x 3 x 3.5 mm, 32 axial slices a total for 150 timepoint/session). Each RS-fMRI session lasted 5 minutes, considered enough duration for a stabilised strength in the functional connectivity analyses (Van Dijk et al., 2009).

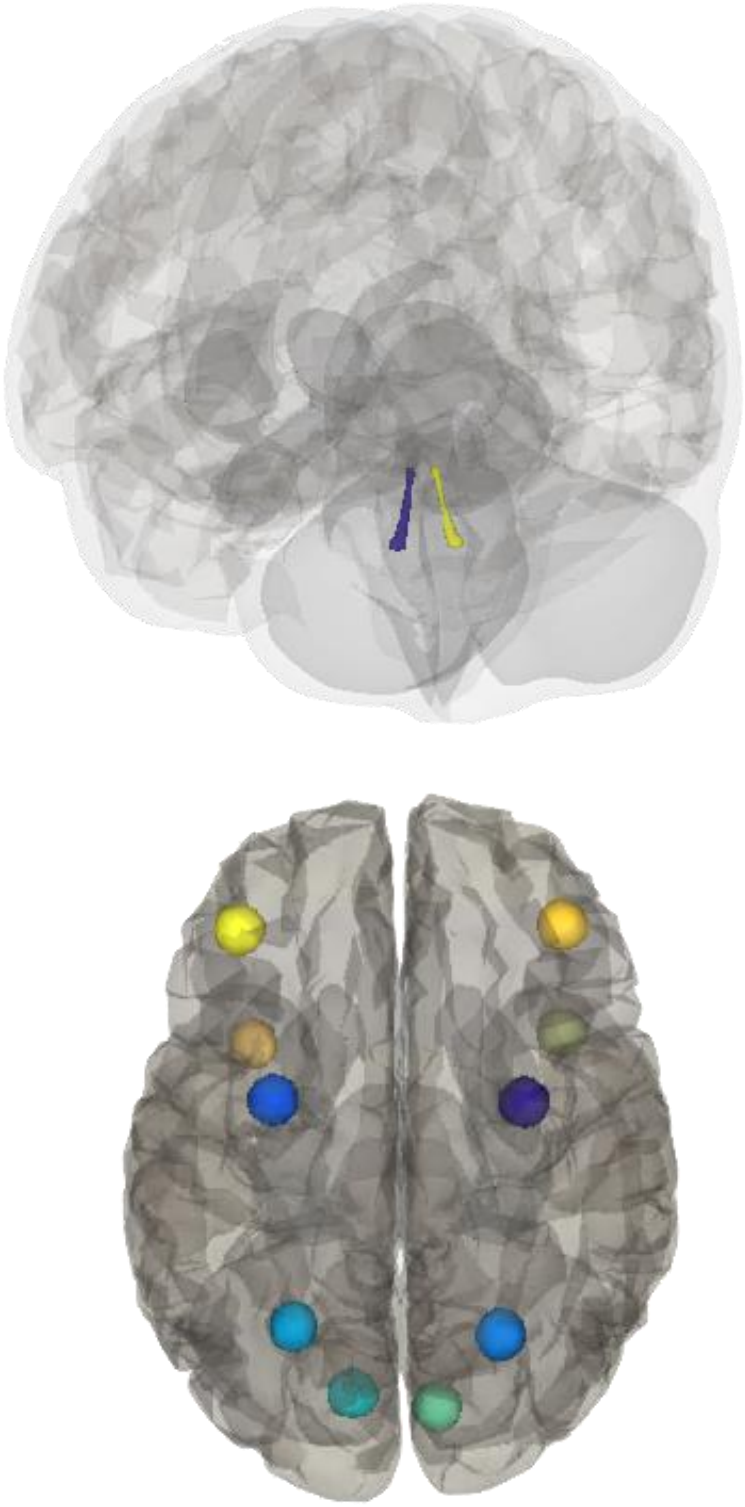

Figure 5.3 The top figure depicts in a left posterolateral view the two standard deviation LC map provided by Keren et al. (2009), and the ten OCN regions in the bottom figure illustrated in a top view. The arrangement of the OCN nodes from frontal to occipital are: DLPFC, anterior insula, FEF, PEF and visual cortex.

Both figures are illustrated on standard MNI brain template. The OCN regions coordinates are listed in Table 4.1.

5.2.6 Image pre-processing

Before conducting functional connectivity analyses, several pre-processing and denoising steps must take place first (for a review, see (Strother, 2006). These steps include realigning and unwarping the functional images, correcting for the slice timing differences, detecting artefacts related to head movement, segmenting and normalising the brain MNI template, and then smoothing the functional data. Simultaneously, anatomical MRI was segmented and normalised to the MNI space and co-registered to the functional images. The analysis pipeline is illustrated in Figure 5.4

Structural and functional volumes were pre-processed and analysed using CONN toolbox (Whitfield-Gabrieli and Nieto-Castanon, 2012, Nieto-Castanon, 2020) (version 20b), which is based on MATLAB (v2019) and SPM (12) fMRI functional connectivity analysis software.

We used methods described by Andersson et al. (2001) to align and unwarp the acquired fMRI using b-spline interpolation, which uses the first scan of the first sessions as a reference image and then co-register and resample all other scans to this reference. The described methods resample the functional data in identified deformation field related to head movement by an estimate the derivatives of the distortion. Then, the temporal differences between the sequentially acquired slices were corrected using the sinc-interpolation slice-timing correction method, which resamples and time-shifts the functional data to the middle of each acquisition time (Henson et al., 1999). At each time point, a bounding box of 140x180x115mm encompassing the brain with six reference points at the centre of the box, any displacement of more than 0.9 cm of these reference points or changes above 5 standard deviations of the global BOLD signal marks the frame as a possible outlier.

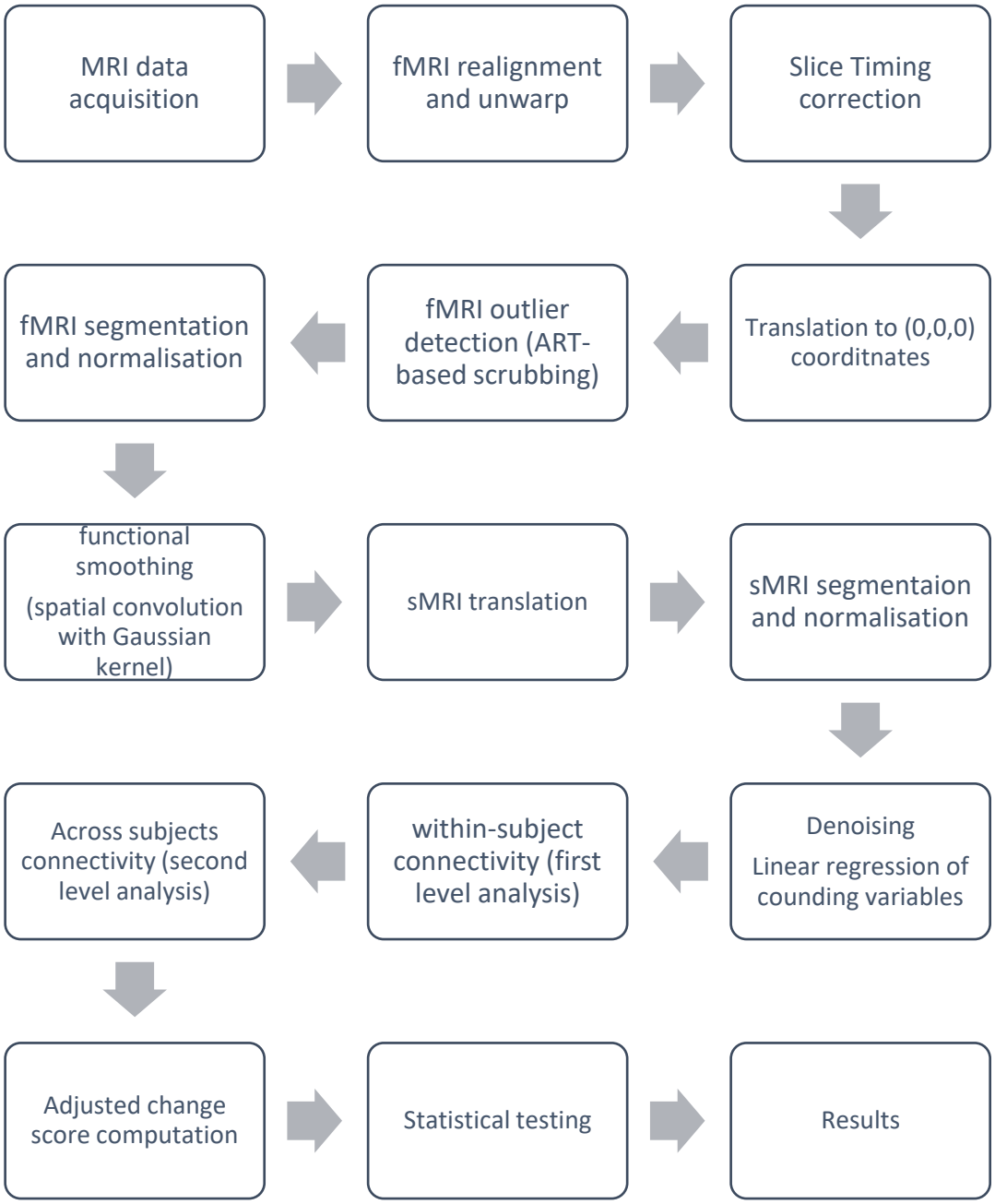

Figure 5.4 Illustrates the fMRI resting-state analysis pipeline from acquisition to statistical analysis.

For the direct tissue segmentation and normalisation, the functional and anatomical data are resampled to a default bounding box (180x216x180mm) using 4th-order spline interpolation, with 1mm isotropic voxels for anatomical and 2mm for functional data to normalise the data into standard MNI space (Ashburner and Friston, 2005). Tissue probability maps (TPM) and non-linear spatial transformation are estimated using iterative tissue classification from the reference images (function or anatomical) that best converge between the posterior and prior TPMs. Then to decrease the residual variability and optimise the BOLD signal-to-noise ratio, functional data were smoothed using an 8 mm full-width half maximum (FWHM) Gaussian kernel (Mikl et al., 2008).

5.2.7 Denoising the functional data

After conducting a preliminary quality control assessment on the pre-processed data, the data was denoised using linear regression and filtering temporal band-pass. We performed Ordinary Least Squares regression to remove estimated potential confounding factors for each voxel using a different method for each founder. An anatomical component-based noise correction (Behzadi et al., 2007) was used to remove cerebrospinal fluid and white matter noise components. Identified outlier scans with excessive movement are scrubbed on the subject-level (Power et al., 2014). Less significant movements are regressed using twelve movement-related parameters, three rotation and three translation parameters and their first-order derivatives (Friston, 1994). We then applied a band-pass filter (0.008 – 0.09 Hz) to the BOLD data using a discrete cosine transform windowing operation to exclude noise resulting from physiological cardiovascular (0.6 – 1.2 Hz) and respiratory (0.1 – 0.5) cycles (Cordes et al., 2001, Hallquist et al., 2013).

5.2.8 Functional connectivity estimation

Functional connectivity was computed using the Fisher-transformed bivariate correlation coefficient for each subject, where r is the matrix of correlation coefficients, Z is the Fisher-transformed ROI-ROI connectivity matrix, and R is the BOLD time series for each ROI.

$$r(i,j) = \frac{\int R_i(t)R_j(t)dt}{\left(\int R_i^2(t)dt \int R_j^2(t)dt\right)^{\frac{1}{2}}}$$

$$Z(i,j) = tanh^{-1}(r(i,j))$$

Then, we tested the functional connectivity between all connectivity pairs of the OCN (Table 4.1) and the LC by using a multivariate parametric general linear model analysis (Jafri et al., 2008). The model determines the maximal lagged correlation to evaluate the latency differences and mitigate its impact on the measured connectivity. We controlled for the multiple comparisons using the false discover rate (FDR) correction (Benjamini and Hochberg, 1995). This testing process generated a T-statistical matrix of the resting state connections associated with a significant FDR-corrected p-value (<.05).

We computed the change in functional connectivity by subtracting the pre-training from the post-training Fisher-transformed correlation values for each region/subject. Our baseline data tended to be negatively correlated with the change in connectivity, where higher baseline score had less positive or more negative change score. To account for the natural variation in baseline connectivity and the explore the effect of the RECOGNeyes training, we aimed to account for the regression to the mean phenomenon (Barnett et al., 2005). This phenomenon describes the tendency of large variation (unusually high or low) in a measured baseline data to return to the population mean at a repeated measure. Thus, we computed an adjusted change score (AdCS), represented by the computed standardised residuals of the linear regression for the change in connectivity as a dependent variable and the pre-training (baseline) connectivity as a predictor. This process produced an AdCS, which relates the changes in functional connectivity, and

the varying exposure to RECOGNeye cognitive training while adjusting for the regression to the mean phenomenon.

5.3 Results

5.3.1 Participants and sample demographics

A total of 35 participants were recruited (20 females) aged 19-31 years (24 avg age). A formal diagnosis of ADHD or SpLD was confirmed in 34 participants, while one participant refused to disclose his/her diagnosis. Only 33 subjects completed the pre- and post-task fMRI sessions, which led to the exclusion of the two subjects who had missing data sets from the analyses.

Table 5.2 RECOGNeyes sample diagnostic information (N=35). ADD: attention deficit disorder, ADHD-PI: attention-concentration deficit type.

Diagnosis (No. of subjects)	Subtype	Treatment	Notes
ADHD (6)	2 ADHD 1 ADHD-PI 1 ADD 1 comorbid dyspraxia 1 comorbid dyspraxia and dyslexia	1 Dextroamphetamine 1 Methylphenidate 1 Concerta XL 1 Elvanse 70mg once daily 1 Elvanse 30mg and Atomoxetine 1 unknown and non-compliant	Concerta XL is a sustained release formulation of methylphenidate. Elvanse is lisdexamfetamine, a precursor to dextroamphetamine. Dextroamphetamine, methylphenidate, and lisdexamfetamine are all psychostimulants.
Dyslexia (26)	17 pure dyslexia 8 comorbid dyspraxia 1 comorbid dysgraphia		
Dyspraxia (2)	2 dyspraxia/dyspraxia tendencies		

The severity of ADHD symptoms were assessed using the self-reported Conners' Adult ADHD Rating Scales (Conners et al., 1999). The scale has a normalized T-score population reference value of 50. Higher scores indicates more severe or more frequent problems. Waitt (2022) reported significant differences in this sample on the inattention/memory problems measures from their population reference T-score, *mean*=59.88, *Std. Dev*= 10.398, $t(31)=5.372$, $p < .001$, and on the

impulsivity/emotional lability measure, *mean*=45.52, Std Dev= 8.258, *t*(32) = - 3.12, *p* = .004 (Waitt, 2022). This implies that our sample has more inattention/memory problems and less impulsivity/emotional lability ADHD symptoms than the reference population, which makes it an appropriate sample representing the inattentive ADHD.

5.3.2 Training Exposure

The average RECOGNeyes training exposure across all participants was 129.09 (± 57.71) minutes. This indicates that participants, on average, had 8.5 (± 3.24) each session lasted 15.4 (± 4.8) minutes. Nonetheless, participants did show good compliance towards their allocated training schedules, evident in the mean minutes of exposure per group detailed in Table 5.3.

Table 5.3 RECOGNeyes training allocation and total minutes trained

Training sessions regime	Assigned subjects	Actual training exposure (mean ± S.D)
2	11	94.12 ± 22.82
3	12	137.75 ± 64.14
4	12	152.48 ± 61.70
Total	35	129.09 ± 57.71

5.3.3 Antisaccade performance

The analysis of antisaccade performance was done and reported by Waitt (2022). Their results showed a mean RT latency difference between antisaccade and prosaccade on Day1 of (M= 34.016 ± 32.915), which decreased significantly on Day2 (M = 14.903 ± 22.714). Moreover, the difference between trial types decreased significantly in Day2 compared to Day1, *t*(30) = -3.911, *p = .000* . Furthermore, their results showed an increased response accuracy (measured by d' score) on Day2 relative to Day1, *t*(30)= 3.811, *p* = .001. Their results indicate a significant effect of RECOGNeyes training on increasing response accuracy and decreasing the RT for both trial types prominently in antisaccade trials.

5.3.4 Pupil dilation changes

The pupillometry analysis was part of the data analyses carried out by (Waitt, 2022), which revealed a task-related phasic pupil dilatation in response to the cue presentation reaching maximum area after saccade onset. During the anticipatory period, prosaccade exhibited greater pupil size than antisaccade.

In accordance with previous findings (Wang et al., 2016, Karatekin et al., 2010), imperative stimulus presentation induced a significantly greater pupil dilatation rate in antisaccade trials than in prosaccade. This dilatation rate was greater on Day2 than on Day1, prominently in the first 100 ms post-stimulus presentation. This finding indicates that antisaccade trials are associated with greater arousal and effort.

In addition, they reported a significant negative correlation between RT and pupil dilation rate during the cue to target and target to saccade. The correlation was greater for antisaccade trials than prosaccade. Their results indicates greater pupil dilation rate predicts faster RT (Waitt, 2022).

5.3.5 Data pre-processing quality

While five subjects exhibited excessive motion in the scanner, which accounted for most of the excluded scans, the remaining subjects illustrated sustained stability within the scanner. The maximum head movement recorded was 3.47 mm. However, the average maximum head movement per subject was 0.95 cm (*SD* = ± 0.81 cm), and the mean motion was 0.11 mm (*SD* = ± 0.03 cm) (Figure 5.5).

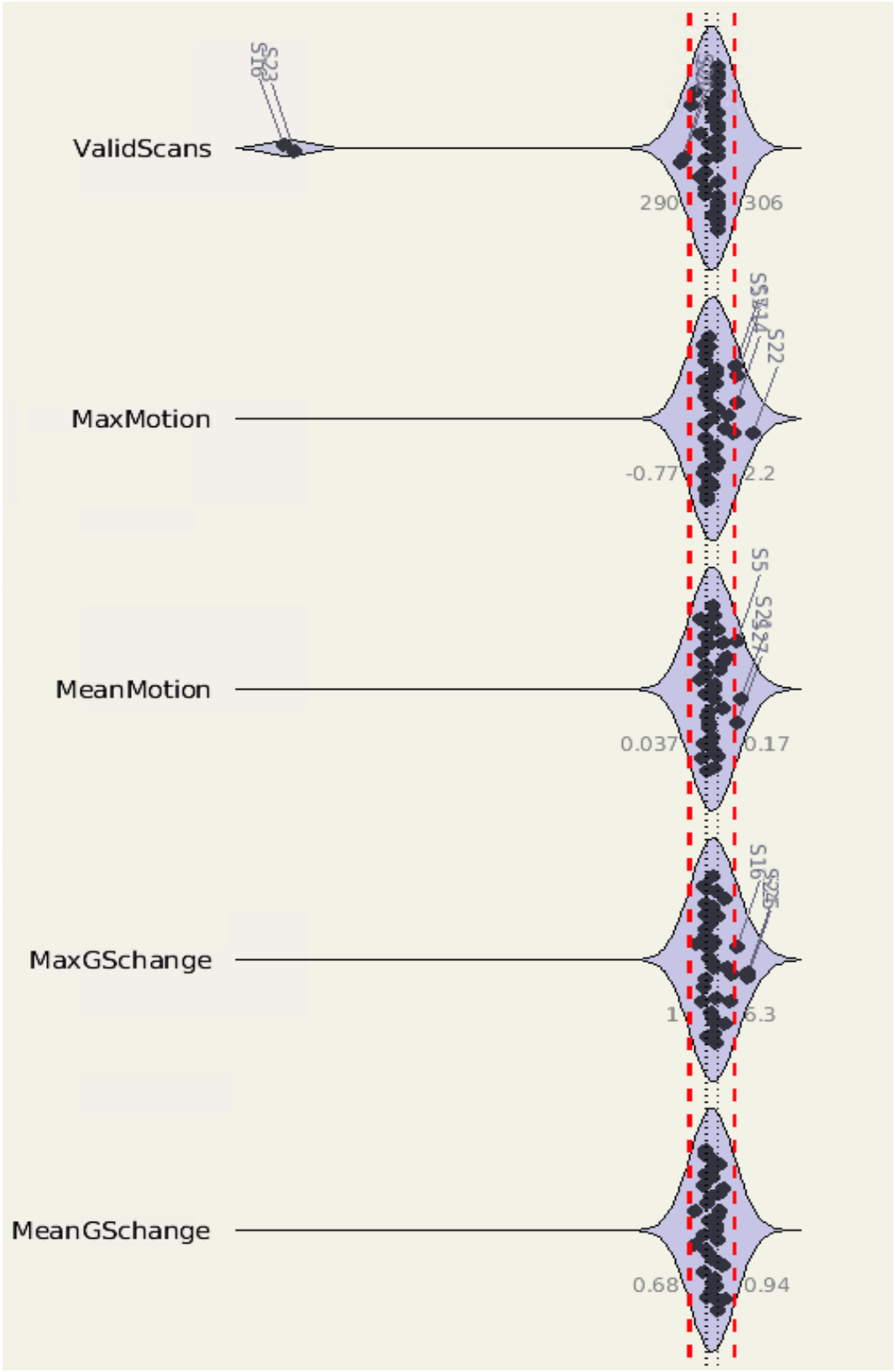

Figure 5.5 Quality assessment parameters of the acquired fMRI data. The missing sessions in two subjects affect the total number of valid scans depicted in S16 and S23.The black dotted lines depicts the 1st and 3rd quartiles, and the red dashed lines depict the 1st (- 1.5 IQR) and 3rd (+ 1.5 IQR) quartiles.

We evaluated the co-registered structural and functional scans to the MNI template to examine the quality of tissue segmentation and co-registration. The structural scans showed an excellent co-registration to the MNI grey matter (TPM) templates averaged across all subjects (Figure 5.6 A). The functional data illustrated a good co-registration with the MNI grey matter's TPM template for the cerebral cortex. The fMRI segmented data illustrated better co-registration with the grey matter of the Regional MNI templates than to TPM (Figure 5.6 B and C).

Outlier identification process using head movement and changes in the global signal resulted in the exclusion of 81 scans out of 9900 total scans (0.82%). This example is from S22, which exhibited the maximum number of outliers and recorded maximum motion. The carpet plot illustrates the change in the BOLD global signal before and after performing the denoising process (Figure 5.7). Furthermore, as described in section 5.2.7, denoising (regressing) the computed confounders and normalising the global signal corrected the skewness of the functional connectivity data. It enhanced the distribution of the functional connectivity correlations between the separate voxels in the brain.

A)

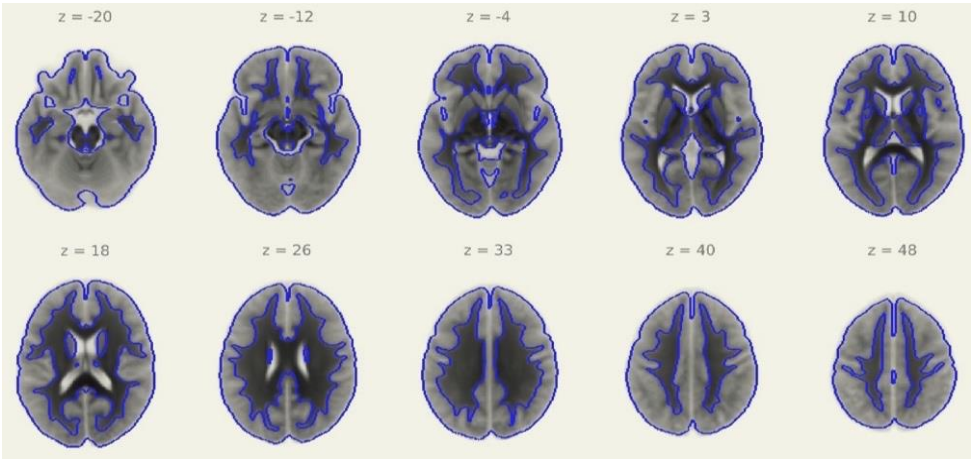

B)

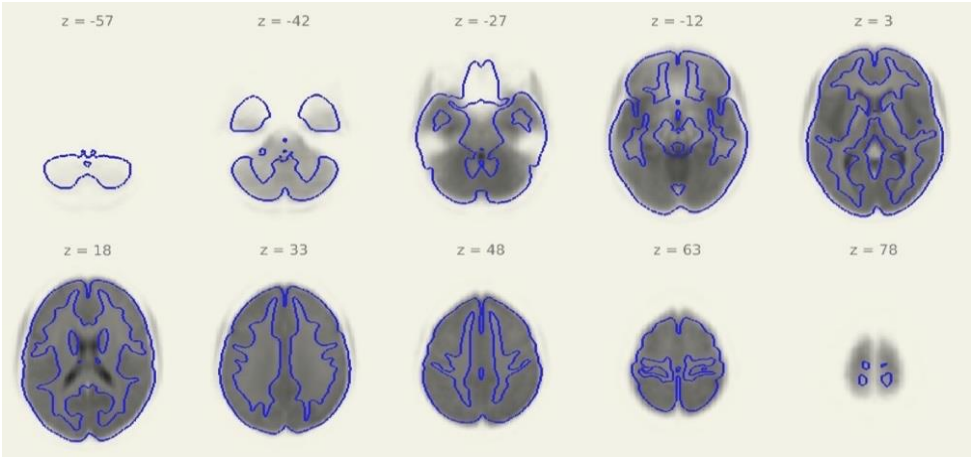

C)

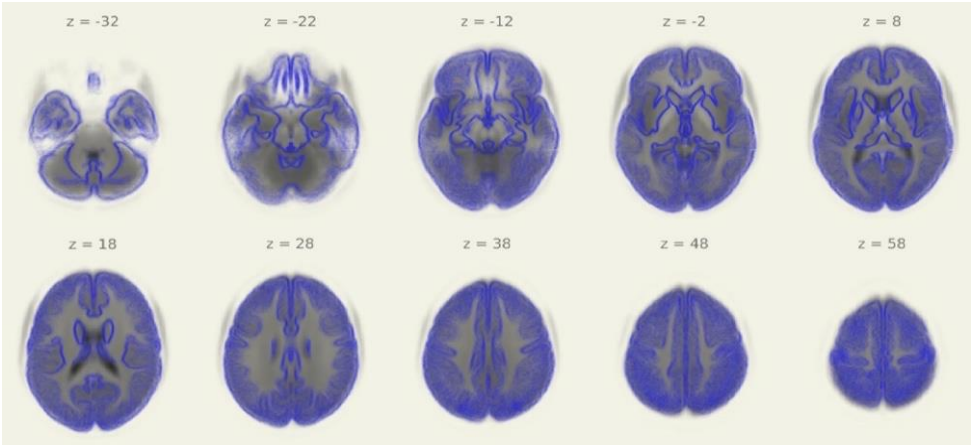

Figure 5.6 The quality of the segmentation and co-registration process. A) the average anatomical scan (across subjects) co-registration to the MNI TPM showing excellent alignment to the boundaries of the MNI template (blue solid line). B) the smoothed fMRI scans co-registration to the MNI TPM maps and C) to the grey matter of the ROI templates. Z= slice level.
ROI templates.

A)

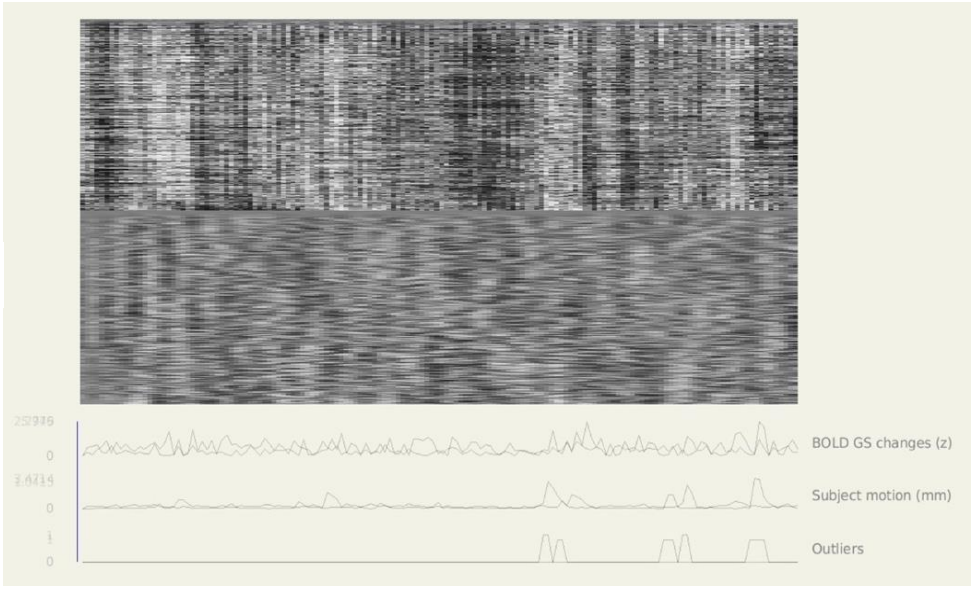

B)

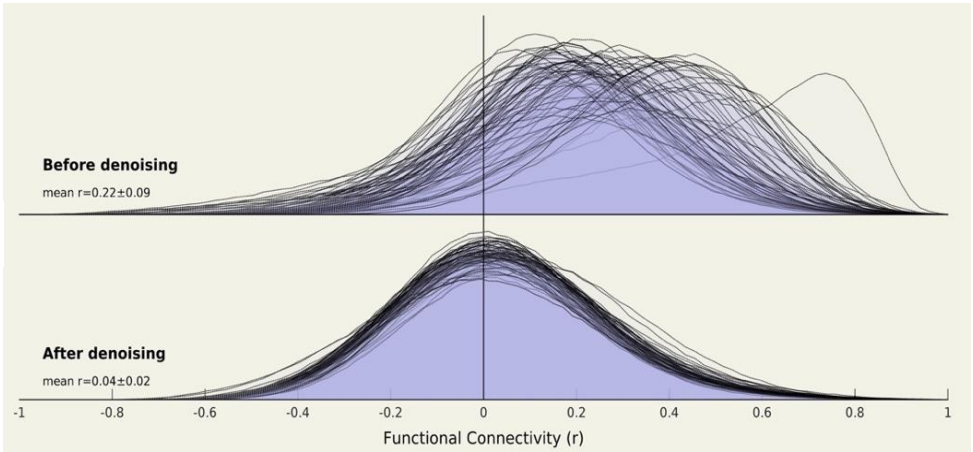

Figure 5.7 The effects of performing the denoising process, A) on the averaged carpet plot of S22 across the two resting-state sessions. The X-axis represent the scan's timeseries and on the Y-axis the BOLD signal of each voxel in the scan. The upper half of the plot depicts the BOLD signal before denoising, and the lower part of the carpet plot is the BOLD signal after denoising. The change in BOLD global signal estimates is depicted on the first timeline below the carpet plot followed a track of subject's motion and the last timeline illustrates the identified outlier scans based on the change in BOLD signal and the amount of recorded motion. B) On improving the functional connectivity across the different voxels in the brain across all subjects and both resting states.

5.3.6 Resting-state functional connectivity patterns

In Rest1 functional connectivity analysis (Figure 5.8 A), there was significant inter-hemispheric connectivity between all the homologous OCN regions. The locus coeruleus showed functional connectivity only to the visual cortices bilaterally. Both visual cortices illustrated a second connection to the anterior insula bilaterally. On the other hand, the anterior insula bilaterally exhibited a functional connection with the FEF and the DLPFC in both hemispheres. While the right DLPFC had connections to the FEF and the PEF bilaterally, the left DLPFC showed functional correlations with its ipsilateral FEF and PEF. The strongest inter-regional connection was between bilateral FEF and both PEF.

In Day2 resting state (Rest2) (Figure 5.8 B), there was a strengthening of all Rest1 connections except for the correlation between the locus coeruleus and the right visual cortex, which was lost. In addition, there were new connections between the bilateral visual regions, bilateral FEF and the left DLPFC.

To examine the effect of time on modulating the OCN functional connectivity. As the correlation between the regions is not directional (orthogonal), i.e., the measured correlation value does not differ whether the region is a seed or test region. There were fifteen edges within each hemisphere, totaling thirty edges between the cortical OCN. Using the BOLD signal as the dependent measure, we conducted a three-way repeated measures ANOVA, using three within-subjects factors; Time (two-level; Rest1, Rest2), Hemisphere (two-level: left, right), and connections (15-level; DLPFC-FEF, DLPFC-AntIns, DLPFC-PEF, DLPFC-V1, DLPFC-LC, FEF-AntIns, FEF-PEF, FEF-V1, FEF-LC, AntIns-PEF, AntIns-V1, AntIns-LC, PEF-V1, PEF-LC, V1-LC).

There was no significant main effect or interaction of Time. We then examined the change in connectivity in Rest2 from Rest1 by subtracting Rest1 correlations from Rest2. There was a trend-level effect of connections to exhibit a different change, $F(8, 248.8) = 1.943$, $p = .054$. These results imply the presence of consistent resting state connectivity modulations across subjects in Rest2 relative to Rest1. However, it does not reach a significant difference level in Rest2 from Rest1.

A

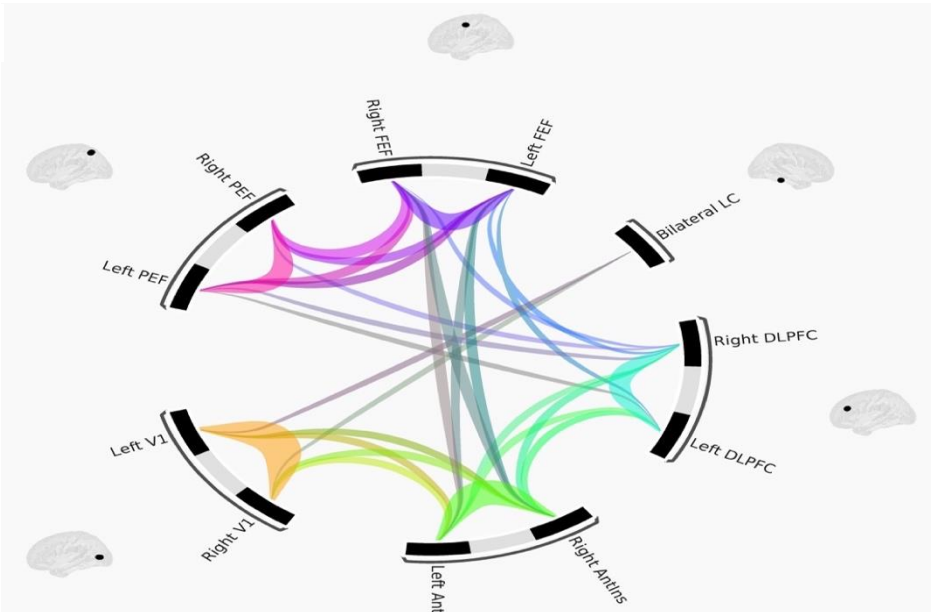

B

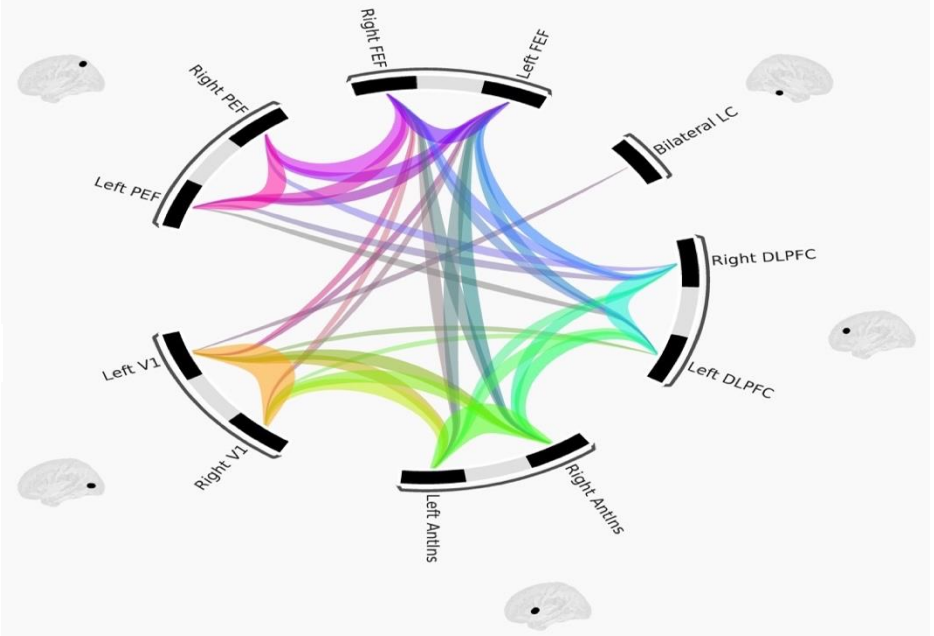

Figure 5.8 The resting state functional connectivity between the OCN regions and the LC. A) Rest1 showing a strong inter-hemispheric correlation between the homologous OCN regions, and bilateral FEF connectivity with the PEF and the AntIns bilaterally. While the AntIns exhibit with the DLPFC and Visual cortices bilaterally, the visual regions are the only ones to have connections with the LC. B) Rest2 functional connectivity Illustrating a strengthening of Rest1 correlation except for right V1 to LC. In addition, V1 bilaterally exhibited new connections with the FEF and the left DLPFC. Illustrated have varying significance level (p <.05) represented by the connection thickness (thicker line = greater statistical value).

5.3.7 RECOGNeyes training effects on the OCN

We set out to investigate if these observed changes correlate to the effect of RECOGNeye training over the two weeks. To achieve this, we used the adjusted change scores (AdCS) as our dependent variable, described in section 5.2.8, to examine the correlations between the total trained minutes on RECOGNeyes and the resting state functional connectivity changes.

First, we sought to examine the inter-homotopic regional connectivity, as it showed greater connectivity in Rest1 and Rest2. We conducted two-way mixed-design ANOVA with the total trained minutes as the between-subjects factor and the AdCS for the homotopic regions as the within-subjects factor (five-level; DLPFC, FEF, AntIns, V1). The results showed a significant between-subjects effect of total minutes trained, $F(1,31)=7.188$, $p=012$, illustrating a decreased inter-homotopic connectivity associated with increased total minutes trained. This finding suggests a decrease in the connectivity between the putative OCN homotopic regions is associated with RECOGNeyes training, which would benefit children with ADHD who have greater homotopic connectivity than normal controls (Jiang et al., 2019).

Then, we investigated the total trained minutes' effect on the interhemispheric connectivity changes for non-homotopic regions. We conducted a repeated measure ANOVA, with total exposure (minutes trained) to RECOGNeyes training as the between-subjects covariate and interhemispheric connections as the within-subjects factors. There was no main effect of Connections or between-subjects effect of total minutes trained. This indicates that the RECOGNeyes training did not modulate the interhemispheric resting-state connectivity apart from the homologous OCN pairs.

Next, we examined the total trained minutes' effect on modulating the intrahemispheric resting-state connectivity. We used a three-way mixed-design ANOVA, with total trained minutes as the between-subjects factor and two within-subjects factors; Hemisphere (two-level; right, left) and Connection (ten-level; DLPFC-FEF, DLPFC-AntIns, DLPFC-PEF, DLPFC-V1, FEF-AntIns, FEF-PEF, FEF-V1, AntIns-PEF, AntIns-V1, PEF-V1).

There was a significant main effect of Hemisphere, $F(1,31) = 4.651$, $p = .039$. However, there was a significant Hemisphere by training exposure effect, $F(1, 31) = 5.509$, $p = .025$. We examined the parameter estimates for the intrahemispheric connection to interpret this finding and used Sidak multiple comparisons correction. The Left intrahemispheric connectivity exhibited a positive trend with total minutes trained, which was significant for the DLPFC-FEF, $p = .031$, and the DLPFC-PEF, $p = .044$. On the other hand, the right intrahemispheric exhibited a negative association with the total minutes trained, which reached a significant level in the anterior insula to the primary visual connection, $p = .046$. These findings suggest that the total trained minutes on RECOGNeyes introduced neuromodulatory changes apparent in the intrahemispheric resting-state functional connectivity in a dose-related manner, which decreased the right and increased the left intrahemispheric connectivity. The baseline connectivity was stronger in the right than the left hemisphere. Thus, this change in connectivity strength with RECOGNeyes training is in the direction of equalizing the connectivity within the two hemispheres.

5.3.8 Locus coeruleus functional connectivity

Our resting-state functional connectivity results (Figure 5.8) show a significant LC-V1 connection, bilaterally in Rest1 and to the left V1 in Rest2. Furthermore, in our sample, preparatory PD exhibited a greater dilatation rate, on Day2, in response to the imperative stimulus in antisaccade trials than prosaccade, which reflects increased arousal in antisaccade trials (section 5.3.4). Hence, we sought to investigate the correlation between the antisaccade dilatation and the resting-state functional connectivity between the LC and V1 bilaterally by conducting a Pearson's correlation test between the LC-V1 resting-state functional connectivity and the PD rate during the preparatory period in the antisaccade and prosaccade trials on Day1 and Day2. The results showed a significant positive correlation between the antisaccade PD rate during the preparatory period on Day2 and the LC-V1 connectivity in Rest2, $r(30) = .374$, $p = .042$, but not for Day1 with Rest1. This finding suggests a possible increased recruitment efficacy of the visual cortex by the LC during the preparatory period due to a systematic increase induced by the RECOGNeyes training effect.

To examine this hypothesis, we examined the difference between the correlations LC-V1 (in Rest1 and Rest2) with PD rate for prosaccade and antisaccade (cue-stimulus and stimulus to saccade) (Fisher, 1921, Soper, 2022). The results showed no significant differences between the correlations.

This finding suggests a plausible alternative hypothesis that a greater increase in LC-V1 connectivity is associated with a greater increase in arousal reflected in the preparatory PD rates for antisaccade trials. We investigated this explanation by computing each subject's change in LC-V1 connectivity (Rest2 - Rest1) and PD rates (Day2 – Day1). Then we examined the correlation between the change in LC-V1 connectivity and the change in PD. There was a significant positive correlation between the LC-left V1, $r(29) = .438$, $p = .018$, right V1, $r(29) = .429$, $p = .02$, and the mean LC-V1, $r(29) = .449$, $p = .015$, with the change of preparatory PD rate in antisaccade trials. These findings imply that greater preparatory arousal changes in antisaccade trials are associated with greater changes in the LC- left V1 more than the right V1 resting-state functional connectivity (Figure 5.9).

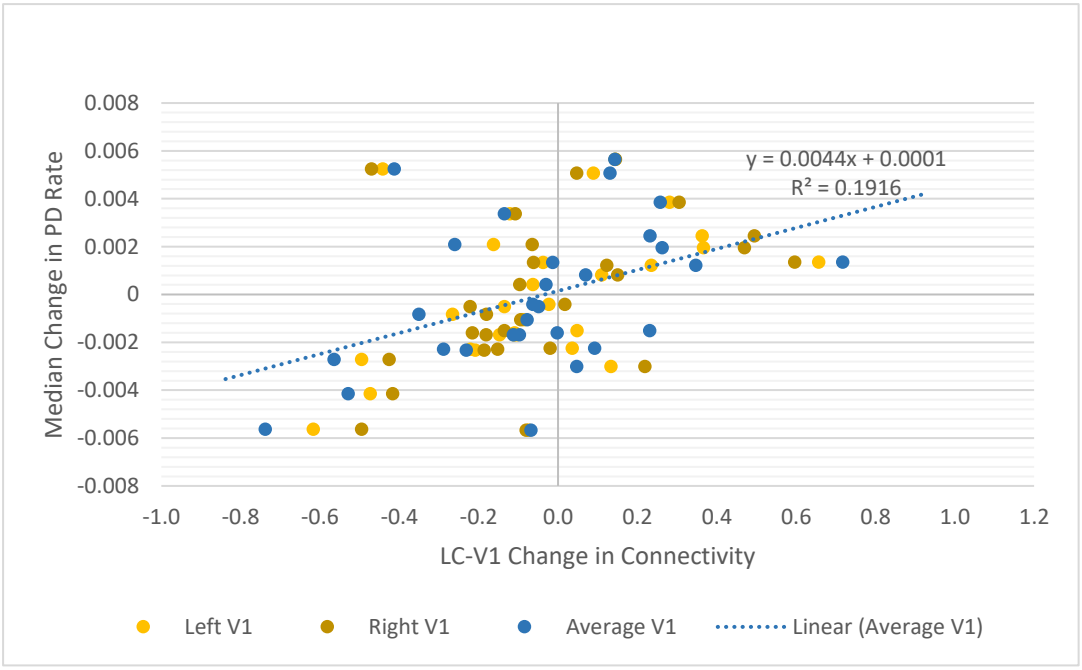

Figure 5.9 Scatter plot illustrating the significant positive Pearson correlation between the antisaccade PD rate changes during the preparatory period (Day2-Day1) with the LC-V1 change in connectivity (Rest2-Rest1).

5.4 Discussion

The RECOGNeyes game, as a computerised cognitive training tool, has shown high acceptability and good compliance in a sample of ADHD and SpLD patients. This training significantly improved the participants' reaction times on the antisaccade task for both trial types and enhanced their performance's accuracy (Waitt, 2022).

The OCN resting-state functional connectivity after RECOGNeyes training exhibited different connectivity patterns from the baseline, which summarised in the following three points. 1) New connections emerged after the RECOGNeyes training. The visual cortices established new connections in Rest2 with the FEFs bilaterally and with the left DLPFC. At the same time, the left DLPFC showed new connection with the right FEF in Rest2. 2) Most of the existing connections between the OCN regions in Rest1 were strengthened after RECOGNeyes training. 3) The LC to the right V1 connection decreased to a non-significant level in Rest2. Given the functional hemispheric differences in attention (right hemisphere in baseline tonic attention and in the VAN, left hemisphere engagement in faster phasic attention) (Petersen and Posner, 2012, Corbetta and Shulman, 2002), the crucial involvement of the FEF and DLPFC in planning and execution top-down control (Buschman and Miller, 2007, Connolly et al., 2002). This change of connectivity pattern after the completion of RECOGNeyes training, imply a possible beneficial effect of RECOGNeyes training on strengthening the functional connectivity of the decision-making centres in the putative OCN. However, further investigations are required to confirm or refute this relationship, as the method we used to examine the change in connectivity failed to find a connection that survives the correction of multiple comparisons. This finding suggests that more prolonged or intensive training regimes could augment these changes given the observed correlation between RECOGNeyes training amount and the change in connectivity.

Jiang et al. (2019) reported a significantly increased inter-hemispheric connectivity between mirroring voxels in children with ADHD compared to children without ADHD for regions in the superior frontal, middle occipital, and anterior cerebellar regions. Furthermore, Chen et al. (2021) investigated the mirror overflow

phenomenon of ADHD children using resting-state functional connectivity of the somatomotor network. They found increased interhemispheric connectivity in ADHD children compared to typically developing ones. The increase in interhemispheric connectivity was positively correlated with the motor overflow severity. Interestingly, our data show that RECOGNeyes training had a significant modulatory impact on the OCN's RE-FC, which exhibited a significant correlation with the amount of training done. More time spent on RECOGNeyes training is negatively correlated with the inter-homotopic connectivity of the OCN regions. This indicates the possible beneficial therapeutic effect of RECOGNeyes in ADHD and supports our suggestion that changes in the OCN RE-FC after RECOGNeyes training could be augmented with increasing the total minutes spent training or the duration of the training program.

In addition, we found a dose-related training modulation on the intra-hemispheric connectivity, whereby the left intrahemispheric connectivity increased with training and the right one decreased. This finding could reflect a possible disengagement mechanism where the left hemisphere, which exhibited lower connectivity at baseline, strengthened its independence by increasing connectivity. This connectivity change led to a decrease in the right hemisphere connectivity caused by the left hemisphere's dependence on its function.

We did not find a correlation between the PD rate in the antisaccade task and LC-V1 connectivity on Day1. However, our results illustrated that the antisaccade preparatory PD rate on Day2 is highly correlated with the LC-V1 resting-state functional connectivity in Rest2. Given the significantly greater correlation between RT and PD rate on the antisaccade task in Day2 reported by Waitt (2022), these findings indicate that performance efficiency on the antisaccade is mediated by LC-V1 functional connectivity. Furthermore, the change in the resting-state functional connectivity between the LC-V1 was significantly correlated with the change in PD rate in the antisaccade. This indicates that faster PD rate predicts greater change in LC-V1 connectivity specifically in periods of increased arousal such as the antisaccade task. In addition, this finding imply that the change in the LC-V1 connectivity allow for enhanced visual cortex recruitment by the LC during increased arousal periods represented by the preparatory period in antisaccade trials.

Chapter 6 General Discussion and concluding remarks

In this thesis, we investigated the neuroplastic changes associated with using two different neuromodulation techniques. The first is active tDCS, as an external non-invasive tool of neuromodulation, concurrent with the performance of active inhibitory cognitive control tasks. The second neuromodulation tool was an extended computerised cognitive training game targeted for gaze-control enhancement. Using the same inhibitory control task, we employed different methodologies on two samples to assess the induced cortical neuroplasticity of two different neuromodulation techniques. We used the MEG's high temporal and spatial resolution to measure the instantaneous changes in regional cortical activity during the concurrent task performance and active tDCS. We used pupillometry to assess autonomic nervous system reactivity during task performance. We employed resting state functional connectivity analysis methods to evaluate the MEG and fMRI changes related to neuroplastic changes in cortical and subcortical regions.

In this chapter, we will review the main findings from the preceding chapters in light of the hypotheses specified in section 1.8. We will discuss their applications and implications relevant to the theme that links these hypotheses: brain stimulation effects on the function of the oculomotor control network.

6.1 Resting-state changes associated with treatment conditions

In both treatment conditions, there was a widespread increase in resting state functional connectivity in the Rest2 relative to Rest1 across the cerebral cortex. The increase in connectivity was prominent in the lateral parietal, lateral occipital, lateral temporal, median and posterior cingulate regions. In addition, the active tDCS condition (Figure 2.6) exhibited a greater connectivity increase in frontal regions than the sham condition (Figure 2.5). This change in functional connectivity was supported by the significant increase with time in the degree centrality for the Alpha (Figure 2.8), Beta (Figure 2.10), and cross-frequency connectivity (Figure 2.11). The increase in connectivity was not confined to the OCN (Figure 1.3) (Munoz and Everling, 2004). However, it might reflect an increase in arousal consistent with the widespread LC-

NE innervation to the cortical regions reported in Chapter 3 and discussed below in section 6.2.

Our knowledge of the neurophysiological mechanisms underlie the cognitive training effects on regional cortical activity and inter-regional connectivity is still developing (for detailed reviews, see (Duda and Sweet, 2020, van Balkom et al., 2020, Kelly and Garavan, 2005)). However, the growing evidence from fMRI studies suggests that task-relevant cortical regions exhibit increased activity following short cognitive training, which decreases with a prolonged training regime. Changes in the BOLD signal are difficult to interpret using oscillatory neural signals. Mantini et al. (2007) showed that BOLD signals are associated with different oscillatory signatures in different networks. For example, the Alpha and Beta bands' resting-state activity is positively correlated with fMRI DMN activity and negatively correlated with the DAN and the visual processing networks. Contrasting the antisaccade task performance and the associated treatment condition effects illustrated a different connectivity pattern between the treatment conditions (Figure 2.7). In the sham condition, there was a prominent increase in the connectivity of the occipital, parietal, temporal and limbic cortical regions, with right hemisphere dominance, to the rest of the cortex in Alpha, Beta, and cross-frequency connectivity. In contrast, the active tDCS condition exhibited a prevailing Alpha-band connectivity increase in the left hemisphere for the frontal, parietal, temporal and limbic regions. It is worth noting that the increases in connectivity observed in both conditions might be attributed to engagement in the task. However, some of these changes might reflect a placebo effect in the sham condition, similar to the response to active treatment.

These functional connectivity changes were supported by significant degree-centrality changes prominent in the occipital regions for the sham condition and in the frontal regions for the active tDCS condition (Figure 2.9 and Figure 2.12). The Alpha-band degree-centrality increase of the occipital brain regions following the sham condition is consistent with the prominent role of the visual cortex in both pro- and antisaccade trials (Romei et al., 2010), and the visual processing network (Mantini et al., 2007). This suggests that the post-task changes in Alpha-band connectivity in the sham condition reflect a disengagement of the previously engaged

cortical regions during task performance required for alertness and bottom-up visual processing (Petersen and Posner, 2012, Posner and Petersen, 1990).

On the other hand, the increased Alpha-band centrality in the frontal regions in the active tDCS is consistent with the expected effect of delivering asymmetric tDCS to the frontal cortex. However, this observed pattern of increased Alpha band connectivity in the frontal regions could reflect the disengagement of previously active executive cortical regions involved in the top-down cognitive control required for task performance (Fries, 2015, Jensen and Mazaheri, 2010, Hwang et al., 2016).

These findings support our hypothesis that, compared to the sham condition, a single session of tDCS delivered during the antisaccade task performance would lead to short-term plastic changes in the resting-state network connectivity, persisting for at least several minutes after the treatment. However, we did not find supporting evidence for the hypothesis that the changes in resting state connectivity would be related explicitly to modulation patterns of brain activity observed during the antisaccade task.

6.2 Engagement of the autonomic nervous system during the antisaccade task

Our results illustrated a persistent increase in pupil dilation throughout the time of the antisaccade task up to 500 ms post-stimulus presentation. This increase in pupil dilation represents the activity of the Locus Coeruleus – Norepinephrine (LC-NE) system (Gabay et al., 2011, Aston-Jones and Cohen, 2005). The prosaccade trials exhibited a faster increase in pupil dilation during the preparatory period up to 100 ms before the imperative stimulus presentation, when the antisaccade took over and illustrated a faster increase in pupil dilation up to the end of the period of interest (Figure 3.4). The rate of change in pupil dilation supported this finding by demonstrating a greater increase in antisaccade pupil dilation rate beginning 400 ms post-cue presentation (Figure 3.5). The change in pupil dilation rate was greater following the imperative stimulus presentation in both trial types reflecting the phasic mode activity of the LC-NE. The putative event-related pupil dilation rate confirmed these findings by illustrating a greater event-related pupil dilation rate for

the stimulus to saccade event relative to the cue to stimulus in both trial types, which was more prominent in the antisaccade trials relative to prosaccade (Figure 3.6). This finding reflected the increased arousal and cognitive processing demands associated with the antisaccade trials relative to prosaccades, consistent with a negative correlation with the reaction time of both trial types (Figure 3.8) and prominently with the antisaccade trials (Figure 3.7).

The persistent increased arousal during the antisaccade task performance and the LC-NE system's continuous engagement indicates greater activation of the sympathetic nervous system. Given the widely distributed norepinephrine fibre projections from the Locus Coeruleus to the cerebral cortex(Aston-Jones et al., 1991), this observation is consistent with the widespread increase in the resting state connectivity that persisted after the task completion in both treatment conditions reported in Chapter 2.

6.3 Effects of treatment conditions on cerebral activity during the antisaccade task performance

During task performance, we observed several shared findings between both treatment conditions, which supports previous findings of common physiological processes. In addition, several neuromodulation effects were associated with the active tDCS relative to the sham condition. In the following sections, we will summarize and discuss these findings in light of theories of attention network (Posner and Petersen, 1990), gating by inhibition (Jensen and Mazaheri, 2010) and the communication through coherence (Fries, 2015).

6.3.1 Shared modulation between Treatment conditions

The shared ERSP between the treatment conditions summarised in the following sections indicates the presence of essential neurophysiological processes that were not modulated by receiving a single session of tDCS stimulation.

6.3.1.1 Preparatory oscillatory modulations

During the preparatory period, we found that the Alpha band modulation exhibited an increase in FEF synchronisation and PEF desynchronisation Figure 4.11. Given the established role of the Alpha band in disengaging the irrelative regions to the task in the gating by inhibition theory (Hwang et al., 2014, Jensen and Mazaheri, 2010), these findings indicate the active recruitment of the PEF in preparation for spatial stimulus detection and the disengagement of the FEF to prevent the initiation of an immature saccadic response. Moreover, we found a decrease in FEF and an increase in PEF desynchronisation for both examined Beta bands (Figure 4.5, Figure 4.7) during the second part of the preparatory period.

Given the functional roles of the Beta band in long-distance communication and active recruitment and engagement of task-relevant regions suggested by the CTC theory (Fries, 2015, Engel and Fries, 2010), these findings support the proposed role of the FEF in sustaining ocular fixation and the PEF preparation for spatial localisation of the imperative stimulus (Munoz and Everling, 2004, Coe and Munoz, 2017).

6.3.1.2 DLPFC cognitive control

Our results provide supporting evidence for role differences of the right and left DLPFC in active inhibitory cognitive control during the performance of the antisaccade task (Figure 4.3) (Hwang et al., 2014, Gaymard et al., 1998). The Left DLPFC showed more engagement in the antisaccade trials, while the right DLPFC was more engaged during the prosaccade trials. The desynchronisation of the Alpha band reflected this engagement (Jensen and Mazaheri, 2010). This result supports lateralising the decision-making process in the top-down cognitive control process towards the left DLPFC for the antisaccade (Pierrot-Deseilligny et al., 1991a, Hwang et al., 2014).

6.3.1.3 Stimulus-related oscillatory modulation

Our results support the proposed PEF role in the vector inversion mechanism involved in the antisaccade task performance (Moon et al., 2007, Belyusar et al., 2013, Corbetta et al., 2000). Overall, the contralateral presented stimuli were associated with greater Alpha synchronisation across hemispheres and regions. However, these modulations in the PEF differed significantly for each trial type (Figure 4.10). The contralateral stimulus relative to ipsilateral ones had greater Alpha desynchronisation for prosaccade trials throughout the post-stimulus period in the left PEF. In the antisaccade trials, an initial greater Alpha desynchronisation was associated with contralateral stimuli, which reverses 140 ms post-stimulus presentation towards ipsilateral stimuli dominance. This finding indicates a trial-type specific PEF engagement pattern in response to presented stimuli. As Alpha-band is proposed to regulate a cortical disengagement mechanism (Jensen and Mazaheri, 2010), the left PEF exhibits greater engagement for contralateral presented stimulus maintained throughout the prosaccade trials and inversion of engagement 140 ms post-stimulus in antisaccade trials.

Furthermore, in our results, the PEF response in the low-Beta band differed between trial types. The PEF illustrated greater low-Beta desynchronisation for antisaccade trials throughout the post-stimulus period. Conversely, the prosaccade was associated with a decrease in desynchrony, which commenced at 220 ms and peaked at 300 ms post-stimulus presentation. This timing encompasses the mean of the median RTs in our sample (*mean* = 245.6, Std Dev= 36.1). These findings suggest that PEF plays a significant role in saccade initiation in the prosaccade trials. The absence of this peak in antisaccade trials supports this suggestion, as the FEF is expected to initiate the top-down controlled saccadic response for antisaccade trials Figure 4.12)

6.3.2 Effects of active tDCS

First, active tDCS, relative to the Sham condition, was associated with increased Alpha desynchronisation in the right hemisphere during the preparatory period (Figure 4.4), which persisted during the post-stimulus presentation period across trial types prevailing in the ipsilateral prosaccade trials (Figure 4.11). This finding might implicate the effect of asymmetric electrode positioning of the anode over the right F4 and the cathode electrode over the Fp1 position (Figure 2.2). Alternatively, it could suggest the effect of tDCS in enhancing tonic attention by decreasing Alpha inhibition over the right hemisphere, which has a closer relationship with LC and is implicated in the posterior attention network (Posner and Petersen, 1990, Aston-Jones and Cohen, 2005).

Secondly, the active tDCS condition exhibited a non-specific greater low-Beta band desynchronisation during the second half of the preparatory period, which then converges to reach the same level of desynchronisation as the Sham condition (Figure 4.6). This result suggests a more precise timing of the inhibition of inappropriate motor activity in the active tDCS condition compared to the Sham. Thirdly, the active tDCS modulated the low-Beta band during the post-stimulus period in a stimulus and trial-type sensitive manner. The active tDCS increased the low-Beta band synchronisation for contralateral prosaccade trials in the FEF and the right hemisphere (Figure 4.13 and Figure 4.14, respectively).

To interpret these findings, we should consider the following functional roles; a) the right hemisphere's role in the dorsal attention network and maintaining essential tonic attention for reflexive behaviour (bottom-up cognitive processing) (Spagna et al., 2020, Sturm and Willmes, 2001). b) The established role of the FEF in initiating voluntary saccades (Gaymard et al., 1999). c) The functional roles of Alpha and Beta band oscillations (Fries, 2015, Engel and Fries, 2010). Our findings indicate a beneficial effect of active tDCS stimulation over the F4 region in inducing functional cortical enhancement in regions responsible for bottom-up cognitive processing and voluntary control of saccades.

6.4 Effect of gaze control training on resting state functional connectivity

We aimed to examine the effect of RECOGNeyes as a tool of inhibitory cognitive control training on modulating the resting-state fMRI connectivity between the OCN regions. Our results demonstrated changes in the measured functional connectivity, which was associated with the amount of exposure to RECOGNeyes training. Furthermore, we demonstrated the feasibility of measuring the BOLD signal from LC, which we used to examine its connectivity with the OCN and its relationship with the measured PD during the antisaccade task.

6.4.1.1 Resting-state functional connectivity before and after RECOGNeyes

At baseline, resting state OCN connectivity exhibited a strong correlation between the mirroring OCN regions in the two hemispheres. The LC illustrated functional connectivity with bilateral primary visual cortices. Primary visual regions exhibit functional correlation with the anterior insula. The anterior insula illustrated functional connectivity to both the DLPFC and FEF bilaterally. The right DLPFC demonstrate connectivity with the FEF and PEF both bilaterally. The left DLPFC connected significantly with the left PEF and left FEF (Figure 5.8 A).

After completing the RECOGNeyes training, the OCN illustrated an augmentation of all the Rest1 connections except for the LC to the right primary visual cortex, which decreased to a non-significant correlation. In addition, there were new connections between the bilateral FEF and the bilateral primary visual cortex. The left DLPFC established new connections with bilateral visual cortices and with the right FEF (Figure 5.8 B).

Considering the different physiological roles of each hemisphere in attention (the right hemisphere is involved in the bottom-up processing and the posterior attention network, and the left hemisphere is engaged in phasic attention) (Petersen and Posner, 2012, Corbetta and Shulman, 2002), and the pivotal role of the DLPFC and FEF in executing top-down control and planning of the antisaccade and behaviour (Buschman and Miller, 2007, Connolly et al., 2002), these changes in resting state connectivity imply that RECOGNeyes training strengthens the connectivity of the

decision-making centres (DLPFC and FEF) to other regions in the OCN to facilitate top-down control of eye-movements. Our results only showed a trend level of significance for this change in connectivity. Given the significant correlation observed between the adjusted change score and the amount of training spent on RECOGNeyes, this finding indicates that modulating the training regime by increasing the training duration would produce positive training effects.

6.4.1.2 RECOGNeyes training effects

The total minutes trained on RECOGNeyes were negatively correlated with the inter-homotopic, which indicates that the more time spent on RECOGNeyes training, the less inter-hemispheric connectivity between the mirroring OCN. As patients with ADHD illustrate increased connectivity between mirroring cortical regions (Chen et al., 2021, Jiang et al., 2019), this effect demonstrates the promising potential for the RECOGNeyes game as a therapeutic tool in ADHD and SpLD.

Moreover, at baseline, the right hemisphere exhibited greater intra-hemispheric connectivity than the left hemisphere. The time spent on RECOGNeyes training was negatively correlated with the right intra-hemispheric and positively correlated with the left intra-hemispheric connectivity. This implies that RECOGNeyes training modulates the inter and intra-hemispheric connectivity to balance the difference and facilitate hemispheric functional independence, which is essential for a healthy cortical connectivity (Jiang et al., 2019, Chen et al., 2021). Furthermore, these connectivity changes suggest that RECOGNeyes training decreases the dependence on the reflexive bottom-up processing dormant in the right hemisphere and increases the efficacy of the left hemisphere's role in phasic alertness and its capacity for the oculomotor cognitive control of the gaze direction (Munoz and Everling, 2004, Posner and Petersen, 1990).

6.4.1.3 LC-V1 functional connectivity and PDR

There was a positive correlation between the antisaccade PDR on Day2 and the LC to V1 connectivity during Rest2, which was insignificant for Day1 with Rest1. Furthermore, we found a positive correlation between the change in LC-V1

connectivity and the change in pupil dilation rate from baseline to after the completion of RECOGNeyes training (Figure 5.9). This finding indicates that a greater change in LC-V1 connectivity is associated with greater pupil dilation rate changes in both directions, which supports the putative physiological role of the LC-NE system of modulating arousal, PD and alertness suggested by the adaptive gain theory (Aston-Jones and Cohen, 2005).

Furthermore, when considering A) the replicated negative correlation between the pupil dilation rate and the reaction time in the antisaccade task reported from different samples (here in sections 5.3.4 and 3.3.2 and by Wang et al. (2015) and Karatekin et al. (2010)), and B) the correlation between increased LC-V1 connectivity and greater the pupil dilation rate following RECOGNeye training completion, these findings suggest potential beneficial neuromodulation effects associated with RECOGNeyes training that increases the alertness required for optimum performance in the antisaccade task and that it can produce behavioural changes with a modified training regime.

6.5 Limitations

One of the limitations of this thesis is the sample size and heterogeneity in both studies. The tDCS study sample size did not reach to the calculated sample size (60 participants, 30 in each treatment condition) to achieve the desired effect size. This means that some of our analyses might be underpowered. Furthermore, the concurrent application of tDCS during the MEG session introduced a significant artefact on the measured MEG signal. This led to the further exclusion of six subjects from the MEG task analysis (for details, see section 2.3.3).

Furthermore, our results did not show that active tDCS enhanced participants' task performance nor modulated autonomic effects associated with changes in pupil dilation. We had to use a 1.25 mA because the introduced MEG noise artefacts were unacceptable at 2mA stimulation. Given the previous evidence of optimum tDCS stimulation at 2mA (Max et al., 2021, Stagg and Nitsche, 2011), and the observation that performance changes did not reach a significant difference between Treatment

conditions, it would be intriguing to examine these effects using higher tDCS current amplitude, longer duration or after concurrent active tDCS with cognitive task repeated sessions. In addition, the antisaccade performance analysis could have benefited from examining the learning effect by comparing the performance in the first set of trials to the last set. Our investigation examined the effect of a single montage of active tDCS. It would be informative to examine the effects of reversed electrode placement or symmetric tDCS montages that might result in opposing or more beneficial effects with the antisaccade task.

Despite the interesting findings associated with the used LC map, localising a small region within the neural complexity of the brainstem using a predefined map is an added limitation to the results discussed in this thesis. This map does not provide a definite signal that is only related to the LC, rather it contains noise from neighbouring regions. This noise might mask the actual changes associated with the LC function and hinder its validity.

In addition, the time constraints of the PhD prevented the conduction of several planned and prepared analyses in both studies. In the tDCS study, for example, the antisaccade task accuracy measures, learning effect analysis, network-specific analysis, and response-locked analysis. These analyses will add greater insight into the network connectivity and the physiological ERSP changes in the OCN associated with the saccadic response, specifically on the spatial remapping process.

6.6 Impacts and future directions

We provide supportive evidence for the physiological roles of the OCN regions in the inhibitory cognitive control process. Our work supports the proposed roles of the left DLPFC in decision-making, the FEF in saccade initiation, and the PEF in spatial localisation of salient stimuli and in the vector remapping process involved in redirecting the saccadic eye movements. In our results, the Alpha band modulation was the frequency band implicated in these processes. In contrast, the low-Beta band in the PEF demonstrated trial type-specific changes with increased synchronisation for prosaccade trials around the reaction times, suggesting its involvement in the saccade initiation. However, further work is needed to establish the role of Theta, Delta and Gamma in these processes.

Furthermore, our work shows a neuromodulation effect for tDCS on the OCN involved in the antisaccade task. These modulations were prominent in the frontal eye fields and the right hemisphere. The effect of active tDCS produced different short-term neuroplasticity effects on the resting state networks' functional connectivity. The active tDCS increased the functional connectivity of the frontal regions, while the sham condition exhibited prominent connectivity in the occipital regions. However, examining the effective connectivity between the different OCN regions during task performance and comparing both treatment conditions can lead to further our knowledge of the OCN. Future work should investigate the different tDCS parameters and protocols to identify the most suitable settings for stimulating different cortical regions. Longitudinal studies would provide better insight into the long-term neuroplasticity effect of multiple sessions of active tDCS.

We provided evidence for the efficacy of computerised cognitive training as a neuromodulation tool in introducing neuroplasticity that modulated OCN in the training tasks. Moreover, in the light of the adaptive gain theory (Aston-Jones and Cohen, 2005), we provide evidence of a resting state connection between the LC and the visual cortex. the change in the LC to the visual region connection correlates with the arousal level associated with task performance. This indicates the feasibility and

the validity of measuring fMRI signal from the LC that corresponds with physiological measures of arousal.

The combination of these findings indicates the feasibility and efficacy of using non-invasive neuromodulation techniques to modulate the functional connectivity of brain networks. This provides a promising therapeutic tool for mental disorder patients who suffer from cortical connectivity abnormalities. For example, patients with ADHD suffer from increased homotopic connectivity that results in abnormal motor movements called mirror overflow (Chen et al., 2021) could benefit from a modified version of the RECOGNeye training game that decreases this homotopic connectivity and enhances the independence of both hemispheres.

Furthermore, studies of functional connectivity in schizophrenia point towards reduced connectivity of the left prefrontal cortex among other cortical and subcortical regions (Friston et al., 2016). Our results show a significant effect of a single session of tDCS targeting the DLPFC in introducing neuroplastic changes in the targeted region among other frontal and central regions. This finding demonstrates the promising potential of tDCS as a therapeutic intervention combined with certain cognitive tasks to modulate brain connectivity in the active cortical networks in these tasks.

We expect future research work to demonstrate the beneficial effect of combining active tDCS with cognitive training. These effects will include more efficient learning effects associated with multiple stimulation sessions of adjusted stimulation parameters. This learning enhancement should result from the facilitated neuroplasticity effect caused by the augmentation of naturally occurring neural communications associated with cognitive functioning. Once supportive evidence exists, the tDCS and cognitive training combination will have diverse applications in the clinical and public sectors. These applications could vary, including and not limited to A) treatment of mental disorders, which exhibit deficits of certain cognitive functions, and B) reducing the time required for cognitive learning and skills acquisition among the general population.

6.7 Conclusion

This thesis examined the neuromodulation effects of active tDCS while participants performed an active inhibitory cognitive control task. Moreover, we investigated the effect of RECOGNeye as a computerised cognitive training on modulating functional cortical connectivity. The active tDCS and the RECOGNeyes cognitive training produced neuroplastic changes in the functional connectivity of the cortical regions involved in the OCN. Both techniques had beneficial neuromodulatory effects related to the antisaccade task's performance, resulting in a measured short-term neuroplastic effect for active tDCS and relatively long-term effects for RECOGNeyes.

References

ABD-ALRAZAQ, A., ALAJLANI, M., ALHUWAIL, D., TORO, C. T., GIANNICCHI, A., AHMED, A., MAKHLOUF, A. & HOUSEH, M. 2022a. The Effectiveness and Safety of Serious Games for Improving Cognitive Abilities Among Elderly People With Cognitive Impairment: Systematic Review and Meta-Analysis. *JMIR Serious Games,* 10**,** e34592.

ABD-ALRAZAQ, A., ALHUWAIL, D., AHMED, A. & HOUSEH, M. 2022b. Effectiveness of Serious Games for Improving Executive Functions Among Older Adults With Cognitive Impairment: Systematic Review and Meta-analysis. *JMIR Serious Games,* 10**,** e36123.

ABIKOFF, H. 1991. Cognitive Training in ADHD Children: Less to It Than Meets the Eye. *Journal of Learning Disabilities,* 24**,** 205-209.

AHMAD, S., CH, A. H., BATOOL, A., SITTAR, K. & MALIK, M. 2016. Play and Cognitive Development: Formal Operational Perspective of Piaget's Theory. *Journal of Education and Practice,* 7**,** 72-79.

AINSWORTH, B. & GARNER, M. 2013. Attention control in mood and anxiety disorders: evidence from the antisaccade task. *Human Psychopharmacology: Clinical and Experimental,* 28**,** 274-280.

ALLOWAY, T. P. 2009. Working memory, but not IQ, predicts subsequent learning in children with learning difficulties. *European journal of psychological assessment,* 25**,** 92.

AMARO, E. & BARKER, G. J. 2006. Study design in fMRI: Basic principles. *Brain and Cognition,* 60**,** 220-232.

AMERICAN PSYCHIATRIC, A. 2013. *Diagnostic and Statistical Manual of Mental Disorders (DSM-5®),* Washington, UNITED STATES, American Psychiatric Publishing.

ANDERSSON, J. L., HUTTON, C., ASHBURNER, J., TURNER, R. & FRISTON, K. 2001. Modeling geometric deformations in EPI time series. *Neuroimage,* 13**,** 903-19.

ANTAL, A., VARGA, E. T., KINCSES, T. Z., NITSCHE, M. A. & PAULUS, W. 2004. Oscillatory brain activity and transcranial direct current stimulation in humans. *Neuroreport,* 15**,** 1307-1310.

APPLEBY, B. S., DUGGAN, P. S., REGENBERG, A. & RABINS, P. V. 2007. Psychiatric and neuropsychiatric adverse events associated with deep brain stimulation: A meta-analysis of ten years' experience. *Movement Disorders,* 22**,** 1722-1728.

ARIEL, R. & CASTEL, A. D. 2014. Eyes wide open: Enhanced pupil dilation when selectively studying important information. *Experimental brain research,* 232**,** 337-344.

ARNS, M., CLARK, C. R., TRULLINGER, M., DEBEUS, R., MACK, M. & ANIFTOS, M. 2020. Neurofeedback and Attention-Deficit/Hyperactivity-Disorder (ADHD) in Children: Rating the Evidence and Proposed Guidelines. *Applied Psychophysiology and Biofeedback,* 45**,** 39-48.

ARNS, M., HEINRICH, H. & STREHL, U. 2014. Evaluation of neurofeedback in ADHD: The long and winding road. *Biological Psychology,* 95**,** 108-115.

ARON, A. R. 2007. The Neural Basis of Inhibition in Cognitive Control. *The Neuroscientist,* 13**,** 214-228.

ASHBURNER, J. & FRISTON, K. J. 2005. Unified segmentation. *Neuroimage,* 26**,** 839-51.

ASTON-JONES, G. & COHEN, J. D. 2005. An integrative theory of locus coeruleus-norepinephrine function: adaptive gain and optimal performance. *Annu. Rev. Neurosci.,* 28**,** 403-450.

ASTON-JONES, G., RAJKOWSKI, J. & COHEN, J. 1999. Role of locus coeruleus in attention and behavioral flexibility. *Biological Psychiatry,* 46**,** 1309-1320.

ASTON-JONES, G., RAJKOWSKI, J., KUBIAK, P. & ALEXINSKY, T. 1994. Locus coeruleus neurons in monkey are selectively activated by attended cues in a vigilance task. *Journal of Neuroscience,* 14**,** 4467-4480.

ASTON-JONES, G., SHIPLEY, M., CHOUVET, G., ENNIS, M., VAN BOCKSTAELE, E., PIERIBONE, V., SHIEKHATTAR, R., AKAOKA, H., DROLET, G. & ASTIER, B. 1991. Afferent regulation of locus coeruleus neurons: anatomy, physiology and pharmacology. *Progress in brain research,* 88**,** 47-75.

BAGGETTA, P. & ALEXANDER, P. A. 2016. Conceptualization and Operationalization of Executive Function. *Mind, brain and education,* 10**,** 10-33.

BAHAR-FUCHS, A., MARTYR, A., GOH, A. M. Y., SABATES, J. & CLARE, L. 2019. Cognitive training for people with mild to moderate dementia. *Cochrane Database of Systematic Reviews*.

BAILLET, S., MOSHER, J. C. & LEAHY, R. M. 2001. Electromagnetic brain mapping. *IEEE Signal Processing Magazine,* 18**,** 14-30.

BARI, A. & ROBBINS, T. W. 2013. Inhibition and impulsivity: behavioral and neural basis of response control. *Prog Neurobiol,* 108**,** 44-79.

BARNES, G. R. & HILLEBRAND, A. 2003. Statistical flattening of MEG beamformer images. *Human brain mapping,* 18**,** 1-12.

BARNETT, A. G., VAN DER POLS, J. C. & DOBSON, A. J. 2005. Regression to the mean: what it is and how to deal with it. *International Journal of Epidemiology,* 34**,** 215-220.

BARONE, J. & ROSSITER, H. E. 2021. Understanding the Role of Sensorimotor Beta Oscillations. *Frontiers in Systems Neuroscience,* 15.

BASANOVIC, J., MYLES, O. & MACLEOD, C. 2022. Do the eyes have it? A comparison of eye-movement and attentional-probe-based approaches to indexing attentional control within the antisaccade paradigm. *Quarterly Journal of Experimental Psychology***,** 17470218221083556.

BAŞAR, E. 2013. Brain oscillations in neuropsychiatric disease. *Dialogues Clin Neurosci,* 15**,** 291-300.

BAYS, P. M. & HUSAIN, M. 2007. Spatial remapping of the visual world across saccades. *Neuroreport,* 18**,** 1207-13.

BECKMANN, C. F., DELUCA, M., DEVLIN, J. T. & SMITH, S. M. 2005. Investigations into resting-state connectivity using independent component analysis. *Philos Trans R Soc Lond B Biol Sci,* 360**,** 1001-13.

BEHZADI, Y., RESTOM, K., LIAU, J. & LIU, T. T. 2007. A component based noise correction method (CompCor) for BOLD and perfusion based fMRI. *Neuroimage,* 37**,** 90-101.

BELLATO, A., ARORA, I., HOLLIS, C. & GROOM, M. J. 2020. Is autonomic nervous system function atypical in attention deficit hyperactivity disorder (ADHD)? A systematic review of the evidence. *Neuroscience & Biobehavioral Reviews,* 108**,** 182-206.

BELYUSAR, D., SNYDER, A. C., FREY, H.-P., HARWOOD, M. R., WALLMAN, J. & FOXE, J. J. 2013. Oscillatory alpha-band suppression mechanisms during the rapid attentional shifts required to perform an anti-saccade task. *NeuroImage,* 65**,** 395-407.

BENARROCH, E. E. 2018. Locus coeruleus. *Cell and Tissue Research,* 373**,** 221-232.

BENJAMINI, Y. & HOCHBERG, Y. 1995. Controlling the False Discovery Rate: A Practical and Powerful Approach to Multiple Testing. *Journal of the Royal Statistical Society: Series B (Methodological),* 57**,** 289-300.

BERDENIS VAN BERLEKOM, A., MUFLIHAH, C. H., SNIJDERS, G. J., MACGILLAVRY, H. D., MIDDELDORP, J., HOL, E. M., KAHN, R. S. & DE WITTE, L. D. 2020. Synapse pathology in schizophrenia: a meta-analysis of postsynaptic elements in postmortem brain studies. *Schizophrenia bulletin,* 46**,** 374-386.

BERRIDGE, C. W. 2008. Noradrenergic modulation of arousal. *Brain research reviews,* 58**,** 1-17.

BERRIDGE, C. W. & WATERHOUSE, B. D. 2003. The locus coeruleus–noradrenergic system: modulation of behavioral state and state-dependent cognitive processes. *Brain Research Reviews,* 42**,** 33-84.

BIANCIARDI, M., FUKUNAGA, M., VAN GELDEREN, P., HOROVITZ, S. G., DE ZWART, J. A., SHMUELI, K. & DUYN, J. H. 2009. Sources of functional magnetic resonance imaging signal fluctuations in the human brain at rest: a 7 T study. *Magnetic Resonance Imaging,* 27**,** 1019-1029.

BIRAN, R., MARTIN, D. C. & TRESCO, P. A. 2005. Neuronal cell loss accompanies the brain tissue response to chronically implanted silicon microelectrode arrays. *Exp Neurol,* 195**,** 115-26.

BIRN, R. M., MURPHY, K. & BANDETTINI, P. A. 2008. The effect of respiration variations on independent component analysis results of resting state functional connectivity. *Human brain mapping,* 29**,** 740-750.

BISWAL, B., YETKIN, F. Z., HAUGHTON, V. M. & HYDE, J. S. 1995. Functional connectivity in the motor cortex of resting human brain using echo-planar MRI. *Magn Reson Med,* 34**,** 537-41.

BJORNSSON, C., OH, S. J., AL-KOFAHI, Y., SMITH, K. L., TURNER, J., DE, S., ROYSAM, B., SHAIN, W. & KIM, S. J. 2006. Effects of insertion conditions on tissue strain and vascular damage during neuroprosthetic device insertion. *Journal of neural engineering,* 3**,** 196-207.

BLASER, E., EGLINGTON, L., CARTER, A. S. & KALDY, Z. 2014. Pupillometry Reveals a Mechanism for the Autism Spectrum Disorder (ASD) Advantage in Visual Tasks. *Scientific Reports,* 4**,** 4301.

BOETS, B., OP DE BEECK, H. P., VANDERMOSTEN, M., SCOTT, S. K., GILLEBERT, C. R., MANTINI, D., BULTHÉ, J., SUNAERT, S., WOUTERS, J. & GHESQUIÈRE, P. 2013. Intact but less accessible phonetic representations in adults with dyslexia. *Science,* 342**,** 1251-1254.

BOUFFARD, M. A. 2019. The Pupil. *Continuum (Minneap Minn),* 25**,** 1194-1214.

BOUZIANE, C., CAAN, M. W. A., TAMMINGA, H. G. H., SCHRANTEE, A., BOTTELIER, M. A., DE RUITER, M. B., KOOIJ, S. J. J. & RENEMAN, L. 2018. ADHD and maturation of brain white matter: A DTI study in medication naive children and adults. *NeuroImage: Clinical,* 17**,** 53-59.

BRADLEY, M. M., MICCOLI, L., ESCRIG, M. A. & LANG, P. J. 2008. The pupil as a measure of emotional arousal and autonomic activation. *Psychophysiology,* 45**,** 602-607.

BRAKOWSKI, J., SPINELLI, S., DÖRIG, N., BOSCH, O. G., MANOLIU, A., HOLTFORTH, M. G. & SEIFRITZ, E. 2017. Resting state brain network function in major

depression – Depression symptomatology, antidepressant treatment effects, future research. *Journal of Psychiatric Research,* 92**,** 147-159.

BRAVER, T. S. 2012. The variable nature of cognitive control: a dual mechanisms framework. *Trends Cogn Sci,* 16**,** 106-13.

BROOKES, M. J., HALE, J. R., ZUMER, J. M., STEVENSON, C. M., FRANCIS, S. T., BARNES, G. R., OWEN, J. P., MORRIS, P. G. & NAGARAJAN, S. S. 2011a. Measuring functional connectivity using MEG: methodology and comparison with fcMRI. *Neuroimage,* 56**,** 1082-1104.

BROOKES, M. J., TEWARIE, P. K., HUNT, B. A. E., ROBSON, S. E., GASCOYNE, L. E., LIDDLE, E. B., LIDDLE, P. F. & MORRIS, P. G. 2016. A multi-layer network approach to MEG connectivity analysis. *NeuroImage,* 132**,** 425-438.

BROOKES, M. J., VRBA, J., ROBINSON, S. E., STEVENSON, C. M., PETERS, A. M., BARNES, G. R., HILLEBRAND, A. & MORRIS, P. G. 2008. Optimising experimental design for MEG beamformer imaging. *Neuroimage,* 39**,** 1788-802.

BROOKES, M. J., WOOLRICH, M., LUCKHOO, H., PRICE, D., HALE, J. R., STEPHENSON, M. C., BARNES, G. R., SMITH, S. M. & MORRIS, P. G. 2011b. Investigating the electrophysiological basis of resting state networks using magnetoencephalography. *Proceedings of the National Academy of Sciences,* 108**,** 16783-16788.

BROOKES, M. J., WOOLRICH, M. W. & BARNES, G. R. 2012. Measuring functional connectivity in MEG: A multivariate approach insensitive to linear source leakage. *NeuroImage,* 63**,** 910-920.

BRUCE, C. J., GOLDBERG, M. E., BUSHNELL, M. C. & STANTON, G. B. 1985. Primate frontal eye fields. II. Physiological and anatomical correlates of electrically evoked eye movements. *Journal of Neurophysiology,* 54**,** 714-734.

BUCKNER, R. L., SEPULCRE, J., TALUKDAR, T., KRIENEN, F. M., LIU, H., HEDDEN, T., ANDREWS-HANNA, J. R., SPERLING, R. A. & JOHNSON, K. A. 2009. Cortical Hubs Revealed by Intrinsic Functional Connectivity: Mapping, Assessment of Stability, and Relation to Alzheimer's Disease. *The Journal of Neuroscience,* 29**,** 1860.

BUSCHKUEHL, M. & JAEGGI, S. M. 2010. Improving intelligence: A literature review. *Swiss medical weekly,* 140**,** 266-272.

BUSCHMAN, T. J. & MILLER, E. K. 2007. Top-down versus bottom-up control of attention in the prefrontal and posterior parietal cortices. *Science,* 315**,** 1860-2.

BUZSÁKI, G., ANASTASSIOU, C. A. & KOCH, C. 2012. The origin of extracellular fields and currents — EEG, ECoG, LFP and spikes. *Nature Reviews Neuroscience,* 13**,** 407.

CAVANAGH, P., HUNT, A. R., AFRAZ, A. & ROLFS, M. 2010. Visual stability based on remapping of attention pointers. *Trends in cognitive sciences,* 14**,** 147-153.

CAYE, A., SWANSON, J. M., COGHILL, D. & ROHDE, L. A. 2019. Treatment strategies for ADHD: an evidence-based guide to select optimal treatment. *Molecular Psychiatry,* 24**,** 390-408.

CHAKAROV, V., NARANJO, J. R., SCHULTE-MÖNTING, J., OMLOR, W., HUETHE, F. & KRISTEVA, R. 2009. Beta-Range EEG-EMG Coherence With Isometric Compensation for Increasing Modulated Low-Level Forces. *Journal of Neurophysiology,* 102**,** 1115-1120.

CHANDLER, D. J., GAO, W.-J. & WATERHOUSE, B. D. 2014. Heterogeneous organization of the locus coeruleus projections to prefrontal and motor cortices. *Proceedings of the National Academy of Sciences,* 111**,** 6816-6821.

CHEN, C., LIDSTONE, D., CROCETTI, D., MOSTOFSKY, S. H. & NEBEL, M. B. 2021. Increased interhemispheric somatomotor functional connectivity and mirror overflow in ADHD. *NeuroImage: Clinical,* 31**,** 102759.

CHINDEMI, G., ABDELLAH, M., AMSALEM, O., BENAVIDES-PICCIONE, R., DELATTRE, V., DORON, M., ECKER, A., JAQUIER, A. T., KING, J., KUMBHAR, P., MONNEY, C., PERIN, R., RÖSSERT, C., TUNCEL, A. M., VAN GEIT, W., DEFELIPE, J., GRAUPNER, M., SEGEV, I., MARKRAM, H. & MULLER, E. B. 2022. A calcium-based plasticity model for predicting long-term potentiation and depression in the neocortex. *Nature Communications,* 13**,** 3038.

CHUNG, S. W., HOY, K. E. & FITZGERALD, P. B. 2015. Theta-burst stimulation: a new form of TMS treatment for depression? *Depression and anxiety,* 32**,** 182-192.

CITRI, A. & MALENKA, R. C. 2008. Synaptic Plasticity: Multiple Forms, Functions, and Mechanisms. *Neuropsychopharmacology,* 33**,** 18-41.

CLAYTON, D. F., ANREITER, I., ARISTIZABAL, M., FRANKLAND, P. W., BINDER, E. B. & CITRI, A. 2020. The role of the genome in experience-dependent plasticity: Extending the analogy of the genomic action potential. *Proceedings of the National Academy of Sciences,* 117**,** 23252-23260.

COE, B. C. & MUNOZ, D. P. 2017. Mechanisms of saccade suppression revealed in the anti-saccade task. *Philosophical Transactions of the Royal Society B: Biological Sciences,* 372**,** 20160192.

COFFMAN, B. A., CLARK, V. P. & PARASURAMAN, R. 2014. Battery powered thought: Enhancement of attention, learning, and memory in healthy adults using transcranial direct current stimulation. *NeuroImage,* 85**,** 895-908.

COLCLOUGH, G. L., BROOKES, M. J., SMITH, S. M. & WOOLRICH, M. W. 2015. A symmetric multivariate leakage correction for MEG connectomes. *NeuroImage,* 117**,** 439-448.

COLCLOUGH, G. L., WOOLRICH, M. W., TEWARIE, P. K., BROOKES, M. J., QUINN, A. J. & SMITH, S. M. 2016. How reliable are MEG resting-state connectivity metrics? *NeuroImage,* 138**,** 284-293.

COLE, S. R. & VOYTEK, B. 2017. Brain Oscillations and the Importance of Waveform Shape. *Trends in Cognitive Sciences,* 21**,** 137-149.

COLLINS, P. 2016. *The remediation of oculomotor and attentional deficits of children with ADHD: identifying and training control mechanisms based on ocular data.* University of Nottingham.

CONNERS, C., ERHARDT, D., EPSTEIN, J., PARKER, J., SITARENIOS, G. & SPARROW, E. 1999. Self-ratings of ADHD symptoms in adults I: Factor structure and normative data. *Journal of Attention Disorders,* 3**,** 141-151.

CONNOLLY, J. D., GOODALE, M. A., MENON, R. S. & MUNOZ, D. P. 2002. Human fMRI evidence for the neural correlates of preparatory set. *Nature Neuroscience,* 5**,** 1345-1352.

CORBETTA, M., KINCADE, J. M., OLLINGER, J. M., MCAVOY, M. P. & SHULMAN, G. L. 2000. Voluntary orienting is dissociated from target detection in human posterior parietal cortex. *Nature Neuroscience,* 3**,** 292-297.

CORBETTA, M., PATEL, G. & SHULMAN, G. L. 2008. The Reorienting System of the Human Brain: From Environment to Theory of Mind. *Neuron,* 58**,** 306-324.

CORBETTA, M. & SHULMAN, G. L. 2002. Control of goal-directed and stimulus-driven attention in the brain. *Nature Reviews Neuroscience,* 3**,** 201-215.

CORDES, D., HAUGHTON, V. M., ARFANAKIS, K., CAREW, J. D., TURSKI, P. A., MORITZ, C. H., QUIGLEY, M. A. & MEYERAND, M. E. 2001. Frequencies contributing to functional connectivity in the cerebral cortex in "resting-state" data. *AJNR Am J Neuroradiol,* 22**,** 1326-33.

CORDES, D., HAUGHTON, V. M., ARFANAKIS, K., WENDT, G. J., TURSKI, P. A., MORITZ, C. H., QUIGLEY, M. A. & MEYERAND, M. E. 2000. Mapping functionally related regions of brain with functional connectivity MR imaging. *American journal of neuroradiology,* 21**,** 1636-1644.

CORTESE, S., FERRIN, M., BRANDEIS, D., BUITELAAR, J., DALEY, D., DITTMANN, R. W., HOLTMANN, M., SANTOSH, P., STEVENSON, J. & STRINGARIS, A. 2015. Cognitive training for attention-deficit/hyperactivity disorder: meta-analysis of clinical and neuropsychological outcomes from randomized controlled trials. *Journal of the American Academy of Child & Adolescent Psychiatry,* 54**,** 164-174.

CORTESE, S., FERRIN, M., BRANDEIS, D., HOLTMANN, M., AGGENSTEINER, P., DALEY, D., SANTOSH, P., SIMONOFF, E., STEVENSON, J., STRINGARIS, A., SONUGA-BARKE, E. J. S., ASHERSON, P., BANASCHEWSKI, T., BRANDEIS, D., BUITELAAR, J., COGHILL, D., CORTESE, S., DALEY, D., DANCKAERTS, M., DITTMANN, R. W., DÖPFNER, M., FERRIN, M., HOLLIS, C., HOLTMANN, M., KONOFAL, E., LECENDREUX, M., ROTHENBERGER, A., SANTOSH, P., SERGEANT, J. A., SIMONOFF, E., SONUGA-BARKE, E. J., SOUTULLO, C., STEINHAUSEN, H., STEVENSON, J., STRINGARIS, A., TAYLOR, E., VAN DER OORD, S., WONG, I. & ZUDDAS, A. 2016. Neurofeedback for Attention-Deficit/Hyperactivity Disorder: Meta-Analysis of Clinical and Neuropsychological Outcomes From Randomized Controlled Trials. *Journal of the American Academy of Child & Adolescent Psychiatry,* 55**,** 444-455.

D'ANGOUR, A. 2013. Plato and play: Taking education seriously in ancient Greece. *American Journal of Play,* 5**,** 293-307.

DAMOISEAUX, J. S., ROMBOUTS, S. A., BARKHOF, F., SCHELTENS, P., STAM, C. J., SMITH, S. M. & BECKMANN, C. F. 2006. Consistent resting-state networks across healthy subjects. *Proc Natl Acad Sci U S A,* 103**,** 13848-53.

DAN, E. L., DÎNŞOREANU, M. & MUREŞAN, R. C. Accuracy of Six Interpolation Methods Applied on Pupil Diameter Data. 2020 IEEE International Conference on Automation, Quality and Testing, Robotics (AQTR), 21-23 May 2020 2020. 1-5.

DAVID, O. & FRISTON, K. J. 2003. A neural mass model for MEG/EEG: coupling and neuronal dynamics. *Neuroimage,* 20**,** 1743-55.

DE LUCA, M., BECKMANN, C. F., DE STEFANO, N., MATTHEWS, P. M. & SMITH, S. M. 2006. fMRI resting state networks define distinct modes of long-distance interactions in the human brain. *Neuroimage,* 29**,** 1359-67.

DE OLIVEIRA ROSA, V., ROSA FRANCO, A., ABRAHÃO SALUM JÚNIOR, G., MOREIRA-MAIA, C. R., WAGNER, F., SIMIONI, A., DE FRAGA BASSOTTO, C., R. MORITZ, G., SCHAFFER AGUZZOLI, C., BUCHWEITZ, A., SCHMITZ, M., RUBIA, K. & PAIM ROHDE, L. A. 2020. Effects of computerized cognitive training as add-on treatment to stimulants in ADHD: a pilot fMRI study. *Brain Imaging and Behavior,* 14**,** 1933-1944.

DE PASQUALE, F., DELLA PENNA, S., SNYDER, A. Z., LEWIS, C., MANTINI, D., MARZETTI, L., BELARDINELLI, P., CIANCETTA, L., PIZZELLA, V. & ROMANI, G. L. 2010. Temporal dynamics of spontaneous MEG activity in brain networks. *Proceedings of the National Academy of Sciences,* 107**,** 6040-6045.

DE PASQUALE, F., DELLA PENNA, S., SNYDER, A. Z., MARZETTI, L., PIZZELLA, V., ROMANI, G. L. & CORBETTA, M. 2012. A cortical core for dynamic integration of functional networks in the resting human brain. *Neuron,* 74**,** 753-764.

DEFELIPE, J. & FARIÑAS, I. 1992. The pyramidal neuron of the cerebral cortex: morphological and chemical characteristics of the synaptic inputs. *Prog Neurobiol,* 39**,** 563-607.

DEIBER, M.-P., HASLER, R., COLIN, J., DAYER, A., AUBRY, J.-M., BAGGIO, S., PERROUD, N. & ROS, T. 2020. Linking alpha oscillations, attention and inhibitory control in adult ADHD with EEG neurofeedback. *NeuroImage: Clinical,* 25**,** 102145.

DÉMONET, J. F., TAYLOR, M. J. & CHAIX, Y. 2004. Developmental dyslexia. *Lancet,* 363**,** 1451-60.

DETERDING, S., KHALED, R., NACKE, L. & DIXON, D. 2011. Gamification: Toward a definition. *Proceedings of CHI 2011 Workshop Gamification: Using Game Design Elements in Non-Game Contexts***,** 6-9.

DIAMOND, A. 2013. Executive Functions. *Annual Review of Psychology,* 64**,** 135-168.

DUDA, B. M. & SWEET, L. H. 2020. Functional brain changes associated with cognitive training in healthy older adults: A preliminary ALE meta-analysis. *Brain Imaging and Behavior,* 14**,** 1247-1262.

DUHAMEL, J.-R., COLBY, C. L. & GOLDBERG, M. E. 1992. The updating of the representation of visual space in parietal cortex by intended eye movements. *Science,* 255**,** 90-92.

ELDRETH, D. A., PATTERSON, M. D., PORCELLI, A. J., BISWAL, B. B., REBBECHI, D. & RYPMA, B. 2006. Evidence for multiple manipulation processes in prefrontal cortex. *Brain research,* 1123**,** 145-156.

ENGEL, A. K. & FRIES, P. 2010. Beta-band oscillations—signalling the status quo? *Current Opinion in Neurobiology,* 20**,** 156-165.

ENOCHS, W. S., PETHERICK, P., BOGDANOVA, A., MOHR, U. & WEISSLEDER, R. 1997. Paramagnetic metal scavenging by melanin: MR imaging. *Radiology,* 204**,** 417-423.

ENRIQUEZ-GEPPERT, S., SMIT, D., PIMENTA, M. G. & ARNS, M. 2019. Neurofeedback as a Treatment Intervention in ADHD: Current Evidence and Practice. *Curr Psychiatry Rep,* 21**,** 46.

ESPINOZA, R. T. & KELLNER, C. H. 2022. Electroconvulsive therapy. *New England Journal of Medicine,* 386**,** 667-672.

EVDOKIMIDIS, I., SMYRNIS, N., CONSTANTINIDIS, T., STEFANIS, N., AVRAMOPOULOS, D., PAXIMADIS, C., THELERITIS, C., EFSTRATIADIS, C., KASTRINAKIS, G. & STEFANIS, C. 2002. The antisaccade task in a sample of 2,006 young men. *Experimental Brain Research,* 147**,** 45-52.

EVERLING, S. & MUNOZ, D. P. 2000. Neuronal correlates for preparatory set associated with pro-saccades and anti-saccades in the primate frontal eye field. *J Neurosci,* 20**,** 387-400.

EVERLING, S., SPANTEKOW, A., KRAPPMANN, P. & FLOHR, H. 1998. Event-related potentials associated with correct and incorrect responses in a cued antisaccade task. *Experimental Brain Research,* 118**,** 27-34.

EYSENCK, M. W., DERAKSHAN, N., SANTOS, R. & CALVO, M. G. 2007. Anxiety and cognitive performance: attentional control theory. *Emotion,* 7**,** 336-53.

EYSENCK, M. W. & KEANE, M. T. 2020. *Cognitive Psychology: A Student's Handbook,* Milton, Milton: Taylor & Francis Group.

FAN, J., BYRNE, J., WORDEN, M. S., GUISE, K. G., MCCANDLISS, B. D., FOSSELLA, J. & POSNER, M. I. 2007. The Relation of Brain Oscillations to Attentional Networks. *The Journal of Neuroscience,* 27**,** 6197-6206.

FAN, J., MCCANDLISS, B. D., FOSSELLA, J., FLOMBAUM, J. I. & POSNER, M. I. 2005. The activation of attentional networks. *Neuroimage,* 26**,** 471-479.

FAN, J., MCCANDLISS, B. D., SOMMER, T., RAZ, A. & POSNER, M. I. 2002. Testing the efficiency and independence of attentional networks. *J Cogn Neurosci,* 14**,** 340-7.

FAUL, F., ERDFELDER, E., LANG, A. G. & BUCHNER, A. 2007. G*Power 3: a flexible statistical power analysis program for the social, behavioral, and biomedical sciences. *Behav Res Methods,* 39**,** 175-91.

FEINBERG, I. 1982. Schizophrenia: Caused by a fault in programmed synaptic elimination during adolescence? *Journal of Psychiatric Research,* 17**,** 319-334.

FIELDING, J., CLOUGH, M., BEH, S., MILLIST, L., SEARS, D., FROHMAN, A. N., LIZAK, N., LIM, J., KOLBE, S., RENNAKER, R. L., FROHMAN, T. C., WHITE, O. B. & FROHMAN, E. M. 2015. Ocular motor signatures of cognitive dysfunction in multiple sclerosis. *Nature Reviews Neurology,* 11**,** 637-645.

FILMER, H. L., DUX, P. E. & MATTINGLEY, J. B. 2014. Applications of transcranial direct current stimulation for understanding brain function. *Trends Neurosci,* 37**,** 742-53.

FISCHER, B. & WEBER, H. 1993. Express saccades and visual attention. *Behavioral and Brain Sciences,* 16**,** 553-567.

FISHER, R. A. 1921. 014: On the" Probable Error" of a Coefficient of Correlation Deduced from a Small Sample.

FLEMING, T. M., BAVIN, L., STASIAK, K., HERMANSSON-WEBB, E., MERRY, S. N., CHEEK, C., LUCASSEN, M., LAU, H. M., POLLMULLER, B. & HETRICK, S. 2017.

Serious games and gamification for mental health: current status and promising directions. *Frontiers in psychiatry,* 7**,** 215.

FOOD AND DRUG ADMINISTRATION, H. 2018. Neurological Devices; Reclassification of Electroconvulsive Therapy Devices; Effective Date of Requirement for Premarket Approval for Electroconvulsive Therapy Devices for Certain Specified Intended Uses. Final order. *Fed Regist,* 83**,** 66103-24.

FOX, M. D., SNYDER, A. Z., VINCENT, J. L., CORBETTA, M., VAN ESSEN, D. C. & RAICHLE, M. E. 2005. The human brain is intrinsically organized into dynamic, anticorrelated functional networks. *Proc Natl Acad Sci U S A,* 102**,** 9673-8.

FOX, M. D., ZHANG, D., SNYDER, A. Z. & RAICHLE, M. E. 2009. The global signal and observed anticorrelated resting state brain networks. *J Neurophysiol,* 101**,** 3270-83.

FOXE, J. & SNYDER, A. 2011. The Role of Alpha-Band Brain Oscillations as a Sensory Suppression Mechanism during Selective Attention. *Frontiers in Psychology,* 2.

FOXE, J. J., SIMPSON, G. V. & AHLFORS, S. P. 1998. Parieto-occipital~ 1 0Hz activity reflects anticipatory state of visual attention mechanisms. *Neuroreport,* 9**,** 3929-3933.

FRIES, P. 2015. Rhythms for Cognition: Communication through Coherence. *Neuron,* 88**,** 220-35.

FRISTON, K., BROWN, H. R., SIEMERKUS, J. & STEPHAN, K. E. 2016. The dysconnection hypothesis (2016). *Schizophrenia research,* 176**,** 83-94.

FRISTON, K. J. 1994. Functional and effective connectivity in neuroimaging: A synthesis. *Human Brain Mapping,* 2**,** 56-78.

FRISTON, K. J. 1998. The disconnection hypothesis. *Schizophrenia Research,* 30**,** 115-125.

FRITH, U. 1999. Paradoxes in the definition of dyslexia. *Dyslexia,* 5**,** 192-214.

GABAY, S., PERTZOV, Y. & HENIK, A. 2011. Orienting of attention, pupil size, and the norepinephrine system. *Attention, Perception, & Psychophysics,* 73**,** 123-129.

GARCÍA-BAOS, A., TOMAS, D., OLIVEIRA, I., COLLINS, P., ECHEVARRIA, C., ZAPATA, L. P., LIDDLE, E. & SUPER, H. 2019. Novel interactive eye-tracking game for training attention in children with attention-deficit/hyperactivity disorder. *The primary care companion for CNS disorders,* 21**,** 26348.

GAREY, L., ONG, W., PATEL, T., KANANI, M., DAVIS, A., MORTIMER, A., BARNES, T. & HIRSCH, S. 1998. Reduced dendritic spine density on cerebral cortical pyramidal neurons in schizophrenia. *Journal of Neurology, Neurosurgery & Psychiatry,* 65**,** 446-453.

GASIOROWSKA, A., WYDRYCH, M., DRAPICH, P., ZADROZNY, M., STECZKOWSKA, M., NIEWIADOMSKI, W. & NIEWIADOMSKA, G. 2021. The Biology and Pathobiology of Glutamatergic, Cholinergic, and Dopaminergic Signaling in the Aging Brain. *Frontiers in Aging Neuroscience,* 13.

GAU, S. S.-F., CHEN, S.-J., CHOU, W.-J., CHENG, H., TANG, C.-S., CHANG, H.-L., TZANG, R.-F., WU, Y.-Y., HUANG, Y.-F. & CHOU, M.-C. 2008. National survey of adherence, efficacy, and side effects of methylphenidate in children with attention-deficit/hyperactivity disorder in Taiwan. *The Journal of clinical psychiatry,* 69**,** 12448.

GAYMARD, B., PLONER, C. J., RIVAUD, S., VERMERSCH, A. I. & PIERROT-DESEILLIGNY, C. 1998. Cortical control of saccades. *Experimental Brain Research,* 123**,** 159-163.

GAYMARD, B., PLONER, C. J., RIVAUD-PÉCHOUX, S. & PIERROT-DESEILLIGNY, C. 1999. The frontal eye field is involved in spatial short-term memory but not in reflexive saccade inhibition. *Exp Brain Res,* 129**,** 288-301.

GAYNES, B. N., LLOYD, S. W., LUX, L., GARTLEHNER, G., HANSEN, R. A., BRODE, S., JONAS, D. E., EVANS, T. S., VISWANATHAN, M. & LOHR, K. N. 2014. Repetitive transcranial magnetic stimulation for treatment-resistant depression: a systematic review and meta-analysis. *The Journal of clinical psychiatry,* 75**,** 29758.

GENTRY, S. V., GAUTHIER, A., L'ESTRADE EHRSTROM, B., WORTLEY, D., LILIENTHAL, A., TUDOR CAR, L., DAUWELS-OKUTSU, S., NIKOLAOU, C. K., ZARY, N., CAMPBELL, J. & CAR, J. 2019. Serious Gaming and Gamification Education in Health Professions: Systematic Review. *J Med Internet Res,* 21**,** e12994.

GERALDO, A., DORES, A. R., CASTRO-CALDAS, A. & BARBOSA, F. 2022. Functional connectivity as a neural correlate of cognitive rehabilitation programs' efficacy: A systematic review. *Current Psychology*.

GEVA, R., ZIVAN, M., WARSHA, A. & OLCHIK, D. 2013. Alerting, orienting or executive attention networks: differential patters of pupil dilations. *Frontiers in Behavioral Neuroscience,* 7.

GILZENRAT, M. S., NIEUWENHUIS, S., JEPMA, M. & COHEN, J. D. 2010. Pupil diameter tracks changes in control state predicted by the adaptive gain theory of locus coeruleus function. *Cognitive, Affective, & Behavioral Neuroscience,* 10**,** 252-269.

GREICIUS, M. D., KRASNOW, B., REISS, A. L. & MENON, V. 2003. Functional connectivity in the resting brain: A network analysis of the default mode hypothesis. *Proceedings of the National Academy of Sciences,* 100**,** 253-258.

GROSBRAS, M. H., LAIRD, A. R. & PAUS, T. 2005. Cortical regions involved in eye movements, shifts of attention, and gaze perception. *Human brain mapping,* 25**,** 140-154.

GROSS, J. 2019. Magnetoencephalography in Cognitive Neuroscience: A Primer. *Neuron,* 104**,** 189-204.

GROUP, M. C. 2004. National Institute of Mental Health Multimodal Treatment Study of ADHD Follow-up: 24-Month Outcomes of Treatment Strategies for Attention-Deficit/Hyperactivity Disorder. *Pediatrics,* 113**,** 754-761.

GUO, J., LUO, X., WANG, E., LI, B., CHANG, Q., SUN, L. & SONG, Y. 2019. Abnormal alpha modulation in response to human eye gaze predicts inattention severity in children with ADHD. *Developmental Cognitive Neuroscience,* 38**,** 100671.

HABER, S. N., LIU, H., SEIDLITZ, J. & BULLMORE, E. 2022. Prefrontal connectomics: from anatomy to human imaging. *Neuropsychopharmacology,* 47**,** 20-40.

HABGOOD, M. J. & AINSWORTH, S. E. 2011. Motivating children to learn effectively: Exploring the value of intrinsic integration in educational games. *The Journal of the Learning Sciences,* 20**,** 169-206.

HAEGENS, S., NÁCHER, V., LUNA, R., ROMO, R. & JENSEN, O. 2011. α-Oscillations in the monkey sensorimotor network influence discrimination performance by rhythmical inhibition of neuronal spiking. *Proc Natl Acad Sci U S A,* 108**,** 19377-82.

HALL, A. 2008. Specific learning difficulties. *Psychiatry,* 7**,** 260-265.

HALLETT, P. E. 1978. Primary and secondary saccades to goals defined by instructions. *Vision Research,* 18**,** 1279-1296.

HALLEZ, H., VANRUMSTE, B., GRECH, R., MUSCAT, J., DE CLERCQ, W., VERGULT, A., D'ASSELER, Y., CAMILLERI, K. P., FABRI, S. G., VAN HUFFEL, S. & LEMAHIEU, I. 2007. Review on solving the forward problem in EEG source analysis. *Journal of NeuroEngineering and Rehabilitation,* 4**,** 46.

HALLQUIST, M. N., HWANG, K. & LUNA, B. 2013. The nuisance of nuisance regression: spectral misspecification in a common approach to resting-state fMRI preprocessing reintroduces noise and obscures functional connectivity. *Neuroimage,* 82**,** 208-25.

HÄMÄLÄINEN, M., HARI, R., ILMONIEMI, R. J., KNUUTILA, J. & LOUNASMAA, O. V. 1993. Magnetoencephalography---theory, instrumentation, and applications to noninvasive studies of the working human brain. *Reviews of Modern Physics,* 65**,** 413-497.

HAMANI, C. & LOZANO, A. M. 2006. Hardware-Related Complications of Deep Brain Stimulation: A Review of the Published Literature. *Stereotactic and Functional Neurosurgery,* 84**,** 248-251.

HAMILTON, J. P., CHEN, M. C. & GOTLIB, I. H. 2013. Neural systems approaches to understanding major depressive disorder: An intrinsic functional organization perspective. *Neurobiology of Disease,* 52**,** 4-11.

HAMPSON, M., DRIESEN, N. R., SKUDLARSKI, P., GORE, J. C. & CONSTABLE, R. T. 2006. Brain connectivity related to working memory performance. *J Neurosci,* 26**,** 13338-43.

HAMPSON, M., PETERSON, B. S., SKUDLARSKI, P., GATENBY, J. C. & GORE, J. C. 2002. Detection of functional connectivity using temporal correlations in MR images. *Human Brain Mapping,* 15**,** 247-262.

HÄNDEL, B. F., HAARMEIER, T. & JENSEN, O. 2011. Alpha Oscillations Correlate with the Successful Inhibition of Unattended Stimuli. *Journal of Cognitive Neuroscience,* 23**,** 2494-2502.

HAYES, T. R. & PETROV, A. A. 2016. Mapping and correcting the influence of gaze position on pupil size measurements. *Behavior Research Methods,* 48**,** 510-527.

HEEGER, D. J. & RESS, D. 2002. What does fMRI tell us about neuronal activity? *Nature Reviews Neuroscience,* 3**,** 142-151.

HENSON, R., BUECHEL, C., JOSEPHS, O. & FRISTON, K. 1999. The slice-timing problem in event-related fMRI. *NeuroImage,* 9**,** 125-.

HESS, E. H. & POLT, J. M. 1960. Pupil Size as Related to Interest Value of Visual Stimuli. *Science,* 132**,** 349-350.

HILL, N. T. M., MOWSZOWSKI, L., NAISMITH, S. L., CHADWICK, V. L., VALENZUELA, M. & LAMPIT, A. 2016. Computerized Cognitive Training in Older Adults With Mild Cognitive Impairment or Dementia: A Systematic Review and Meta-Analysis. *American Journal of Psychiatry,* 174**,** 329-340.

HIPP, J. F., HAWELLEK, D. J., CORBETTA, M., SIEGEL, M. & ENGEL, A. K. 2012. Large-scale cortical correlation structure of spontaneous oscillatory activity. *Nature Neuroscience,* 15**,** 884-890.

HOLLANDER, E. & ROSEN, J. 2000. Impulsivity. *Journal of Psychopharmacology,* 14**,** S39-S44.

HOLSHEIMER, J. 2003. Letters to the Editor. *Neuromodulation: Technology at the Neural Interface,* 6**,** 270-272.

HORN, A. & FOX, M. D. 2020. Opportunities of connectomic neuromodulation. *NeuroImage,* 221**,** 117180.

HOSSEINI, S. M. H., PRITCHARD-BERMAN, M., SOSA, N., CEJA, A. & KESLER, S. R. 2016. Task-based neurofeedback training: A novel approach toward training executive functions. *NeuroImage,* 134**,** 153-159.

HOWELLS, F. M., STEIN, D. J. & RUSSELL, V. A. 2012. Synergistic tonic and phasic activity of the locus coeruleus norepinephrine (LC-NE) arousal system is required for optimal attentional performance. *Metab Brain Dis,* 27**,** 267-74.

HOWES, O. D., CUMMINGS, C., CHAPMAN, G. E. & SHATALINA, E. 2023. Neuroimaging in schizophrenia: an overview of findings and their implications for synaptic changes. *Neuropsychopharmacology,* 48**,** 151-167.

HSU, T.-Y., HSU, Y.-F., WANG, H.-Y. & WANG, C.-A. 2021. Role of the frontal eye field in human pupil and saccade orienting responses. *European Journal of Neuroscience,* 54**,** 4283-4294.

HUANG, M. X., MOSHER, J. C. & LEAHY, R. M. 1999. A sensor-weighted overlapping-sphere head model and exhaustive head model comparison for MEG. *Physics in Medicine and Biology,* 44**,** 423-440.

HUANG, M. X., SHIH, J. J., LEE, R. R., HARRINGTON, D. L., THOMA, R. J., WEISEND, M. P., HANLON, F., PAULSON, K. M., LI, T., MARTIN, K., MILLERS, G. A. & CANIVE, J. M. 2004. Commonalities and differences among vectorized beamformers in electromagnetic source imaging. *Brain Topogr,* 16**,** 139-58.

HUSTER, R. J. & RAUD, L. 2018. A Tutorial Review on Multi-subject Decomposition of EEG. *Brain Topography,* 31**,** 3-16.

HUTTON, S. B. & ETTINGER, U. 2006. The antisaccade task as a research tool in psychopathology: A critical review. *Psychophysiology,* 43**,** 302-313.

HWANG, K., GHUMAN, A. S., MANOACH, D. S., JONES, S. R. & LUNA, B. 2014. Cortical Neurodynamics of Inhibitory Control. *The Journal of Neuroscience,* 34**,** 9551.

HWANG, K., GHUMAN, A. S., MANOACH, D. S., JONES, S. R. & LUNA, B. 2016. Frontal preparatory neural oscillations associated with cognitive control: A developmental study comparing young adults and adolescents. *NeuroImage,* 136**,** 139-148.

HWANG, K., VELANOVA, K. & LUNA, B. 2010. Strengthening of Top-Down Frontal Cognitive Control Networks Underlying the Development of Inhibitory Control: A Functional Magnetic Resonance Imaging Effective Connectivity Study. *The Journal of Neuroscience,* 30**,** 15535.

ISAACS, B. R., MULDER, M. J., GROOT, J. M., VAN BERENDONK, N., LUTE, N., BAZIN, P. L., FORSTMANN, B. U. & ALKEMADE, A. 2020. 3 versus 7 Tesla magnetic resonance imaging for parcellations of subcortical brain structures in clinical settings. *PLoS One,* 15**,** e0236208.

JACKSON, A., MAVOORI, J. & FETZ, E. E. 2006. Long-term motor cortex plasticity induced by an electronic neural implant. *Nature,* 444**,** 56-60.

JACKSON, A. F. & BOLGER, D. J. 2014. The neurophysiological bases of EEG and EEG measurement: A review for the rest of us. *Psychophysiology,* 51**,** 1061-1071.

JENSEN, O. & BONNEFOND, M. 2013. Prefrontal α- and β-band oscillations are involved in rule selection. *Trends Cogn Sci,* 17**,** 10-2.

JENSEN, O. & MAZAHERI, A. 2010. Shaping functional architecture by oscillatory alpha activity: gating by inhibition. *Front Hum Neurosci,* 4**,** 186.

JENSEN, P. S., HINSHAW, S. P., KRAEMER, H. C., LENORA, N., NEWCORN, J. H., ABIKOFF, H. B., MARCH, J. S., ARNOLD, L. E., CANTWELL, D. P., CONNERS, C. K., ELLIOTT, G. R., GREENHILL, L. L., HECHTMAN, L., HOZA, B., PELHAM, W. E., SEVERE, J. B., SWANSON, J. M., WELLS, K. C., WIGAL, T. & VITIELLO, B. 2001. ADHD Comorbidity Findings From the MTA Study: Comparing Comorbid Subgroups. *Journal of the American Academy of Child & Adolescent Psychiatry,* 40**,** 147-158.

JIANG, K., YI, Y., LI, L., LI, H., SHEN, H., ZHAO, F., XU, Y. & ZHENG, A. 2019. Functional network connectivity changes in children with attention-deficit hyperactivity disorder: A resting-state fMRI study. *International Journal of Developmental Neuroscience,* 78**,** 1-6.

JODOJ, E., CHIANG, C. & ASTON-JONES, G. 1998. Potent excitatory influence of prefrontal cortex activity on noradrenergic locus coeruleus neurons. *Neuroscience,* 83**,** 63-79.

JOHNSTONE, S. J., ROODENRYS, S. J., JOHNSON, K., BONFIELD, R. & BENNETT, S. J. 2017. Game-based combined cognitive and neurofeedback training using Focus Pocus reduces symptom severity in children with diagnosed AD/HD and subclinical AD/HD. *International Journal of Psychophysiology,* 116**,** 32-44.

JOSHI, S., LI, Y., KALWANI, RISHI M. & GOLD, JOSHUA I. 2016. Relationships between Pupil Diameter and Neuronal Activity in the Locus Coeruleus, Colliculi, and Cingulate Cortex. *Neuron,* 89**,** 221-234.

KAMIŃSKI, J., BRZEZICKA, A., GOLA, M. & WRÓBEL, A. 2012. Beta band oscillations engagement in human alertness process. *International Journal of Psychophysiology,* 85**,** 125-128.

KANG, O. E., HUFFER, K. E. & WHEATLEY, T. P. 2014. Pupil Dilation Dynamics Track Attention to High-Level Information. *PLOS ONE,* 9**,** e102463.

KARATEKIN, C., BINGHAM, C. & WHITE, T. 2010. Oculomotor and Pupillometric Indices of Pro- and Antisaccade Performance in Youth-Onset Psychosis and Attention Deficit/Hyperactivity Disorder. *Schizophrenia Bulletin,* 36**,** 1167-1186.

KATZ, P. S. & FROST, W. N. 1996. Intrinsic neuromodulation: altering neuronal circuits from within. *Trends in Neurosciences,* 19**,** 54-61.

KEESER, D., MEINDL, T., BOR, J., PALM, U., POGARELL, O., MULERT, C., BRUNELIN, J., MÖLLER, H.-J., REISER, M. & PADBERG, F. 2011. Prefrontal Transcranial Direct Current Stimulation Changes Connectivity of Resting-State Networks during fMRI. *The Journal of Neuroscience,* 31**,** 15284.

KELLY, A. M. & GARAVAN, H. 2005. Human functional neuroimaging of brain changes associated with practice. *Cereb Cortex,* 15**,** 1089-102.

KELLY, S. P., LALOR, E. C., REILLY, R. B. & FOXE, J. J. 2006. Increases in alpha oscillatory power reflect an active retinotopic mechanism for distracter suppression during sustained visuospatial attention. *Journal of neurophysiology,* 95**,** 3844-3851.

KEREN, N. I., LOZAR, C. T., HARRIS, K. C., MORGAN, P. S. & ECKERT, M. A. 2009. In vivo mapping of the human locus coeruleus. *Neuroimage,* 47**,** 1261-7.

KHANNA, P. & CARMENA, J. M. 2017. Beta band oscillations in motor cortex reflect neural population signals that delay movement onset. *eLife,* 6**,** e24573.

KIM, S.-G., RICHTER, W. & UĞURBIL, K. 1997. Limitations of temporal resolution in functional MRI. *Magnetic Resonance in Medicine,* 37**,** 631-636.

KIRK, H. E., GRAY, K., RIBY, D. M. & CORNISH, K. M. 2015. Cognitive training as a resolution for early executive function difficulties in children with intellectual disabilities. *Research in Developmental Disabilities,* 38**,** 145-160.

KIRK, H. E., GRAY, K. M., ELLIS, K., TAFFE, J. & CORNISH, K. M. 2016. Computerised attention training for children with intellectual and developmental disabilities: a randomised controlled trial. *Journal of Child Psychology and Psychiatry,* 57**,** 1380-1389.

KLEIN, C. & FOERSTER, F. 2001. Development of prosaccade and antisaccade task performance in participants aged 6 to 26 years. *Psychophysiology,* 38**,** 179-89.

KNYAZEV, G. G. 2007. Motivation, emotion, and their inhibitory control mirrored in brain oscillations. *Neuroscience & Biobehavioral Reviews,* 31**,** 377-395.

KOELEWIJN, T., DE KLUIVER, H., SHINN-CUNNINGHAM, B. G., ZEKVELD, A. A. & KRAMER, S. E. 2015. The pupil response reveals increased listening effort when it is difficult to focus attention. *Hearing Research,* 323**,** 81-90.

KOFLER, M. J., HARMON, S. L., ADUEN, P. A., DAY, T. N., AUSTIN, K. E., SPIEGEL, J. A., IRWIN, L. & SARVER, D. E. 2018. Neurocognitive and behavioral predictors of social problems in ADHD: A Bayesian framework. *Neuropsychology,* 32**,** 344-355.

KÜHN, S., VANDERHASSELT, M.-A., DE RAEDT, R. & GALLINAT, J. 2012. Why ruminators won't stop: the structural and resting state correlates of rumination and its relation to depression. *Journal of affective disorders,* 141**,** 352-360.

KUO, M.-F. & NITSCHE, M. A. 2012. Effects of Transcranial Electrical Stimulation on Cognition. *Clinical EEG and Neuroscience,* 43**,** 192-199.

LAENG, B., SIROIS, S. & GREDEBÄCK, G. 2012. Pupillometry: A Window to the Preconscious? *Perspect Psychol Sci,* 7**,** 18-27.

LAMPIT, A., HALLOCK, H., SUO, C., NAISMITH, S. L. & VALENZUELA, M. 2015. Cognitive training-induced short-term functional and long-term structural plastic change is related to gains in global cognition in healthy older adults: a pilot study. *Frontiers in aging neuroscience,* 7**,** 14.

LAN, M. J., CHHETRY, B. T., LISTON, C., MANN, J. J. & DUBIN, M. 2016. Transcranial magnetic stimulation of left dorsolateral prefrontal cortex induces brain morphological changes in regions associated with a treatment resistant major depressive episode: an exploratory analysis. *Brain stimulation,* 9**,** 577-583.

LENARTOWICZ, A., MAZAHERI, A., JENSEN, O. & LOO, S. K. 2018. Aberrant Modulation of Brain Oscillatory Activity and Attentional Impairment in Attention-Deficit/Hyperactivity Disorder. *Biological Psychiatry: Cognitive Neuroscience and Neuroimaging,* 3**,** 19-29.

LEUNG, I. H. K., WALTON, C. C., HALLOCK, H., LEWIS, S. J. G., VALENZUELA, M. & LAMPIT, A. 2015. Cognitive training in Parkinson disease. *Neurology,* 85**,** 1843.

LEWIS, C. M., BALDASSARRE, A., COMMITTERI, G., ROMANI, G. L. & CORBETTA, M. 2009. Learning sculpts the spontaneous activity of the resting human brain. *Proc Natl Acad Sci U S A,* 106**,** 17558-63.

LEWIS, P. M., THOMSON, R. H., ROSENFELD, J. V. & FITZGERALD, P. B. 2016. Brain Neuromodulation Techniques:A Review. *The Neuroscientist,* 22**,** 406-421.

LI, M. C. & COOK, M. J. 2018. Deep brain stimulation for drug-resistant epilepsy. *Epilepsia,* 59**,** 273-290.

LI, S., HU, N., ZHANG, W., TAO, B., DAI, J., GONG, Y., TAN, Y., CAI, D. & LUI, S. 2019. Dysconnectivity of Multiple Brain Networks in Schizophrenia: A Meta-Analysis of Resting-State Functional Connectivity. *Frontiers in Psychiatry,* 10.

LIEBETANZ, D., NITSCHE, M. A., TERGAU, F. & PAULUS, W. 2002. Pharmacological approach to the mechanisms of transcranial DC-stimulation-induced after-effects of human motor cortex excitability. *Brain,* 125**,** 2238-2247.

LISANBY, S. H. 2007. Electroconvulsive therapy for depression. *New England Journal of Medicine,* 357**,** 1939-1945.

LISMAN, J. 1989. A mechanism for the Hebb and the anti-Hebb processes underlying learning and memory. *Proceedings of the National Academy of Sciences,* 86**,** 9574-9578.

LOBEL, E., KAHANE, P., LEONARDS, U., GROSBRAS, M., LEHÉRICY, S., LE BIHAN, D. & BERTHOZ, A. 2001. Localization of human frontal eye fields: anatomical and functional findings of functional magnetic resonance imaging and intracerebral electrical stimulation. *J Neurosurg,* 95**,** 804-15.

LOGOTHETIS, N. K. 2008. What we can do and what we cannot do with fMRI. *Nature,* 453**,** 869-878.

LOGOTHETIS, N. K., PAULS, J., AUGATH, M., TRINATH, T. & OELTERMANN, A. 2001. Neurophysiological investigation of the basis of the fMRI signal. *Nature,* 412**,** 150-157.

LOUTHRENOO, O., BOONCHOODUANG, N., LIKHITWEERAWONG, N., CHAROENKWAN, K. & SRISURAPANONT, M. 2021. The Effects of Neurofeedback on Executive Functioning in Children With ADHD: A Meta-Analysis. *Journal of Attention Disorders,* 26**,** 976-984.

LOYER CARBONNEAU, M., DEMERS, M., BIGRAS, M. & GUAY, M.-C. 2021. Meta-Analysis of Sex Differences in ADHD Symptoms and Associated Cognitive Deficits. *Journal of Attention Disorders,* 25**,** 1640-1656.

LUAN, S., WILLIAMS, I., NIKOLIC, K. & CONSTANDINOU, T. G. 2014. Neuromodulation: present and emerging methods. *Frontiers in Neuroengineering,* 7.

LUBIANIKER, N., PARET, C., DAYAN, P. & HENDLER, T. 2022. Neurofeedback through the lens of reinforcement learning. *Trends in Neurosciences,* 45**,** 579-593.

LUO, Y., WEIBMAN, D., HALPERIN, J. M. & LI, X. 2019. A Review of Heterogeneity in Attention Deficit/Hyperactivity Disorder (ADHD). *Frontiers in Human Neuroscience,* 13.

LYNAM, D. R., SMITH, G. T., WHITESIDE, S. P. & CYDERS, M. A. 2006. The UPPS-P: Assessing five personality pathways to impulsive behavior. *West Lafayette, IN: Purdue University*.

LYNCH, M. A. 2004. Long-Term Potentiation and Memory. *Physiological Reviews,* 84**,** 87-136.

MACDONALD, A. W., COHEN, J. D., STENGER, V. A. & CARTER, C. S. 2000. Dissociating the role of the dorsolateral prefrontal and anterior cingulate cortex in cognitive control. *Science,* 288**,** 1835-1838.

MACEY, P. M., MACEY, K. E., KUMAR, R. & HARPER, R. M. 2004. A method for removal of global effects from fMRI time series. *NeuroImage,* 22**,** 360-366.

MAKEIG, S. 1993. Auditory event-related dynamics of the EEG spectrum and effects of exposure to tones. *Electroencephalography and Clinical Neurophysiology,* 86**,** 283-293.

MAKEIG, S., DEBENER, S., ONTON, J. & DELORME, A. 2004. Mining event-related brain dynamics. *Trends in Cognitive Sciences,* 8**,** 204-210.

MALENKA, R. C. & BEAR, M. F. 2004. LTP and LTD: An Embarrassment of Riches. *Neuron,* 44**,** 5-21.

MANTINI, D., PERRUCCI, M. G., DEL GRATTA, C., ROMANI, G. L. & CORBETTA, M. 2007. Electrophysiological signatures of resting state networks in the human brain. *Proc Natl Acad Sci U S A,* 104**,** 13170-5.

MARGARI, L., BUTTIGLIONE, M., CRAIG, F., CRISTELLA, A., DE GIAMBATTISTA, C., MATERA, E., OPERTO, F. & SIMONE, M. 2013. Neuropsychopathological comorbidities in learning disorders. *BMC neurology,* 13**,** 1-6.

MARKHAM, J. A. & GREENOUGH, W. T. 2004. Experience-driven brain plasticity: beyond the synapse. *Neuron Glia Biol,* 1**,** 351-63.

MARSHALL, T. R., ESTERER, S., HERRING, J. D., BERGMANN, T. O. & JENSEN, O. 2016. On the relationship between cortical excitability and visual oscillatory responses — A concurrent tDCS–MEG study. *NeuroImage,* 140**,** 41-49.

MARZBANI, H., MARATEB, H. R. & MANSOURIAN, M. 2016. Neurofeedback: A Comprehensive Review on System Design, Methodology and Clinical Applications. *Basic Clin Neurosci,* 7**,** 143-58.

MATEOS-APARICIO, P. & RODRÍGUEZ-MORENO, A. 2019. The Impact of Studying Brain Plasticity. *Front Cell Neurosci,* 13**,** 66.

MATHÔT, S. 2018. Pupillometry: Psychology, Physiology, and Function. *Journal of cognition,* 1**,** 16-16.

MATHÔT, S. & THEEUWES, J. 2011. Visual attention and stability. *Philosophical Transactions: Biological Sciences,* 366**,** 516-527.

MAX, S. M., PLEWNIA, C., ZIPFEL, S., GIEL, K. E. & SCHAG, K. 2021. Combined antisaccade task and transcranial direct current stimulation to increase response inhibition in binge eating disorder. *European Archives of Psychiatry and Clinical Neuroscience,* 271**,** 17-28.

MAZZETTI, C., STAUDIGL, T., MARSHALL, T. R., ZUMER, J. M., FALLON, S. J. & JENSEN, O. 2019. Hemispheric Asymmetry of Globus Pallidus Relates to Alpha Modulation in Reward-Related Attentional Tasks. *The Journal of Neuroscience,* 39**,** 9221.

MCGLASHAN, T. H. & HOFFMAN, R. E. 2000. Schizophrenia as a Disorder of Developmentally Reduced Synaptic Connectivity. *Archives of General Psychiatry,* 57**,** 637-648.

MCGOUGH, J. J., SMALLEY, S. L., MCCRACKEN, J. T., YANG, M., DEL'HOMME, M., LYNN, D. E. & LOO, S. 2005. Psychiatric comorbidity in adult attention deficit hyperactivity disorder: findings from multiplex families. *American Journal of Psychiatry,* 162**,** 1621-1627.

MCLEOD, S. 2019. Vygotsky's Zone of Proximal Development and Scaffolding. *Simply psychology*.

MCNAB, F., VARRONE, A., FARDE, L., JUCAITE, A., BYSTRITSKY, P., FORSSBERG, H. & KLINGBERG, T. 2009. Changes in cortical dopamine D1 receptor binding associated with cognitive training. *Science,* 323**,** 800-2.

MCNAIR, D. M., DROPPLEMAN, L. F. & LORR, M. 1992. *Edits manual for the profile of mood states: POMS*, Edits.

MEDENDORP, W. P., GOLTZ, H. C. & VILIS, T. 2005. Remapping the Remembered Target Location for Anti-Saccades in Human Posterior Parietal Cortex. *Journal of Neurophysiology,* 94**,** 734-740.

MEHTA, T. R., MONEGRO, A., NENE, Y., FAYYAZ, M. & BOLLU, P. C. 2019. Neurobiology of ADHD: A Review. *Current Developmental Disorders Reports,* 6**,** 235-240.

MEHTA, U. M., IBRAHIM, F. A., SHARMA, M. S., VENKATASUBRAMANIAN, G., THIRTHALLI, J., BHARATH, R. D., BOLO, N. R., GANGADHAR, B. N. & KESHAVAN, M. S. 2021. Resting-state functional connectivity predictors of treatment response in schizophrenia - A systematic review and meta-analysis. *Schizophr Res,* 237**,** 153-165.

MENON, V. 2011. Large-scale brain networks and psychopathology: a unifying triple network model. *Trends in Cognitive Sciences,* 15**,** 483-506.

MIKL, M., MAREČEK, R., HLUŠTÍK, P., PAVLICOVÁ, M., DRASTICH, A., CHLEBUS, P., BRÁZDIL, M. & KRUPA, P. 2008. Effects of spatial smoothing on fMRI group inferences. *Magnetic Resonance Imaging,* 26**,** 490-503.

MILES, K., MCMAHON, C., BOISVERT, I., IBRAHIM, R., DE LISSA, P., GRAHAM, P. & LYXELL, B. 2017. Objective Assessment of Listening Effort: Coregistration of Pupillometry and EEG. *Trends in Hearing,* 21**,** 2331216517706396.

MILLER, E. & WALLIS, J. 2009. Executive function and higher-order cognition: definition and neural substrates. *Encyclopedia of neuroscience,* 4.

MILLER, E. K. & COHEN, J. D. 2001. An Integrative Theory of Prefrontal Cortex Function. *Annual Review of Neuroscience,* 24**,** 167-202.

MIYAKE, A. & FRIEDMAN, N. P. 2012. The Nature and Organization of Individual Differences in Executive Functions: Four General Conclusions. *Curr Dir Psychol Sci,* 21**,** 8-14.

MOELLER, F. G., BARRATT, E. S., DOUGHERTY, D. M., SCHMITZ, J. M. & SWANN, A. C. 2001. Psychiatric aspects of impulsivity. *American journal of psychiatry,* 158**,** 1783-1793.

MOLL, K., KUNZE, S., NEUHOFF, N., BRUDER, J. & SCHULTE-KÖRNE, G. 2014. Specific learning disorder: Prevalence and gender differences. *PLoS one,* 9**,** e103537.

MOLL, K., SNOWLING, M. J. & HULME, C. 2020. Introduction to the Special Issue "Comorbidities between Reading Disorders and Other Developmental Disorders". *Scientific Studies of Reading,* 24**,** 1-6.

MOON, S. Y., BARTON, J. J., MIKULSKI, S., POLLI, F. E., CAIN, M. S., VANGEL, M., HÄMÄLÄINEN, M. S. & MANOACH, D. S. 2007. Where left becomes right: a magnetoencephalographic study of sensorimotor transformation for antisaccades. *Neuroimage,* 36**,** 1313-23.

MORENO-GARCÍA, I., CANO-CRESPO, A. & RIVERA, F. 2022. Results of Neurofeedback in Treatment of Children with ADHD: A Systematic Review of Randomized Controlled Trials. *Applied Psychophysiology and Biofeedback,* 47**,** 145-181.

MUNAKATA, Y. & PFAFFLY, J. 2004. Hebbian learning and development. *Developmental Science,* 7**,** 141-148.

MUNOZ, D. P. & EVERLING, S. 2004. Look away: the anti-saccade task and the voluntary control of eye movement. *Nature Reviews Neuroscience,* 5**,** 218.

NADIM, F. & BUCHER, D. 2014. Neuromodulation of neurons and synapses. *Current Opinion in Neurobiology,* 29**,** 48-56.

NI, H.-C., HUNG, J., WU, C.-T., WU, Y.-Y., CHANG, C.-J., CHEN, R.-S. & HUANG, Y.-Z. 2017. The impact of single session intermittent theta-burst stimulation over the dorsolateral prefrontal cortex and posterior superior temporal sulcus on adults with autism spectrum disorder. *Frontiers in neuroscience,* 11**,** 255.

NIETO-CASTANON, A. 2020. *Handbook of functional connectivity Magnetic Resonance Imaging methods in CONN*.

NITSCHE, M. A., COHEN, L. G., WASSERMANN, E. M., PRIORI, A., LANG, N., ANTAL, A., PAULUS, W., HUMMEL, F., BOGGIO, P. S., FREGNI, F. & PASCUAL-LEONE, A. 2008. Transcranial direct current stimulation: State of the art 2008. *Brain Stimul,* 1**,** 206-23.

NITSCHE, M. A., FRICKE, K., HENSCHKE, U., SCHLITTERLAU, A., LIEBETANZ, D., LANG, N., HENNING, S., TERGAU, F. & PAULUS, W. 2003. Pharmacological

Modulation of Cortical Excitability Shifts Induced by Transcranial Direct Current Stimulation in Humans. *The Journal of Physiology,* 553**,** 293-301.

NIXON, N. L., LIDDLE, P. F., NIXON, E., WORWOOD, G., LIOTTI, M. & PALANIYAPPAN, L. 2014. Biological vulnerability to depression: linked structural and functional brain network findings. *British Journal of Psychiatry,* 204**,** 283-289.

NOLTE, G. 2003. The magnetic lead field theorem in the quasi-static approximation and its use for magnetoencephalography forward calculation in realistic volume conductors. *Phys Med Biol,* 48**,** 3637-52.

NORTON, E. S., BEACH, S. D. & GABRIELI, J. D. 2015. Neurobiology of dyslexia. *Current opinion in neurobiology,* 30**,** 73-78.

NOTTURNO, F., MARZETTI, L., PIZZELLA, V., UNCINI, A. & ZAPPASODI, F. 2014. Local and remote effects of transcranial direct current stimulation on the electrical activity of the motor cortical network. *Human Brain Mapping,* 35**,** 2220-2232.

O'NEILL, G. C., TEWARIE, P. K., COLCLOUGH, G. L., GASCOYNE, L. E., HUNT, B. A. E., MORRIS, P. G., WOOLRICH, M. W. & BROOKES, M. J. 2017. Measurement of dynamic task related functional networks using MEG. *NeuroImage,* 146**,** 667-678.

OGAWA, S., LEE, T.-M., KAY, A. R. & TANK, D. W. 1990. Brain magnetic resonance imaging with contrast dependent on blood oxygenation. *proceedings of the National Academy of Sciences,* 87**,** 9868-9872.

OH, S., CHOI, J., HAN, D. H. & KIM, E. 2023. Effects of game-based digital therapeutics on attention deficit hyperactivity disorder in children and adolescents as assessed by parents or teachers: a systematic review and meta-analysis. *European Child & Adolescent Psychiatry*.

OOSTENVELD, R., FRIES, P., MARIS, E. & SCHOFFELEN, J.-M. 2011. FieldTrip: Open Source Software for Advanced Analysis of MEG, EEG, and Invasive Electrophysiological Data. *Computational Intelligence and Neuroscience,* 2011**,** 156869.

OSIMO, E. F., BECK, K., REIS MARQUES, T. & HOWES, O. D. 2019. Synaptic loss in schizophrenia: a meta-analysis and systematic review of synaptic protein and mRNA measures. *Molecular psychiatry,* 24**,** 549-561.

PAAS, F. G. & VAN MERRIËNBOER, J. J. 1994. Instructional control of cognitive load in the training of complex cognitive tasks. *Educational psychology review,* 6**,** 351-371.

PAES, A. H. P., BAKKER, A. & SOE-AGNIE, C. J. 1997. Impact of Dosage Frequency on Patient Compliance. *Diabetes Care,* 20**,** 1512-1517.

PALVA, S. & PALVA, J. M. 2007. New vistas for α-frequency band oscillations. *Trends in Neurosciences,* 30**,** 150-158.

PARÉ, M. & MUNOZ, D. P. 1996. Saccadic reaction time in the monkey: advanced preparation of oculomotor programs is primarily responsible for express saccade occurrence. *J Neurophysiol,* 76**,** 3666-81.

PARHIALA, P., TORPPA, M., EKLUND, K., ARO, T., POIKKEUS, A. M., HEIKKILÄ, R. & AHONEN, T. 2015. Psychosocial functioning of children with and without dyslexia: A follow-up study from ages four to nine. *Dyslexia,* 21**,** 197-211.

PASQUALOTTO, A., MAZZONI, N., BENTENUTO, A., MULÈ, A., BENSO, F. & VENUTI, P. 2021. Effects of cognitive training programs on executive function in children and adolescents with autism spectrum disorder: a systematic review. *Brain sciences,* 11**,** 1280.

PENNINGTON, B. F. 2006. From single to multiple deficit models of developmental disorders. *Cognition,* 101**,** 385-413.

PENNINGTON, B. F. & OLSON, R. K. 2005. Genetics of Dyslexia. *The science of reading: A handbook.* Malden: Blackwell Publishing.

PERICA, M. I., CALABRO, F. J., LARSEN, B., FORAN, W., YUSHMANOV, V. E., HETHERINGTON, H., TERVO-CLEMMENS, B., MOON, C.-H. & LUNA, B. 2022. Development of frontal GABA and glutamate supports excitation/inhibition balance from adolescence into adulthood. *Progress in Neurobiology,* 219**,** 102370.

PETERSEN, S. E. & POSNER, M. I. 2012. The attention system of the human brain: 20 years after. *Annual review of neuroscience,* 35**,** 73.

PFURTSCHELLER, G. 1992. Event-related synchronization (ERS): an electrophysiological correlate of cortical areas at rest. *Electroencephalogr Clin Neurophysiol,* 83**,** 62-9.

PIAGET, J. 2013. *Play, dreams and imitation in childhood*, Routledge.

PIERROT-DESEILLIGNY, C., MÜRI, R. M., PLONER, C. J., GAYMARD, B., DEMERET, S. & RIVAUD-PECHOUX, S. 2003. Decisional role of the dorsolateral prefrontal cortex in ocular motor behaviour. *Brain,* 126**,** 1460-73.

PIERROT-DESEILLIGNY, C., RIVAUD, S., GAYMARD, B. & AGID, Y. 1991a. Cortical control of memory-guided saccades in man. *Experimental Brain Research,* 83**,** 607-617.

PIERROT-DESEILLIGNY, C. H., RIVAUD, S., GAYMARD, B. & AGID, Y. 1991b. CORTICAL CONTROL OF REFLEXIVE VISUALLY-GUIDED SACCADES. *Brain,* 114**,** 1473-1485.

PISELLA, L., ALAHYANE, N., BLANGERO, A., THERY, F., BLANC, S. & PELISSON, D. 2011. Right-hemispheric dominance for visual remapping in humans. *Philosophical Transactions of the Royal Society B: Biological Sciences,* 366**,** 572-585.

POLANCZYK, G. V., SALUM, G. A., SUGAYA, L. S., CAYE, A. & ROHDE, L. A. 2015. Annual research review: A meta-analysis of the worldwide prevalence of mental disorders in children and adolescents. *J Child Psychol Psychiatry,* 56**,** 345-65.

PORTILLO-LARA, R., TAHIRBEGI, B., CHAPMAN, C., GODING, J. & GREEN, R. 2021. Mind the gap: State-of-the-art technologies and applications for EEG-based brain–computer interfaces. *APL Bioengineering,* 5**,** 031507.

POSNER, M. I. 1980. Orienting of Attention. *Quarterly Journal of Experimental Psychology,* 32**,** 3-25.

POSNER, M. I. & PETERSEN, S. E. 1990. The attention system of the human brain. *Annual review of neuroscience,* 13**,** 25-42.

POSNER, M. I. & ROTHBART, M. K. 2007. Research on attention networks as a model for the integration of psychological science. *Annu Rev Psychol,* 58**,** 1-23.

POWER, J. D., MITRA, A., LAUMANN, T. O., SNYDER, A. Z., SCHLAGGAR, B. L. & PETERSEN, S. E. 2014. Methods to detect, characterize, and remove motion artifact in resting state fMRI. *Neuroimage,* 84**,** 320-41.

PRENSKY, M. 2001. Fun, play and games: What makes games engaging. *Digital game-based learning,* 5**,** 5-31.

PROUDFOOT, M., WOOLRICH, M. W., NOBRE, A. C. & TURNER, M. R. 2014. Magnetoencephalography. *Practical Neurology,* 14**,** 336.

PTAK, R. & MÜRI, R. 2013. The parietal cortex and saccade planning: lessons from human lesion studies. *Frontiers in Human Neuroscience,* 7.

PUIGDEMONT, D., PORTELLA, M. J., PÉREZ-EGEA, R., MOLET, J., GIRONELL, A., DE DIEGO-ADELIÑO, J., MARTÍN, A., RODRÍGUEZ, R., ÀLVAREZ, E. & ARTIGAS, F. 2015. A randomized double-blind crossover trial of deep brain stimulation of the subcallosal cingulate gyrus in patients with treatment-resistant depression: a pilot study of relapse prevention. *Journal of Psychiatry and Neuroscience,* 40**,** 224-231.

PUPÍKOVÁ, M., ŠIMKO, P., GAJDOŠ, M. & REKTOROVÁ, I. 2021. Modulation of Working Memory and Resting-State fMRI by tDCS of the Right Frontoparietal Network. *Neural Plasticity,* 2021**,** 5594305.

QIU, M.-G., YE, Z., LI, Q.-Y., LIU, G.-J., XIE, B. & WANG, J. 2011. Changes of Brain Structure and Function in ADHD Children. *Brain Topography,* 24**,** 243-252.

RAHMANI, E., MAHVELATI, A., ALIZADEH, A., MOKHAYERI, Y., RAHMANI, M., ZARABI, H. & HASSANVANDI, S. 2022. Is neurofeedback effective in children with ADHD? A systematic review and meta-analysis. *Neurocase,* 28**,** 84-95.

RAICHLE, M. E. 2015. The Brain's Default Mode Network. *Annual Review of Neuroscience,* 38**,** 433-447.

RAICHLE, M. E., MACLEOD, A. M., SNYDER, A. Z., POWERS, W. J., GUSNARD, D. A. & SHULMAN, G. L. 2001. A default mode of brain function. *Proceedings of the National Academy of Sciences,* 98**,** 676-682.

RAINE, A. & BENISHAY, D. 1995. The SPQ-B: A brief screening instrument for schizotypal personality disorder. *Journal of personality disorders,* 9**,** 346.

RAMAT, S., LEIGH, R. J., ZEE, D. S. & OPTICAN, L. M. 2006. What clinical disorders tell us about the neural control of saccadic eye movements. *Brain,* 130**,** 10-35.

RAMUS, F., ROSEN, S., DAKIN, S. C., DAY, B. L., CASTELLOTE, J. M., WHITE, S. & FRITH, U. 2003. Theories of developmental dyslexia: insights from a multiple case study of dyslexic adults. *Brain,* 126**,** 841-865.

RAPOPORT, J. L., GIEDD, J. N., BLUMENTHAL, J., HAMBURGER, S., JEFFRIES, N., FERNANDEZ, T., NICOLSON, R., BEDWELL, J., LENANE, M. & ZIJDENBOS, A. 1999. Progressive cortical change during adolescence in childhood-onset schizophrenia: a longitudinal magnetic resonance imaging study. *Archives of general psychiatry,* 56**,** 649-654.

REIS, J., SCHAMBRA, H. M., COHEN, L. G., BUCH, E. R., FRITSCH, B., ZARAHN, E., CELNIK, P. A. & KRAKAUER, J. W. 2009. Noninvasive cortical stimulation enhances motor skill acquisition over multiple days through an effect on consolidation. *Proceedings of the National Academy of Sciences,* 106**,** 1590-1595.

REZAEI SHARIF, A., NOROOZI HOMAYOON, M. & ALMASI, M. 2022. The effectiveness of neurofeedback and cognitive-behavioral play therapy and Combined method on working memory of children with specific learning disabilities. *Journal of Learning Disabilities,* 12**,** 47-61.

RIVAUD, S., MÜRI, R. M., GAYMARD, B., VERMERSCH, A. I. & PIERROT-DESEILLIGNY, C. 1994. Eye movement disorders after frontal eye field lesions in humans. *Exp Brain Res,* 102**,** 110-20.

RIZZOLATTI, G., RIGGIO, L., DASCOLA, I. & UMILTÁ, C. 1987. Reorienting attention across the horizontal and vertical meridians: evidence in favor of a premotor theory of attention. *Neuropsychologia,* 25**,** 31-40.

ROACH, B. J. & MATHALON, D. H. 2008. Event-Related EEG Time-Frequency Analysis: An Overview of Measures and An Analysis of Early Gamma Band Phase Locking in Schizophrenia. *Schizophrenia Bulletin,* 34**,** 907-926.

ROBINSON, S. Functional neuroimaging by Synthetic Aperture Magnetometry (SAM). 1999.

ROLFS, M., JONIKAITIS, D., DEUBEL, H. & CAVANAGH, P. 2011. Predictive remapping of attention across eye movements. *Nature Neuroscience,* 14**,** 252-256.

ROMEI, V., GROSS, J. & THUT, G. 2010. On the Role of Prestimulus Alpha Rhythms over Occipito-Parietal Areas in Visual Input Regulation: Correlation or Causation? *The Journal of Neuroscience,* 30**,** 8692.

ROSA, P. G. P., ZUGMAN, A., CERQUEIRA, C. T., SERPA, M. H., DE SOUZA DURAN, F. L., ZANETTI, M. V., BASSITT, D. P., ELKIS, H., CRIPPA, J. A. S. & SALLET, P. C. 2021. Cortical surface abnormalities are different depending on the stage of schizophrenia: A cross-sectional vertexwise mega-analysis of thickness, area and gyrification. *Schizophrenia research,* 236**,** 104-114.

ROSSI, S., ANTAL, A., BESTMANN, S., BIKSON, M., BREWER, C., BROCKMÖLLER, J., CARPENTER, L. L., CINCOTTA, M., CHEN, R., DASKALAKIS, J. D., DI LAZZARO, V., FOX, M. D., GEORGE, M. S., GILBERT, D., KIMISKIDIS, V. K., KOCH, G., ILMONIEMI, R. J., LEFAUCHEUR, J. P., LEOCANI, L., LISANBY, S. H., MINIUSSI, C., PADBERG, F., PASCUAL-LEONE, A., PAULUS, W., PETERCHEV, A. V., QUARTARONE, A., ROTENBERG, A., ROTHWELL, J., ROSSINI, P. M., SANTARNECCHI, E., SHAFI, M. M., SIEBNER, H. R., UGAWA, Y., WASSERMANN, E. M., ZANGEN, A., ZIEMANN, U. & HALLETT, M. 2021. Safety and recommendations for TMS use in healthy subjects and patient populations, with updates on training, ethical and regulatory issues: Expert Guidelines. *Clinical Neurophysiology,* 132**,** 269-306.

ROSSI, S., HALLETT, M., ROSSINI, P. M., PASCUAL-LEONE, A. & GROUP, S. O. T. C. 2009. Safety, ethical considerations, and application guidelines for the use of transcranial magnetic stimulation in clinical practice and research. *Clinical neurophysiology,* 120**,** 2008-2039.

RUSHWORTH, M. F. S., HADLAND, K. A., PAUS, T. & SIPILA, P. K. 2002. Role of the Human Medial Frontal Cortex in Task Switching: A Combined fMRI and TMS Study. *Journal of Neurophysiology,* 87**,** 2577-2592.

SAKAS, D. E., PANOURIAS, I. G., SIMPSON, B. A. & KRAMES, E. S. 2007. An introduction to operative neuromodulation and functional neuroprosthetics, the new frontiers of clinical neuroscience and biotechnology. *Acta Neurochir Suppl,* 97**,** 3-10.

SALEH, M., REIMER, J., PENN, R., OJAKANGAS, C. L. & HATSOPOULOS, N. G. 2010. Fast and Slow Oscillations in Human Primary Motor Cortex Predict Oncoming Behaviorally Relevant Cues. *Neuron,* 65**,** 461-471.

SALVADOR, A. F., DE LIMA, K. A. & KIPNIS, J. 2021. Neuromodulation by the immune system: a focus on cytokines. *Nature reviews. Immunology,* 21**,** 526-541.

SARA, SUSAN J. & BOURET, S. 2012. Orienting and Reorienting: The Locus Coeruleus Mediates Cognition through Arousal. *Neuron,* 76**,** 130-141.

SARA, S. J. & HERVE-MINVIELLE, A. 1995. Inhibitory influence of frontal cortex on locus coeruleus neurons. *Proceedings of the National Academy of Sciences,* 92**,** 6032-6036.

SARAFYAZD, M. & JAZAYERI, M. 2019. Hierarchical reasoning by neural circuits in the frontal cortex. *Science,* 364**,** eaav8911.

SARPAL, D. K., TARCIJONAS, G., CALABRO, F. J., FORAN, W., HAAS, G. L., LUNA, B. & MURTY, V. P. 2022. Context-specific abnormalities of the central executive network in first-episode psychosis: relationship with cognition. *Psychological Medicine,* 52**,** 2299-2308.

SARVAS, J. 1987. Basic mathematical and electromagnetic concepts of the biomagnetic inverse problem. *Physics in Medicine and Biology,* 32**,** 11-22.

SASAKI, M., SHIBATA, E., TOHYAMA, K., TAKAHASHI, J., OTSUKA, K., TSUCHIYA, K., TAKAHASHI, S., EHARA, S., TERAYAMA, Y. & SAKAI, A. 2006. Neuromelanin magnetic resonance imaging of locus ceruleus and substantia nigra in Parkinson's disease. *Neuroreport,* 17**,** 1215-8.

SASLOW, M. G. 1967. Effects of Components of Displacement-Step Stimuli Upon Latency for Saccadic Eye Movement. *Journal of the Optical Society of America,* 57**,** 1024-1029.

SATTERTHWAITE, T. D., WOLF, D. H., LOUGHEAD, J., RUPAREL, K., ELLIOTT, M. A., HAKONARSON, H., GUR, R. C. & GUR, R. E. 2012. Impact of in-scanner head motion on multiple measures of functional connectivity: relevance for studies of neurodevelopment in youth. *Neuroimage,* 60**,** 623-632.

SAUSENG, P., KLIMESCH, W., STADLER, W., SCHABUS, M., DOPPELMAYR, M., HANSLMAYR, S., GRUBER, W. R. & BIRBAUMER, N. 2005. A shift of visual spatial attention is selectively associated with human EEG alpha activity. *European journal of neuroscience,* 22**,** 2917-2926.

SAYAL, K., PRASAD, V., DALEY, D., FORD, T. & COGHILL, D. 2018. ADHD in children and young people: prevalence, care pathways, and service provision. *Lancet Psychiatry,* 5**,** 175-186.

SCHAEFFER, D. J., AMLUNG, M. T., LI, Q., KRAFFT, C. E., AUSTIN, B. P., DYCKMAN, K. A. & MCDOWELL, J. E. 2013. Neural correlates of behavioral variation in healthy adults' antisaccade performance. *Psychophysiology,* 50**,** 325-33.

SCHALL, J. D. 2004. On the role of frontal eye field in guiding attention and saccades. *Vision Research,* 44**,** 1453-1467.

SCHOFFELEN, J.-M. & GROSS, J. 2009. Source connectivity analysis with MEG and EEG. *Human Brain Mapping,* 30**,** 1857-1865.

SCHWALB, J. M. & HAMANI, C. 2008. The History and Future of Deep Brain Stimulation. *Neurotherapeutics,* 5**,** 3-13.

SCHWARTZ, E. S., EDGAR, J. C., GAETZ, W. C. & ROBERTS, T. P. L. 2010. Magnetoencephalography. *Pediatric Radiology,* 40**,** 50-58.

SEARS, S. M. & HEWETT, S. J. 2021. Influence of glutamate and GABA transport on brain excitatory/inhibitory balance. *Experimental Biology and Medicine,* 246**,** 1069-1083.

SEELEY, W. W., MENON, V., SCHATZBERG, A. F., KELLER, J., GLOVER, G. H., KENNA, H., REISS, A. L. & GREICIUS, M. D. 2007. Dissociable intrinsic connectivity networks for salience processing and executive control. *J Neurosci,* 27**,** 2349-56.

SEHM, B., SCHÄFER, A., KIPPING, J., MARGULIES, D., CONDE, V., TAUBERT, M., VILLRINGER, A. & RAGERT, P. 2012. Dynamic modulation of intrinsic functional connectivity by transcranial direct current stimulation. *Journal of Neurophysiology,* 108**,** 3253-3263.

SEKIHARA, K., NAGARAJAN, S. S., POEPPEL, D. & MARANTZ, A. 2004. Asymptotic SNR of scalar and vector minimum-variance beamformers for neuromagnetic source reconstruction. *IEEE Transactions on Biomedical Engineering,* 51**,** 1726-1734.

SELF, D. R., DE VRIES HENRY, E., FINDLEY, C. S. & REILLY, E. 2006. Thrill seeking: the type T personality and extreme sports. *International Journal of Sport Management and Marketing,* 2**,** 175-190.

SERENO, M., PITZALIS, S. & MARTINEZ, A. 2001. Mapping of contralateral space in retinotopic coordinates by a parietal cortical area in humans. *Science,* 294**,** 1350-1354.

SHELINE, Y. I., BARCH, D. M., PRICE, J. L., RUNDLE, M. M., VAISHNAVI, S. N., SNYDER, A. Z., MINTUN, M. A., WANG, S., COALSON, R. S. & RAICHLE, M. E. 2009. The default mode network and self-referential processes in depression. *Proceedings of the National Academy of Sciences,* 106**,** 1942-1947.

SHERMAN, M. A., LEE, S., LAW, R., HAEGENS, S., THORN, C. A., HÄMÄLÄINEN, M. S., MOORE, C. I. & JONES, S. R. 2016. Neural mechanisms of transient neocortical beta rhythms: Converging evidence from humans, computational modeling, monkeys, and mice. *Proc Natl Acad Sci U S A,* 113**,** E4885-94.

SHMUELI, K., VAN GELDEREN, P., DE ZWART, J. A., HOROVITZ, S. G., FUKUNAGA, M., JANSMA, J. M. & DUYN, J. H. 2007. Low-frequency fluctuations in the cardiac

rate as a source of variance in the resting-state fMRI BOLD signal. *Neuroimage,* 38**,** 306-320.

SIEGLE, G. J., ICHIKAWA, N. & STEINHAUER, S. 2008. Blink before and after you think: blinks occur prior to and following cognitive load indexed by pupillary responses. *Psychophysiology,* 45**,** 679-87.

SITARAM, R., ROS, T., STOECKEL, L., HALLER, S., SCHARNOWSKI, F., LEWIS-PEACOCK, J., WEISKOPF, N., BLEFARI, M. L., RANA, M., OBLAK, E., BIRBAUMER, N. & SULZER, J. 2017. Closed-loop brain training: the science of neurofeedback. *Nature Reviews Neuroscience,* 18**,** 86-100.

SNOWLING, M. J. 2005. Specific learning difficulties. *Psychiatry,* 4**,** 110-113.

SOMMER, M. A. & WURTZ, R. H. 2006. Influence of the thalamus on spatial visual processing in frontal cortex. *Nature,* 444**,** 374-377.

SOMMER, M. A. & WURTZ, R. H. 2008. Brain circuits for the internal monitoring of movements. *Annu Rev Neurosci,* 31**,** 317-38.

SOPER, D. 2022. Significance of the Difference between Two Correlations Calculator [Software]. *www.danielsoper.com*.

SPAGNA, A., KIM, T. H., WU, T. & FAN, J. 2020. Right hemisphere superiority for executive control of attention. *Cortex,* 122**,** 263-276.

SPITZER, B. & HAEGENS, S. 2017. Beyond the Status Quo: A Role for Beta Oscillations in Endogenous Content (Re)Activation. *eneuro,* 4**,** ENEURO.0170-17.2017.

SRIDHARAN, D., LEVITIN, D. J. & MENON, V. 2008. A critical role for the right fronto-insular cortex in switching between central-executive and default-mode networks. *Proceedings of the National Academy of Sciences,* 105**,** 12569-12574.

STAGG, C. J., BEST, J. G., STEPHENSON, M. C., SHEA, J., WYLEZINSKA, M., KINCSES, Z. T., MORRIS, P. G., MATTHEWS, P. M. & JOHANSEN-BERG, H. 2009. Polarity-Sensitive Modulation of Cortical Neurotransmitters by Transcranial Stimulation. *The Journal of Neuroscience,* 29**,** 5202.

STAGG, C. J., JAYARAM, G., PASTOR, D., KINCSES, Z. T., MATTHEWS, P. M. & JOHANSEN-BERG, H. 2011. Polarity and timing-dependent effects of transcranial direct current stimulation in explicit motor learning. *Neuropsychologia,* 49**,** 800-804.

STAGG, C. J. & NITSCHE, M. A. 2011. Physiological Basis of Transcranial Direct Current Stimulation. *The Neuroscientist,* 17**,** 37-53.

STROTHER, S. C. 2006. Evaluating fMRI preprocessing pipelines. *IEEE Engineering in Medicine and Biology Magazine,* 25**,** 27-41.

STURM, W. & WILLMES, K. 2001. On the functional neuroanatomy of intrinsic and phasic alertness. *Neuroimage,* 14**,** S76-S84.

SWANN, A. C., BJORK, J. M., MOELLER, F. G. & DOUGHERTY, D. M. 2002. Two models of impulsivity: relationship to personality traits and psychopathology. *Biological Psychiatry,* 51**,** 988-994.

TAKEUCHI, H., SEKIGUCHI, A., TAKI, Y., YOKOYAMA, S., YOMOGIDA, Y., KOMURO, N., YAMANOUCHI, T., SUZUKI, S. & KAWASHIMA, R. 2010. Training of Working Memory Impacts Structural Connectivity. *The Journal of Neuroscience,* 30**,** 3297.

TALLON-BAUDRY, C., BERTRAND, O., DELPUECH, C. & PERMIER, J. 1997. Oscillatory gamma-band (30-70 Hz) activity induced by a visual search task in humans. *J Neurosci,* 17**,** 722-34.

TAMBINI, A., KETZ, N. & DAVACHI, L. 2010. Enhanced brain correlations during rest are related to memory for recent experiences. *Neuron,* 65**,** 280-90.

TANG, J., LIAO, Y., SONG, M., GAO, J.-H., ZHOU, B., TAN, C., LIU, T., TANG, Y., CHEN, J. & CHEN, X. 2013. Aberrant default mode functional connectivity in early onset schizophrenia. *PloS one,* 8**,** e71061.

TETI MAYER, J., CHOPARD, G., NICOLIER, M., GABRIEL, D., MASSE, C., GIUSTINIANI, J., VANDEL, P., HAFFEN, E. & BENNABI, D. 2020. Can transcranial direct current stimulation (tDCS) improve impulsivity in healthy and psychiatric adult populations? A systematic review. *Prog Neuropsychopharmacol Biol Psychiatry,* 98**,** 109814.

THAPAR, A., COOPER, M., EYRE, O. & LANGLEY, K. 2013. What have we learnt about the causes of ADHD? *Journal of child psychology and psychiatry, and allied disciplines,* 54**,** 3-16.

THARYAN, P. & ADAMS, C. E. 2005. Electroconvulsive therapy for schizophrenia. *Cochrane Database of Systematic Reviews*.

TROEBINGER, L., LÓPEZ, J. D., LUTTI, A., BESTMANN, S. & BARNES, G. 2014. Discrimination of cortical laminae using MEG. *Neuroimage,* 102**,** 885-893.

TZOURIO-MAZOYER, N., LANDEAU, B., PAPATHANASSIOU, D., CRIVELLO, F., ETARD, O., DELCROIX, N., MAZOYER, B. & JOLIOT, M. 2002. Automated Anatomical Labeling of Activations in SPM Using a Macroscopic Anatomical Parcellation of the MNI MRI Single-Subject Brain. *NeuroImage,* 15**,** 273-289.

UDUPA, K. & CHEN, R. 2015. The mechanisms of action of deep brain stimulation and ideas for the future development. *Progress in Neurobiology,* 133**,** 27-49.

UMENO, M. M. & GOLDBERG, M. E. 1997. Spatial processing in the monkey frontal eye field. I. Predictive visual responses. *J Neurophysiol,* 78**,** 1373-83.

USHER, M., COHEN, J. D., SERVAN-SCHREIBER, D., RAJKOWSKI, J. & ASTON-JONES, G. 1999. The Role of Locus Coeruleus in the Regulation of Cognitive Performance. *Science,* 283**,** 549-554.

VAIDYA, C. J. 2012. Neurodevelopmental abnormalities in ADHD. *Curr Top Behav Neurosci,* 9**,** 49-66.

VAN BALKOM, T. D., VAN DEN HEUVEL, O. A., BERENDSE, H. W., VAN DER WERF, Y. D. & VRIEND, C. 2020. The Effects of Cognitive Training on Brain Network Activity and Connectivity in Aging and Neurodegenerative Diseases: a Systematic Review. *Neuropsychology Review,* 30**,** 267-286.

VAN DIJK, K. R., SABUNCU, M. R. & BUCKNER, R. L. 2012. The influence of head motion on intrinsic functional connectivity MRI. *Neuroimage,* 59**,** 431-438.

VAN DIJK, K. R. A., HEDDEN, T., VENKATARAMAN, A., EVANS, K. C., LAZAR, S. W. & BUCKNER, R. L. 2009. Intrinsic Functional Connectivity As a Tool For Human Connectomics: Theory, Properties, and Optimization. *Journal of Neurophysiology,* 103**,** 297-321.

VAN DOREN, J., ARNS, M., HEINRICH, H., VOLLEBREGT, M. A., STREHL, U. & K. LOO, S. 2019. Sustained effects of neurofeedback in ADHD: a systematic review and meta-analysis. *European Child & Adolescent Psychiatry,* 28**,** 293-305.

VAN VEEN, B. D., VAN DRONGELEN, W., YUCHTMAN, M. & SUZUKI, A. 1997. Localization of brain electrical activity via linearly constrained minimum variance spatial filtering. *IEEE Trans Biomed Eng,* 44**,** 867-80.

VEEN, B. D. V. & BUCKLEY, K. M. 1988. Beamforming: a versatile approach to spatial filtering. *IEEE ASSP Magazine,* 5**,** 4-24.

VELOSO, A., VICENTE, S. G. & FILIPE, M. G. 2020. Effectiveness of cognitive training for school-aged children and adolescents with attention deficit/hyperactivity disorder: a systematic review. *Frontiers in psychology***,** 2983.

VOLLEBREGT, M. A., ZUMER, J. M., TER HUURNE, N., BUITELAAR, J. K. & JENSEN, O. 2016. Posterior alpha oscillations reflect attentional problems in boys with Attention Deficit Hyperactivity Disorder. *Clinical Neurophysiology,* 127**,** 2182-2191.

VON BASTIAN, C. C., BELLEVILLE, S., UDALE, R. C., REINHARTZ, A., ESSOUNNI, M. & STROBACH, T. 2022. Mechanisms underlying training-induced cognitive change. *Nature Reviews Psychology,* 1**,** 30-41.

VYGOTSKY, L. S. & COLE, M. 1978. *Mind in society: Development of higher psychological processes*, Harvard university press.

WAITT, A. E. 2022. *Autonomic and central nervous system correlates of cognitive control training for attentional disorders.* PhD Electronic, University of Nottingham.

WAKAMATSU, K., TABUCHI, K., OJIKA, M., ZUCCA, F. A., ZECCA, L. & ITO, S. 2015. Norepinephrine and its metabolites are involved in the synthesis of neuromelanin derived from the locus coeruleus. *J Neurochem,* 135**,** 768-76.

WALKER, R., HUSAIN, M., HODGSON, T. L., HARRISON, J. & KENNARD, C. 1998. Saccadic eye movement and working memory deficits following damage to human prefrontal cortex. *Neuropsychologia,* 36**,** 1141-59.

WANG, C.-A., BRIEN, D. C. & MUNOZ, D. P. 2015. Pupil size reveals preparatory processes in the generation of pro-saccades and anti-saccades. *European Journal of Neuroscience,* 41**,** 1102-1110.

WANG, C.-A., MCINNIS, H., BRIEN, D. C., PARI, G. & MUNOZ, D. P. 2016. Disruption of pupil size modulation correlates with voluntary motor preparation deficits in Parkinson's disease. *Neuropsychologia,* 80**,** 176-184.

WANG, J., ZUO, X. & HE, Y. 2010. Graph-based network analysis of resting-state functional MRI. *Frontiers in Systems Neuroscience,* 4.

WANG, Y., ZUO, C., XU, Q., HAO, L. & ZHANG, Y. 2021. Attention-deficit/hyperactivity disorder is characterized by a delay in subcortical maturation. *Progress in Neuro-Psychopharmacology and Biological Psychiatry,* 104**,** 110044.

WANG, Z., LIU, J., ZHONG, N., QIN, Y., ZHOU, H. & LI, K. 2012. Changes in the brain intrinsic organization in both on-task state and post-task resting state. *Neuroimage,* 62**,** 394-407.

WHITFIELD-GABRIELI, S. & NIETO-CASTANON, A. 2012. Conn : A Functional Connectivity Toolbox for Correlated and Anticorrelated Brain Networks. *Brain Connectivity,* 2**,** 125-41.

WIEST, G. M., ROSALES, K. P., LOONEY, L., WONG, E. H. & WIEST, D. J. 2022. Utilizing Cognitive Training to Improve Working Memory, Attention, and Impulsivity in School-Aged Children with ADHD and SLD. *Brain Sciences,* 12**,** 141.

WIGAL, T., SWANSON, J. M., REGINO, R., LERNER, M. A., SOLIMAN, I., STEINHOFF, K., GURBANI, S. & WIGAL, S. B. 1999. Stimulant medications for the treatment of ADHD: efficacy and limitations. *Mental Retardation and Developmental Disabilities Research Reviews,* 5**,** 215-224.

WILKINSON, P. 2016. A Brief History of Serious Games. *In:* DÖRNER, R., GÖBEL, S., KICKMEIER-RUST, M., MASUCH, M. & ZWEIG, K. (eds.) *Entertainment Computing and Serious Games: International GI-Dagstuhl Seminar 15283, Dagstuhl Castle, Germany, July 5-10, 2015, Revised Selected Papers.* Cham: Springer International Publishing.

WORDEN, M. S., FOXE, J. J., WANG, N. & SIMPSON, G. V. 2000. Anticipatory biasing of visuospatial attention indexed by retinotopically specific alpha-band electroencephalography increases over occipital cortex. *The Journal of neuroscience: the official journal of the Society for Neuroscience,* 20**,** RC63-RC63.

WU, W. H., HSIAO, H. C., WU, P. L., LIN, C. H. & HUANG, S. H. 2012. Investigating the learning-theory foundations of game-based learning: a meta-analysis. *Journal of Computer Assisted Learning,* 28**,** 265-279.

WURTZ, R. H. 2008. Neuronal mechanisms of visual stability. *Vision research,* 48**,** 2070-2089.

XIONG, J., PARSONS, L. M., GAO, J. H. & FOX, P. T. 1999. Interregional connectivity to primary motor cortex revealed using MRI resting state images. *Human brain mapping,* 8**,** 151-156.

YEO, B. T., KRIENEN, F. M., SEPULCRE, J., SABUNCU, M. R., LASHKARI, D., HOLLINSHEAD, M., ROFFMAN, J. L., SMOLLER, J. W., ZOLLEI, L., POLIMENI, J. R., FISCHL, B., LIU, H. & BUCKNER, R. L. 2011. The organization of the human cerebral cortex estimated by intrinsic functional connectivity. *J Neurophysiol,* 106**,** 1125-65.

YERKES, R. M. & DODSON, J. D. 1908. The relation of strength of stimulus to rapidity of habit-formation. *Journal of Comparative Neurology and Psychology,* 18**,** 459-482.

ZAEHLE, T., SANDMANN, P., THORNE, J. D., JÄNCKE, L. & HERRMANN, C. S. 2011. Transcranial direct current stimulation of the prefrontal cortex modulates working memory performance: combined behavioural and electrophysiological evidence. *BMC neuroscience,* 12**,** 1-11.

ZAITSEV, M., MACLAREN, J. & HERBST, M. 2015. Motion artifacts in MRI: A complex problem with many partial solutions. *Journal of Magnetic Resonance Imaging,* 42**,** 887-901.

ZARAHN, E., AGUIRRE, G. K. & D'ESPOSITO, M. 1997. Empirical analyses of BOLD fMRI statistics. I. Spatially unsmoothed data collected under null-hypothesis conditions. *Neuroimage,* 5**,** 179-97.

ZIEGLER, S., PEDERSEN, M. L., MOWINCKEL, A. M. & BIELE, G. 2016. Modelling ADHD: A review of ADHD theories through their predictions for computational models of decision-making and reinforcement learning. *Neuroscience & Biobehavioral Reviews,* 71**,** 633-656.

ZUCCA, F. A., SEGURA-AGUILAR, J., FERRARI, E., MUÑOZ, P., PARIS, I., SULZER, D., SARNA, T., CASELLA, L. & ZECCA, L. 2017. Interactions of iron, dopamine and neuromelanin pathways in brain aging and Parkinson's disease. *Progress in Neurobiology,* 155**,** 96-119.

ZUCKER, R. S. & REGEHR, W. G. 2002. Short-term synaptic plasticity. *Annual review of physiology,* 64**,** 355-405.

ZUO, X.-N., EHMKE, R., MENNES, M., IMPERATI, D., CASTELLANOS, F. X., SPORNS, O. & MILHAM, M. P. 2012. Network Centrality in the Human Functional Connectome. *Cerebral Cortex,* 22**,** 1862-1875.

Appendices

Appendix I: tDCS advertising flyer

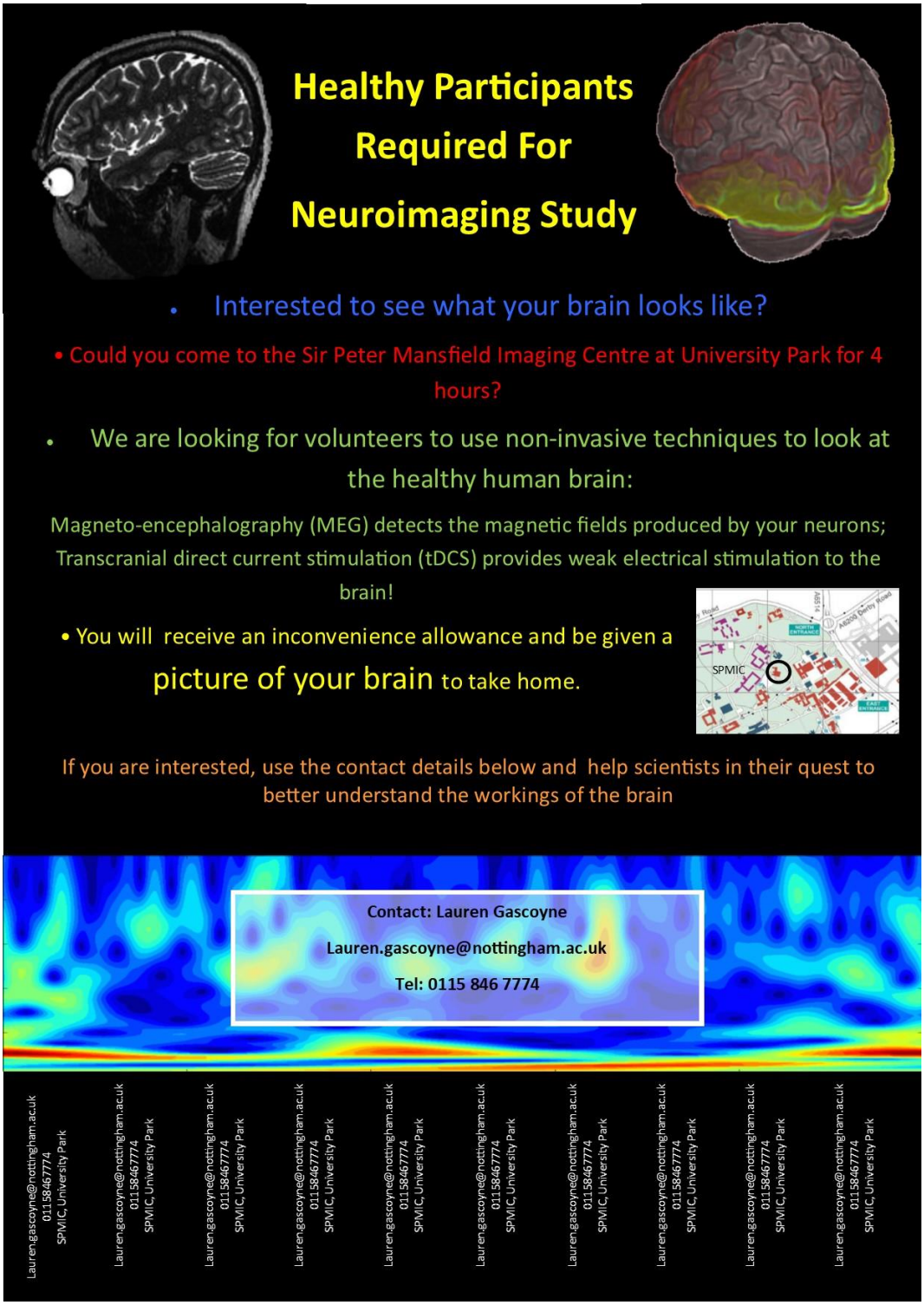

Appendix II: E-mail to approach society and clubs

Dear “society or club name”,

I was wondering if you would be able to assist in online advertisements for a Medical Research Council (MRC) funded study investigating impulsivity and brain stimulation.

Our project is looking at whether we can change impulsive behavior by stimulating the brain sing a technique called transcranial direct current stimulation (tDCS) while undergoing a brain scan using Magnetoencephalography (MEG). We are looking for 60 healthy participants studying at the University of Nottingham to take part in the study. They must be aged 18-40 and not have epilepsy (or other neurological conditions), history of significant head injury, substance misuse, major mental disorder or currently be taking psychotropic medication.

The study will last for up to 4 hours and take place at the Sir Peter Mansfield Centre on University Park. An inconvenience allowance will be offered, and the person will be given an image of their brain to take away with them. We hope this study will help to improve our knowledge about impulsivity, and potentially result in a new therapeutic approach for clinical populations where impulsivity can be harmful.

Would it be possible for the text advertisement below to be placed on the society website/ social media page or distributed to your members by e-mail? We have also attached a flyer if you would also like to circulate this to your group members.

Please do not hesitate to e-mail me on Abdulrhman.shalabi@nottingham.ac.uk if you have any other questions.

Best wishes

Abdulrhman Shalabi and the rest of the study team (Professor Peter Liddle [PI], Dr Katy Jones, Dr Najat Khalifa, Dr Lauren Gascoyne, Dr George O’Neill, Christian Sales, Alice Waitt, Megan Burack, Michael Trubshaw, Abdulrhman Shalabi, Dr Mohammad Katshu, Dr Matt Brookes).

TEXT FOR ADVERTISMENT

“We are looking for students aged 18-40 at the University of Nottingham to help us understand impulsivity.

Our project is looking at whether we can change impulsive behavior by stimulating the brain using a technique called transcranial direct current stimulation (tDCS) while undergoing a brain scan using Magnetoencephalography (MEG). We are looking for 60 healthy participants studying at the University of Nottingham to take part in the study. You must not have epilepsy (or other neurological conditions), history of significant head injury, substance misuse, major mental disorder or currently be taking psychotropic medication.

The study will last for up to 4 hours and take place at the Sir Peter Mansfield Centre on University Park. You will receive an inconvenience allowance and will be given a picture of

your brain to take home with you. We hope this study will help to improve our knowledge about impulsivity, and potentially result in a new therapeutic approach for clinical populations where impulsivity can be harmful.

If you are interested in learning more about the study, please e-mail Lauren Gascoyne (Lauren.Gascoyne@nottingham.ac.uk) or ring **0115 846 7774** *for more information".*

University of Nottingham
Sir Peter Mansfield Imaging Centre

Participant Information Sheet (Healthy Volunteers)

Measuring cortical dynamics of inhibitory control before, during, and after transcranial Direct Current Stimulation (tDCS).

REC Ref: 199-1801

Investigators: Professor Peter Liddle, Dr Katy Jones, Dr Najat Khalifa, Dr Lauren Gascoyne, Dr George O'Neill, Christian Sales, Alice Waitt, Abdulrhman Shalabi, Dr Mohammad Katshu, Megan Burack, Michael Trubshaw, Dr Matt Brookes

What is tDCS?

Transcranial Direct Current Stimulation (tDCS) is a safe technique involving very weak electrical stimulation to the brain using a battery-operated stimulator. Stimulation is delivered via two conductive sponges applied to the scalp and a tiny current is passed between them to stimulate a specific part of the brain. For more information about how this might feel please see the additional tDCS information sheet.

What is Magnetoencephalography?

Magnetoencephalography (MEG) is an alternative technique for directly measuring brain activity. Brain cells communicate with one another by exchanging small electrical currents and these currents induce a magnetic field that is distributed around the head. Such fields are detectable using a MEG scanner and their measurement allows us to determine the location of any electrical activity in the brain, and how the patterns of that electrical activity change over time.

What are we investigating?

MEG measure electromagnetic patterns of brain activity. We will use it in conjunction with tDCS to examine whether tDCS changes brain functioning in areas related to impulse control.

Figure 1: MEG system

A

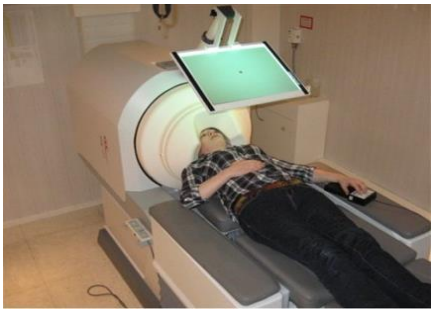

What will it involve for you?

You will be scanned using MEG to measure your brain activity when completing an impulse control task known as the anti-saccade task. This task will involve you looking away from a stimulus repeatedly presented to you on a screen and lasts for about 20 minutes.

If you are happy to continue once you have understood the precise details of the experiment explained to you then we will ask to complete a tDCS safety questionnaire and to sign a consent form. You will then be asked to attend the Imaging Centre for up to 4 hours. On arrival you will be asked to confirm and sign that no details have changed on your safety form. You will then be shown the MEG scanner which will be used during the experiment.

MEG

You will be shown the MEG scanner, and we will explain exactly what you will experience during the experiment. The MEG scan involves you placing your head inside a plastic helmet which contains the sensors which make the measurements. Your head fits into this helmet as far as your nose (see Figure1). Before you are placed in the MEG scanner 3 small coils will be attached to your head at the top of your nose and in-front of both of your ears. These will monitor your head position inside the MEG scanner and will not measure any brain signals. You will feel no sensation from them during scanning.

Because we cannot have any metal near MEG scanners we will then ask you to change into paper clothing, similar to pyjamas, which we will provide. We will then be ready to record your brain activity using MEG. The investigator conducting the study will explain beforehand what will happen during the experiment, what you are required to do and the length of time that you will be scanned for. It is very important that you stay as still as possible throughout the entire duration of all experiments. The signals which we measure get corrupted by movements which make it hard to accurately measure your brain activity unless you remain still.

MRI

After the MEG scan, you will undergo an anatomical MRI scan. Before the scan you will be provided with ear protection as the scanner can be loud. You will also be checked again to make sure you are free of metal, as an MRI scanner contains a strong magnetic field. You will be lying as still as possible inside the scanner for about 15 minutes and we will be creating an image of the structure of your brain for use in further analysis. A picture of your brain can be provided.

The entire study will last up to four hours.

What is the potential for pain, discomfort, distress, inconvenience or changes in lifestyle?

None of the procedures are painful. See separate tDCS information about how this stimulation might feel.

Are there any risks?

MEG is a non-invasive passive scanning technique and involve no risk. MRI is also low risk, though you may feel a slight dizziness on entering the magnetic field, this is normal.

IMPORTANT: What happens if we notice something abnormal on your scan?

While it is extremely unlikely that your scan will show any abnormality, it is unlikely that we would notice anything unusual or abnormal on the images since the Sir Peter Mansfield Imaging Centre (the SPMIC; see Figure 2) is NOT a clinical diagnostic facility and the scans we collect are NOT the same as scans collected by doctors for medical purposes. The pictures will NOT usually be looked at by a radiologist (a doctor qualified to find abnormalities in scans), so this test does NOT replace any tests that your doctor thinks might be needed.

However, there is a possibility that one of the researchers working with your scans might notice something that they consider abnormal. If we suspect that there is something abnormal on your scan we will ask a specialist to review it. If he/ she thinks that further action is necessary we will inform your GP. Your GP may refer you to other medical specialists for further clinical investigation.

It is a requirement of the SPMIC that you give permission for us to inform your GP of such a finding before we can enrol you into the study.

In the unlikely event that we do notice something abnormal on your scan, giving you that information might have the benefit of allowing you to start treatment earlier than you would have otherwise. However, it is also important for you to realise that by providing you with this information there may be implications for your future ability to find employment and obtain insurance.

In 2010 we scanned over 1100 volunteers (most of whom were healthy young people) and happened to notice something that we thought was abnormal on 10 people, of which 3 turned out to be clinical significant problems. However, the chances of detecting an abnormality depend on the region of your body we are scanning, the methods we are using to scan you, your age and your health.

What is in it for you?

You will receive an inconvenience allowance of £40 for participating in the study.

What if something goes wrong?

In case you have a complaint (for example on your treatment by a member of staff) you can initially approach lead investigator Professor Peter Liddle (Institute of Mental Health, Division of Psychiatry and Applied Psychology, University of Nottingham Innovations Park, Triumph Road, Nottingham, NG7 2TU, peter.liddle@nottingham.ac.ukmailto:najat.khalifa@nottingham.ac.uk, 0115 823 0421).

If this does not produce a satisfactory outcome (or in case of something serious happened during or following your participation in the study) you can then contact FMHS Research Ethics Committee Administrator, c/o The University of Nottingham, Faculty PVC Office, B Floor, Medical School, Queen's Medical Centre Campus, Nottingham University Hospitals, Nottingham, NG7 2UH or via E-mail: FMHS-ResearchEthics@nottingham.ac.uk. Please quote ref no: FMHS 199-1801,

What if you decide to leave the study?

You are free to leave the study at any time if you chose to do so without giving a reason. If you do withdraw from the study for medical reasons not associated with the study you will receive an inconvenience allowance proportional to the length of the period of participation, but if you withdraw for any other reason, the inconvenience allowance to be received, if any, shall be at the discretion of the supervising investigator.

Will my taking part in the study be kept confidential?

We will follow ethical and legal practice and all information about you will be handled in confidence.

If you join the study, some parts of the data collected for the study will be looked at by authorised persons from the University of Nottingham who are organising the research. They may also be looked at by authorised people to check that the study is being carried out correctly. All will have a duty of confidentiality to you as a research participant.

All information which is collected about you during the course of the research will be kept **strictly confidential**, stored in a secure and locked office, and on a password protected database. Any information about you which leaves the institution will have your name and address removed (anonymised) and a unique code will be used so that you cannot be recognised from it.

Your personal data (address, telephone number) will be kept for 6 months after the end of the study so that we are able to contact you about the findings of the study *and possible follow-up studies* (unless you advise us that you do not wish to be contacted). All other data (research data) will be kept securely for 7 years. After this time your data will be disposed of securely. During this time all precautions will be taken by all those involved to maintain your confidentiality, only members of the research team will have access to your personal data.

We would also like to seek your consent so that the data may be stored and used in possible future research during and after 7 years– this is optional (please indicate you agree to this on the consent form).

Publication and Dissemination of the Results

The results of this study may be published in the scientific literature and may also be presented at scientific meetings. All such data will be presented anonymously so that none of the volunteers can be identified.

Do you have any further questions?

If you have any questions please ask the person who gave you this sheet or Dr Lauren Gascoyne on Lauren.gascoyne@nottingham.ac.uk.

Don't forget, you do not have to be scanned, and you can change your mind, and withdraw from the study, at any time, even whilst being scanned!

Figure 2: The Sir Peter Mansfield Imaging Centre is situated off the Main Visitors car park in grid E4

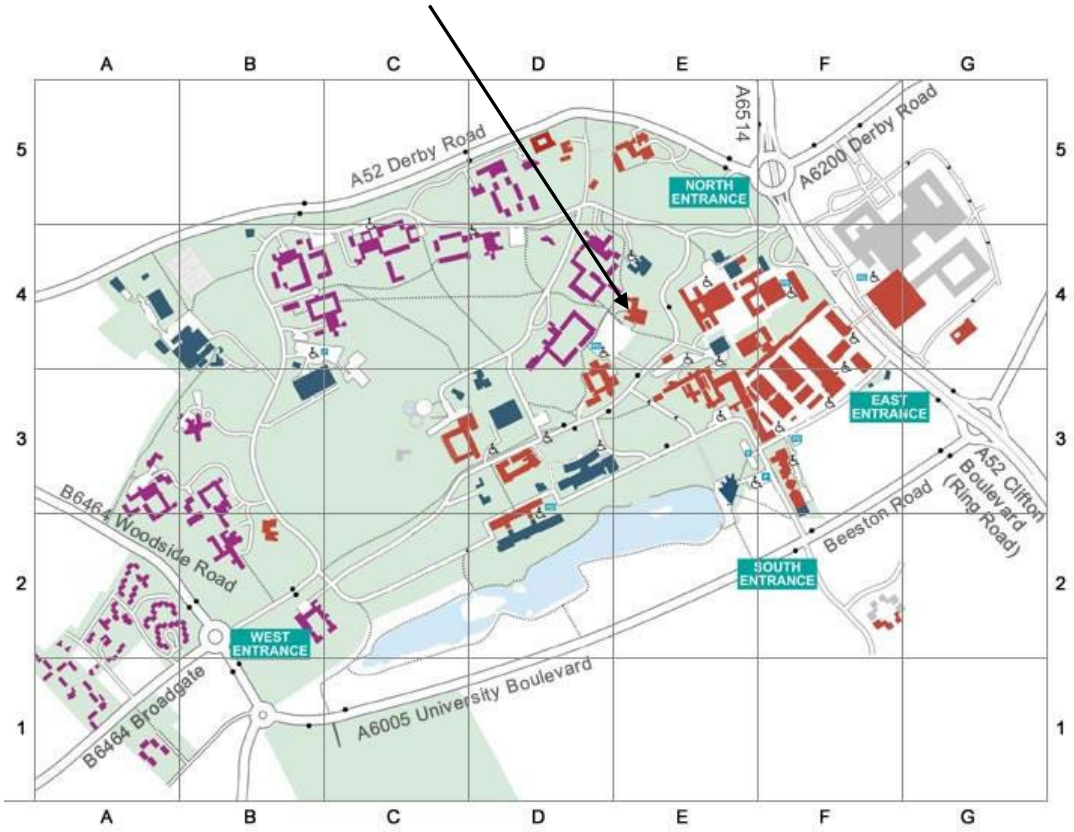

Appendix IV: tDCS Safety Questionnaire

tDCS Safety Questionnaire

Participant ID (to be added by researcher)

Please answer all the questions listed below. For safety reasons, it's of great importance that the information you have given on this safety questionnaire is accurate. Mark Yes or No

1. Do you have epilepsy or have you ever had a convulsion or seizure?
2. Have you ever had head injury?
3. Do you have metal in the brain/skull, e.g. splinters, fragments or clips?
4. Do you have cochlear implants?
5. Do you have an implanted neuro-stimulator (e.g. direct brain stimulation, epidural/subdural stimulation, vagal nerve stimulation)?
6. Have you ever had surgical procedures to your brain?
7. Have you ever had tDCS in the past? If the answer is yes, have you ever had an adverse reaction to it?
8. Have you been diagnosed with a severe psychiatric disorder such as schizophrenia, bipolar disorder, clinical depression?
9. Do you have a cardiac pacemaker or intracardiac lines or metal in your body?
10. Are you taking any medications? Please list _____
11. Do you drink more than 20 units of alcohol per week (a unit being half a pint of medium strength beer, one shot of spirits or a small glass of wine)?
12. Do you use any illicit or non-illicit substances including solvents, cannabis, amphetamine, heroin or new psychoactive substances (previously known as legal highs)?
13. Do you have a sensitive scalp?

For items marked 'Yes', please provide additional information here:

Researcher:	Participant:
Signature:	Signature:
Date:	Date:

Appendix V: Time-frequency spectrograms of the antisaccade task

The following figures are the time-frequency spectrograms (4-40Hz with 2Hz increment) from cue presentation to 500 ms post-stimulus during the performance of the antisaccade task for both treatment conditions labelled by region, trial type and treatment condition.

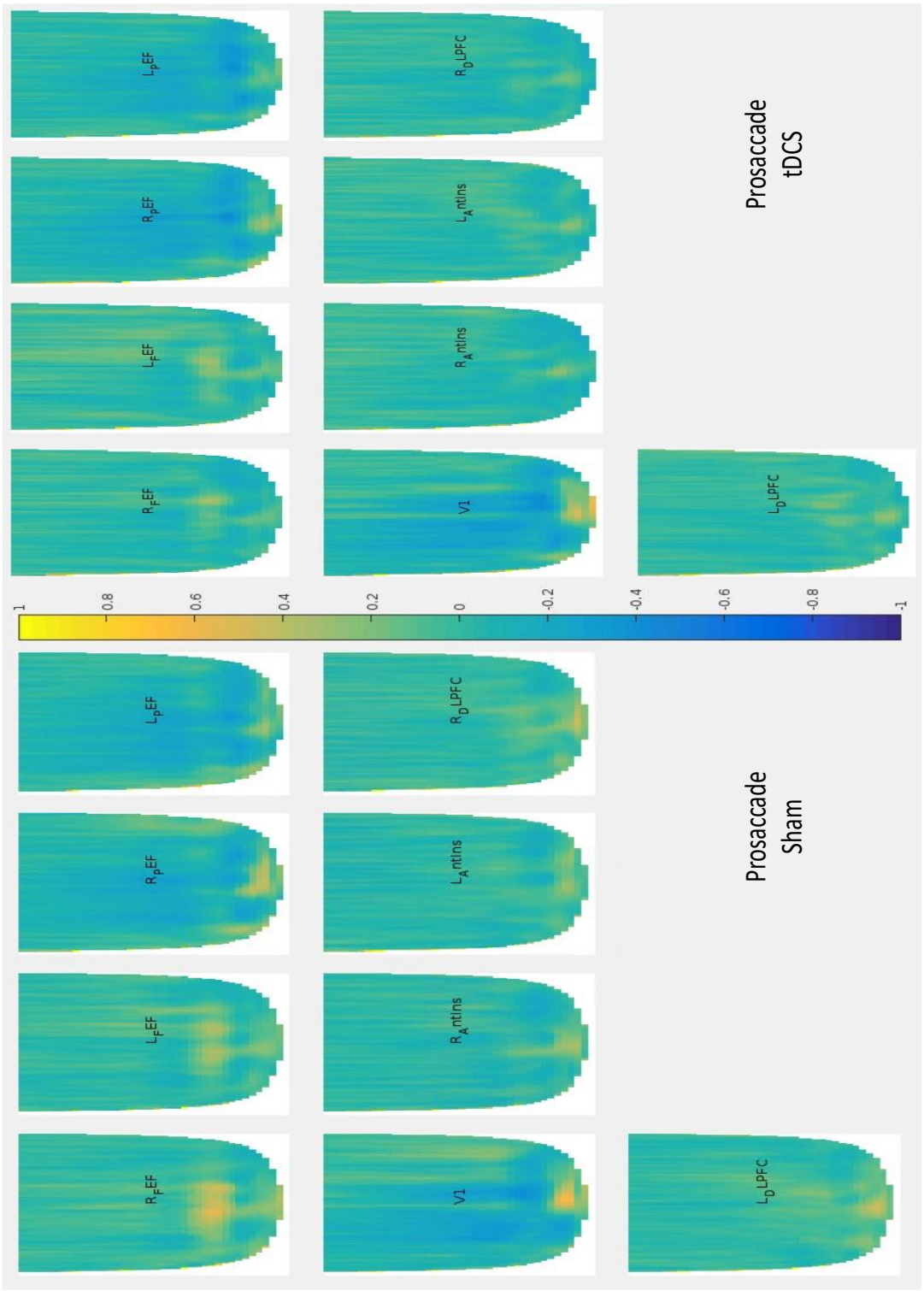

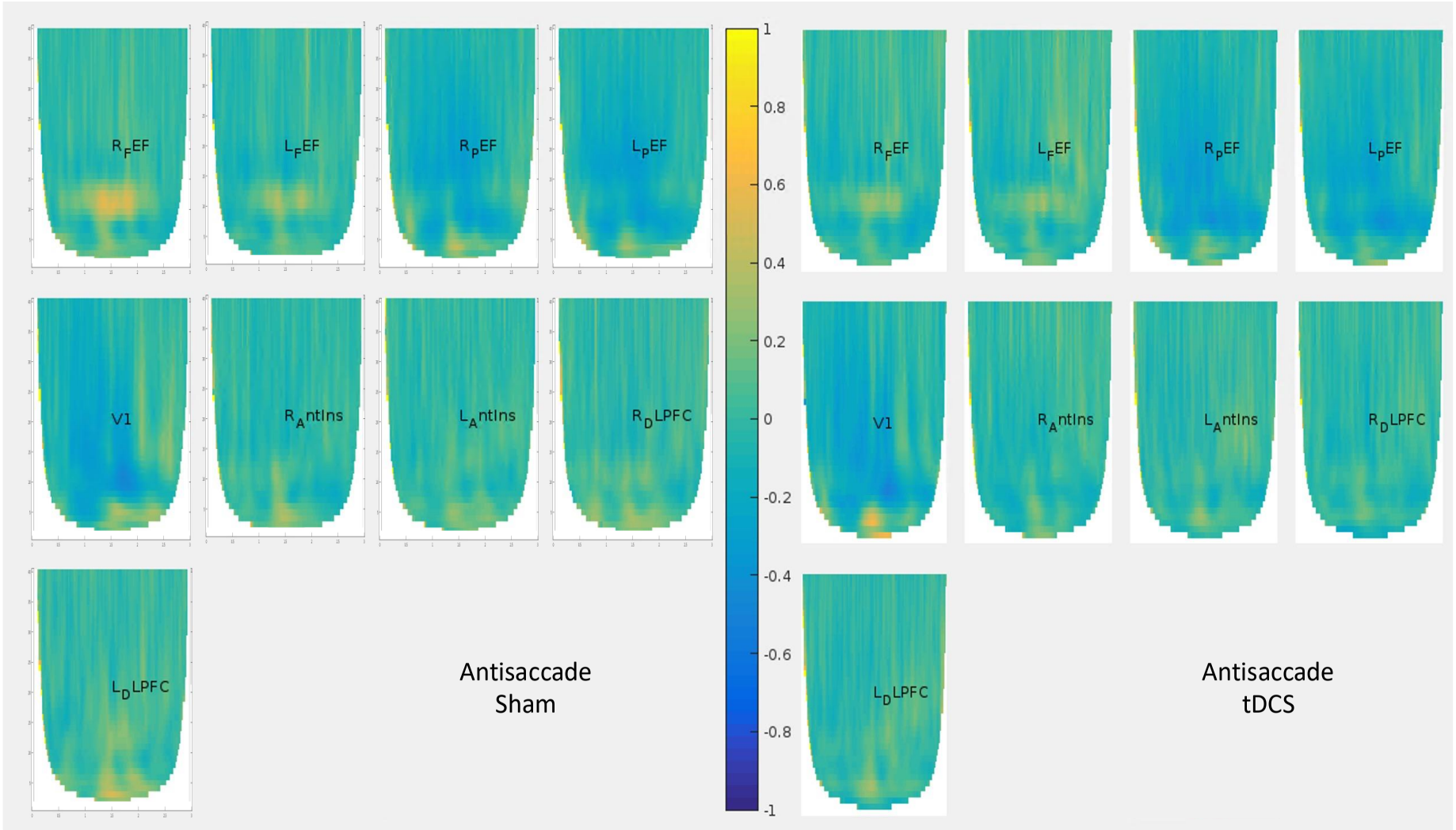
R FEF
L FEF
R PEF
L PEF
V1
R AntIns
L AntIns
R DLPFC
L DLPFC
1
0.8
0.6
0.4
0.2
0
-0.2
-0.4
-0.6
-0.8
-1
Antisaccade
Sham
Antisaccade
tDCS

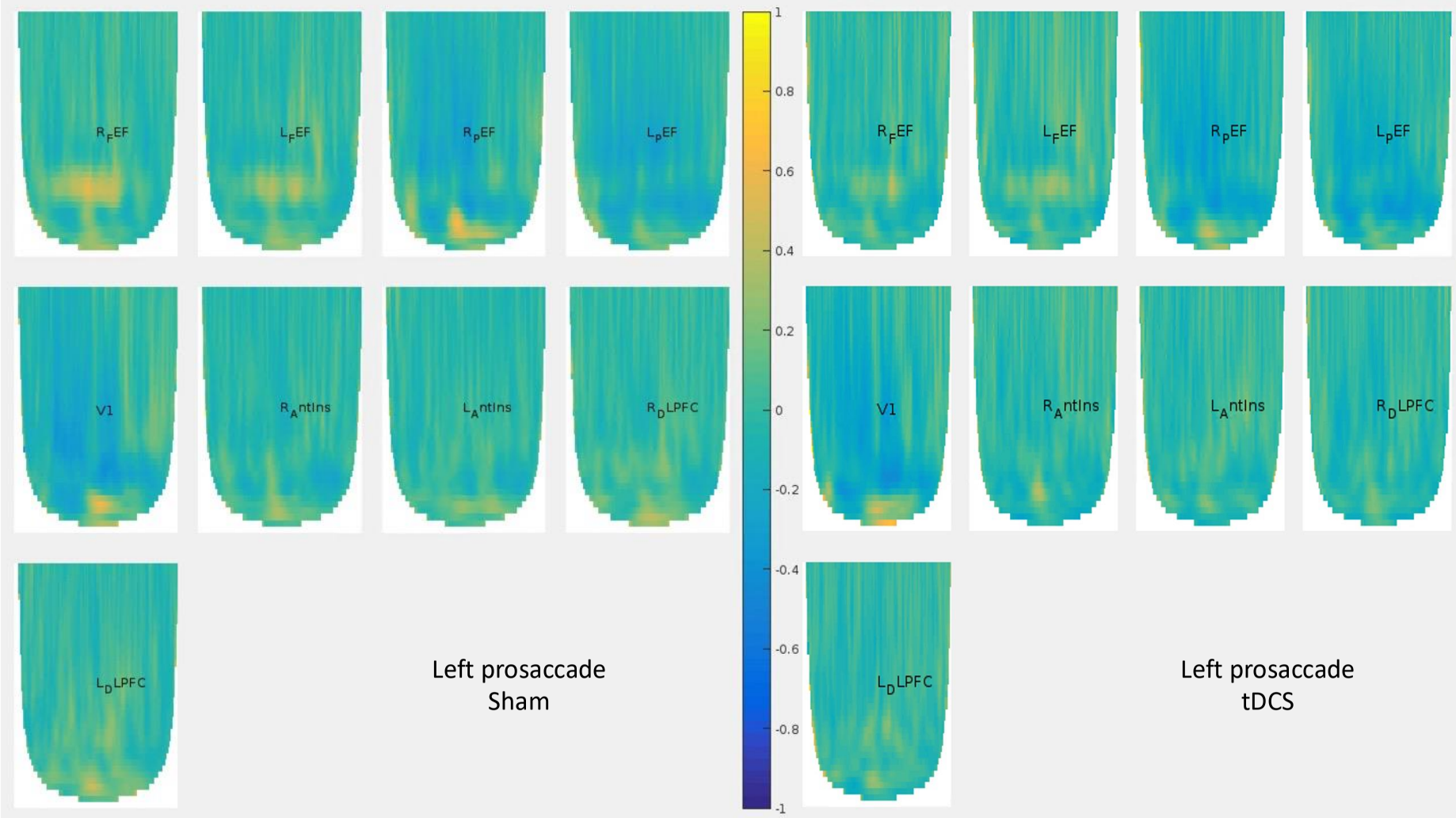
R FEF
L FEF
R PEF
L PEF
V1
R AntIns
L AntIns
R DLPFC
L DLPFC
1
0.8
0.6
0.4
0.2
0
-0.2
-0.4
-0.6
-0.8
-1
R FEF
L FEF
R PEF
L PEF
V1
R AntIns
L AntIns
R DLPFC
L DLPFC
Left prosaccade
Sham
Left prosaccade
tDCS

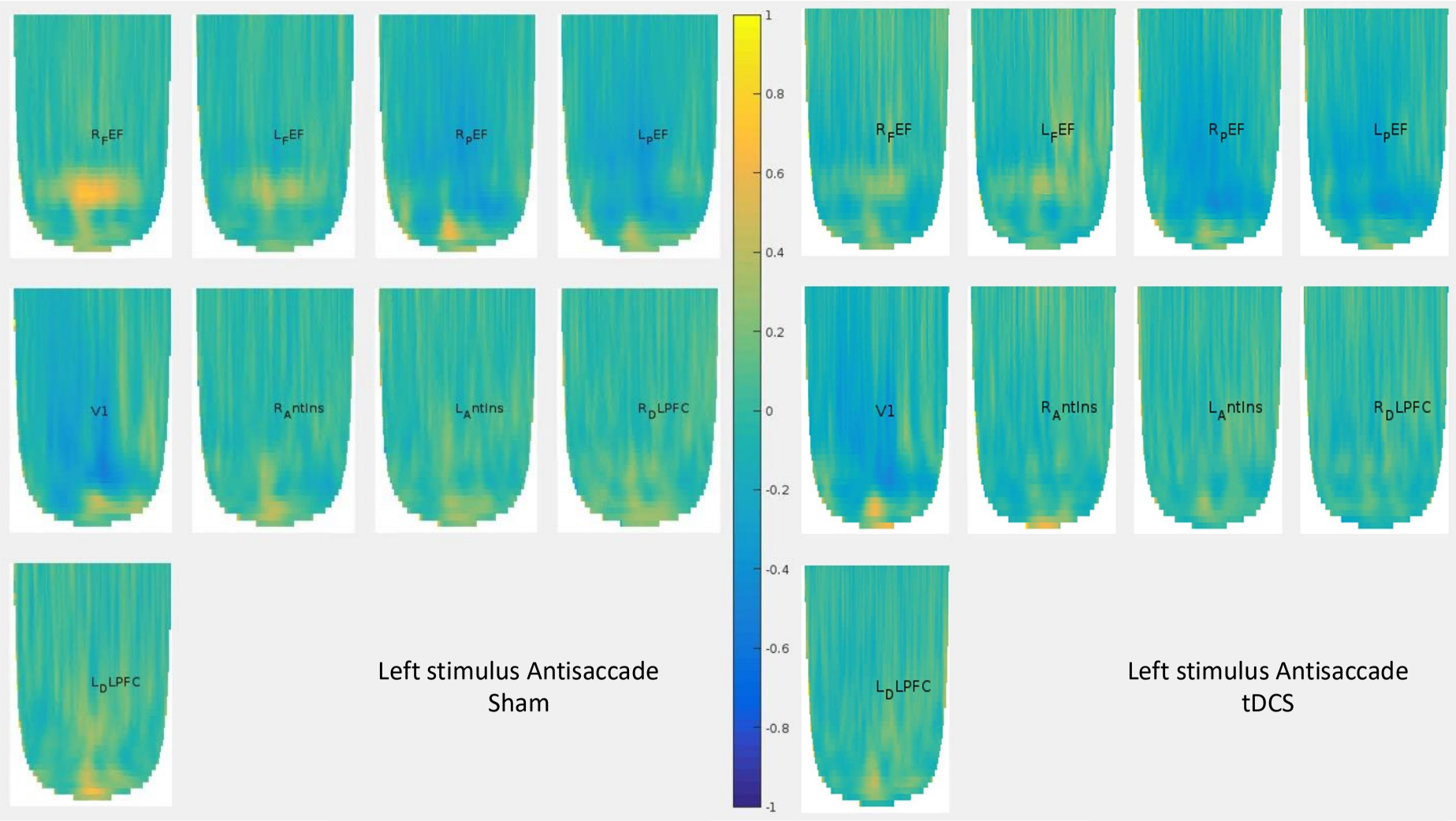
R FEF
L FEF
R PEF
L PEF
V1
R AntIns
L AntIns
R DLPFC
L DLPFC
1
0.8
0.6
0.4
0.2
0
-0.2
-0.4
-0.6
-0.8
-1
R FEF
L FEF
R PEF
L PEF
V1
R AntIns
L AntIns
R DLPFC
L DLPFC
Left stimulus Antisaccade
Sham
Left stimulus Antisaccade
tDCS

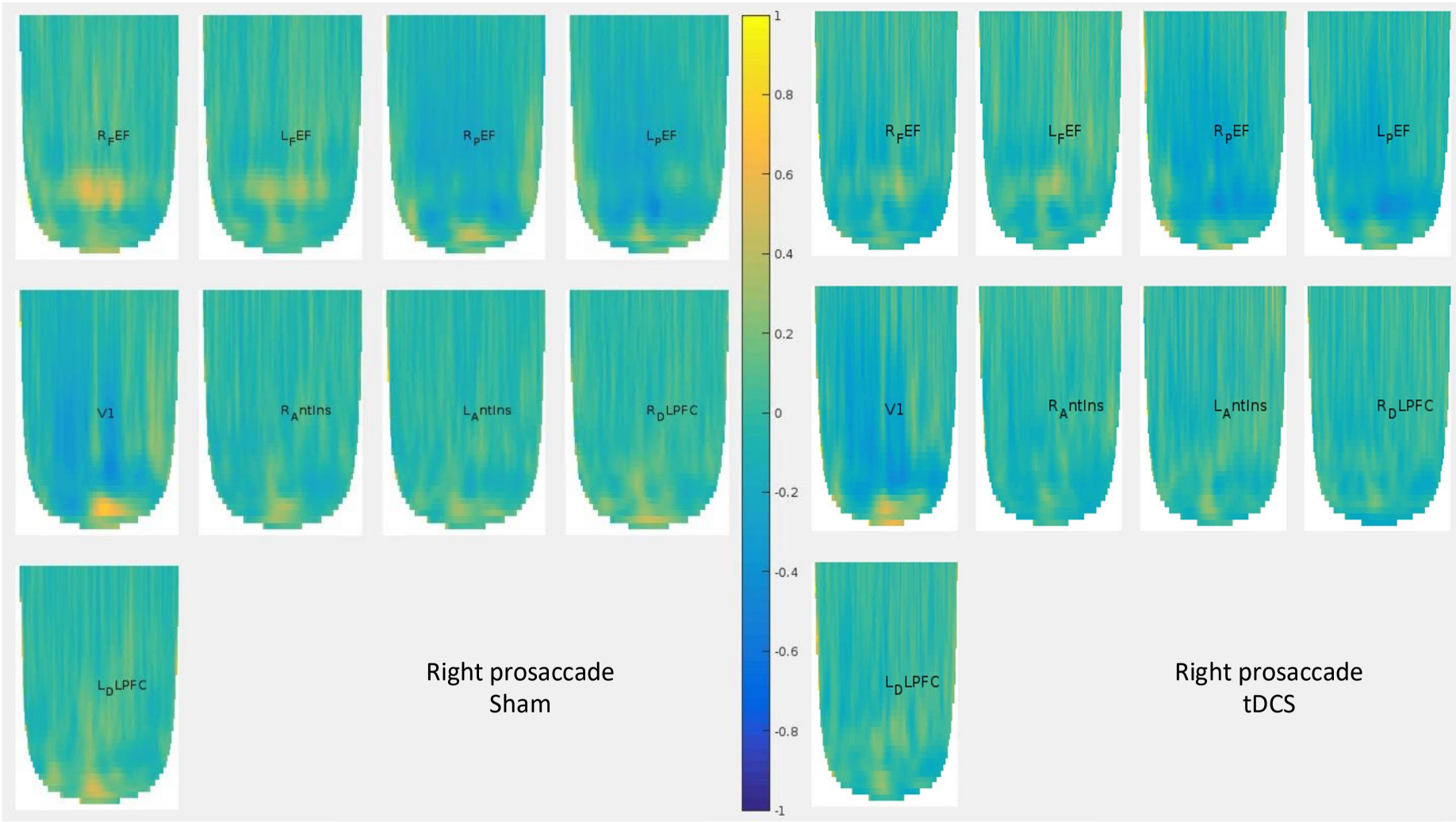
R FEF
L FEF
R PEF
L PEF
V1
R AntIns
L AntIns
R DLPFC
L DLPFC
1
0.8
0.6
0.4
0.2
0
-0.2
-0.4
-0.6
-0.8
-1
Right prosaccade
Sham
Right prosaccade
tDCS

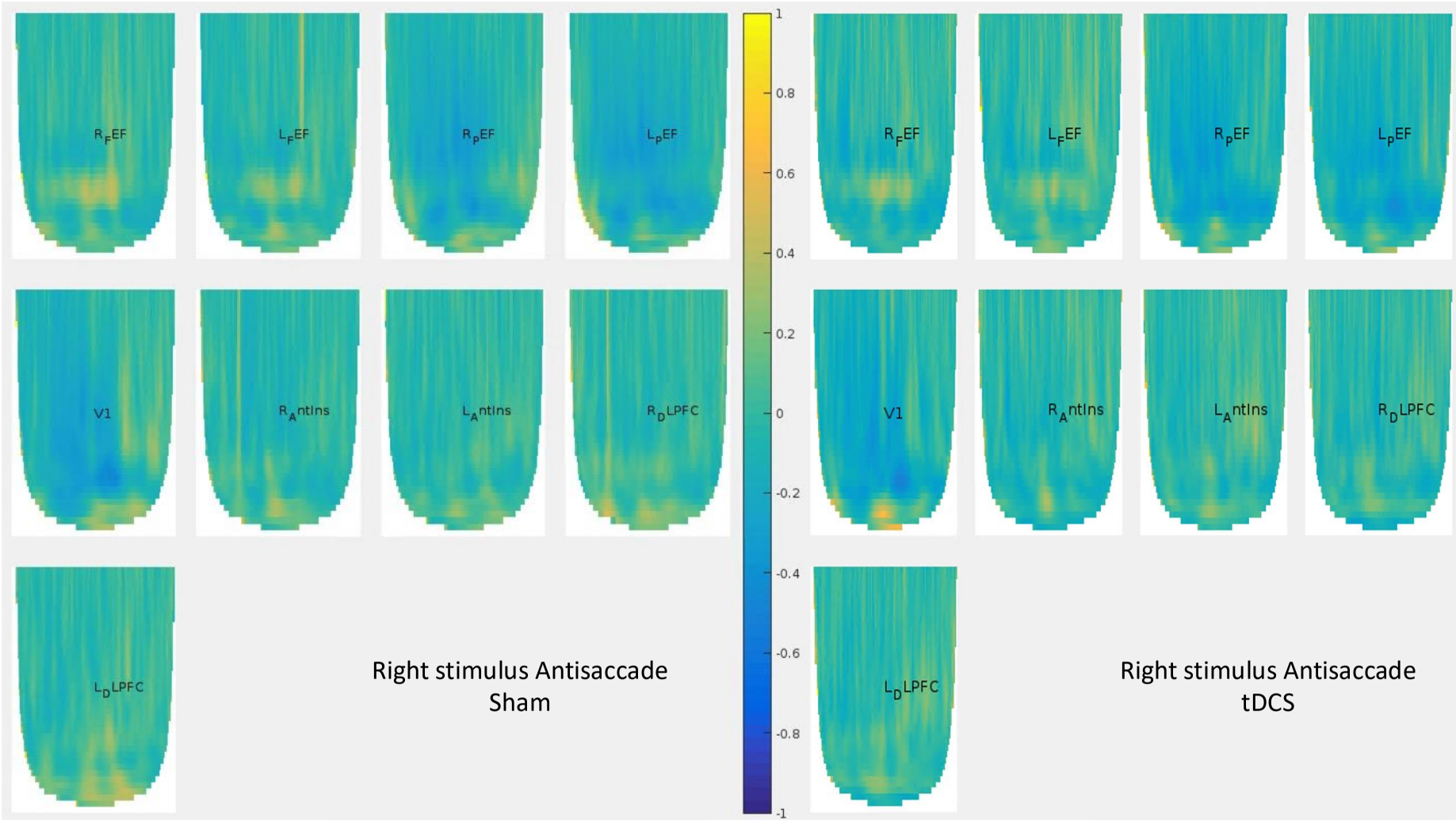
R FEF
L FEF
R PEF
L PEF
V1
R AntIns
L AntIns
R DLPFC
L DLPFC
1
0.8
0.6
0.4
0.2
0
-0.2
-0.4
-0.6
-0.8
-1
R FEF
L FEF
R PEF
L PEF
V1
R AntIns
L AntIns
R DLPFC
L DLPFC
Right stimulus Antisaccade
Sham
Right stimulus Antisaccade
tDCS

Appendix VI: Profile of Mood status (POMS) questionnaire

	Scale	Not at all	A little	Moderately	Quit a lot	Extremely
Tense	TEN	0	1	2	3	4
Angry	ANG	0	1	2	3	4
Worn Out	FAT	0	1	2	3	4
Unhappy	DEP	0	1	2	3	4
Proud	ERA	0	1	2	3	4
Lively	VIG	0	1	2	3	4
Confused	CON	0	1	2	3	4
Sad	DEP	0	1	2	3	4
Active	VIG	0	1	2	3	4
On-edge	TEN	0	1	2	3	4
Grouchy	ANG	0	1	2	3	4
Ashamed	ERA (RS)	0	1	2	3	4
Energetic	VIG	0	1	2	3	4
Hopeless	DEP	0	1	2	3	4
Uneasy	TEN	0	1	2	3	4
Restless	TEN	0	1	2	3	4
Unable to concentrate	CON	0	1	2	3	4
Fatigued	FAT	0	1	2	3	4
Competent	ERA	0	1	2	3	4
Annoyed	ANG	0	1	2	3	4
Discouraged	DEP	0	1	2	3	4
Resentful	ANG	0	1	2	3	4
Nervous	TEN	0	1	2	3	4
Miserable	DEP	0	1	2	3	4
Confident	ERA	0	1	2	3	4
Bitter	ANG	0	1	2	3	4
Exhausted	FAT	0	1	2	3	4
Anxious	TEN	0	1	2	3	4
Helpless	DEP	0	1	2	3	4
Weary	FAT	0	1	2	3	4
Satisfied	ERA	0	1	2	3	4
Bewildered	CON	0	1	2	3	4
Furious	ANG	0	1	2	3	4
Full of Pep	VIG	0	1	2	3	4
Worthless	DEP	0	1	2	3	4
Forgetful	CON	0	1	2	3	4
Vigorous	VIG	0	1	2	3	4
Uncertain about things	CON	0	1	2	3	4
Bushed	FAT	0	1	2	3	4
Embarrassed	ERA (RS)	0	1	2	3	4

TEN= Tension, ANG=Anger, FAT= Fatigue, DEP=Depression, ERA=Esteem related affect, VIG= vigour, CON = Confusion, RS= reverse score
Total Mood Disturbance (TMD)= [TEN+DEP+ANG+FAT+CON]-[VIG+ERA]

Appendix VII Urgency premeditation, perseverance, sensation seeking and positive urgency (UPPS-P) scale

UPPS-P

Below are a number of statements that describe ways in which people act and think. For each statement, please indicate how much you agree or disagree with the statement. If you **Agree Strongly** circle **1**, if you **Agree Somewhat** circle **2**, if you **Disagree somewhat** circle **3**, and if you **Disagree Strongly** circle **4**. Be sure to indicate your agreement or disagreement for every statement below. Also, there are questions on the following pages.

	Agree Strongly	Agree Some	Disagree Some	Disagree Strongly
1. I have a reserved and cautious attitude toward life.	1	2	3	4
2. I have trouble controlling my impulses.	1	2	3	4
3. I generally seek new and exciting experiences and sensations.	1	2	3	4
4. I generally like to see things through to the end.	1	2	3	4
5. When I am very happy, I can't seem to stop myself from doing things that can have bad consequences.	1	2	3	4
6. My thinking is usually careful and purposeful.	1	2	3	4
7. I have trouble resisting my cravings (for food, cigarettes, etc.).	1	2	3	4
8. I'll try anything once.	1	2	3	4
9. I tend to give up easily.	1	2	3	4
10. When I am in great mood, I tend to get into situations that could cause me problems.	1	2	3	4
11. I am not one of those people who blurt out things without thinking.	1	2	3	4
12. I often get involved in things I later wish I could get out of.	1	2	3	4
13. I like sports and games in which you have to choose your next move very quickly.	1	2	3	4
14. Unfinished tasks really bother me.	1	2	3	4
15. When I am very happy, I tend to do things that may cause problems in my life.	1	2	3	4
16. I like to stop and think things over before I do them.	1	2	3	4
17. When I feel bad, I will often do things I later regret in order to make myself feel better now.	1	2	3	4
18. I would enjoy water skiing.	1	2	3	4
19. Once I get going on something I hate to stop.	1	2	3	4
20. I tend to lose control when I am in a great mood.	1	2	3	4
21. I don't like to start a project until I know exactly how to proceed.	1	2	3	4

	Agree Strongly	Agree Some	Disagree Some	Disagree Strongly
22. Sometimes when I feel bad, I can't seem to stop what I am doing even though it is making me feel worse.	1	2	3	4
23. I quite enjoy taking risks.	1	2	3	4
24. I concentrate easily.	1	2	3	4
25. When I am really ecstatic, I tend to get out of control.	1	2	3	4
26. I would enjoy parachute jumping.	1	2	3	4
27. I finish what I start.	1	2	3	4
28. I tend to value and follow a rational, "sensible" approach to things.	1	2	3	4
29. When I am upset I often act without thinking.	1	2	3	4
30. Others would say I make bad choices when I am extremely happy about something.	1	2	3	4
31. I welcome new and exciting experiences and sensations, even if they are a little frightening and unconventional.	1	2	3	4
32. I am able to pace myself so as to get things done on time.	1	2	3	4
33. I usually make up my mind through careful reasoning.	1	2	3	4
34. When I feel rejected, I will often say things that I later regret.	1	2	3	4
35. Others are shocked or worried about the things I do when I am feeling very excited.	1	2	3	4
36. I would like to learn to fly an airplane.	1	2	3	4
37. I am a person who always gets the job done.	1	2	3	4
38. I am a cautious person.	1	2	3	4
39. It is hard for me to resist acting on my feelings.	1	2	3	4
40. When I get really happy about something, I tend to do things that can have bad consequences.	1	2	3	4
41. I sometimes like doing things that are a bit frightening.	1	2	3	4
42. I almost always finish projects that I start.	1	2	3	4
43. Before I get into a new situation I like to find out what to expect from it.	1	2	3	4
44. I often make matters worse because I act without thinking when I am upset.	1	2	3	4
45. When overjoyed, I feel like I can't stop myself from going overboard.	1	2	3	4
46. I would enjoy the sensation of skiing very fast down a high mountain slope.	1	2	3	4
47. Sometimes there are so many little things to be done that I just ignore them all.	1	2	3	4
48. I usually think carefully before doing anything.	1	2	3	4
49. When I am really excited, I tend not to think of the consequences of my actions.	1	2	3	4
50. In the heat of an argument, I will often say things that I later regret.	1	2	3	4
51. I would like to go scuba diving.	1	2	3	4
52. I tend to act without thinking when I am really excited.	1	2	3	4
53. I always keep my feelings under control.	1	2	3	4
54. When I am really happy, I often find myself in situations that I normally wouldn't be comfortable with.	1	2	3	4
55. Before making up my mind, I consider all the advantages and disadvantages.	1	2	3	4
56. I would enjoy fast driving.	1	2	3	4
57. When I am very happy, I feel like it is ok to give in to cravings or overindulge.	1	2	3	4
58. Sometimes I do impulsive things that I later regret.	1	2	3	4
59. I am surprised at the things I do while in a great mood.	1	2	3	4

Scoring Instructions

This is a revised version of the UPPS Impulsive Behavior scale (Whiteside & Lynam, 2001). This version, UPPS-P (Lynam, Smith, Whiteside, & Cyders, 2006), assesses Positive Urgency (Cyders, Smith, Spillane, Fischer, Annus, & Peterson, 2007) in addition to the four pathways assessed in the original version of the scale-- Urgency (now Negative Urgency), (lack of) Premeditation, (lack of) Perseverance, and Sensation Seeking. The scale uses a 1 (agree strongly) to 4 (disagree strongly) response format. Because the items from different scales run in different directions, it is important to make sure that the correct items are reverse-scored. We suggest making all of the scales run in the direction such that higher scores indicate more impulsive behavior. Therefore, we include the scoring key for, (Negative) Urgency, (lack of) Premeditation, (lack of) Perseverance, Sensation Seeking, and Positive Urgency. For each scale, calculate the mean of the available items; this puts the scales on the same metric. We recommend requiring that a participant have at least 70% of the items before a score is calculated.

(Negative) Urgency (all items except 1 are reversed)
items 2 (R), 7(R), 12 (R), 17 (R), 22 (R), 29 (R), 34 (R), 39 (R), 44 (R), 50 (R), 53, 58 (R)

(lack of) Premeditation (no items are reversed)
items 1, 6, 11, 16, 21, 28, 33, 38, 43, 48, 55.

(lack of) Perseverance (two items are reversed)
items 4, 9 (R), 14, 19, 24, 27, 32, 37, 42, 47 (R)

Sensation Seeking (all items are reversed)
items 3 (R), 8 (R), 13 (R), 18 (R), 23 (R), 26 (R), 31 (R), 36 (R), 41 (R), 46 (R), 51 (R), 56 (R)

Positive Urgency (all items are reversed)
items 5 (R), 10 (R), 15 (R), 20 (R), 25 (R), 30 (R), 35 (R), 40 (R), 45 (R), 49 (R), 52 (R), 54 (R), 57 (R), 59 (R)

(R) indicates the item needs to be reverse scored such 1=4, 2=3, 3=2, and 4=1.

Appendix VIII Schizotypal personality questionnaire (SPQ)

As presented by (Raine and Benishay, 1995).

Table 1. Items for the nine subscales in the final 74-item version of the Schizotypal Personality Questionnaire

Ideas of Reference

1. Do you sometimes feel that things you see on the TV or read in the newspaper have a special meaning for you?
10. I am aware that people notice me when I go out for a meal or to see a film.
19. Do some people drop hints about you or say things with a double meaning?
28. Have you ever noticed a common event or object that seemed to be a special sign for you?
37. Do you sometimes see special meanings in advertisements, shop windows, or in the way things are arranged around you?
45. When shopping do you get the feeling that other people are taking notice of you?
53. When you see people talking to each other, do you often wonder if they are talking about you?
60. Do you sometimes feel that other people are watching you?
63. Do you sometimes feel that people are talking about you?

Excessive Social Anxiety

2. I sometimes avoid going to places where there will be many people because I will get anxious.
11. I get very nervous when I have to make polite conversation.
20. Do you ever get nervous when someone is walking behind you?
29. I get anxious when meeting people for the first time.
38. Do you often feel nervous when you are in a group of unfamiliar people?
46. I feel very uncomfortable in social situations involving unfamiliar people.
54. I would feel very anxious if I had to give a speech in front of a large group of people.
71. I feel very uneasy talking to people I do not know well.

Odd Beliefs or Magical Thinking

3. Have you had experiences with the supernatural?
12. Do you believe in telepathy (mind-reading)?
21. Are you sometimes sure that other people can tell what you are thinking?
30. Do you believe in clairvoyancy (psychic forces, fortune telling)?
39. Can other people feel your feelings when they are not there?
47. Have you had experiences with astrology, seeing the future, UFOs, ESP, or a sixth sense?
55. Have you ever felt that you are communicating with another person telepathically (by mind-reading)?

Unusual Perceptual Experiences

4. Have you often mistaken objects or shadows for people, or noises for voices?
13. Have you ever had the sense that some person or force is around you, even though you cannot see anyone?
22. When you look at a person, or yourself in a mirror, have you ever seen the face change right before your eyes?
31. I often hear a voice speaking my thoughts aloud.
40. Have you ever seen things invisible to other people?
48. Do everyday things seem unusually large or small?
56. Does your sense of smell sometimes become unusually strong?
61. Do you ever suddenly feel distracted by distant sounds that you are not normally aware of?
64. Are your thoughts sometimes so strong that you can almost hear them?

Odd or Eccentric Behavior

5. Other people see me as slightly eccentric (odd).
14. People sometimes comment on my unusual mannerisms and habits.
23. Sometimes other people think that I am a little strange.
32. Some people think that I am a very bizarre person.
67. I am an odd, unusual person.
70. I have some eccentric (odd) habits.
74. People sometimes stare at me because of my odd appearance.

No Close Friends

6. I have little interest in getting to know other people.
15. I prefer to keep myself to myself.
24. I am mostly quiet when with other people.

Table 1. Items for the nine subscales in the final 74-item version of the Schizotypal Personality Questionnaire—*Continued*

No Close Friends—*Continued*

33. I find it hard to be emotionally close to other people.
41. Do you feel that there is no one you are really close to outside of your immediate family, or people you can confide in or talk to about personal problems?
49. Writing letters to friends is more trouble than it is worth.
57. I tend to keep in the background on social occasions.
62. I attach little importance to having close friends.
66. Do you feel that you cannot get "close" to people?

Odd Speech

7. People sometimes find it hard to understand what I am saying.
16. I sometimes jump quickly from one topic to another when speaking.
25. I sometimes forget what I am trying to say.
34. I often ramble on too much when speaking.
42. Some people find me a bit vague and elusive during a conversation.
50. I sometimes use words in unusual ways.
58. Do you tend to wander off the topic when having a conversation?
69. I find it hard to communicate clearly what I want to say to people.
72. People occasionally comment that my conversation is confusing.

Constricted Affect

8. People sometimes find me aloof and distant.
17. I am not good at expressing my true feelings by the way I talk and look.
26. I rarely laugh and smile.
35. My "nonverbal" communication (smiling and nodding during a conversation) is not very good.
43. I am poor at returning social courtesies and gestures.
51. I tend to avoid eye contact when conversing with others.
68. I do not have an expressive and lively way of speaking.
73. I tend to keep my feelings to myself.

Suspiciousness

9. I am sure I am being talked about behind my back.
18. Do you often feel that other people have it in for you?
27. Do you sometimes get concerned that friends or coworkers are not really loyal or trustworthy?
36. I feel I have to be on my guard even with friends.
44. Do you often pick up hidden threats or put-downs from what people say or do?
52. Have you found that it is best not to let other people know too much about you?
59. I often feel that others have it in for me.
65. Do you often have to keep an eye out to stop people from taking advantage of you?

Note.—The response format is "yes/no." All items endorsed "yes" score 1 point.

Appendix IX: SPMIC MRI safety questionnaire

The University of Nottingham

Sir Peter Mansfield Magnetic Resonance Centre

MR Volunteer Safety Screening Questionnaire:

NAME	Date of Scan	Date of Birth
ADDRESS	Volunteer Number	
	Ethics Code	
Phone number	Weight	Height if applicable

MR scanning uses strong magnetic fields. For your own safety and the safety of others it is **very important** that you do not go into the magnet halls with any metal in or on your body or clothing. Please answer the following questions carefully and ask if anything is not clear. All information is held in the strictest confidence.

1. Do you have any implants in your body? e.g. replacement joints, drug pumps Y/N
2. Do you have aneurysm clips (clips put around blood vessels during surgery)? Y/N
3. Do you have a pacemaker or artificial heart valve? *(These stop working near MR Scanners)* Y/N
4. Have you ever had any surgery? Please give brief details over. Y/N
   (We do not need to know about uncomplicated caesarean delivery, vasectomy or termination of pregnancy)
5. Do you have any foreign bodies in your body (e.g. shrapnel)? Y/N
6. Have you ever worked in a machine tool shop without eye protection? Y/N
7. Do you wear a hearing aid or cochlear implant? Y/N
8. Could you be pregnant? (Pregnancy tests are available in the female toilets) Y/N
9. Have you ever suffered from tinnitus? Y/N
10. Do you wear dentures, a dental plate or a brace? Y/N
11. Are you susceptible to claustrophobia? Y/N
12. Do you suffer from blackouts, epilepsy or fits? Y/N
13. Do you have any tattoos? (If yes, you may be asked to read and sign another form) Y/N
14. Do you have any body piercing jewellery that cannot be removed? Y/N
15. Do you have any skin patches (trans-dermal patches)? Y/N
16. Do you have a coil in place (IUD) for contraception? Do you know what type? Y/N
17. Do you have any condition that may affect your ability to control your temperature ?
    (e.g. Do you have a fever, cardiovascular disease, hypertension, diabetes or cerebrovascular disease?) Y/N
18. Will you remove all metal including coins, body-piercing jewellery, false-teeth, hearing aids etc. before entering the magnet hall? *(lockers available by the changing rooms)* Y/N
19. Is there anything else you think we should know? Y/N

I have read and understood all the questions **Signature:**	**Date:**
Verified by: **Scanner Operator Only:**	**Date:**

Appendix X: RECOGNeyes advertising flyer

Participant Information Sheet

Effect of RECOGNeyes training on brain networks

Names of Investigators: Dr. Elizabeth Liddle, Prof. Peter Liddle, Dr. Maddie Groom, Ms. Jyothika Kumar, Dr. Lauren Gascoyne

You are being invited to take part in a research study. Before you decide whether or not you wish to participate, it is important for you to understand why the research is being done and what it will involve. Please, take time to read the following information carefully. Talk to others about the study if you wish. Ask us if there is anything that is not clear or if you would like more information. Your participation is voluntary, and you may change your mind about being involved. You are free to withdraw at any point before or during the study. Withdrawal does not require a reason.

Thank you for reading this.

What is the purpose of the study?

We have developed a brain training game called RECOGNeyes with the aim of improving symptoms in people with specific learning difficulties such as attention deficit hyperactivity disorder (ADHD). This game involves using an inexpensive computer mounted eye tracker which tracks the participant's eye movements, allowing their own eyes to become the game controller. You can watch a video about the game here:

https://www.youtube.com/watch?v=HRjK8iJbkao

Developing better treatments depends on being able to measure the changes produced by treatment. Research studies have indicated that changes in the brain are good indicators of treatment effects. Therefore, in this study, our aim is to investigate how training on this game produces changes in the brain networks using magnetic resonance imaging (MRI) and magnetoencephalography (MEG).

Magnetoencephalography (MEG) is a non-invasive brain imaging technique for directly measuring brain activity. Brain cells communicate with one another by exchanging small electrical currents and these currents induce a magnetic field that is distributed around the head. Such fields are detectable using a MEG scanner and their measurement allows us to determine the location of any electrical activity in the brain, and how the patterns of that electrical activity change over time.

Why have I been chosen?

The study will involve healthy people aged 18 to 30, and we are particularly interested in people who have a specific learning difficulty such as ADHD, dyslexia, dyspraxia and dyscalculia. We would like to assess how training on the RECOGNeyes game can change the brain networks and also help with specific learning difficulties. Participants should not have a history of head injury or major medical illnesses and must not have conditions that are unsuitable for a MRI scan (e.g. pregnancy, hearing difficulties such as tinnitus, claustrophobia or metal in the body). Participants who have taken part in any other clinical research project in the last three months will also be excluded.

Do I have to take part?

It is up to you to decide whether or not to take part. If you do, you will be given this information sheet to keep and be asked to sign a consent form. You are still free to withdraw at any time and without giving a reason. A decision to withdraw at any time, or a decision not to take part, will not affect your legal rights.

What will happen to me if I take part?

Once you express an interest in participating in the study, a member of the research team will speak to you in order to explain the study to you in more detail and to make sure that there is nothing that excludes you from the study e.g. being unsuitable for an MRI scan.
The study itself consists of two visits to the Sir Peter Mansfield Imaging Centre (SPMIC), University Park (Nottingham), approximately two weeks apart, during which you will undergo training on the RECOGNeyes game at home. This is explained in more detail below.

First visit:

In the first visit, you will be asked to fill in a rating scale about the behaviours and problems sometimes experienced by adults with ADHD, a questionnaire about your health and also take two short reading tests. You will also be asked for more details regarding your learning difficulties, if any, and also about regular medication intake or any other therapies you are receiving. Then, you will undergo a MEG scan so we can measure your brain activity. This involves you lying in a scanner that covers a part of your head (see the picture below). The researcher will ask you to perform a simple that involve seeing visual images on a screen and responding to them by moving your eyes. The MEG scan consists of short sessions with pauses in between, lasting for

approximately 40 minutes in total. Before the scan we will provide light clothing to wear in the scanner.

Following this, you will undergo a MRI scan (see the picture of the scanner attached below). In the scanner room, you will be asked to lie on your back on a comfortable mat on a sliding bed. You will be given earplugs and pads that will reduce the sound of the scanner. You will also be given a call-bell that can be pushed at any time to stop the procedure and request assistance. Once you are comfortable, the bed will be slid into the scanner. When you lie in the MR scanner, it will cover most of your body, though the scanning will be done only on your head. Further instructions will be read to you through the headphones. We will be in communication with you throughout the scanning session. The MRI scan will last for 25 minutes.

After the scanning sessions, you will be introduced to the RECOGNeyes brain training game and will be provided with a portable eye tracker and a laptop in order to undertake the training at home. A demonstration on how to set up the eye tracker will be provided and then you will be shown how to navigate through the game. Time will be provided for practice on the game tasks and you will be allowed to ask the researcher any questions you may have. Following this, you will take away the eye tracker and laptop for two weeks in order to play the game and undertake a certain number of training sessions per week (maximum 4 per week). Each training session will last for 20 to 30 minutes. You will be given a sealed envelope which will contain information on how many training sessions you need to undertake each week. The first visit will last approximately 3 hours.

Two weeks of RECOGNeyes training:

For two weeks after the first visit, you will undergo RECOGNeyes training at your own convenience using the eye tracker and laptop provided. You will undergo the amount of training per week specified in the envelope provided to you. Details of how to space the training sessions will also be given in the envelope. The laptop will keep a record of your training progress and a log of the time you spend training. An investigator will be available by email or text to help you with your training schedule.

Second visit:

After you have completed training on RECOGNeyes, you will be asked to visit the
Imaging Centre again. The second visit will involve another MEG scan, identical to the first one and a second MRI scan. You will also be asked to do the two reading tests and fill the questionnaire about your health again. The second visit will last approximately 2 hours. At the end of the second visit, you will be asked to fill a brief feedback form.

One of the MRI scanners

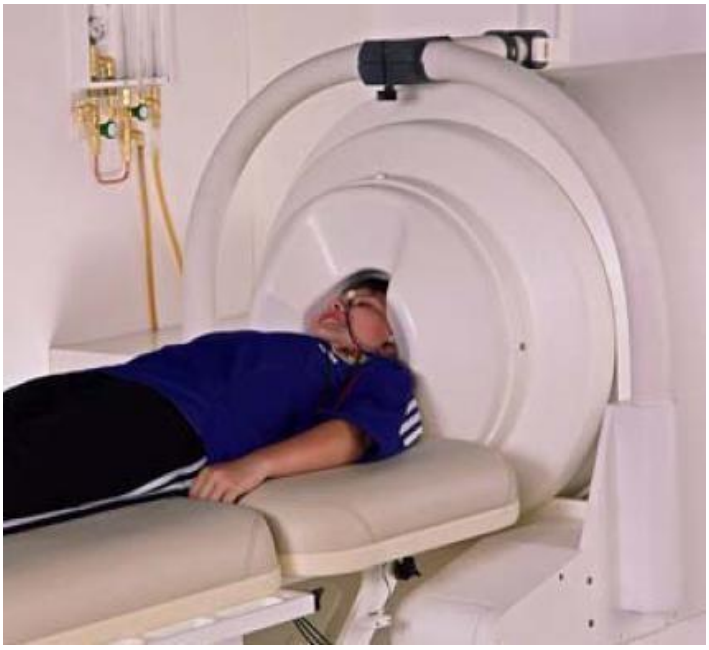

A subject lying in an MEG scanner

What do I have to do?

You must refrain from use of alcohol, cannabis or any other recreational drugs for 24 hours prior to each visit and also prior to undertaking each training session. Otherwise there is nothing that you will have to change about your daily routine. If you are taking regular medication, you should continue with your usual medication schedule.
During the scans, we will give you instructions regarding what we want you to do.

Expenses and payment

You will receive a £60 inconvenience allowance for participating in this study. If we need to exclude you from the experiment on the basis of information from the initial interview or for any other reason related to the study criteria after you arrive at the MR centre, you will still receive the full inconvenience allowance. If you withdraw from the study for medical reasons not associated with the study, you will receive an inconvenience allowance proportional to the length of the period of participation, but if you withdraw for any other reason, the inconvenience allowance to be received, if any, shall be at the discretion of the investigators.

What is the drug, device or procedure that is being tested?

This study is being undertaken in order to examine the effects of the eye-tracking game, RECOGNeyes on your brain networks. No drug is being tested in this study.

What are the side effects of any treatment or procedures received when taking part?

There are no known adverse effects of participating in a magnetic resonance imaging session, provided you do not have any contraindications to participate. Some people feel dizzy in the scanner, but this is rare. There are no known long-term effects of undergoing a MRI scan. Magnetoencephalography is an entirely passive scanning technique and involves no risks at all. If you have any concerns about your participation in this study, please contact Dr. Elizabeth Liddle at 0115 74 84012 or by email at elizabeth.liddle@nottingham.ac.uk. There are also no known adverse effects of using an eyetracker to play a computer game. However, if it makes your eyes feel tired, you can stop at any time.

What are the other possible disadvantages and risks of taking part?

Some people cannot be exposed to the strong magnetic fields in the MRI scanner due to medical/cosmetic procedures that have been performed on them, or accidents which may have resulted in metallic objects entering their bodies. We will therefore carry out a comprehensive safety questionnaire with you to ensure that there is no possibility that it would be unsafe to scan you. In order to obtain good quality images of your brain, you will need to keep as still as possible inside the scanner while you are performing the task. There is also the possibility that you might feel claustrophobic inside the narrow scanner tunnel. However, if you feel very uncomfortable you can stop the experiment at any time by pressing the call-bell.

We do ask that you do not take part if you think that you may be pregnant. There is no evidence that MRI scanning is a danger to a foetus, but the issue has yet to be well studied. If there is any likelihood you might be pregnant we will offer you a pregnancy test on each day of scanning.

What are the possible benefits of taking part?

We cannot promise the study will help you in any way. The purpose of the training game is to enhance attentional control in children and adults. We do anticipate some positive effects of the training on the brain but this work is at

an early stage. We hope that you will find the computer games fun and that exposure to a research study to be an interesting experience. It is hoped that your participation will contribute to research into the development of the intervention aimed at helping people with specific learning difficulties such as ADHD. This might lead to better treatments for children and adults with specific learning difficulties in future.

What if unexpected information becomes available from the study?

The research scan is not the same as a routine clinical scan and therefore cannot be used to make a clinical diagnosis. However, if your scan reveals anything that suggests a possible clinical abnormality, we will inform your GP so that he or she might arrange any further investigations that might be required.

What if there is a problem?

If you have any questions or concerns about your participation in this study, please contact the Chief Investigator Dr. Elizabeth Liddle (details given below). The second point of contact is the FMHS Research Ethics Committee Administrator, c/o The University of Nottingham, Faculty PVC Office, B Floor, Medical School, Queen's Medical Centre Campus, Nottingham University Hospitals, Nottingham, NG7 2UH or via E-mail: FMHS-ResearchEthics@nottingham.ac.uk

Will my taking part in the study be kept confidential?

We will follow ethical and legal practice and all information about you will be handled in confidence.
If you join the study, some parts of your data collected for the study will be looked at by authorised persons from the University of Nottingham who are organising the research. They may also be looked at by authorised people to check that the study is being carried out correctly. All will have a duty of confidentiality to you as a research participant and we will do our best to meet this duty.

All information which is collected about you during the course of the research will be kept **strictly confidential**, stored in a secure and locked office, and on a password protected database. Any information about you which leaves the university will have your name and address removed (anonymised) and a unique code will be used so that you cannot be recognised from it.
Your personal data (address, telephone number) will be kept for 12 months after the end of the study so that we are able to contact you about the findings of the study *and possible follow-up studies* (unless you advise us that you do not wish to be contacted).

All other data (research data) will be kept securely for at least 7 years. During this time all precautions will be taken by all those involved to maintain your confidentiality, only members of the research team will have access to your personal data. When it is finally disposed of this will be done securely.

What will happen if I don't want to carry on with the study?

Your participation is voluntary and you are free to withdraw at any time, without giving any reason, and without your legal rights being affected. If you withdraw then the information collected so far cannot be erased and this information may still be used in the project analysis.

Involvement of the General Practitioner/Family doctor (GP)

If your scan reveals anything that suggests a possible clinical abnormality, we will inform your GP so that he or she might arrange any further investigations that might be required.

What will happen to the results of the research study?

Results from this study will be published in academic journals. You may request copies of any published articles related to this study. You will not be identified in any report or publication.

Who is organising and funding the research?

This study is organised by the investigators listed above at the University of Nottingham. The source of funding for this project is the Medical Research Council.

Who has reviewed the study?

This study has been reviewed and given favourable opinion by the University of Nottingham, Medical School Ethics Committee

Contact Details:

If you are interested in participating in this study or have any questions, please contact Ms. Jyothika Kumar at jyothika.kumar1@nottingham.ac.uk. If you have any concerns, please contact the principal investigator Dr Elizabeth Liddle at 0115 74 84012 or by email at elizabeth.liddle@nottingham.ac.uk.
You will be given a copy of the information sheet and a signed consent form to keep. Thank you very much for considering taking part in our study.

School of Medicine
Division of Psychiatry and Applied Psychology
Institute of Mental Health
Triumph Road, Nottingham NG7 2TU.